

## ***Electronic Supplementary Information***

### **The Mechanism of Oxidative Addition of Pd(0) to Si–H bonds: Electronic Effects, Reaction Mechanism, and Hydrosilylation**

Michael R. Hurst, Lev N. Zakharov, and Amanda. K. Cook\*

#### **Table of Contents**

1. Materials and Methods .....	3
2. General Experimental .....	3
3. Synthesis of Non-Commercial Reagents .....	5
a. Palladium complex, [(μ-dcpe)Pd] <sub>2</sub> .....	5
b. Triaryl silanes .....	6
c. Aryl dimethyl silanes .....	9
d. Deuterated silanes .....	12
e. Other silanes .....	13
4. Characterization of Silyl Palladium Hydrides/Deuterides .....	15
a. General considerations .....	15
b. Triaryl silanes .....	16
c. Aryl dimethyl silanes .....	19
d. Other silanes .....	21
e. Measurements of <sup>2</sup> J <sub>H–Si</sub> .....	23
f. Measurements of <sup>2</sup> J <sub>H–P(trans)</sub> .....	25
5. Equilibrium Studies – Conversion and K <sub>eq</sub> at 298 K .....	27
a. General procedure A .....	27
b. Determination of K <sub>eq</sub> .....	27
c. Equilibrium conversion and Hammett plot data .....	28
i. Triaryl silanes .....	28
ii. Aryl dimethyl silanes .....	29
iii. Additional silanes .....	30
6. Equilibrium Studies – Variable Temperature and van't Hoff Plots .....	31
a. General procedure B .....	31
b. Data with dimethyl aryl silanes 3 .....	32
c. Equilibrium isotope effect .....	39

7.	Reversibility .....	40
a.	Reversibility with respect to temperature .....	40
b.	Reversibility with respect to product distribution .....	42
8.	Competition Studies .....	47
a.	General procedure C .....	47
b.	Results of competition between 5a and 5b-f .....	48
c.	Results of competition between 3a and 3b-f .....	49
9.	Kinetic Studies .....	50
a.	General procedure D .....	50
b.	Kinetics to measure the order in $[(\mu\text{-dcpe})\text{Pd}]_2$ (1) .....	51
c.	Kinetics to measure the order in $\text{HSiPhMe}_2$ (3a) .....	53
d.	Derivation of the rate law .....	55
e.	Kinetics to construct a Hammett plot .....	56
f.	Kinetics to measure KIE .....	62
g.	Kinetics to construct an Eyring plot .....	64
10.	Dynamic Behavior .....	68
a.	Reaction setup, data, spectra, and analysis .....	68
b.	Rates of dynamic exchange as a function of concentration .....	80
c.	ROESY NMR spectrum of 10a/5a mixture .....	86
11.	Catalysis .....	88
a.	Synthesis of hydrosilylation products using an independent method .....	88
b.	Catalytic studies .....	92
12.	Crystallographic information of 10f .....	97
13.	Calculation of $\tau_4$ Structural Parameter of 10f .....	98
14.	NMR and IR Spectra .....	99
a.	Palladium(0) complexes .....	99
b.	Triaryl silanes .....	101
c.	Aryl dimethyl silanes .....	115
d.	Deuterated silanes .....	131
e.	Other silanes .....	136
f.	Silyl Palladium Hydrides/Deuterides .....	141
g.	Hydrosilylation Products .....	184
15.	References .....	195

## 1. Materials and Methods

All syntheses and manipulations were carried out under nitrogen using standard Schlenk (vacuum  $10^{-2}$  mbar) technique or in a nitrogen-filled glovebox unless otherwise indicated. All reagents and solvents were used after drying and stored under nitrogen, unless otherwise indicated. Tetrahydrofuran (THF; Fisher Chemical; HPLC grade, unstabilized), hexanes (Fisher Chemical; HPLC grade), diethyl ether ( $\text{Et}_2\text{O}$ ; B&J Brand; HPLC grade, unstabilized) and acetonitrile (MeCN; Fisher Chemical; HPLC grade) were dispensed under nitrogen from an LC Technology SP-1 solvent system. Benzene (ACS grade) was refluxed overnight with  $\text{CaH}_2$  and distilled under nitrogen before use. The dried solvents were thereafter stored on activated 4Å molecular sieves under nitrogen.  $\text{C}_6\text{D}_6$  and  $\text{C}_7\text{D}_8$  were purchased from Cambridge Isotope Laboratories, degassed by freeze-pump-thaw, and thereafter stored on activated 4Å molecular sieves under nitrogen. All stock solutions were prepared by mass and were dispensed into reaction vessel by difference from syringe, as detailed in the procedure for each experiment.

The following reagents were used from commercial sources without further purification: 1,2-bis(dicyclohexylphosphino)ethane (dcpe; **S2**; Strem Chemicals), trichlorosilane (Alfa Aesar), dimethylchlorosilane (Alfa Aesar), triphenylchlorosilane (TCI America), dimethylphenylchlorosilane (Gelest), lithium aluminum deuteride (Aldrich Chemical), anhydrous hydrazine (Sigma Aldrich), 4-iodotoluene (Oakwood Chemical), 4-iodoanisole (Oakwood Chemical), 4-bromofluorobenzene (TCI America), 4-bromo-N,N,-dimethylaniline (TCI America), 4-bromobenzotrifluoride (Matrix Scientific), palladium acetate (Aldrich), tetraethyl ethylenediphosphonate (Alfa Aesar), triphenylsilane (Alfa Aesar), phenyldimethylsilane (Oakwood), dimethylphenylsilane (Oakwood), triethylsilane (Oakwood), and triethoxysilane (Acros). (dcpe) $\text{PdCl}_2$  (**S1**) was prepared according to a literature procedure.<sup>1, 2</sup>  $\text{Pd}(\text{PCy}_3)_2$  was prepared according to a literature procedure.<sup>3</sup>

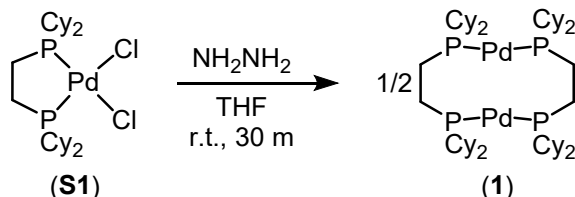
## 2. General Experimental

Nuclear magnetic resonance (NMR) spectra were collected at room temperature (298 K) unless otherwise stated on a Bruker AV-III HD 600 NMR (600.13 MHz for  $^1\text{H}$ ; 150.90 MHz for  $^{13}\text{C}$ ; 564.69 MHz for  $^{19}\text{F}$ ; 119.23 MHz for  $^{29}\text{Si}$ ; 232.94 MHz for  $^{31}\text{P}$ ), Bruker Avance-III HD 500 NMR (499.90 MHz for  $^1\text{H}$ ; 126 MHz for  $^{13}\text{C}$ ; 471 MHz for  $^{19}\text{F}$ ; 99 MHz for  $^{29}\text{Si}$ ; 202.46 MHz for  $^{31}\text{P}$ ), or Varian Inova 500 NMR (499.90 MHz for  $^1\text{H}$ ; 126 MHz for  $^{13}\text{C}$ ; 471 MHz for  $^{19}\text{F}$ ; 99 MHz for  $^{29}\text{Si}$ ; 202.46 MHz for  $^{31}\text{P}$ ).  $^1\text{H}$  and  $^{13}\text{C}$  spectra were referenced to residual solvent peaks ( $\text{C}_6\text{D}_6$ :  $^1\text{H}$   $\delta$  = 7.16 ppm,  $^{13}\text{C}$   $\delta$  = 128.06 ppm;  $\text{C}_7\text{D}_8$ :  $^1\text{H}$   $\delta$  = 2.08, 6.97, 7.01, 7.09 ppm,  $^{13}\text{C}$   $\delta$  = 137.48, 128.87, 127.96, 125.13, 20.43 ppm). Chemical shifts are reported in parts per million (ppm,  $\delta$ ) relative to tetramethylsilane at 0.00 ppm. Peaks are characterized as follows: s (singlet), d (doublet), t (triplet), q (quartet), pent (pentet), sext (sextet), sept (septet), m (multiplet), br (broad), app (apparent), and/or ms (multiple signals). Coupling constants,  $J$ , are reported in Hz. Infrared spectroscopy was performed on a Bruker Alpha II FT-IR spectrometer or an Agilent Nicolet 6700 FT-IR using the ATR sampling technique (vide infra), and peaks are reported in  $\text{cm}^{-1}$ . For catalytic reactions, yields were determined using Gas Chromatography-Mass Spectrometry (GCMS) against an internal standard. GCMS was carried out on a Shimadzu GC-2010 Plus/GCMS-QP2010 SE using a Restek Rtx®-5 (Crossbond 5% diphenyl – 95% dimethyl polysiloxane; 15 m, 0.25 mm ID, 0.25  $\mu\text{m}$  df)

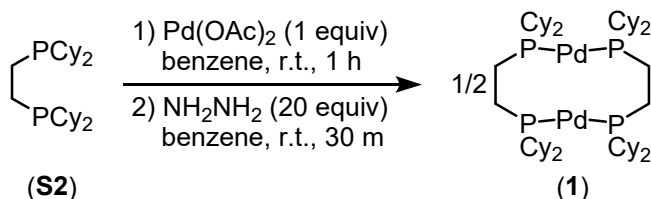
column. High-resolution mass spectrometry (HRMS) was carried out on a Waters XEVO G2-XS TOF mass spectrometer.

### 3. Synthesis of Non-Commercial Reagents

#### a. Palladium complex, $[(\mu\text{-dcpe})\text{Pd}]_2$



$[(\mu\text{-dcpe})\text{Pd}]_2$  (**1**) was synthesized via modified literature procedure:<sup>2</sup> to a 20 mL scintillation vial in a glovebox was added **S1** (180 mg, 0.30 mmol, 1.0 equiv) and THF (5 mL) with stirring. To the suspension, anhydrous  $\text{NH}_2\text{NH}_2$  (0.19 mL, 6.0 mmol, 20 equiv) was added at once by syringe, and the reaction was stirred for 30 minutes. Hexanes (10 mL) was added and the reaction mixture filtered over a Celite plug to collect a deep red solution, which was concentrated under reduced pressure to yield crude  $[(\mu\text{-dcpe})\text{Pd}]_2$ . The material was re-dissolved in hexanes and extracted with MeCN to remove impurities; the hexanes fraction was then concentrated to yield a pure, microcrystalline red solid (124 mg, 0.117 mmol, 78% yield).



Alternatively, **1** was synthesized in a one-pot procedure: to a 20 mL scintillation vial in the glovebox was added  $\text{Pd(OAc)}_2$  (67 mg, 0.30 mmol, 1.0 equiv), **S2** (127 mg, 0.30 mmol, 1.0 equiv.), and benzene (5 mL) with stirring. The reaction was stirred for 1 hour, and anhydrous  $\text{NH}_2\text{NH}_2$  (0.19 mL, 6.0 mmol, 20 equiv.) was added all at once by syringe. The reaction was stirred for 30 minutes more before hexanes (10 mL) was added and the reaction mixture was filtered over a Celite plug to collect a deep red solution. The solution was extracted with MeCN and the hexanes layer concentrated under reduced pressure to yield a pure, microcrystalline red solid (116 mg, 0.109 mmol, 73% yield).

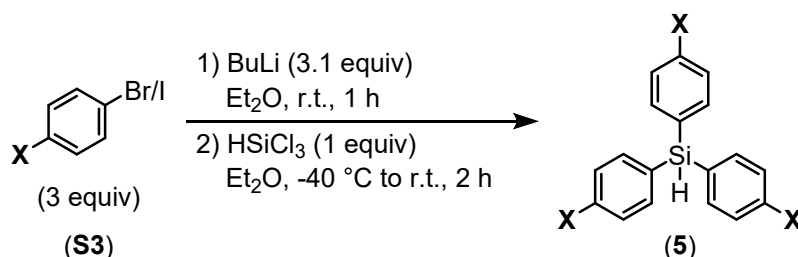
$^1\text{H}$  NMR (600 MHz,  $\text{C}_6\text{D}_6$ , 298 K):  $\delta$  2.28 (app d,  $J$  = 12.5 Hz, 8H), 2.13 (app d,  $J$  = 11.8 Hz, 8H), 1.90 (m, 16H), 1.74 (m, 40H), 1.33 (m, 24H)

$^{13}\text{C}\{^1\text{H}\}$  NMR (151 MHz,  $\text{C}_6\text{D}_6$ , 298 K):  $\delta$  37.2 (t,  $J$  = 3.4 Hz), 31.4 (d,  $J$  = 64.6 Hz), 28.1 (d,  $J$  = 21.5 Hz), 27.3, 22.0 (t,  $J$  = 5.5 Hz)

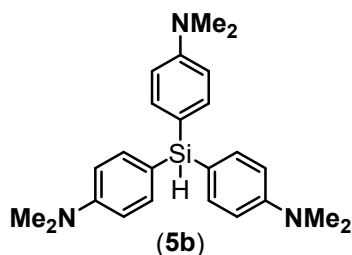
$^{31}\text{P}\{^1\text{H}\}$  NMR (243 MHz,  $\text{C}_6\text{D}_6$ , 298 K):  $\delta$  22.96 (s)

ASAP/HRMS ( $m/z$ ):  $[\text{M}]^+$  calculated for  $\text{C}_{52}\text{H}_{96}\text{P}_4\text{Pd}_2$ : 1056.4532; found 1056.4553

## b. Triaryl silanes



Triaryl silanes were synthesized via modified literature procedure:<sup>4</sup> an oven-dried Schlenk flask was charged with the aryl iodide or aryl bromide (3.33 equiv), which was dissolved in Et<sub>2</sub>O. BuLi (2.5 M in hexanes, 3.41 equiv) was added dropwise and the reaction was left to stir at room temperature for 1 hour. The reaction was cooled to -40 °C in a dry ice/MeCN bath. HSiCl<sub>3</sub> (1.0 equiv) was slowly added, and the reaction allowed to stir for 1 hour at -40 °C, then warmed to room temperature and stirred for an additional 1 hour. The flask was cooled to 0 °C, opened to air, and quenched with NH<sub>4</sub>Cl (saturated aqueous solution). The organic layer was separated, and the aqueous layer extracted twice with Et<sub>2</sub>O. The combined organic layers were dried over MgSO<sub>4</sub> and filtered, and the filtrate was concentrated under reduced pressure to yield the corresponding crude product. Purification details are included below. <sup>1</sup>J<sub>H-Si</sub> values were measured from the <sup>29</sup>Si satellites of the Si-H signal in the <sup>1</sup>H NMR spectrum.



### Tris[4-(*N,N*-dimethylamino)phenyl]silane (**5b**)

Synthesis details: 4-Bromo-*N,N*-dimethylaniline (2.00 g, 10.0 mmol, 3.33 equiv), Et<sub>2</sub>O (20 mL), BuLi (4.12 mL, 10.3 mmol, 3.41 equiv), HSiCl<sub>3</sub> (0.30 mL, 3.0 mmol, 1.0 equiv), quenched with NH<sub>4</sub>Cl (10 mL), extracted with Et<sub>2</sub>O (2 x 25 mL). (1.08 g, 2.77 mmol, 92% yield).

Purification details: A white solid was collected after concentration under reduced pressure. To the solid was added cold hexane, and the insoluble solid was separated by filtration. The filtrate was concentrated under reduced pressure to yield the product as a white solid.

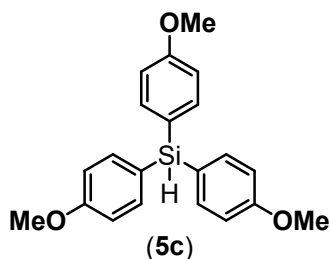
<sup>1</sup>H NMR (500 MHz, C<sub>6</sub>D<sub>6</sub>, 298 K): δ 7.80 (d, *J* = 8.6 Hz, 6H), 6.65 (d, *J* = 8.6 Hz, 6H), 6.05 (s, 1H, <sup>1</sup>J<sub>H-Si</sub> = 189.8 Hz), 2.49 (s, 18H)

<sup>13</sup>C{<sup>1</sup>H} NMR (126 MHz, C<sub>6</sub>D<sub>6</sub>, 298 K): δ 151.7, 137.5, 121.0, 112.7, 39.9

<sup>29</sup>Si{<sup>1</sup>H} NMR (99 MHz, C<sub>6</sub>D<sub>6</sub>, 298 K): δ -19.10

IR (ATR, neat) ν: 2070 cm<sup>-1</sup> (Si-H)

ASAP/HRMS (*m/z*): [M]<sup>+</sup> calculated for C<sub>24</sub>H<sub>31</sub>N<sub>3</sub>Si: 389.2287; found 389.2255



#### Tris(4-methoxyphenyl)silane (**5c**)

Synthesis details: 4-Iodoanisole (2.34 g, 10.0 mmol, 3.33 equiv), Et<sub>2</sub>O (20 mL), BuLi (4.12 mL, 10.3 mmol, 3.41 equiv), HSiCl<sub>3</sub> (0.30 mL, 3.0 mmol, 1.0 equiv), quenched with NH<sub>4</sub>Cl (10 mL), extracted with Et<sub>2</sub>O (2 x 25 mL). (1.05 g, 2.99 mmol, 98% yield).

Purification details: A white, waxy solid was collected after concentration under reduced pressure. To the solid was added cold hexane, and the insoluble solid was separated by filtration. The filtrate was concentrated under reduced pressure to saturation, and the product crystallized after cooling in the freezer to give a white solid.

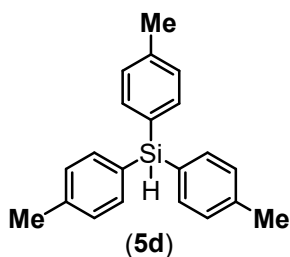
<sup>1</sup>H NMR (600 MHz, C<sub>6</sub>D<sub>6</sub>, 298 K): δ 7.63 (d, *J* = 7.7 Hz, 6H), 6.85 (d, *J* = 7.7 Hz, 6H), 5.85 (s, 1H, <sup>1</sup>*J*<sub>H-Si</sub> = 195.1 Hz), 3.28 (s, 9H)

<sup>13</sup>C{<sup>1</sup>H} NMR (151 MHz, C<sub>6</sub>D<sub>6</sub>, 298 K): δ 161.7, 137.8, 125.4, 114.4, 54.6

<sup>29</sup>Si{<sup>1</sup>H} NMR (99 MHz, C<sub>6</sub>D<sub>6</sub>, 298 K): δ -18.98

IR (ATR, neat) ν: 2136 cm<sup>-1</sup> (Si-H)

ASAP/HRMS (m/z): [M]<sup>+</sup> calculated for C<sub>21</sub>H<sub>22</sub>O<sub>3</sub>Si: 350.1338; found 350.1312



#### Tris(4-methylphenyl)silane (**5d**)

Synthesis details: 4-Iodotoluene (2.18 g, 10.0 mmol, 3.33 equiv), Et<sub>2</sub>O (20 mL), BuLi (4.12 mL, 10.3 mmol, 3.41 equiv), HSiCl<sub>3</sub> (0.30 mL, 3.0 mmol, 1.0 equiv), quenched with NH<sub>4</sub>Cl (10 mL), extracted with Et<sub>2</sub>O (2 x 25 mL). (0.57 g, 1.88 mmol, 63% yield).

Purification details: A white solid was collected after concentration under reduced pressure. To the solid was added cold hexane, and the insoluble solid was separated by filtration. The filtrate was concentrated under reduced pressure to yield the product as a white solid.

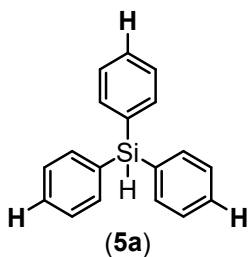
<sup>1</sup>H NMR (500 MHz, C<sub>6</sub>D<sub>6</sub>, 298 K): δ 7.63 (d, *J* = 7.7 Hz, 6H), 7.04 (d, *J* = 7.7 Hz, 6H), 5.81 (s, 1H, <sup>1</sup>*J*<sub>H-Si</sub> = 195.9 Hz), 2.10 (s, 9H)

<sup>13</sup>C{<sup>1</sup>H} NMR (126 MHz, C<sub>6</sub>D<sub>6</sub>, 298 K): δ 139.8, 136.4, 130.8, 129.3, 21.5

<sup>29</sup>Si{<sup>1</sup>H} NMR (99 MHz, C<sub>6</sub>D<sub>6</sub>, 298 K): δ -18.27

IR (ATR, neat) ν: 2114 cm<sup>-1</sup> (Si-H)

ASAP/HRMS (m/z): [M]<sup>+</sup> calculated for C<sub>21</sub>H<sub>22</sub>Si: 302.1491; found 302.1489



Triphenylsilane (**5a**) (commercial, but characterization

provided for reference)

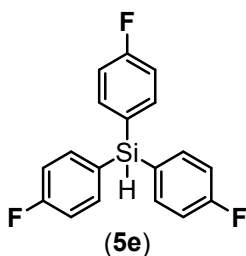
$^1\text{H}$  NMR (500 MHz,  $\text{C}_6\text{D}_6$ , 298 K):  $\delta$  7.59 (d,  $J$  = 6.5 Hz, 6H), 7.20-7.10 (m, 6H, overlapping with  $\text{C}_6\text{H}_6$ ), 5.71 (s, 1H,  $^1J_{\text{H-Si}}$  = 198.0 Hz)

$^{13}\text{C}\{^1\text{H}\}$  NMR (126 MHz,  $\text{C}_6\text{D}_6$ , 298 K):  $\delta$  135.9, 133.4, 129.7, 128.1

$^{29}\text{Si}\{^1\text{H}\}$  NMR (99 MHz,  $\text{C}_6\text{D}_6$ , 298 K):  $\delta$  -17.98

IR (ATR, neat)  $\nu$ : 2118  $\text{cm}^{-1}$  (Si-H)

ASAP/HRMS ( $m/z$ ):  $[\text{M}]^+$  calculated for  $\text{C}_{18}\text{H}_{16}\text{Si}$ : 260.1021; found 260.0986



Tris(4-fluorophenyl)silane (**5e**)

Synthesis details: 4-Iodo-fluorobenzene (1.15 mL, 10.0 mmol, 3.33 equiv),  $\text{Et}_2\text{O}$  (20 mL), BuLi (4.12 mL, 10.3 mmol, 3.41 equiv),  $\text{HSiCl}_3$  (0.30 mL, 3.0 mmol, 1.0 equiv), quenched with  $\text{NH}_4\text{Cl}$  (10 mL), extracted with  $\text{Et}_2\text{O}$  (2 x 25 mL). (0.79 g, 2.5 mmol, 76% yield).

Purification details: A colorless oil was collected after concentration under reduced pressure. To the oil was added cold hexane, and the insoluble solid was separated by filtration. The filtrate was concentrated under reduced pressure to yield the product as a colorless oil.

$^1\text{H}$  NMR (600 MHz,  $\text{C}_6\text{D}_6$ , 298 K):  $\delta$  7.23 (dd,  $J$  = 6.2, 8.6 Hz, 6H), 6.82 (app t,  $J$  = 8.6 Hz, 6H), 5.45 (s, 1H,  $^1J_{\text{H-Si}}$  = 200.9 Hz)

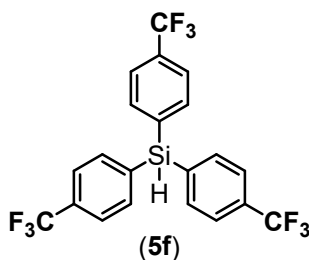
$^{13}\text{C}\{^1\text{H}\}$  NMR (151 MHz,  $\text{C}_6\text{D}_6$ , 298 K):  $\delta$  164.9 (d,  $J$  = 250.0 Hz), 138.1 (d,  $J$  = 7.8 Hz), 128.7 (d,  $J$  = 3.9 Hz), 115.8 (d,  $J$  = 19.9 Hz)

$^{19}\text{F}$  NMR (565 MHz,  $\text{C}_6\text{D}_6$ , 298 K):  $\delta$  -109.73 (m)

$^{29}\text{Si}\{^1\text{H}\}$  NMR (119 MHz,  $\text{C}_6\text{D}_6$ , 298 K):  $\delta$  -19.07

IR (ATR, neat)  $\nu$ : 2132  $\text{cm}^{-1}$  (Si-H)

ASAP/HRMS ( $m/z$ ):  $[\text{M}]^+$  calculated for  $\text{C}_{18}\text{H}_{13}\text{F}_3\text{Si}$ : 314.0739; found 314.0769



Tris[4-(trifluoromethyl)phenyl]silane (**5f**)

Synthesis details: 4-Iodobenzotrifluoride (1.47 mL, 10.0 mmol, 3.33 equiv), Et<sub>2</sub>O (20 mL), BuLi (4.12 mL, 10.3 mmol, 3.41 equiv), HSiCl<sub>3</sub> (0.30 mL, 3.0 mmol, 1.0 equiv), quenched with NH<sub>4</sub>Cl (10 mL), extracted with Et<sub>2</sub>O (2 x 25 mL). (0.40 g, 0.86 mmol, 29% yield).

Purification details: A yellow, waxy solid was collected after concentration under reduced pressure. To the solid was added cold hexane, and the insoluble solid was separated by filtration. The filtrate was concentrated under reduced pressure to saturation, and the product crystallized after cooling in the freezer to give a pale yellow solid.

<sup>1</sup>H NMR (600 MHz, C<sub>6</sub>D<sub>6</sub>, 298 K): δ 7.36 (d, *J* = 7.7 Hz, 6H), 7.20 (d, *J* = 7.7 Hz, 6H), 5.32 (s, 1H, <sup>1</sup>*J*<sub>H-Si</sub> = 206.6 Hz)

<sup>13</sup>C{<sup>1</sup>H} NMR (151 MHz, C<sub>6</sub>D<sub>6</sub>, 298 K): δ 136.4, 136.3, 132.6 (q, *J* = 32.4 Hz), 125.2 (q, *J* = 3.8 Hz), 124.7 (q, *J* = 277.5 Hz)

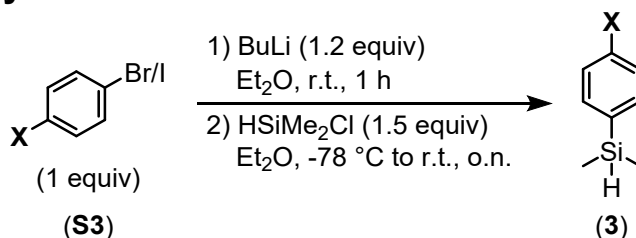
<sup>19</sup>F NMR (565 MHz, C<sub>6</sub>D<sub>6</sub>, 298 K): δ -62.90

<sup>29</sup>Si{<sup>1</sup>H} NMR (99 MHz, C<sub>6</sub>D<sub>6</sub>, 298 K): δ -18.92

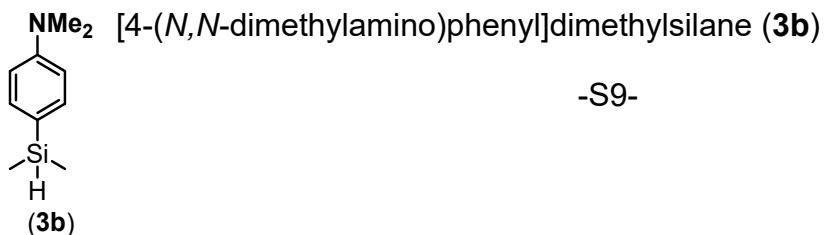
IR (ATR, neat) ν: 2159 cm<sup>-1</sup> (Si-H)

ASAP/HRMS (*m/z*): [*M*]<sup>+</sup> calculated for C<sub>21</sub>H<sub>13</sub>F<sub>9</sub>Si: 464.0643; found 464.0602

### c. Aryl dimethyl silanes



Aryl dimethyl silanes were synthesized via modified literature procedure:<sup>5</sup> an oven-dried Schlenk flask was charged with aryl iodide or aryl bromide (1.0 equiv.), which was dissolved in Et<sub>2</sub>O. BuLi (2.5 M in hexanes, 1.2 equiv.) was added dropwise and the reaction was left to stir at room temperature for 1 hour, after which it was cooled to -78 °C in a dry ice/acetone bath. HSiMe<sub>2</sub>Cl (1.5 equiv.) was added slowly and the reaction mixture stirred at -78 °C while slowly warming to room temperature overnight. The flask was cooled to 0 °C, opened to air, and quenched with NH<sub>4</sub>Cl (saturated aqueous solution). The organic layer was separated and the aqueous layer was extracted twice with Et<sub>2</sub>O. The combined organic layers were dried over MgSO<sub>4</sub> and filtered, and the filtrate was concentrated under reduced pressure to yield the corresponding products as clear, colorless liquids. Note: products are moderately volatile, and care should be taken to avoid their evaporation when drying under vacuum. <sup>1</sup>*J*<sub>H-Si</sub> values were measured from the <sup>29</sup>Si satellites of the Si-H signal in the <sup>1</sup>H NMR spectrum.



**Synthesis details:** 4-Bromo-N,N-dimethylaniline (1.40 g, 7.0 mmol, 1.0 equiv), Et<sub>2</sub>O (20 mL), BuLi (3.36 mL, 8.4 mmol, 1.2 equiv), HSiMe<sub>2</sub>Cl (1.17 mL, 10.5 mmol, 1.5 equiv), quenched with NH<sub>4</sub>Cl (10 mL), extracted with Et<sub>2</sub>O (2 x 25 mL). (0.33 mg, 1.84 mmol, 26% yield).

**Purification details:** Column chromatography: silica, pentane. Collected fractions in pentane were combined, extracted with MeCN and the pentane layer concentrated.

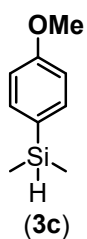
<sup>1</sup>H NMR (600 MHz, C<sub>6</sub>D<sub>6</sub>, 298 K): δ 7.53 (d, *J* = 7.5 Hz, 2H), 6.65 (d, *J* = 7.5 Hz, 2H), 4.80 (sept, <sup>3</sup>*J*<sub>H-H</sub> = 3.7 Hz, <sup>1</sup>*J*<sub>H-Si</sub> = 184.9 Hz, 1H), 2.50 (s, 6H), 0.34 (d, <sup>3</sup>*J*<sub>H-H</sub> = 3.7 Hz, 6H)

<sup>13</sup>C{<sup>1</sup>H} NMR (151 MHz, C<sub>6</sub>D<sub>6</sub>): δ 151.7, 135.5, 122.5, 112.6, 39.9, -3.1

<sup>29</sup>Si{<sup>1</sup>H} NMR (119 MHz, C<sub>6</sub>D<sub>6</sub>, 298 K): δ -18.36

IR (ATR, neat) ν: 2105 cm<sup>-1</sup> (Si-H)

ASAP/HRMS (m/z): [M]<sup>+</sup> calculated for C<sub>10</sub>H<sub>17</sub>NSi: 179.1130; found 179.1097



**(4-methoxyphenyl)dimethylsilane (3c)**

**Synthesis details:** 4-Iodoanisole (1.64 g, 7.0 mmol, 1.0 equiv), Et<sub>2</sub>O (20 mL), BuLi (3.36 mL, 8.4 mmol, 1.2 equiv), HSiMe<sub>2</sub>Cl (1.17 mL, 10.5 mmol, 1.5 equiv), quenched with NH<sub>4</sub>Cl (10 mL), extracted with Et<sub>2</sub>O (2 x 25 mL). Clear, colorless oil (560 mg, 3.4 mmol, 48% yield).

**Purification details:** Column chromatography: silica, pentane.

<sup>1</sup>H NMR (600 MHz, C<sub>6</sub>D<sub>6</sub>, 298 K): δ 7.42 (d, *J* = 6.2 Hz, 2H), 6.85 (d, *J* = 6.2 Hz, 2H), 4.69 (sept, <sup>3</sup>*J*<sub>H-H</sub> = 3.5 Hz, <sup>1</sup>*J*<sub>H-Si</sub> = 187.3 Hz, 1H), 3.31 (s, 3H), 0.26 (d, <sup>3</sup>*J*<sub>H-H</sub> = 3.6, 6H)

<sup>1</sup>H NMR (600 MHz, CDCl<sub>3</sub>, 298 K): δ 7.49 (d, *J* = 8.4 Hz, 2H), 6.94 (d, *J* = 8.4 Hz, 2H), 4.43 (sept, <sup>3</sup>*J*<sub>H-H</sub> = 3.7 Hz, <sup>1</sup>*J*<sub>H-Si</sub> = 187.2 Hz, 1H), 3.83 (s, 3H), 0.34 (d, <sup>3</sup>*J*<sub>H-H</sub> = 3.7 Hz, 6H)

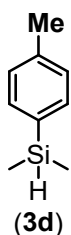
<sup>13</sup>C{<sup>1</sup>H} NMR (151 MHz, C<sub>6</sub>D<sub>6</sub>, 298 K): δ 161.34, 135.83, 128.15 (obscured by C<sub>6</sub>D<sub>6</sub>), 114.18, 54.57, -3.36

<sup>13</sup>C{<sup>1</sup>H} NMR (151 MHz, CDCl<sub>3</sub>, 298 K): δ 160.7, 135.6, 128.4, 113.8, 55.2, -3.4

<sup>29</sup>Si{<sup>1</sup>H} NMR (119 MHz, C<sub>6</sub>D<sub>6</sub>, 298 K): δ -17.81

IR (ATR, neat) ν: 2112 cm<sup>-1</sup> (Si-H)

ASAP/HRMS (m/z): [M]<sup>+</sup> calculated for C<sub>9</sub>H<sub>14</sub>OSi: 166.0814; found 166.0783



**(4-methylphenyl)dimethylsilane (3d)**

**Synthesis details:** 4-Iodotoluene (1.53 g, 7.0 mmol, 1.0 equiv), Et<sub>2</sub>O (20 mL), BuLi (3.36 mL, 8.4 mmol, 1.2 equiv), HSiMe<sub>2</sub>Cl (1.17 mL, 10.5 mmol, 1.5 equiv), quenched with NH<sub>4</sub>Cl (10 mL), extracted with Et<sub>2</sub>O (2 x 25 mL). Clear, colorless oil (850 mg, 5.7 mmol, 81% yield).

**Purification details:** Column chromatography: silica, pentane.

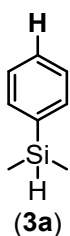
<sup>1</sup>H NMR (600 MHz, C<sub>6</sub>D<sub>6</sub>, 298 K): δ 7.44 (d, *J* = 7.0 Hz, 2H), 7.06 (d, *J* = 7.0 Hz, 2H), 4.67 (sept, <sup>3</sup>*J*<sub>H-H</sub> = 3.7 Hz, <sup>1</sup>*J*<sub>H-Si</sub> = 187.0 Hz, 1H), 2.13 (s, 3H), 0.25 (d, <sup>3</sup>*J*<sub>H-H</sub> = 3.7, 6H)

<sup>13</sup>C{<sup>1</sup>H} NMR (151 MHz, C<sub>6</sub>D<sub>6</sub>): δ 139.2, 134.5, 133.9, 129.1, 21.5, -3.6

<sup>29</sup>Si{<sup>1</sup>H} NMR (119 MHz, C<sub>6</sub>D<sub>6</sub>, 298 K): δ -17.50

IR (ATR, neat) ν: 2114 cm<sup>-1</sup> (Si-H)

ASAP/HRMS (m/z): [M]<sup>+</sup> calculated for C<sub>9</sub>H<sub>14</sub>Si: 150.0865; found 150.0823



Phenyltrimethylsilane (**3a**) (commercial, but characterization provided for reference)

<sup>1</sup>H NMR (600 MHz, C<sub>6</sub>D<sub>6</sub>, 298 K): δ 7.46 (br s, 2H), 7.18 (br s, 3H), 4.62 (sept, <sup>3</sup>*J*<sub>H-H</sub> = 3.5 Hz, <sup>1</sup>*J*<sub>H-Si</sub> = 188.2 Hz, 1H), 0.21 (d, <sup>3</sup>*J*<sub>H-H</sub> = 3.5, 6H)

<sup>1</sup>H NMR (600 MHz, CDCl<sub>3</sub>, 298 K): δ 7.56 (m, 2H), 7.38 (m, 3H), 4.44 (sept, <sup>3</sup>*J*<sub>H-H</sub> = 3.7 Hz, <sup>1</sup>*J*<sub>H-Si</sub> = 188.3 Hz, 1H), 0.37 (d, <sup>3</sup>*J*<sub>H-H</sub> = 3.7 Hz, 6H)

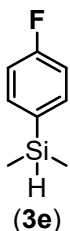
<sup>13</sup>C{<sup>1</sup>H} NMR (151 MHz, C<sub>6</sub>D<sub>6</sub>, 298 K): δ 137.1, 134.0, 129.2, (one aryl peak hidden under benzene peak), -4.1

<sup>13</sup>C{<sup>1</sup>H} NMR (151 MHz, CDCl<sub>3</sub>, 298 K): δ 137.6, 134.2, 129.3, 128.0, -3.6

<sup>29</sup>Si{<sup>1</sup>H} NMR (119 MHz, C<sub>6</sub>D<sub>6</sub>, 298 K): δ -17.20

IR (ATR, neat) ν: 2118 cm<sup>-1</sup> (Si-H)

ASAP/HRMS (m/z): [M]<sup>+</sup> calculated for C<sub>8</sub>H<sub>12</sub>Si: 136.0708; found 136.0680



(4-fluorophenyl)dimethylsilane (**3e**)

**Synthesis details:** 4-Fluoro-bromobenzene (1.2 mL g, 11 mmol, 1.0 equiv), Et<sub>2</sub>O (20 mL), BuLi (3.36 mL, 8.4 mmol, 1.2 equiv), HSiMe<sub>2</sub>Cl (1.17 mL, 10.5 mmol, 1.5 equiv), quenched with NH<sub>4</sub>Cl (10 mL), extracted with Et<sub>2</sub>O (2 x 25 mL). Clear, colorless oil (440 mg, 2.8 mmol, 26% yield).

**Purification details:** Filtered solution of the crude product in ether through a cotton plug and concentration under vacuum. Distillation at 40 °C, 1 Torr into a collection flask cooled with an acetone/dry ice bath.

<sup>1</sup>H NMR (500 MHz, C<sub>6</sub>D<sub>6</sub>, 298 K): δ 7.21 (dd, *J* = 6.3, 8.4 Hz, 2H), 6.85 (app t, *J* = 8.9 Hz, 2H), 4.53 (sept, <sup>3</sup>*J*<sub>H-H</sub> = 3.8 Hz, <sup>1</sup>*J*<sub>H-Si</sub> = 188.8 Hz, 1H), 0.15 (d, <sup>3</sup>*J*<sub>H-H</sub> = 3.8, 6H)

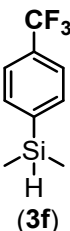
<sup>13</sup>C{<sup>1</sup>H} NMR (151 MHz, C<sub>6</sub>D<sub>6</sub>, 298 K): δ 164.4 (d, *J* = 248.1 Hz), 136.3 (d, *J* = 7.5 Hz), 132.9 (d, *J* = 3.9 Hz), 115.4 (d, *J* = 19.6 Hz), -3.7

<sup>19</sup>F NMR (565 MHz, C<sub>6</sub>D<sub>6</sub>, 298 K): δ -111.56 (m)

<sup>29</sup>Si{<sup>1</sup>H} NMR (119 MHz, C<sub>6</sub>D<sub>6</sub>, 298 K): δ -17.31

IR (ATR, neat) ν: 2120 cm<sup>-1</sup> (Si-H)

ASAP/HRMS (m/z): [M]<sup>+</sup> calculated for C<sub>8</sub>H<sub>11</sub>FSi: 154.0614; found 154.0593



[4-(trifluoromethyl)phenyl]dimethylsilane (**3f**)

Synthesis details: 4-Bromobenzotrifluoride (0.98 mL, 7.0 mmol, 1.0 equiv), Et<sub>2</sub>O (20 mL), BuLi (3.36 mL, 8.4 mmol, 1.2 equiv), HSiMe<sub>2</sub>Cl (1.17 mL, 10.5 mmol, 1.5 equiv), quenched with NH<sub>4</sub>Cl (10 mL), extracted with Et<sub>2</sub>O (2 x 25 mL). Clear, pale yellow oil (150 mg, 0.73 mmol, 10% yield).

Purification details: Column chromatography: silica, pentane. Extraction of product dissolved in pentane with MeCN, separation of the layers, concentration of the pentane layer under reduced pressure.

<sup>1</sup>H NMR (600 MHz, C<sub>6</sub>D<sub>6</sub>, 298 K): δ 7.37 (d, *J* = 7.4 Hz, 2H), 7.24 (d, *J* = 7.4 Hz, 2H), 4.46 (sept, <sup>3</sup>*J*<sub>H-H</sub> = 3.9 Hz, <sup>1</sup>*J*<sub>H-Si</sub> = 190.8 Hz, 1H), 0.11 (d, <sup>3</sup>*J*<sub>H-H</sub> = 3.9, 6H)

<sup>13</sup>C{<sup>1</sup>H} NMR (151 MHz, C<sub>6</sub>D<sub>6</sub>, 298 K): δ 142.4, 134.6, 131.4 (q, *J* = 32.2 Hz), 125.0 (q, *J* = 274 Hz), 124.6 (q, *J* = 3.8 Hz), -4.12

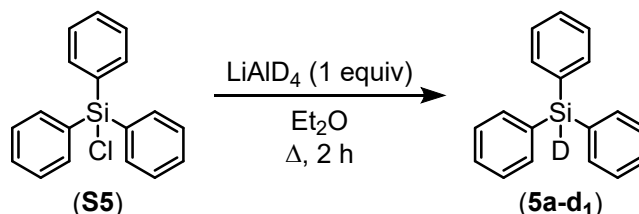
<sup>19</sup>F NMR (565 MHz, C<sub>6</sub>D<sub>6</sub>, 298 K): δ -62.63

<sup>29</sup>Si{<sup>1</sup>H} NMR (119 MHz, C<sub>6</sub>D<sub>6</sub>, 298 K): δ -16.72

IR (ATR, neat) ν: 2126 cm<sup>-1</sup> (Si-H)

ASAP/HRMS (*m/z*): [*M*]<sup>+</sup> calculated for C<sub>9</sub>H<sub>11</sub>F<sub>3</sub>Si: 204.0582; found 205.0564

#### d. Deuterated silanes



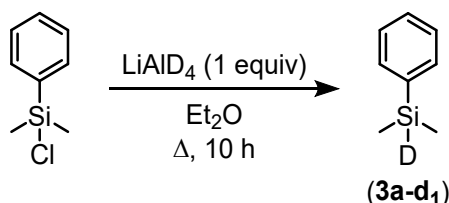
DSiPh<sub>3</sub> was prepared via modified literature procedure:<sup>6</sup> to an oven-dried Schlenk flask was added ClSiPh<sub>3</sub> (300 mg, 1.0 mmol, 1.0 equiv.) and degassed Et<sub>2</sub>O (15 mL) with stirring. LiAlD<sub>4</sub> (42 mg, 1.0 mmol, 1.0 equiv.) was added to the reaction, and the flask was equipped with a reflux condenser. The reaction mixture was heated to reflux and stirred overnight. The reaction was cooled to room temperature and quenched with H<sub>2</sub>O. The reaction mixture was extracted with Et<sub>2</sub>O and the organics filtered through Celite. The collected clear liquid was concentrated under reduced pressure to yield **5a-d<sub>1</sub>** as a viscous, clear, colorless oil (250 mg, 0.82 mmol, 82% yield).

<sup>1</sup>H NMR (600 MHz, C<sub>6</sub>D<sub>6</sub>, 298 K): δ 7.59 (dd, *J* = 7.8 Hz, 1.5 Hz, 6 H), 7.17-7.13 (m, 9H).

<sup>13</sup>C{<sup>1</sup>H} NMR (151 MHz, C<sub>6</sub>D<sub>6</sub>, 298 K): δ 136.2, 133.7, 130.1, 128.4

IR (ATR, neat) ν: 1539 cm<sup>-1</sup> (Si-D)

ASAP/HRMS (*m/z*): [*M*]<sup>+</sup> calculated for C<sub>18</sub>H<sub>15</sub>DSi: 261.1084; found 261.0945



DSiPhMe<sub>2</sub> was prepared according to literature procedure:<sup>7</sup> to an oven-dried Schlenk flask was added LiAlD<sub>4</sub> (170 mg, 4.0 mmol, 2.7 equiv.) and Et<sub>2</sub>O (15 mL) with stirring. PhMe<sub>2</sub>SiCl (0.26 mL, 1.5 mmol, 1.0 equiv) was added to the suspension via syringe, and the flask was equipped with a reflux condenser. The reaction mixture was heated to reflux and stirred overnight. The reaction was cooled to room temperature and quenched by slow addition of 10 wt% NaOH (aqueous solution). The product was then extracted into Et<sub>2</sub>O, and the organic layer was separated, dried over MgSO<sub>4</sub>, filtered, and concentrated under reduced pressure. The crude product was purified via vacuum distillation (room temperature, 1 Torr) into a collection flask cooled with an acetone/dry ice bath to give **3a-d<sub>1</sub>** as a clear colorless oil (33 mg, 0.24 mmol, 16% yield).

<sup>1</sup>H NMR (600 MHz, C<sub>6</sub>D<sub>6</sub>, 298 K): δ 7.47 (m, 2H), 7.19 (m, 3H), 0.21 (s, 6H).

<sup>1</sup>H NMR (600 MHz, CDCl<sub>3</sub>, 298 K): δ 7.55 (m, 2H), 7.37 (m, 3H), 0.35 (s, 6H).

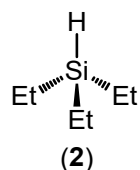
<sup>13</sup>C{<sup>1</sup>H} NMR (151 MHz, C<sub>6</sub>D<sub>6</sub>, 298 K): δ 137.4, 134.3, 129.5, (one aryl peak hidden under benzene peak), -3.84

<sup>13</sup>C{<sup>1</sup>H} NMR (151 MHz, CDCl<sub>3</sub>, 298 K): δ 137.6, 134.2, 129.3, 128.0, -3.84

IR (ATR, neat) ν: 1539 cm<sup>-1</sup> (Si–D)

ASAP/HRMS (m/z): [M]<sup>+</sup> calculated for C<sub>8</sub>H<sub>11</sub>DSi: 137.0771; found 137.0676

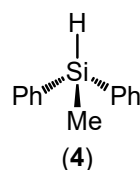
## e. Other silanes



Triethylsilane (**2**) (commercial, but characterization provided for reference)

<sup>1</sup>H NMR (600 MHz, C<sub>6</sub>D<sub>6</sub>, 298 K): δ 3.90 (sept, <sup>3</sup>J<sub>H–H</sub> = 3.1 Hz, <sup>1</sup>J<sub>H–Si</sub> = 177.5 Hz, 1H), 0.97 (t, *J* = 8.0 Hz, 9 H), 0.55 (qd, <sup>3</sup>J<sub>H–H</sub> = 8.0 Hz, 3.1 Hz, 6 H)

ASAP/HRMS (m/z): [M]<sup>+</sup> calculated for C<sub>6</sub>H<sub>16</sub>Si: 116.1021; found 116.1059



Methylphenyldiphenylsilane (**4**) (commercial, but characterization provided for reference)

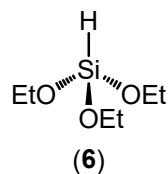
<sup>1</sup>H NMR (600 MHz, C<sub>6</sub>D<sub>6</sub>, 298 K): δ 7.51 (m, 4H), 7.16–7.15 (ms, 6H, overlapping with benzene), 5.14 (q, <sup>3</sup>J<sub>H–H</sub> = 3.8 Hz, <sup>1</sup>J<sub>H–Si</sub> = 193.3 Hz, 1H), 0.46 (d, <sup>3</sup>J<sub>H–H</sub> = 3.8 Hz, 3H)

<sup>13</sup>C{<sup>1</sup>H} NMR (151 MHz, C<sub>6</sub>D<sub>6</sub>, 298 K): δ 135.6, 135.2, 129.8, (one aryl peak overlapping with benzene), -4.9

<sup>29</sup>Si{<sup>1</sup>H} NMR (119 MHz, C<sub>6</sub>D<sub>6</sub>, 298 K): δ -17.63

IR (ATR, neat) ν: 2118 cm<sup>-1</sup> (Si–D)

ASAP/HRMS (m/z): [M]<sup>+</sup> calculated for C<sub>13</sub>H<sub>14</sub>Si: 198.0865; found 198.0818



Triethoxysilane (**6**) (commercial, but characterization provided for reference)

<sup>1</sup>H NMR (600 MHz, C<sub>6</sub>D<sub>6</sub>, 298 K): δ 4.60 (s, <sup>1</sup>J<sub>H–Si</sub> = 285.8 Hz, 1H), 3.77 (q, <sup>3</sup>J<sub>H–H</sub> = 7.0 Hz, 6H), 1.13 (t, <sup>3</sup>J<sub>H–H</sub> = 7.0 Hz, 9 H)

<sup>13</sup>C{<sup>1</sup>H} NMR (151 MHz, C<sub>6</sub>D<sub>6</sub>, 298 K): δ 58.0, 18.1

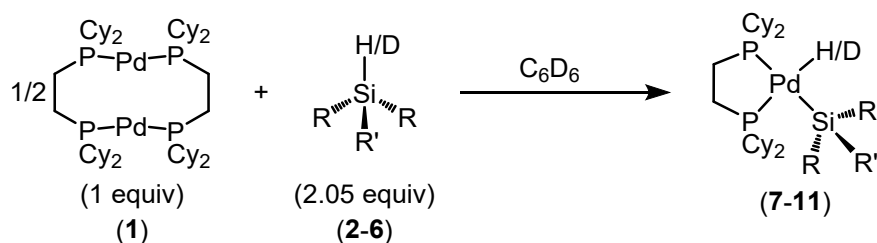
<sup>29</sup>Si{<sup>1</sup>H} NMR (119 MHz, C<sub>6</sub>D<sub>6</sub>, 298 K): δ -59.16

IR (ATR, neat) ν: 2192 cm<sup>-1</sup> (Si–D)

ASAP/HRMS (m/z): [M]<sup>+</sup> calculated for C<sub>6</sub>H<sub>16</sub>O<sub>3</sub>Si: 164.0869; found 164.0905

## 4. Characterization of Silyl Palladium Hydrides/Deuterides

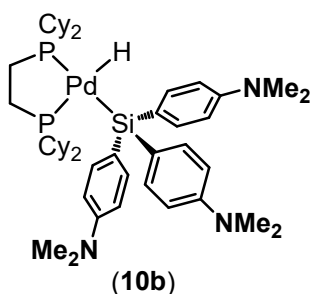
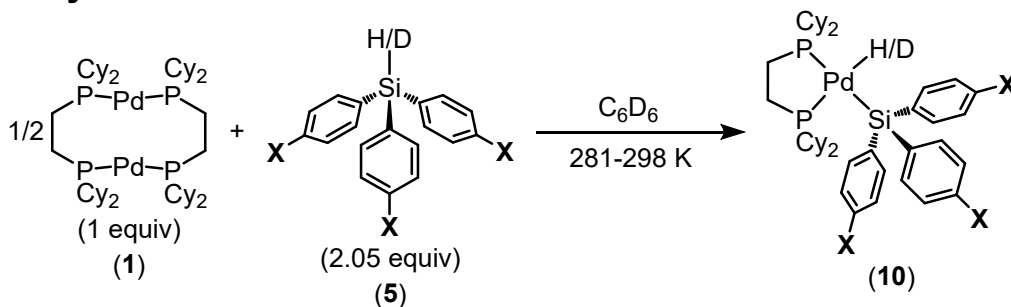
### a. General considerations



The silyl palladium hydrides were formed and characterized *in situ*.  $[(\mu\text{-dcpe})\text{Pd}]_2$  (**1**) (4.2 mg, 0.0040 mmol, 1.0 equiv) and the corresponding silane (**2-6**) (0.0082 mmol, 2.05 equiv.) were dissolved in  $\text{C}_6\text{D}_6$  in an NMR tube. Because a slight excess of silane was used, NMR spectra show unconsumed silane. When the reaction does not proceed to completion, the only species observed by NMR are **1**, silane, and (silyl)Pd(H).

In cases of low conversion (primarily for electron-rich silanes), spectra were collected at reduced temperatures to increase equilibrium concentration of the (silyl)Pd(H). IR spectra were recorded by placing an aliquot on the IR ATR stage, allowed the solvent to evaporate, and then the spectrum was recorded; these IR spectra are therefore of the product in solid form. HRMS spectra were obtained by reacting 1 equivalent of  $[(\text{dcpe})\text{Pd}]_2$  with 4 equivalents of the silane in benzene and the reaction mixture was dried, taking care to expose the reaction mixtures only minimally to air during sample preparation. For the products of volatile dimethylaryl silanes, effort was made to evaporate only the solvent of the reaction but not the silane, maintaining the condition of excess silane.  $J_{\text{H-Si}}$  values were measured from the  $^{29}\text{Si}$  satellites of the Pd-H signal in the  $^1\text{H}$  NMR spectrum and are reported in section e below for complexes **9-11**.  $^2J_{\text{H-P(trans)}}$  and  $^2J_{\text{H-P(cis)}}$  values were measured, when observable, from the  $^1\text{H}$ -coupled  $^{31}\text{P}$  NMR spectra at low temperature and are reported in section f below.

### b. Triaryl silanes



(dcpe)Pd(H)[Si(4-NMe<sub>2</sub>-Ph)<sub>3</sub>] (**10b**)

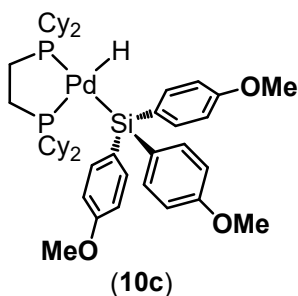
<sup>1</sup>H NMR (600 MHz, C<sub>6</sub>D<sub>6</sub>, 281 K): δ 8.15 (d, *J* = 6.9 Hz, 6H), 6.83 (d, *J* = 6.9 Hz, 6H), 2.58 (s, 18H), 2.0-1.0 (ms, overlapping with **1**), -1.23 (t, *J* = 75.0 Hz, 1H)

<sup>13</sup>C{<sup>1</sup>H} NMR (151 MHz, C<sub>6</sub>D<sub>6</sub>, 281 K): δ 150.1, 138.5, (2 peaks obscured by C<sub>6</sub>D<sub>6</sub>), 40.60, 36.0, 34.8 (d, *J* = 14.0 Hz), 30.3, 29.4, 29.2, 27.8, 27.6 (d, *J* = 8.1 Hz), 26.9, 26.6, 22.39

<sup>29</sup>Si{<sup>1</sup>H} NMR (119 MHz, C<sub>6</sub>D<sub>6</sub>, 281 K): δ 7.30 (t, *J* = 104.5 Hz) $^{31}\text{P}\{^1\text{H}\}$  NMR (243 MHz,  $\text{C}_6\text{D}_6$ , 281 K):  $\delta$  55.09

IR (ATR, neat)  $\nu$ : 1881  $\text{cm}^{-1}$  (Pd–H)

ASAP/HRMS (m/z): [M]<sup>+</sup> calculated for C<sub>50</sub>H<sub>79</sub>N<sub>3</sub>P<sub>2</sub>PdSi:  
917.4553; found 917.4476



(dcpe)Pd(H)[Si(4-OMe-Ph)<sub>3</sub>] (**10c**)

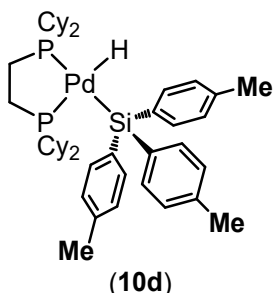
<sup>1</sup>H NMR (600 MHz, C<sub>6</sub>D<sub>6</sub>, 298 K): δ 8.05 (d, *J* = 8.5 Hz, 6H), 6.99 (d, *J* = 8.5 Hz, 6H), 3.38 (s, 9H), 1.84-1.08 (ms, 48H), -1.59 (t, *J* = 76.4 Hz, 1H)

<sup>13</sup>C{<sup>1</sup>H} NMR (151 MHz, C<sub>6</sub>D<sub>6</sub>, 298 K): δ 159.7, 140.4, 138.7, 113.2, 54.6, 34.9 (d, *J* = 14.4 Hz), 30.4 (d, *J* = 8.3 Hz), 29.3, 27.5 (d, *J* = 9.2 Hz), 27.3 (d, *J* = 13.5 Hz), 26.6, 22.4 (m)

<sup>29</sup>Si{<sup>1</sup>H} NMR (119 MHz, C<sub>6</sub>D<sub>6</sub>, 298 K) δ 6.26 (t, *J* = 78.7 Hz) $^{31}\text{P}\{^1\text{H}\}$  NMR (243 MHz,  $\text{C}_6\text{D}_6$ , 298 K):  $\delta$  56.49

IR (ATR, neat)  $\nu$ : 1873  $\text{cm}^{-1}$  (Pd–H)

ASAP/HRMS (m/z): [M]<sup>+</sup> calculated for C<sub>47</sub>H<sub>70</sub>O<sub>3</sub>P<sub>2</sub>PdSi:  
878.3604; found 878.3541



(dcpe)Pd(H)[Si(4-Me-Ph)<sub>3</sub>] (**10d**)

<sup>1</sup>H NMR (600 MHz, C<sub>6</sub>D<sub>6</sub>, 298 K): δ 8.05 (d, *J* = 7.3 Hz, 6 H), 7.17 (d, under C<sub>6</sub>D<sub>6</sub>, 6 H), 2.19 (s, 9H), 1.81-1.10 (ms, 48H), -1.61 (t, *J* = 76.8 Hz, 1H)

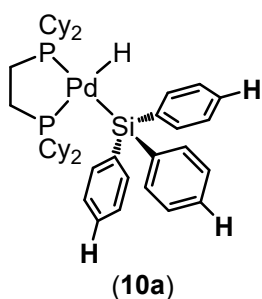
<sup>13</sup>C{<sup>1</sup>H} NMR (151 MHz, C<sub>6</sub>D<sub>6</sub>, 298 K): δ 145.6 (t, *J* = 5.1 Hz), 137.7, 136.1, (one aryl peak overlapping with benzene), 34.9 (d, *J* = 13.6 Hz), 30.4 (d, *J* = 7.9 Hz), 29.3, 27.5 (d, *J* = 8.8 Hz), 27.2 (d, *J* = 13.5 Hz), 26.57, 22.3 (m)

<sup>29</sup>Si{<sup>1</sup>H} NMR (119 MHz, C<sub>6</sub>D<sub>6</sub>, 298 K): δ 7.18 (t, *J* = 78.1 Hz)

<sup>31</sup>P{<sup>1</sup>H} NMR (243 MHz, C<sub>6</sub>D<sub>6</sub>, 298 K): δ 56.58

IR (ATR, neat) ν: 1868 cm<sup>-1</sup> (Pd–H)

ASAP/HRMS (m/z): [M]<sup>+</sup> calculated for C<sub>47</sub>H<sub>70</sub>P<sub>2</sub>PdSi: 830.3757; found 830.3744



(dcpe)Pd(H)(SiPh<sub>3</sub>) (**10a**)

<sup>1</sup>H NMR (600 MHz, C<sub>6</sub>D<sub>6</sub>, 298 K): δ 8.10 (d, *J* = 7.2 Hz, 6H), 7.30 (t, *J* = 7.2 Hz, 6H), 7.20 (t, *J* = 7.2 Hz, 3H), 1.77-1.09 (ms, 48H), -1.74 (t, *J* = 77.5 Hz, 1H)

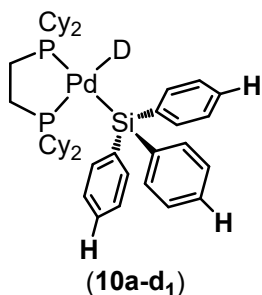
<sup>13</sup>C{<sup>1</sup>H} NMR (151 MHz, C<sub>6</sub>D<sub>6</sub>, 298 K): δ 148.8 (t, *J* = 5.1 Hz), 137.6, 127.3, 127.1, 34.8 (d, *J* = 13.1 Hz), 30.3 (d, *J* = 7.9 Hz), 29.3, 27.5 (d, *J* = 8.8 Hz), 27.2 (d, *J* = 13.3 Hz), 26.5, 22.3 (m)

<sup>29</sup>Si{<sup>1</sup>H} NMR (119 MHz, C<sub>6</sub>D<sub>6</sub>, 298 K): δ 8.24 (t, *J* = 79.1 Hz)

<sup>31</sup>P{<sup>1</sup>H} NMR (243 MHz, C<sub>6</sub>D<sub>6</sub>, 298 K): δ 57.16

IR (ATR, neat) ν: 1868 cm<sup>-1</sup> (Pd–H)

ASAP/HRMS (m/z): [M]<sup>+</sup> calculated for C<sub>44</sub>H<sub>64</sub>P<sub>2</sub>PdSi: 788.3287; found 788.3333



(dcpe)Pd(D)(SiPh<sub>3</sub>) (**10a-d<sub>1</sub>**)

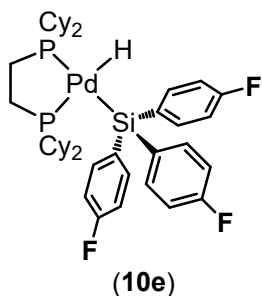
<sup>1</sup>H NMR (600 MHz, C<sub>7</sub>D<sub>8</sub>, 281 K): δ 8.03 (d, *J* = 7.2 Hz, 6H), 7.29 (t, *J* = 7.2 Hz, 6H), 7.19 (t, *J* = 7.2 Hz, 3H), 1.76-1.11 (ms, 48H)

<sup>13</sup>C{<sup>1</sup>H} NMR (151 MHz, C<sub>7</sub>D<sub>8</sub>, 281 K): δ 148.8 (t, *J* = 5.1 Hz), 127.2, 127.0, (one aryl peak overlapping with toluene), 34.7 (d, *J* = 13.1 Hz), 30.2 (d, *J* = 7.9 Hz), 29.2, 27.5 (d, *J* = 8.8 Hz), 27.2 (d, *J* = 13.3 Hz), 26.5, 22.4 (m)

<sup>29</sup>Si{<sup>1</sup>H} NMR (119 MHz, C<sub>7</sub>D<sub>8</sub>, 281 K): δ 8.30

<sup>31</sup>P{<sup>1</sup>H} NMR (243 MHz, C<sub>6</sub>D<sub>6</sub>, 298 K): δ 57.07 (m)

ASAP/HRMS (m/z): [M]<sup>+</sup> calculated for C<sub>44</sub>H<sub>63</sub>DP<sub>2</sub>PdSi: 789.3350; found 789.3221



(dcpe)Pd(H)[Si(4-F-Ph)<sub>3</sub>] (**10e**)

<sup>1</sup>H NMR (600 MHz, C<sub>6</sub>D<sub>6</sub>, 298 K): δ 7.85 (dd, *J* = 6.6, 8.5 Hz, 6H), 7.01 (app t, *J* = 8.5 Hz, 6H), 1.90-1.02 (ms, 48H), -2.03 (t, *J* = 78.3 Hz, 1H)

<sup>13</sup>C{<sup>1</sup>H} NMR (151 MHz, C<sub>6</sub>D<sub>6</sub>, 298 K): δ 163.4 (d, *J* = 245.5 Hz), 144.0 (d, *J* = 4.4 Hz), 139.0 (d, *J* = 6.7 Hz), 114.3 (d, *J* = 18.8 Hz), 34.8 (d, *J* = 13.4 Hz), 30.3 (d, *J* = 7.6 Hz), 29.3, 27.4 (d, *J* = 8.9 Hz), 27.1 (d, *J* = 13.1 Hz), 26.5, 22.3 (m)

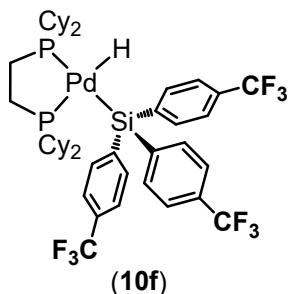
<sup>19</sup>F NMR (471 MHz, C<sub>6</sub>D<sub>6</sub>, 298 K): δ -115.41 (m)

<sup>29</sup>Si{<sup>1</sup>H} NMR (119 MHz, C<sub>6</sub>D<sub>6</sub>, 298 K): δ 7.44 (t, *J* = 81.7 Hz)

<sup>31</sup>P{<sup>1</sup>H} NMR (243 MHz, C<sub>6</sub>D<sub>6</sub>, 298 K): δ 58.08

IR (ATR, neat) ν: 1876 cm<sup>-1</sup> (Pd-H)

ASAP/HRMS (m/z): [M]<sup>+</sup> calculated for C<sub>44</sub>H<sub>61</sub>F<sub>3</sub>P<sub>2</sub>PdSi: 842.3005; found 842.3083



(dcpe)Pd(H)[Si(4-CF<sub>3</sub>-Ph)<sub>3</sub>] (**10f**)

<sup>1</sup>H NMR (600 MHz, C<sub>6</sub>D<sub>6</sub>, 298 K): δ 7.89 (d, *J* = 7.7 Hz, 6H), 7.54 (d, *J* = 7.7 Hz, 6H), 1.60-0.97 (m, 48H), -2.34 (t, *J* = 80.0 Hz, 1H)

<sup>13</sup>C{<sup>1</sup>H} NMR (151 MHz, C<sub>6</sub>D<sub>6</sub>, 298 K): δ 152.7 (t, *J* = 5.3 Hz), 137.4, 129.7 (q, *J* = 31.8 Hz), 125.5 (q, *J* = 272.2 Hz), 124.1 (d, *J* = 3.79 Hz), 34.9 (d, *J* = 14.8 Hz), 30.3 (d, *J* = 7.2 Hz), 29.3, 27.3 (d, *J* = 9.0 Hz), 27.1 (d, *J* = 13.1 Hz), 26.4, 22.4 (m)

<sup>19</sup>F NMR (565 MHz, C<sub>6</sub>D<sub>6</sub>, 298 K): δ -62.13

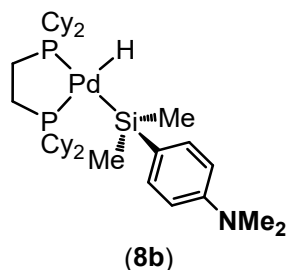
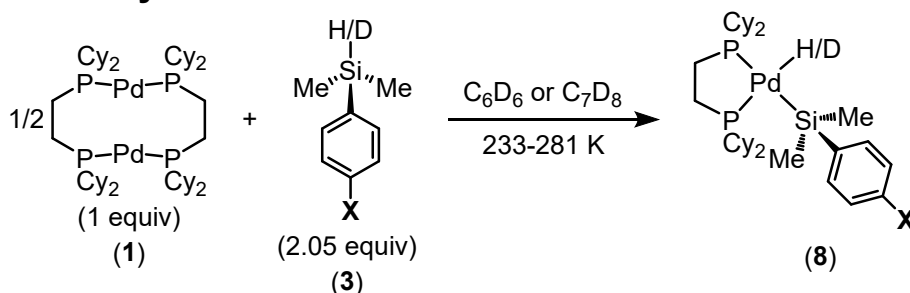
<sup>29</sup>Si{<sup>1</sup>H} NMR (119 MHz, C<sub>6</sub>D<sub>6</sub>, 298 K): δ 8.99 (t, *J* = 81.2 Hz)

<sup>31</sup>P{<sup>1</sup>H} NMR (243 MHz, C<sub>6</sub>D<sub>6</sub>, 298 K): δ 59.62 (br)

IR (ATR, neat) ν: 1875 cm<sup>-1</sup> (Pd-H)

ASAP/HRMS (m/z): [M]<sup>+</sup> calculated for C<sub>47</sub>H<sub>61</sub>F<sub>9</sub>P<sub>2</sub>PdSi: 992.2909; found 992.2858

### c. Aryl dimethyl silanes



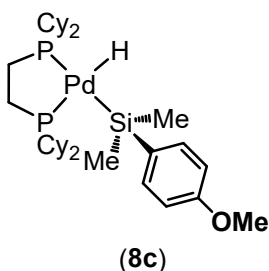
(dcpe)Pd(H)[Si(4-NMe<sub>2</sub>-Ph)Me<sub>2</sub>] (**8b**)

Note: because the conversion is low, many of the peaks are indistinguishable from starting materials. Reported in the <sup>1</sup>H NMR are the distinguishable peaks.

<sup>1</sup>H NMR (600 MHz, C<sub>6</sub>D<sub>6</sub>): δ 8.00 (d, *J* = 8.0 Hz, 2H), 6.80 (d, *J* = 8.0 Hz, 2H), -1.39 (t, *J* = 74.9 Hz, 1H)

<sup>31</sup>P{<sup>1</sup>H} NMR (243 MHz, C<sub>6</sub>D<sub>6</sub>): δ 56.44

ASAP/HRMS (*m/z*): [M]<sup>+</sup> calculated for C<sub>36</sub>H<sub>65</sub>NP<sub>2</sub>PdSi: 707.3396; found 707.3314



(dcpe)Pd(H)[Si(4-OMe-Ph)Me<sub>2</sub>] (**8c**)

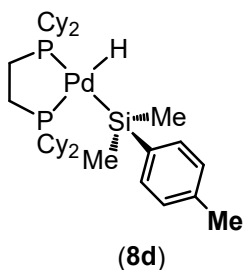
<sup>1</sup>H NMR (500 MHz, C<sub>6</sub>D<sub>6</sub>, 281 K): δ 8.02 (d, *J* = 7.7 Hz, 2H), 7.04 (d, *J* = 7.7 Hz, 2H), 3.40 (s, 3H), 2.30–1.07 (ms, overlapping with **1**), -1.55 (t, *J* = 74.8 Hz, 1H)

<sup>13</sup>C{<sup>1</sup>H} NMR (151 MHz, C<sub>7</sub>D<sub>8</sub>, 233 K): δ 136.1, 112.8, (two aryl peaks overlapping with toluene), 54.1, 34.8 (d, *J* = 11.0 Hz), 29.8 (br), 28.7, 27.2 (d, *J* = 8.1 Hz), 27.1 (d, *J* = 13.1 Hz), 26.3, 10.3

<sup>31</sup>P{<sup>1</sup>H} NMR (202 MHz, C<sub>6</sub>D<sub>6</sub>, 281 K): δ 56.05

IR (ATR, neat) ν: 1862 cm<sup>-1</sup> (Pd–H)

ASAP/HRMS (*m/z*): [M]<sup>+</sup> calculated for C<sub>35</sub>H<sub>62</sub>OP<sub>2</sub>PdSi: 694.3080; found 694.2939



(dcpe)Pd(H)[Si(4-Me-Ph)Me<sub>2</sub>] (**8d**)

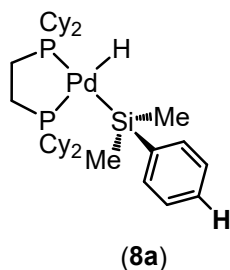
<sup>1</sup>H NMR (500 MHz, C<sub>6</sub>D<sub>6</sub>, 281 K): δ 8.02 (d, *J* = 7.3 Hz, 2H), 7.23 (d, *J* = 7.3 Hz, 2H), 2.25 (s, 3H), 1.93–1.12 (ms, overlapping with **1**), -1.57 (t, *J* = 74.9 Hz, 1H)

<sup>13</sup>C{<sup>1</sup>H} NMR (151 MHz, C<sub>7</sub>D<sub>8</sub>, 233 K): δ 135.0 (three aryl peaks overlapping with toluene), 34.9 (br), 29.8 (d, *J* = 8.02 Hz), 28.7, 27.17 (br), 26.3, (one tolyl peak overlapping with toluene), 9.9 (t, *J* = 7 Hz).

<sup>31</sup>P{<sup>1</sup>H} NMR (202 MHz, C<sub>6</sub>D<sub>6</sub>, 281 K): δ 56.06

IR (ATR, neat) ν: 1860 cm<sup>-1</sup> (Pd–H)

ASAP/HRMS (*m/z*): [M]<sup>+</sup> calculated for C<sub>35</sub>H<sub>62</sub>P<sub>2</sub>PdSi: 678.3131; found 678.3248



(dcpe)Pd(H)(SiPhMe<sub>2</sub>) (**8a**)

<sup>1</sup>H NMR (500 MHz, C<sub>6</sub>D<sub>6</sub>, 281 K): δ 8.08 (d, *J* = 6.0 Hz, 2H), 7.38 (t, *J* = 6.0 Hz, 2H), 1.91-1.04 (ms, overlapping with **1**), -1.63 (t, *J* = 75.2 Hz, 1H)

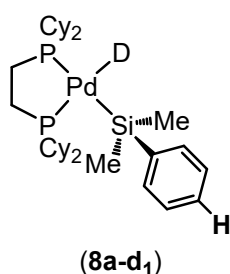
<sup>13</sup>C{<sup>1</sup>H} NMR (151 MHz, C<sub>7</sub>D<sub>8</sub>, 233 K): δ 137.5, 134.8, 127.2, 126.4, 34.9 (d, *J* = 13.2 Hz), 29.8 (d, *J* = 8.0 Hz), 28.7, 27.1, 27.0, 26.7, 26.3, 9.7 (t, *J* = 6.1 Hz)

<sup>29</sup>Si{<sup>1</sup>H} NMR (119 MHz, C<sub>7</sub>D<sub>8</sub>, 233 K): δ -2.10 (t, *J* = 76.8 Hz)

<sup>31</sup>P{<sup>1</sup>H} NMR (202 MHz, C<sub>6</sub>D<sub>6</sub>, 281 K): δ 56.27

IR (ATR, neat) ν: 1862 cm<sup>-1</sup> (Pd–H)

ASAP/HRMS (m/z): [M]<sup>+</sup> calculated for C<sub>34</sub>H<sub>60</sub>P<sub>2</sub>PdSi: 664.2974; found 664.3025



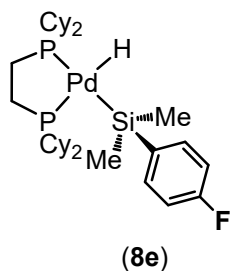
(dcpe)Pd(D)(SiPhMe<sub>2</sub>) (**8a-d<sub>1</sub>**)

<sup>1</sup>H NMR (600 MHz, C<sub>7</sub>D<sub>8</sub>, 253 K): δ 8.04 (d, *J* = 7.7 Hz, 2H), 7.38 (t, 7.7 Hz, 3H), 1.82-1.08 (ms, overlapping with **1**)

<sup>13</sup>C{<sup>1</sup>H} NMR (151 MHz, C<sub>7</sub>D<sub>8</sub>, 253 K): δ 153.0, 134.8, 127.2, 126.4, 35.0 (d, *J* = 13.4 Hz), 30.0 (d, *J* = 8.1 Hz), 28.9, 27.3, 27.2, 27.1, 26.4, 9.6 (t, 6.3 Hz)

<sup>31</sup>P{<sup>1</sup>H} NMR (243 MHz, C<sub>7</sub>D<sub>8</sub>, 253 K): δ 56.69

ASAP/HRMS (m/z): [M]<sup>+</sup> calculated for C<sub>34</sub>H<sub>59</sub>DP<sub>2</sub>PdSi: 665.3037; found 665.3053



(dcpe)Pd(H)[Si(4-F-Ph)Me<sub>2</sub>] (**8e**)

<sup>1</sup>H NMR (500 MHz, C<sub>6</sub>D<sub>6</sub>, 281 K): δ 7.92 (t, *J* = 7.0 Hz, 2H), 7.07 (t, *J* = 8.6 Hz, 2H), 1.86-1.05 (ms, overlapping with **1**), -1.72 (t, *J* = 75.6 Hz, 1H)

<sup>13</sup>C{<sup>1</sup>H} NMR (151 MHz, C<sub>7</sub>D<sub>8</sub>, 233 K): δ 162.8 (d, *J* = 242.5 Hz) 136.5 (d, *J* = 6.2 Hz), (one aryl peak overlapping with toluene and/or unresolved from baseline), 114.0 (d, *J* = 18.4 Hz), 34.9 (d, *J* = 12.7 Hz), 29.8 (d, *J* = 7.6 Hz), 28.7, 27.2, 27.1, 27.0, 26.3, 9.91 (t, *J* = 5.8 Hz)

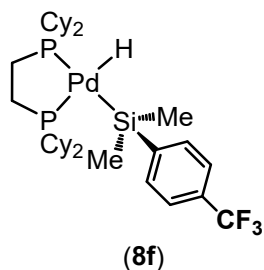
<sup>19</sup>F NMR (471 MHz, C<sub>6</sub>D<sub>6</sub>, 281 K): δ -116.8 (m)

<sup>29</sup>Si{<sup>1</sup>H} NMR (119 MHz, C<sub>7</sub>D<sub>8</sub>, 233 K): δ -1.63 (t, *J* = 79.4 Hz)

<sup>31</sup>P{<sup>1</sup>H} NMR (202 MHz, C<sub>6</sub>D<sub>6</sub>, 281 K): δ 56.66

IR (ATR, neat) ν: 1864 cm<sup>-1</sup> (Pd–H)

ASAP/HRMS (m/z): [M]<sup>+</sup> calculated for C<sub>34</sub>H<sub>59</sub>FP<sub>2</sub>PdSi: 682.2880; found 682.2971



(dcpe)Pd(H)[Si(4-CF<sub>3</sub>-Ph)Me<sub>2</sub>] (**8f**)

<sup>1</sup>H NMR (500 MHz, C<sub>6</sub>D<sub>6</sub>, 281 K): δ 7.96 (d, *J* = 6.4 Hz, 2H), 7.58 (d, *J* = 6.4 Hz, 2H), 1.91-1.03 (ms, overlapping with **1**), -1.89 (t, *J* = 76.4 Hz, 1H)

<sup>13</sup>C{<sup>1</sup>H} NMR (151 MHz, C<sub>7</sub>D<sub>8</sub>, 253 K): δ 134.8, 123.4 (q, *J* = 4.2 Hz), (three aryl peaks overlapping with toluene and/or unresolved from baseline), 35.0 (d, *J* = 4.3 Hz), 29.9 (d, *J* = 7.7 Hz), 28.9, 27.2, 27.1, 27.1, 26.3, 9.0 (d, *J* = 6.5 Hz)

<sup>19</sup>F NMR (471 MHz, C<sub>6</sub>D<sub>6</sub>, 281 K): δ -61.68

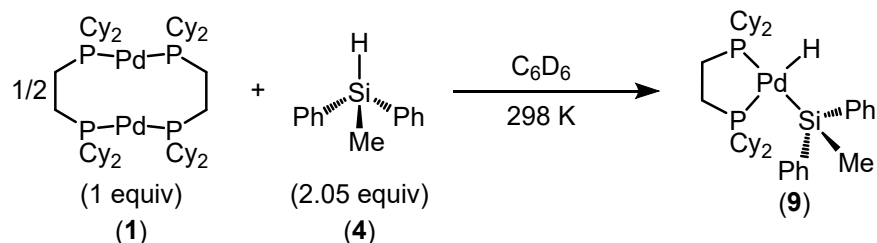
<sup>29</sup>Si{<sup>1</sup>H} NMR (119 MHz, C<sub>7</sub>D<sub>8</sub>, 253 K): δ -1.88 (t, *J* = 78.9 Hz)

<sup>31</sup>P{<sup>1</sup>H} NMR (202 MHz, C<sub>6</sub>D<sub>6</sub>, 281 K): δ 57.15

IR (ATR, neat) ν: 1866 cm<sup>-1</sup> (Pd-H)

ASAP/HRMS (m/z): [M]<sup>+</sup> calculated for C<sub>35</sub>H<sub>59</sub>F<sub>3</sub>P<sub>2</sub>PdSi: 732.2848; found 732.2851

#### d. Other silanes



<sup>1</sup>H NMR (600 MHz, C<sub>6</sub>D<sub>6</sub>, 298 K): δ 8.07 (d, *J* = 7.4 Hz, 4H), 7.32 (t, *J* = 7.3 Hz, 4H), 7.19 (t, *J* = 7.3 Hz, 2H), 1.85 (br d, *J* = 10.9, 4H), 1.62-1.66 (ms, 12H), 1.54 (br d, *J* = 8.9, 8H), 1.36 (m, 4H), 1.25 (s, 3 H), 1.25-1.05 (ms, 20H), -1.69 (t, *J* = 76.5 Hz, 1H)

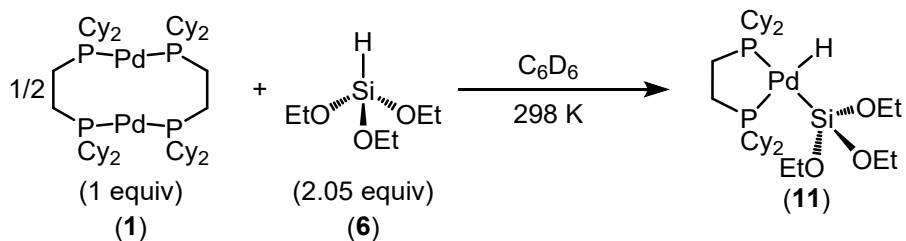
<sup>13</sup>C{<sup>1</sup>H} NMR (151 MHz, C<sub>6</sub>D<sub>6</sub>, 298 K): δ 151.3 (t, *J* = 5.3 Hz), 136.2, 127.4, 126.8, 35.1 (d, *J* = 13.0 Hz), 30.3 (d, *J* = 8.0 Hz), 29.3, 27.4 (d, *J* = 8.8 Hz), 27.3 (d, *J* = 13.6 Hz), 26.5, 22.6 (dd, *J* = 14.5, 20.7 Hz), 7.6 (t, *J* = 6.6 Hz)

<sup>29</sup>Si{<sup>1</sup>H} NMR (119 MHz, C<sub>6</sub>D<sub>6</sub>, 298 K): δ 2.02 (t, *J* = 77.9 Hz)

<sup>31</sup>P{<sup>1</sup>H} NMR (243 MHz, C<sub>6</sub>D<sub>6</sub>, 298 K): δ 56.86

IR (ATR, neat) ν: 1866 cm<sup>-1</sup> (Pd-H)

ASAP/HRMS (m/z): [M]<sup>+</sup> calculated for C<sub>39</sub>H<sub>62</sub>P<sub>2</sub>PdSi: 726.3131; found 726.3151



<sup>1</sup>H NMR (600 MHz, C<sub>6</sub>D<sub>6</sub>, 298 K): δ 4.33 (q, *J* = 7.0 Hz, 6 H), 2.27-1.09 (ms, overlapping with **1**), -1.98 (d, *J* = 154 Hz, 1H)

<sup>13</sup>C{<sup>1</sup>H} NMR (151 MHz, C<sub>6</sub>D<sub>6</sub>, 298 K): δ 57.3, 35.0 (br), 30.2 (d, *J* = 43.2 Hz), 29.3, 27.6 (br), 26.6 (d, *J* = 28.0 Hz)

<sup>29</sup>Si{<sup>1</sup>H} NMR (119 MHz, C<sub>6</sub>D<sub>6</sub>, 298 K): δ -4.6 (d, *J* = 235.5 Hz)

<sup>31</sup>P{<sup>1</sup>H} NMR (243 MHz, C<sub>6</sub>D<sub>6</sub>, 298 K): δ 60.42 (s, 1P), 57.10 (s, 1P)

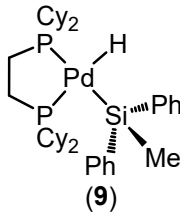
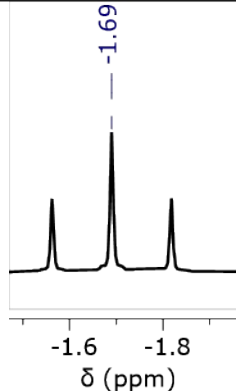
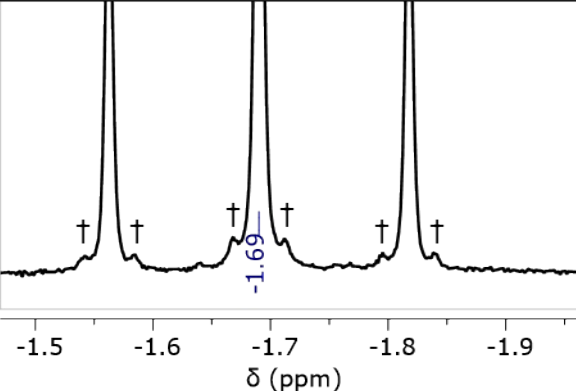
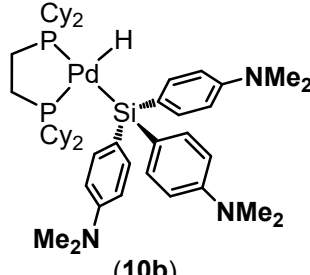
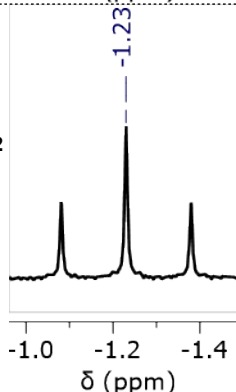
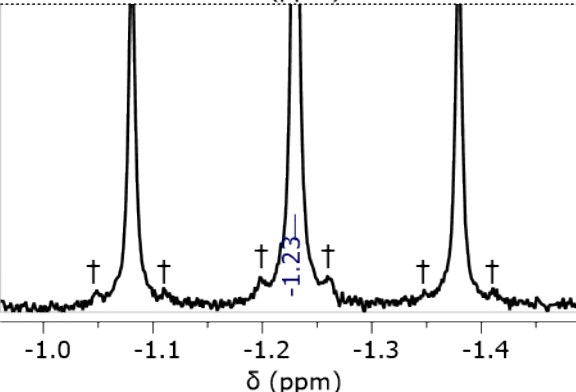
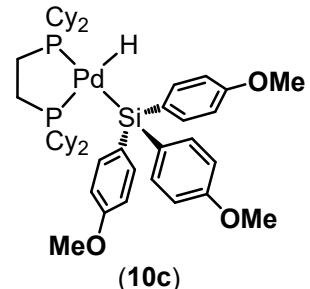
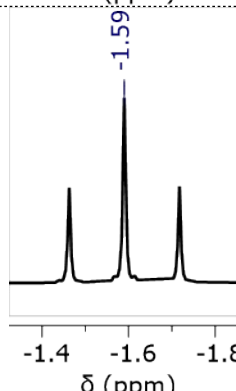
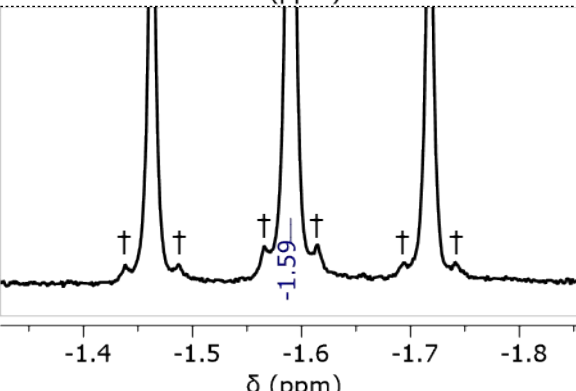
IR (ATR, neat) ν: 1838 cm<sup>-1</sup> (Pd-H)

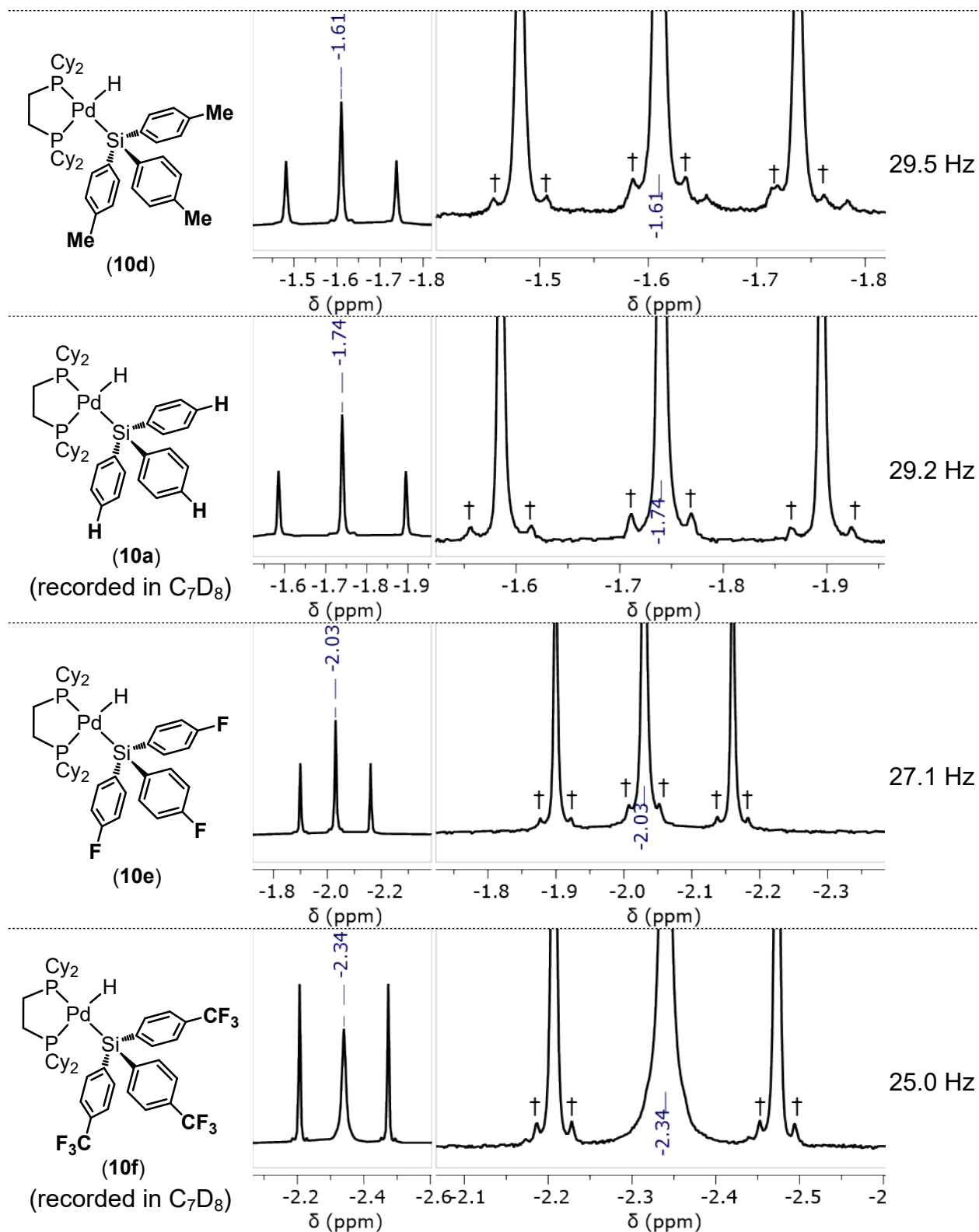
ASAP/HRMS (*m/z*): [M]<sup>+</sup> calculated for C<sub>32</sub>H<sub>64</sub>O<sub>3</sub>P<sub>2</sub>PdSi: 692.3135; found 692.3105

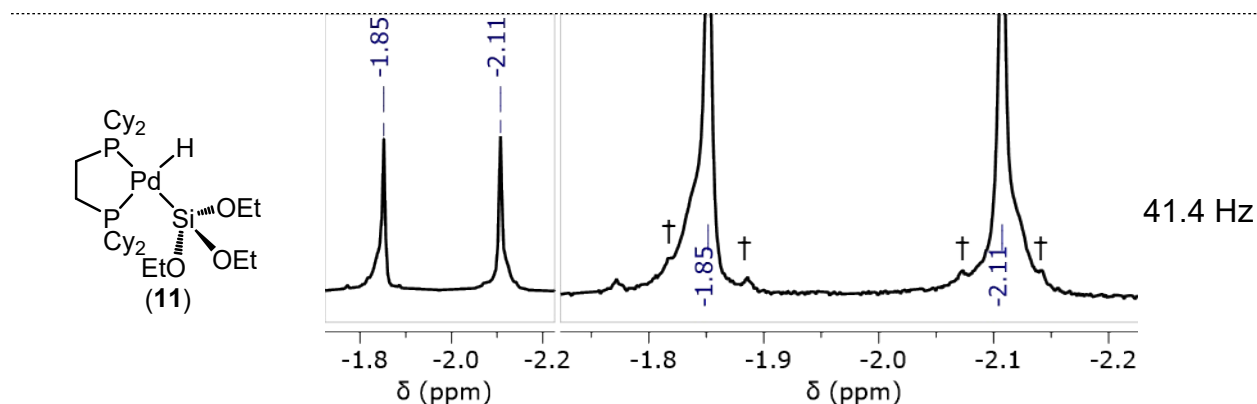
### e. Measurements of $^2J_{\text{H-Si}}$

$J_{\text{H-Si}}$  values were measured using the  $^{29}\text{Si}$  satellites, when visible, in the hydride signal in the  $^1\text{H}$  NMR spectrum (measured in  $\text{C}_6\text{D}_6$  at 298 K, unless otherwise indicated). Below is a table of the  $J_{\text{H-Si}}$  values and an image of the hydride signals showing the  $^{29}\text{Si}$  satellites (labelled with †) for complexes **9-11**. No satellites were visible for complexes **7** or **8**.

**Table S1.**  $^1\text{H}$  NMR spectra, hydride region of complexes **9-11** and  $J_{\text{H-Si}}$  values.

Complex	Zoom-in of hydride region of $^1\text{H}$ NMR spectra. Left, vertical-scaled to show full hydride peak. Right, vertical zoom-in to show satellites.		$J_{\text{H-Si}}$
 (9)			26.0 Hz
 (10b)			31.5 Hz
 (10c)			29.3 Hz

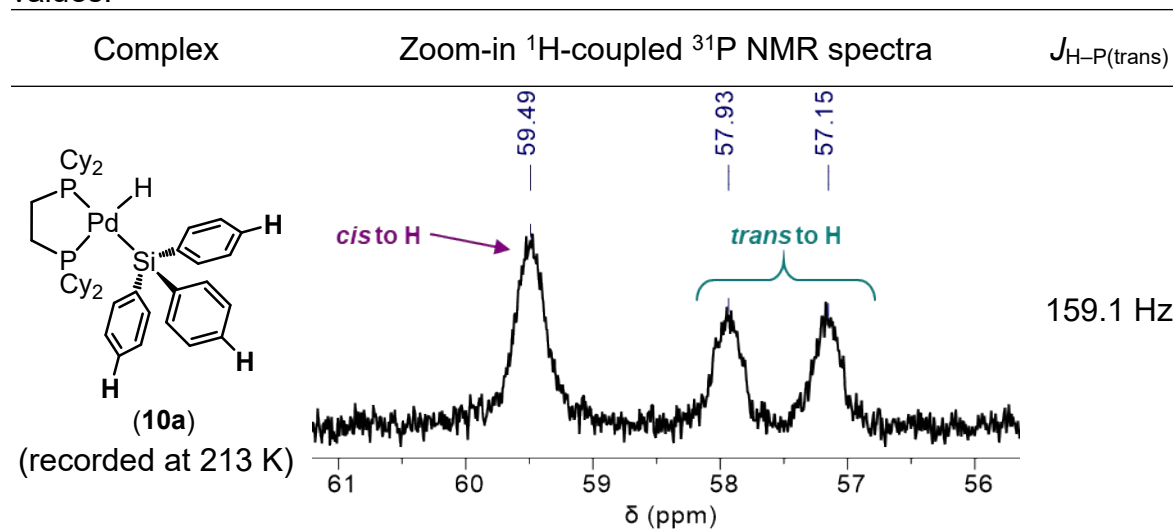


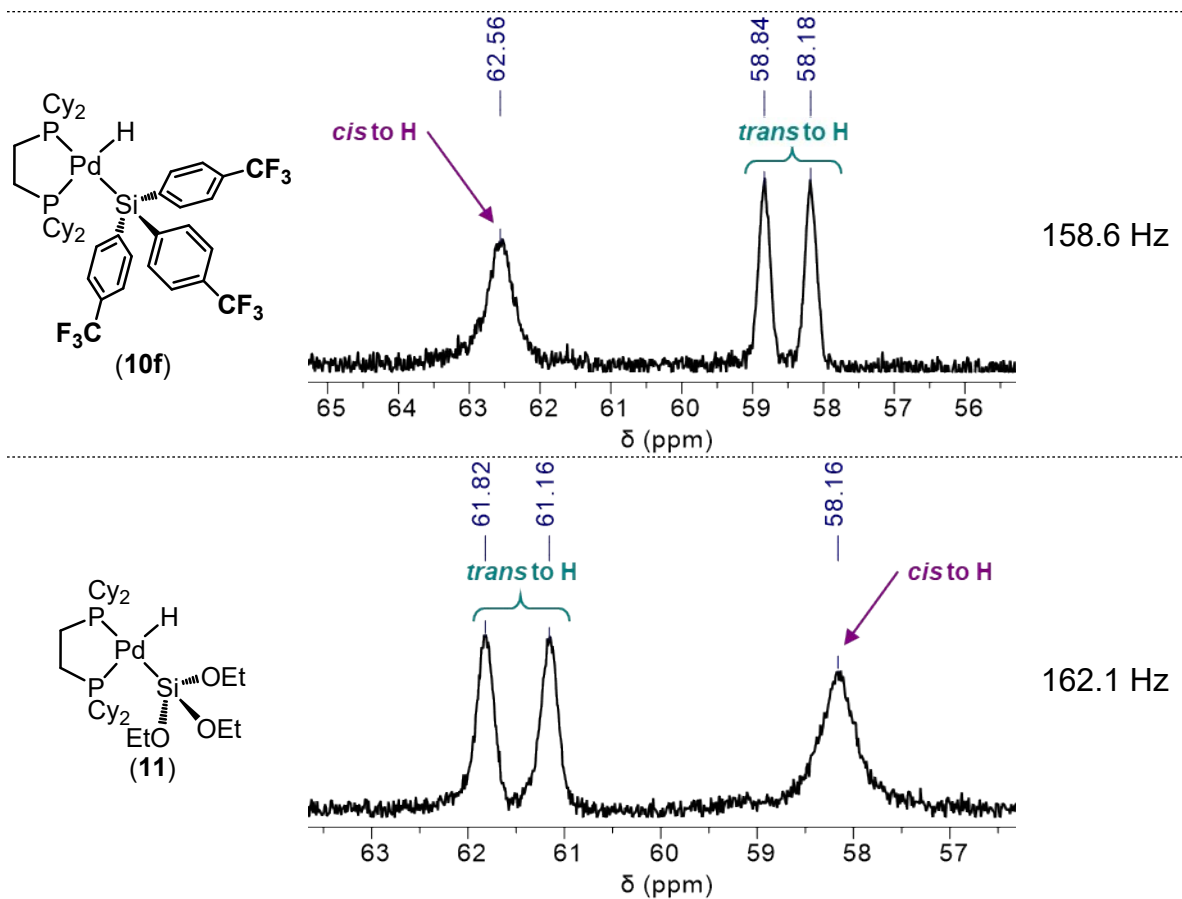


#### f. Measurements of $^2J_{\text{H-P(trans)}}$

$^2J_{\text{H-P(trans)}}$  values were measured from the  $^1\text{H}$ -coupled  $^{31}\text{P}$  NMR spectra, (measured in  $\text{C}_7\text{D}_8$  at 233 K, unless otherwise indicated). Below is a table of the coupling constants and an image of the phosphorus signals showing the coupling for complexes **10a**, **10e**, and **11**.

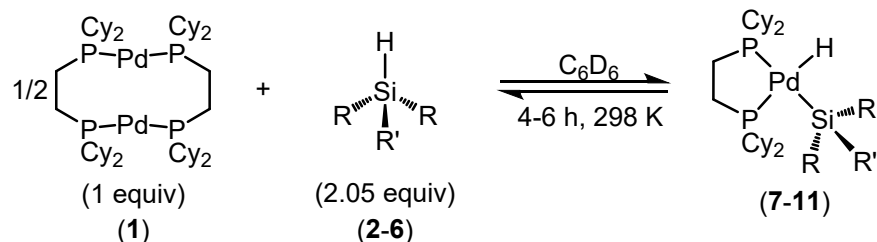
**Table S2.**  $^1\text{H}$ -coupled  $^{31}\text{P}$  NMR spectra of complexes **10a**, **10e**, and **11** and  $J_{\text{H-P(trans)}}$  values.





## 5. Equilibrium Studies – Conversion and $K_{eq}$ at 298 K

### a. General procedure A



In a nitrogen-filled glovebox, stock solutions of **1** (13.3 mM) and silane (**2-6**) (54.7 mM) were prepared by weighing out the reagents and diluting with  $\text{C}_6\text{D}_6$ . **1** (0.30 mL of stock solution, 0.0040 mmol, 1.0 equiv), the appropriate silane (0.15 mL of stock solution, 0.0082 mmol, 2.05 equiv), and additional  $\text{C}_6\text{D}_6$  (0.15 mL) were added to an NMR tube using disposable 1-mL syringes. Then, the NMR tube was capped and the reaction was allowed to react for 4-6 hours in the glovebox, after which it was further sealed with Teflon tape to prevent exposure to air and moisture and removed from the glovebox for analysis by NMR. The integrations of each  $^3\text{1P}\{^1\text{H}\}$  NMR peak corresponding to the product (**7-11**) and **1** were used to determine percent conversion in each reaction. All averages have standard deviations <1%.

### b. Determination of $K_{eq}$

Equilibrium constants were determined from the conversion values. An example calculation is given below, using **1**, **3a**, and **5a** as representative reactants and product. (abbreviations: *i*=initial, *f*=final at equilibrium)

$$[\mathbf{1}]_i = 0.0067 \text{ M}$$

$$[\mathbf{3a}]_i = 0.0137 \text{ M}$$

At equilibrium, conversion to **5a** is 42%. Therefore,

$$[\mathbf{1}]_f = [\mathbf{1}]_i * (100\% - \%conversion) = 0.0067 \text{ M} * (100\% - 42\%) = 0.0039 \text{ M}$$

$$[\mathbf{8a}]_f = (2 * [\mathbf{1}]_i) * \%conversion = (2 * 0.0067 \text{ M}) * 42\% = 0.0056 \text{ M}$$

$$[\mathbf{3a}]_f = [\mathbf{3a}]_i - [\mathbf{8a}]_f = 0.0137 \text{ M} - 0.0056 \text{ M} = 0.0081 \text{ M}$$

$$K_{eq} = \frac{[\mathbf{8a}]^2}{[\mathbf{1}][\mathbf{3a}]^2} = \frac{[0.0056 \text{ M}]^2}{[0.0039 \text{ M}][0.0081 \text{ M}]^2} = 124 \text{ M}^{-1}$$

It is important to note here that these reactions were run under **nonstandard conditions**. Standard conditions for reactions in solution are 25 °C, 1 atm, and 1 M. Because of this deviation from standard conditions, certain correlations (e.g., a  $K_{eq}$  value equal to 1 corresponding to  $\Delta G^\circ = 0$  kcal/mol) do not apply. This is exemplified in the example above, where at a conversion close to 50%,  $K_{eq}$  is far from 1. Under our conditions, conversion of exactly 50% would lead to  $K_{eq} = 272$ , so this value should be used as a measure of whether the reaction favors the products or the reactants.

To construct the Hammett plot for the aryl dimethyl silanes (**3**), values for  $\sigma_p$  were taken from reference 8. The values of  $\log(K_X/K_H)$  for X = NMe<sub>2</sub>, OMe, Me, F, and CF<sub>3</sub> were plotted as a function of  $\sigma_p$ . Using Microsoft Excel, the data were fit to a curve for the

function  $y = mx + b$ , where  $y = \log(K_X/K_H)$  input,  $m =$  sensitivity constant  $\rho$  output,  $x = \sigma_p$  input, and  $b =$  intercept output.

### c. Equilibrium conversion and Hammett plot data

#### i. Triaryl silanes

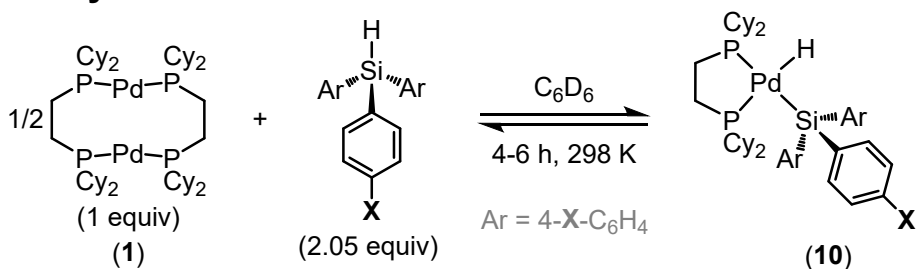


**Table S3.** Conversions and  $K_{\text{eq}}$  values for oxidative addition of triaryl silanes.

X-group	Silane ( <b>5</b> )	Product ( <b>10</b> )	Trial	Conversion	Average conversion	$K_{\text{eq}}$
-NMe <sub>2</sub>	<b>5b</b>	<b>10b</b>	1	39%	40%	100
			2	43%		
			3	38%		
-OMe	<b>5c</b>	<b>10c</b>	1	97%	97%	1.1 x 10 <sup>6</sup>
			2	96%		
-Me	<b>5d</b>	<b>10d</b>	1	98%	99%	2.2 x 10 <sup>7</sup>
			2	100%		
			3	100%		
-H	<b>5a</b>	<b>10a</b>	1	100%	100%	--
			2	100%		
			3	100%		
-F	<b>5e</b>	<b>10e</b>	1	100%	100%	--
			2	100%		
-CF <sub>3</sub>	<b>5f</b>	<b>10f</b>	1	100%	100%	--
			2	100%		

## ii. Aryl dimethyl silanes

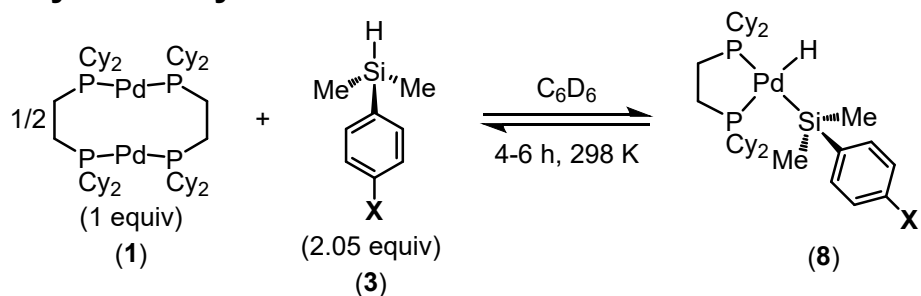


**Table S4.** Conversions and  $K_{\text{eq}}$  values for oxidative addition of dimethyl aryl silanes.

X-group	Silane (3)	Product (8)	Trial	Conversion	Average conversion	$K_{\text{eq}}$
-NMe <sub>2</sub>	<b>3b</b>	<b>8b</b>	1	12%	10%	1.9
			2	9%		
			3	9%		
-OMe	<b>3c</b>	<b>8c</b>	1	25%	30%	35
			2	31%		
			3	33%		
-Me	<b>3d</b>	<b>8d</b>	1	34%	33%	50
			2	30%		
			3	35%		
-H	<b>3a</b>	<b>8a</b>	1	44%	42%	124
			2	40%		
-F	<b>3e</b>	<b>8e</b>	1	56%	54%	400
			2	54%		
			3	52%		
-CF <sub>3</sub>	<b>3f</b>	<b>8f</b>	1	95%	93%	1.7 x 10 <sup>5</sup>
			2	90%		

**Table S5.** Data derived from values in Table S4 for construction of Hammett Plot.

X-group	$\sigma_p$ for X-group	$\log(K_X/K_H)$	Error in $\log(K_X/K_H)$
-NMe <sub>2</sub>	-0.83	-1.8	0.2
-OMe	-0.27	-0.6	0.2
-Me	-0.17	-0.4	0.1
-H	0	0	-
-F	0.06	0.51	0.07
-CF <sub>3</sub>	0.54	3.14	0.08

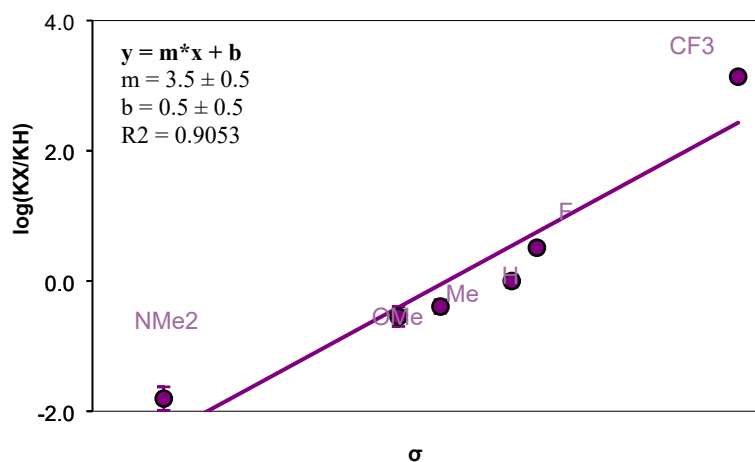


**Figure S1.** Hammett plot of equilibrium constants for conversion to **8**.

### iii. Additional silanes

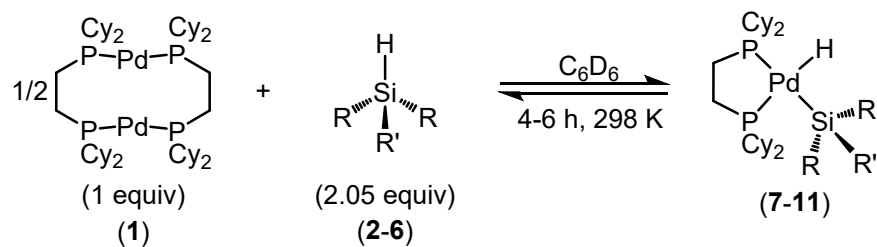
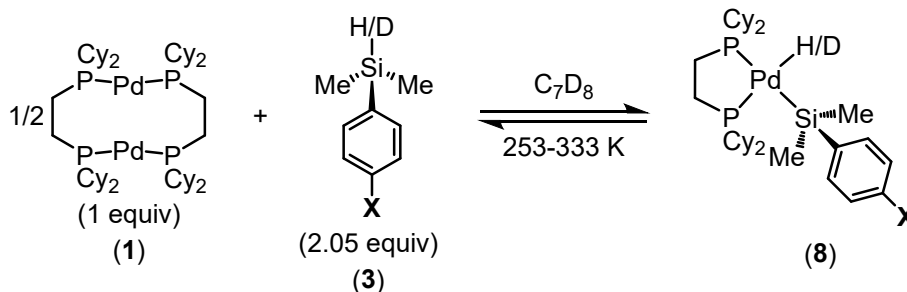


**Table S6.** Conversions and  $K_{\text{eq}}$  values for oxidative addition of other silanes.

R-group	R'-group	Silane	Product	Trial	Conversion	Average conversion	$K_{\text{eq}}$
Et	Et	<b>2</b>	<b>7</b>	1	0%	0%	0
				2	0%		
Ph	Me	<b>4</b>	<b>9</b>	1	97%	97%	$1.1 \times 10^6$
				2	96%		
OEt	OEt	<b>6</b>	<b>11</b>	1	82%	91%	$1.2 \times 10^5$
				2	95%		
				3	97%		

## 6. Equilibrium Studies – Variable Temperature and van't Hoff Plots

### a. General procedure B



In a nitrogen-filled glovebox, stock solutions of **1** (13.3 mM) and silane (**3**) (54.7 mM) were prepared by weighing out the reagents and diluting with C<sub>7</sub>D<sub>8</sub>. **1** (0.30 mL of stock solution, 0.004 mmol, 1.0 equiv), the appropriate silane (0.15 mL of stock solution, 0.0082 mmol, 2.05 equiv), and additional C<sub>7</sub>D<sub>8</sub> (0.15 mL) were added to a screw-top NMR tube using disposable 1-mL syringes. The NMR tube was capped and the reaction was allowed to react at room temperature for 4 h. Then, the NMR tube was removed from the glovebox for analysis by NMR. The sample was inserted into the NMR at -40 °C, and initial <sup>31</sup>P{<sup>1</sup>H} and <sup>1</sup>H spectra were collected after sample was sufficiently cooled. The sample was gradually warmed in 20 °C increments, allowing 10 minutes to equilibrate at each temperature before spectra were collected. The effect of temperature was qualitatively evaluated by observing changes in <sup>31</sup>P and <sup>1</sup>H peak shape. Additionally, if both **1** and **8** are present at equilibrium, the integrations of each <sup>31</sup>P{<sup>1</sup>H} NMR peak were used to determine relative concentrations and K<sub>eq</sub> values. Significant peak broadening is observed at sufficiently low temperatures (see section 10 (Dynamic Behavior) below), and therefore, integrations are less reliable and are not used to calculate K<sub>eq</sub>. Van't Hoff plots of ln(K<sub>eq</sub>) against 1/T were constructed with this data where available.

To construct the van't Hoff plot for the aryl dimethyl silanes (**3**), ln(K<sub>eq</sub>) was plotted as a function of 1/T. Using Microsoft Excel, the data were fit to a curve for the function  $y = mx + b$ , where  $y = \ln(K_{eq})$  input,  $m = -\Delta H \cdot R^{-1}$  output,  $x = T^{-1}$  input, and  $b = \Delta S \cdot R^{-1}$  output, as illustrated below.

$$\ln(K_{eq}) = \left( \frac{-\Delta H}{R} \right) \left( \frac{1}{T} \right) + \frac{\Delta S}{R}$$

$$y = (m) (x) + b$$

Gibbs free energy was found using the following equation:

$$\Delta G = \Delta H - T\Delta S$$

## b. Data with dimethyl aryl silanes 3

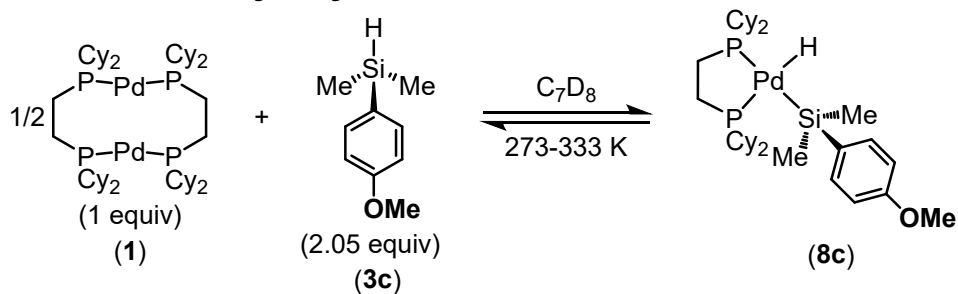


**Table S7.** Conversion,  $K_{eq}$ , and  $\ln(K_{eq})$  values for conversion to **8c** as a function of temperature.

Temperature (K)	1/T (K <sup>-1</sup> )	Conversion	$K_{eq}$	$\ln(K_{eq})$
273	0.00366	52%	330	5.8
293	0.00341	30%	37	3.6
298	0.00336	17%	26	3.3
313	0.00319	18%	8.3	2.1
333	0.00300	10%	2.0	0.67

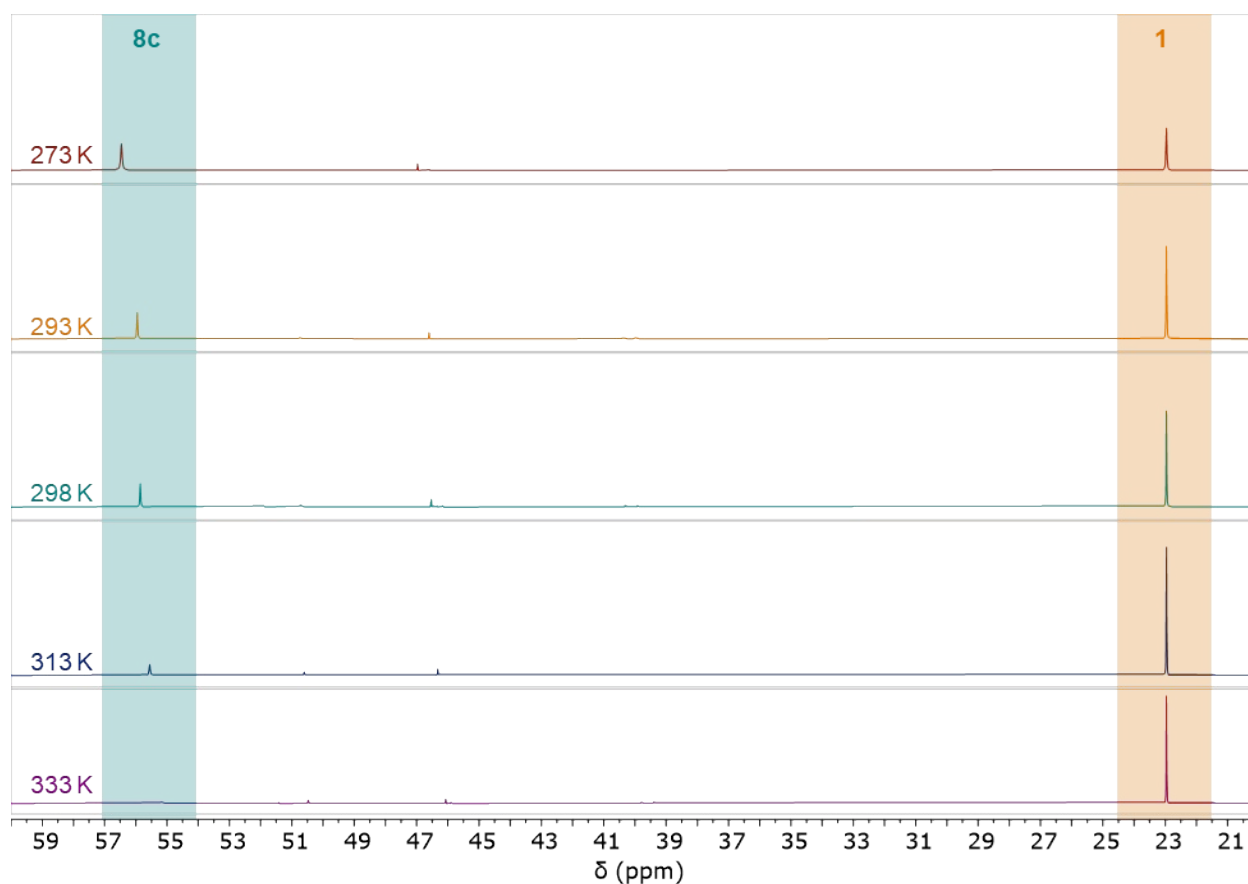


**Figure S2.**  $^{31}P\{^1H\}$  NMR spectra of conversion to **8c** as a function of temperature.

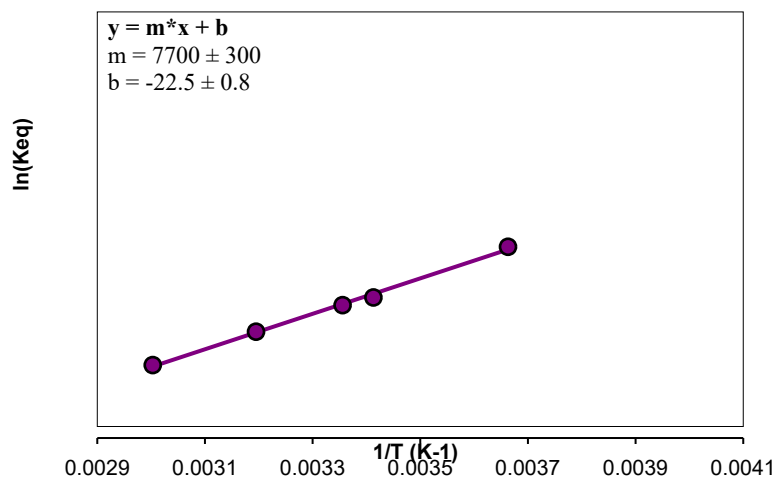


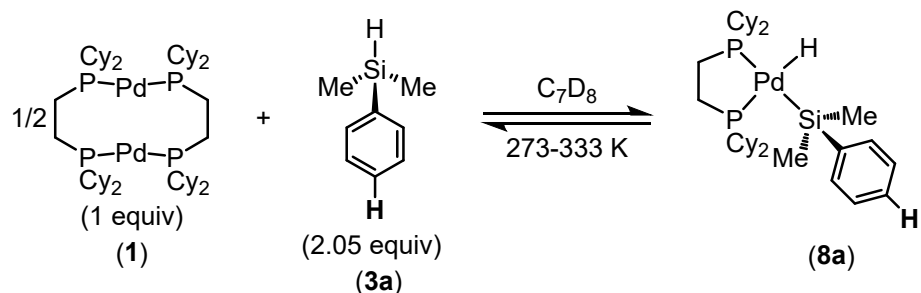
**Figure S3.** van't Hoff plot for **8c**.

$$\Delta H = -15.3 \pm 0.5 \text{ kcal} \cdot \text{mol}^{-1}$$

$$\Delta S = -45 \pm 2 \text{ cal} \cdot \text{mol}^{-1} \cdot \text{K}^{-1}$$

$$\Delta G_{298\text{K}} = -2.0 \pm 0.5 \text{ kcal} \cdot \text{mol}^{-1}$$

$$\Delta G_{233\text{K}} = -4.9 \pm 0.5 \text{ kcal} \cdot \text{mol}^{-1}$$



Note: two trials were run, and the average of the two conversions is reported below.

**Table S8.** Conversion,  $K_{eq}$ , and  $\ln(K_{eq})$  values for conversion to **8a** as a function of temperature.

Temperature (K)	1/T ( $K^{-1}$ )	Conversion	$K_{eq}$	$\ln(K_{eq})$
233	0.00429	95 $\pm$ 1%	500000 $\pm$ 100000	13.1 $\pm$ 0.3
253	0.00395	93 $\pm$ 1%	170000 $\pm$ 20000	12.1 $\pm$ 0.1
273	0.00366	71 $\pm$ 4%	2600 $\pm$ 600	7.9 $\pm$ 0.2
293	0.00341	46 $\pm$ 0%	184 $\pm$ 0	5.2 $\pm$ 0
298	0.00336	40 $\pm$ 0%	102 $\pm$ 0	4.6 $\pm$ 0
313	0.00319	27 $\pm$ 3%	26 $\pm$ 5	3.3 $\pm$ 0.2
333	0.00300	16 $\pm$ 2%	6 $\pm$ 1	1.7 $\pm$ 0.2

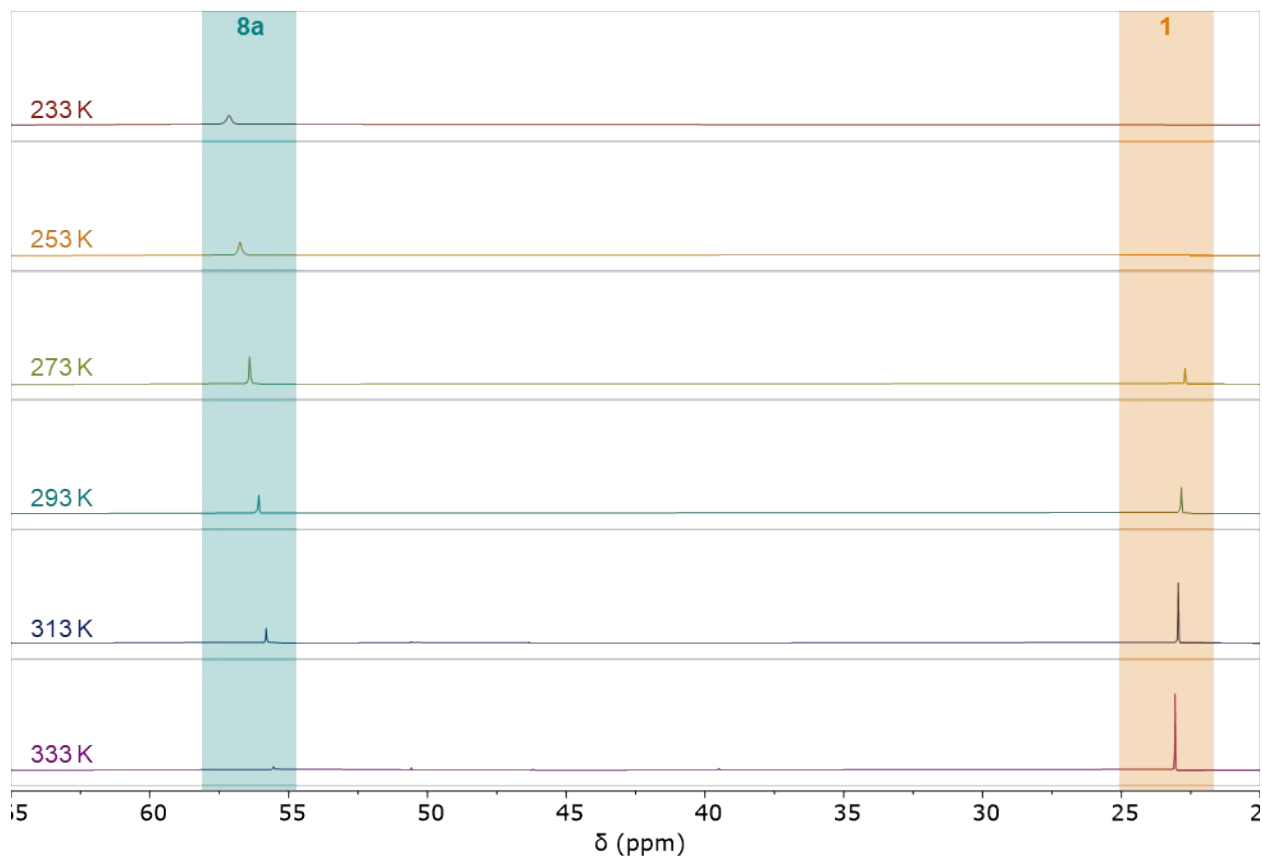


**Figure S4.**  $^{31}P\{^1H\}$  NMR spectra of conversion to **8a** as a function of temperature.

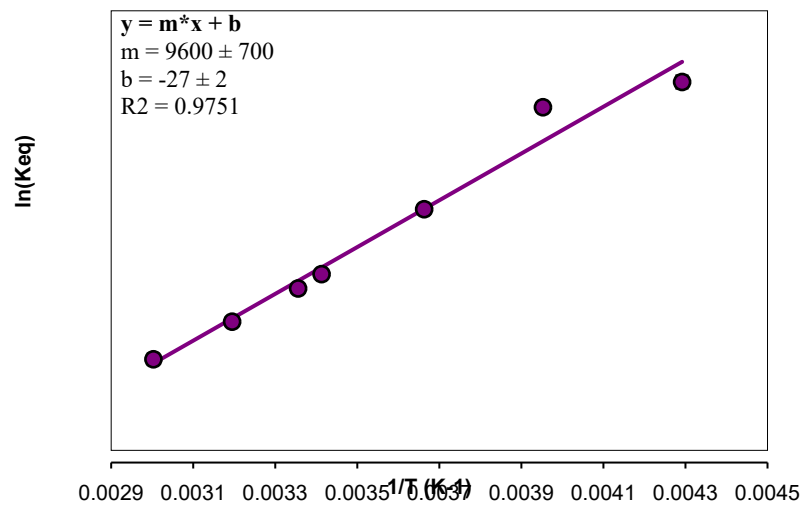


**Figure S5.** van't Hoff plot for **8a**.

$\Delta H = -19 \pm 1$	kcal•mol <sup>-1</sup>
$\Delta S = -54 \pm 5$	cal•mol <sup>-1</sup> •K <sup>-1</sup>
$\Delta G_{298K} = -3 \pm 1$	kcal•mol <sup>-1</sup>
$\Delta G_{233K} = -6 \pm 1$	kcal•mol <sup>-1</sup>

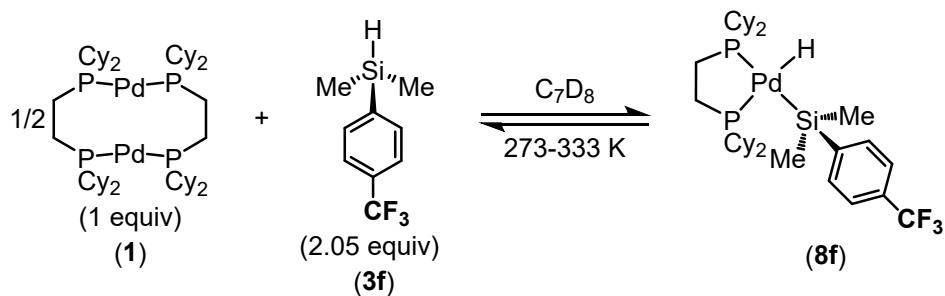


**Table S9.** Conversion,  $K_{eq}$ , and  $\ln(K_{eq})$  values for conversion to **8f** as a function of temperature.

Temperature (K)	1/T ( $K^{-1}$ )	Conversion	$K_{eq}$	$\ln(K_{eq})$
273	0.00366	99%	$1.2 \times 10^7$	16
298	0.00336	88%	46000	11
313	0.00319	74%	3900	8.3
333	0.00300	59%	670	6.5

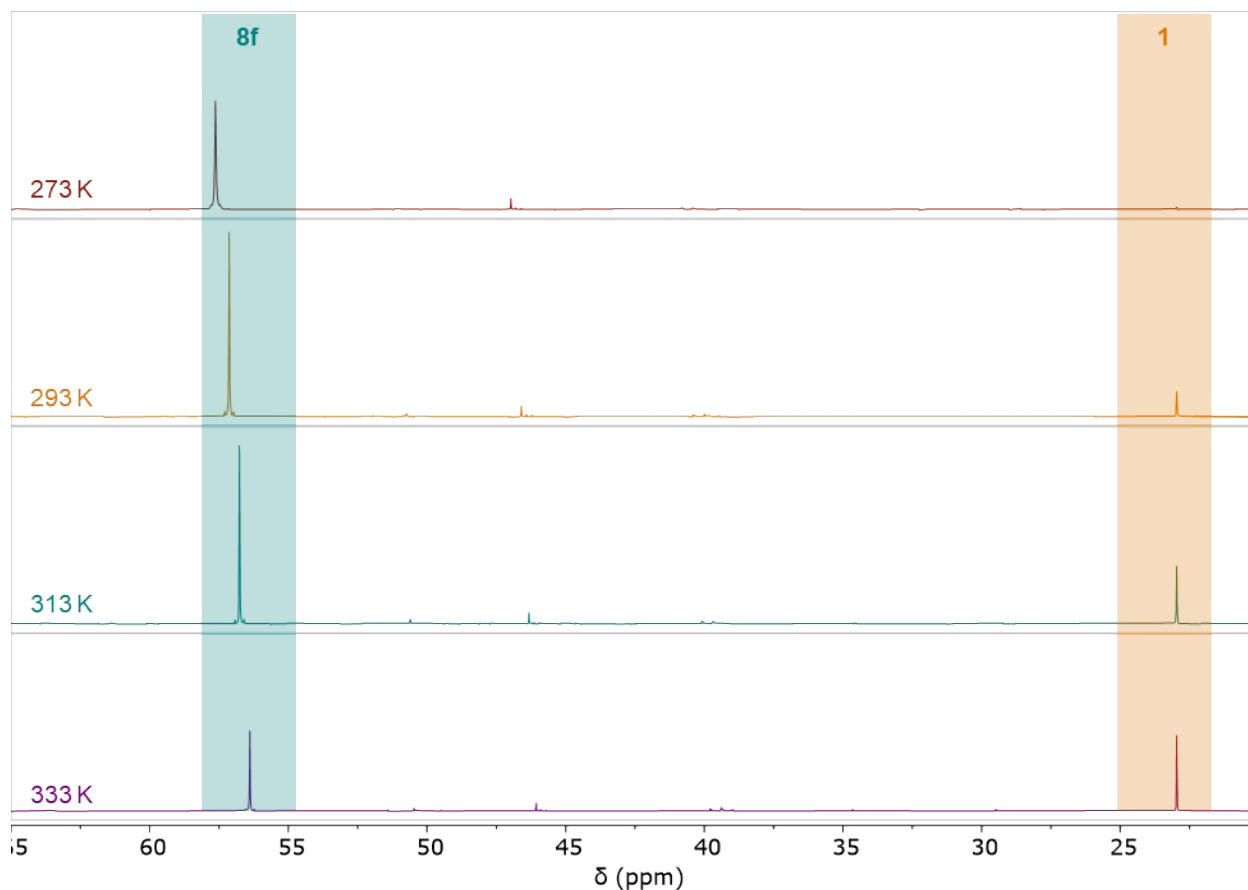


**Figure S6.**  $^{31}P\{^1H\}$  NMR spectra of conversion to **8f** as a function of temperature.

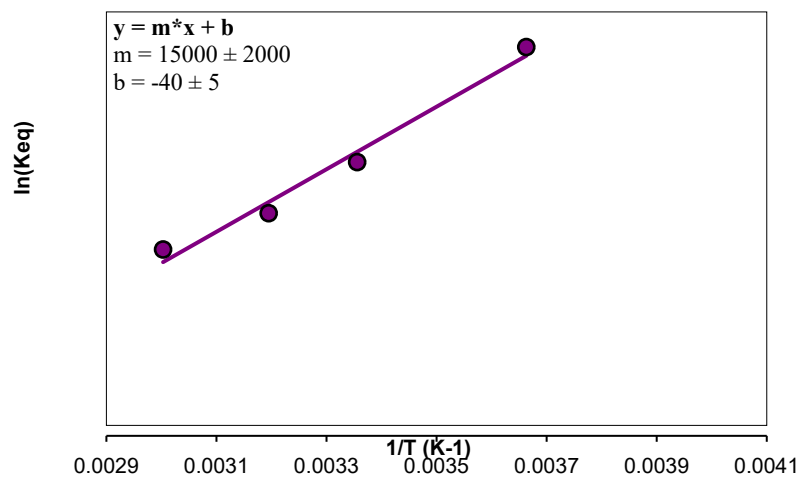
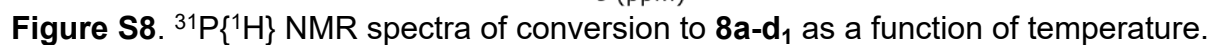


**Figure S7.** van't Hoff plot for **8f**.

$$\begin{aligned}
 \Delta H &= -30 \pm 3 \text{ kcal} \cdot \text{mol}^{-1} \\
 \Delta S &= -80 \pm 10 \text{ cal} \cdot \text{mol}^{-1} \cdot \text{K}^{-1} \\
 \Delta G_{298\text{K}} &= -7 \pm 3 \text{ kcal} \cdot \text{mol}^{-1} \\
 \Delta G_{233\text{K}} &= -12 \pm 3 \text{ kcal} \cdot \text{mol}^{-1}
 \end{aligned}$$



Temperature (K)	1/T (K <sup>-1</sup> )	Conversion	K <sub>eq</sub>	ln(K <sub>eq</sub> )
233	0.00429	83 ± 3%	16000 ± 3000	9.7 ± 0.2
253	0.00395	81 ± 4%	11000 ± 3000	9.3 ± 0.3
273	0.003666	54 ± 3%	410 ± 60	6.0 ± 0.1
293	0.00341	29 ± 2%	34 ± 4	3.5 ± 0.1
298	0.00336	28.0 ± 0.7%	28 ± 1	3.33 ± 0.05
313	0.00319	18.0 ± 0.9%	7.9 ± 0.7	2.06 ± 0.09
333	0.00300	10 ± 2%	1.7 ± 0.7	0.6 ± 0.4



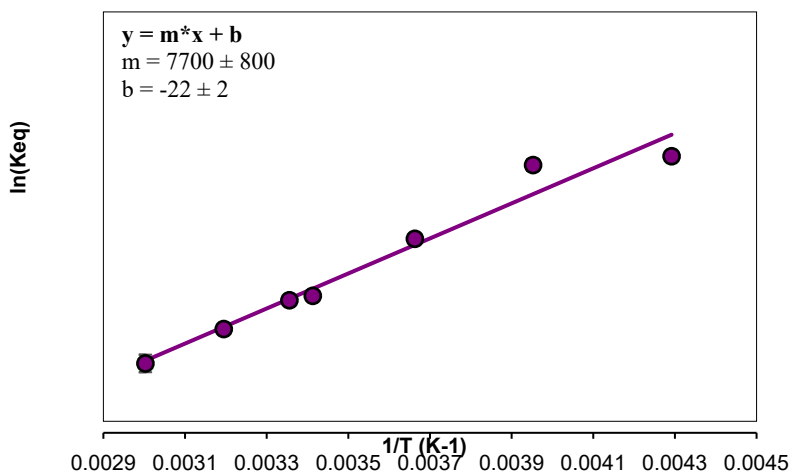
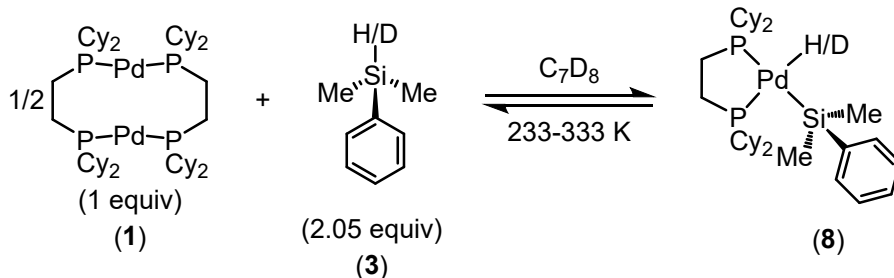


**Figure S9.** van't Hoff plot for **8a-d<sub>1</sub>**.

$$\begin{aligned}\Delta H &= -15 \pm 1 && \text{kcal} \cdot \text{mol}^{-1} \\ \Delta S &= -45 \pm 5 && \text{cal} \cdot \text{mol}^{-1} \cdot \text{K}^{-1} \\ \Delta G_{298\text{K}} &= -2 \pm 1 && \text{kcal} \cdot \text{mol}^{-1} \\ \Delta G_{233\text{K}} &= -5 \pm 1 && \text{kcal} \cdot \text{mol}^{-1}\end{aligned}$$

### c. Equilibrium isotope effect



General procedure B was used. Using the  $K_{eq}$  values determined at a range of temperatures for **3a** and **3a-d<sub>1</sub>** (see section 6b above) equilibrium isotope effects (EIE) were determined at multiple temperatures.

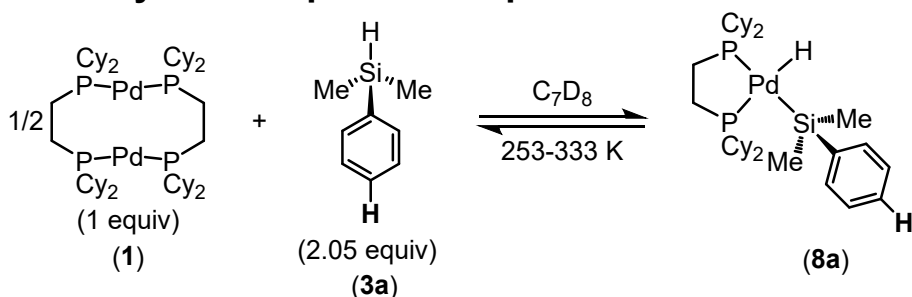
$$EIE = \frac{K_H}{K_D}$$

**Table S11.** Conversion,  $K_{eq}$ , and EIE values for conversion to **8a** and **8a-d<sub>1</sub>** as a function of temperature

Temperature (K)	Conversion to <b>8a</b>	Conversion to <b>8a-d<sub>1</sub></b>	$K_H$	$K_D$	EIE
233	$95 \pm 1\%$	$83 \pm 3\%$	$500000 \pm 100000$	$16000 \pm 3000$	$30 \pm 10$
253	$93 \pm 1\%$	$81 \pm 4\%$	$170000 \pm 20000$	$11000 \pm 3000$	$16 \pm 4$
273	$71 \pm 4\%$	$54 \pm 3\%$	$2600 \pm 600$	$410 \pm 60$	$6 \pm 2$
293	$46 \pm 0\%$	$29 \pm 2\%$	$184 \pm 0$	$34 \pm 4$	$5.5 \pm 0.6$
298	$40 \pm 0\%$	$28.0 \pm 0.7\%$	$102 \pm 0$	$28 \pm 1$	$3.4 \pm 0.2$
313	$27 \pm 3\%$	$18.0 \pm 0.9\%$	$26 \pm 5$	$7.9 \pm 0.7$	$3.3 \pm 0.7$
333	$16 \pm 2\%$	$10 \pm 2\%$	$6 \pm 1$	$1.7 \pm 0.7$	$3 \pm 1$

## 7. Reversibility

### a. Reversibility with respect to temperature



In a nitrogen-filled glovebox, stock solutions of **1** (13.3 mM) and **3a** (54.7 mM) were prepared by weighing out the reagents and diluting with  $C_7D_8$ . **1** (0.30 mL of stock solution, 0.004 mmol, 1.0 equiv), **3a** (0.15 mL of stock solution, 0.0082 mmol, 2.05 equiv), and additional  $C_7D_8$  (0.15 mL) were added to a screw-top NMR tube using disposable 1-mL syringes. The NMR tube was capped and the reaction was allowed to react at room temperature for 4 h. Then, the NMR tube was removed from the glovebox for analysis by NMR. The sample was inserted into the NMR which was precooled to  $-40\text{ }^{\circ}\text{C}$ , and initial  $^{31}\text{P}\{^1\text{H}\}$  and  $^1\text{H}$  spectra were collected after sample was sufficiently cooled. The sample was gradually warmed in  $20\text{ }^{\circ}\text{C}$  increments to  $60\text{ }^{\circ}\text{C}$ , allowing 10 minutes to equilibrate at each temperature before spectra were collected (red, orange, yellow, green, and blue spectra in Figure S10 below). Then, the sample was allowed to cool back down to room temperature (298 K), and spectra were recorded (purple spectrum in Figure S10 below). The integrations of the peaks corresponding to **1** and **8a** by  $^{31}\text{P}\{^1\text{H}\}$  NMR were used to determine conversion.

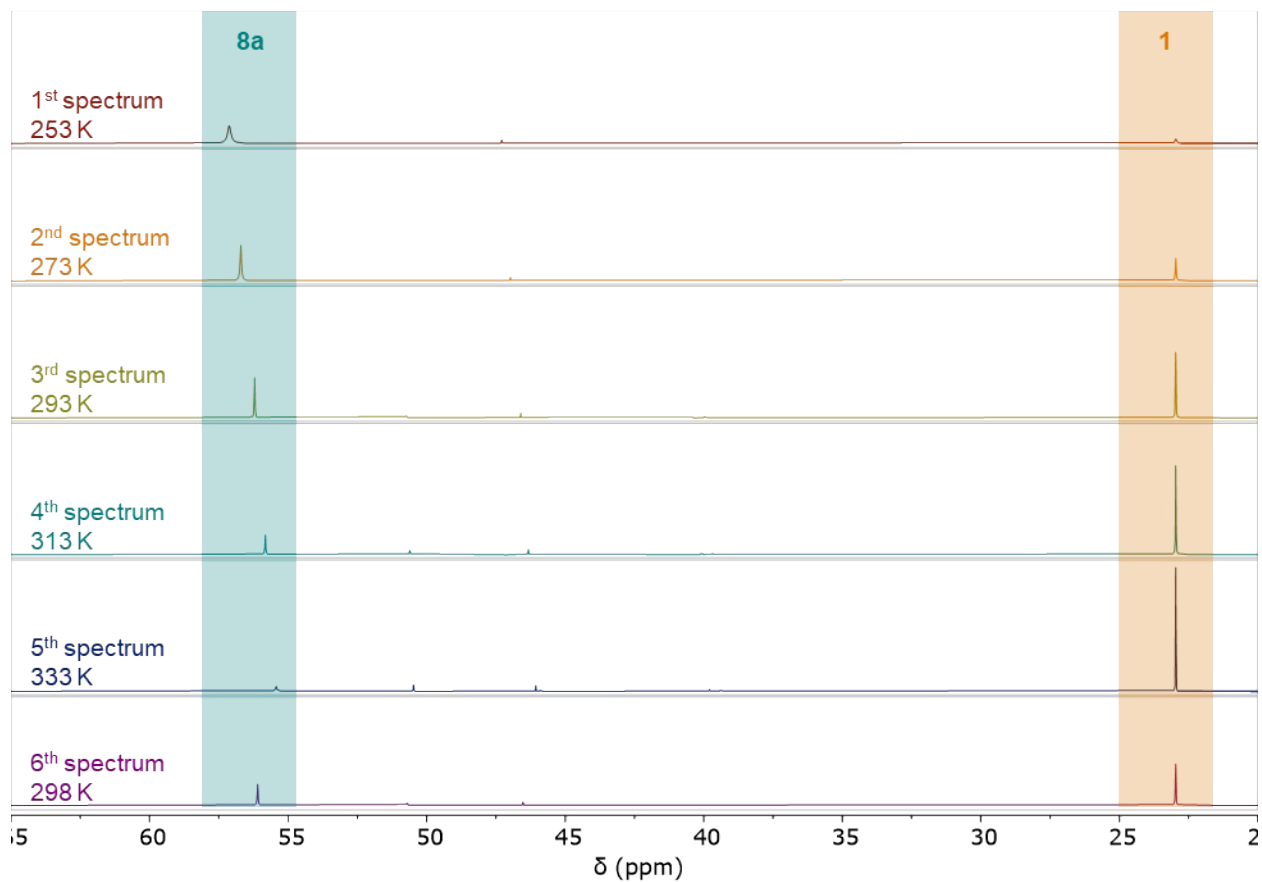
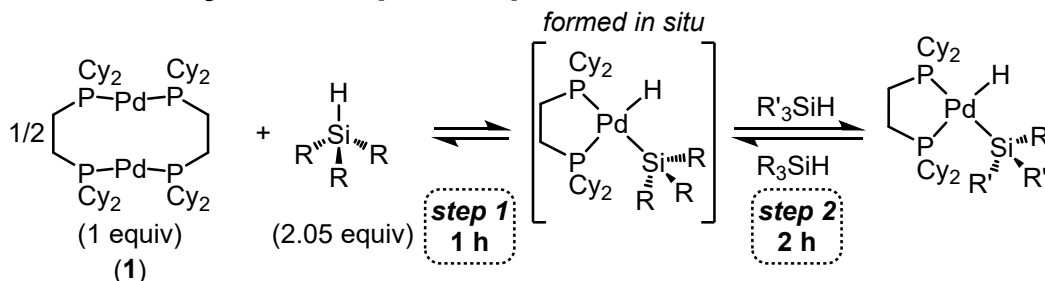


**Figure S10.**  $^{31}\text{P}\{^1\text{H}\}$  NMR spectra of conversion to **8a** as a function of temperature showing that the reaction is reversible with respect to temperature.

**Table S12.** Conversion values to **8a** as a function of temperature and order.

Spectrum order	Temperature (K)	Conversion to <b>8a</b>
1 <sup>st</sup>	253	88%
2 <sup>nd</sup>	273	72%
3 <sup>rd</sup>	293	44%
4 <sup>th</sup>	313	27%
5 <sup>th</sup>	333	17%
6 <sup>th</sup>	298	41%

## b. Reversibility with respect to product distribution



In a nitrogen-filled glovebox, stock solutions of **1** (13.3 mM), **5a** (54.7 mM), **5d** (54.7 mM), and **5e** (54.7 mM) were prepared by weighing out the reagents and diluting with C<sub>7</sub>D<sub>8</sub>. **1** (0.30 mL of stock solution, 0.004 mmol, 1.0 equiv) and one of the silanes (0.15 mL of stock solution, 0.0082 mmol, 2.05 equiv) were added to a screw-top NMR tube using disposable 1-mL syringes. The NMR tube was capped and the reaction was allowed to react at room temperature for 1 h. Then, the NMR tube was removed from the glovebox for analysis by NMR. The integrations of the peaks corresponding to **1** and **10a**, **10d**, or **10e** by <sup>31</sup>P{<sup>1</sup>H} NMR were used to determine relative concentrations of each species. Then, the NMR tube was brought back into the glovebox, and a different silane was added to the NMR tube (0.15 mL of stock solution, 0.0082 mmol, 2.05 equiv) via a disposable 1-mL syringe. The reaction was allowed to react at room temperature for 2 h. The NMR tube was removed from the glovebox for analysis by NMR. The integrations of the peaks corresponding to **1** and **10a**, **10d**, and/or **10e** by <sup>31</sup>P{<sup>1</sup>H} NMR were used to determine relative concentrations of each species.

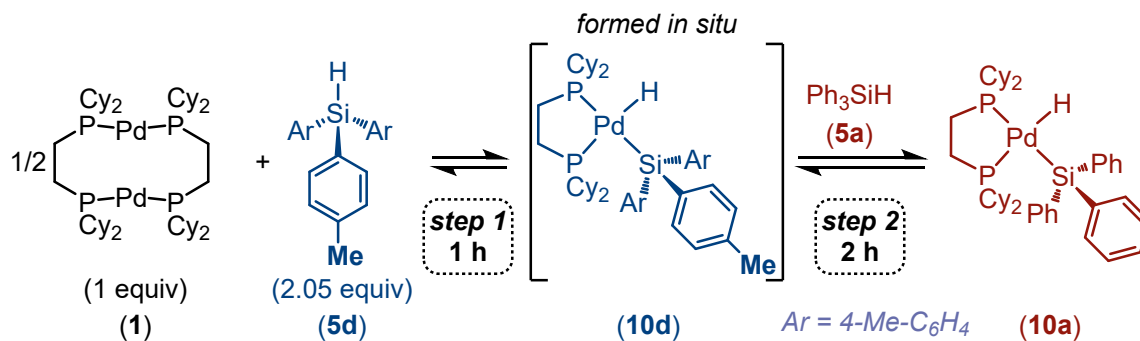


**Table S13.** Equilibrium conversions to **10d** and **10a** when **5d** was added first.

Step	Conversion to <b>10d</b>	Conversion to <b>10a</b>
1	98%	---
2	23%	77%

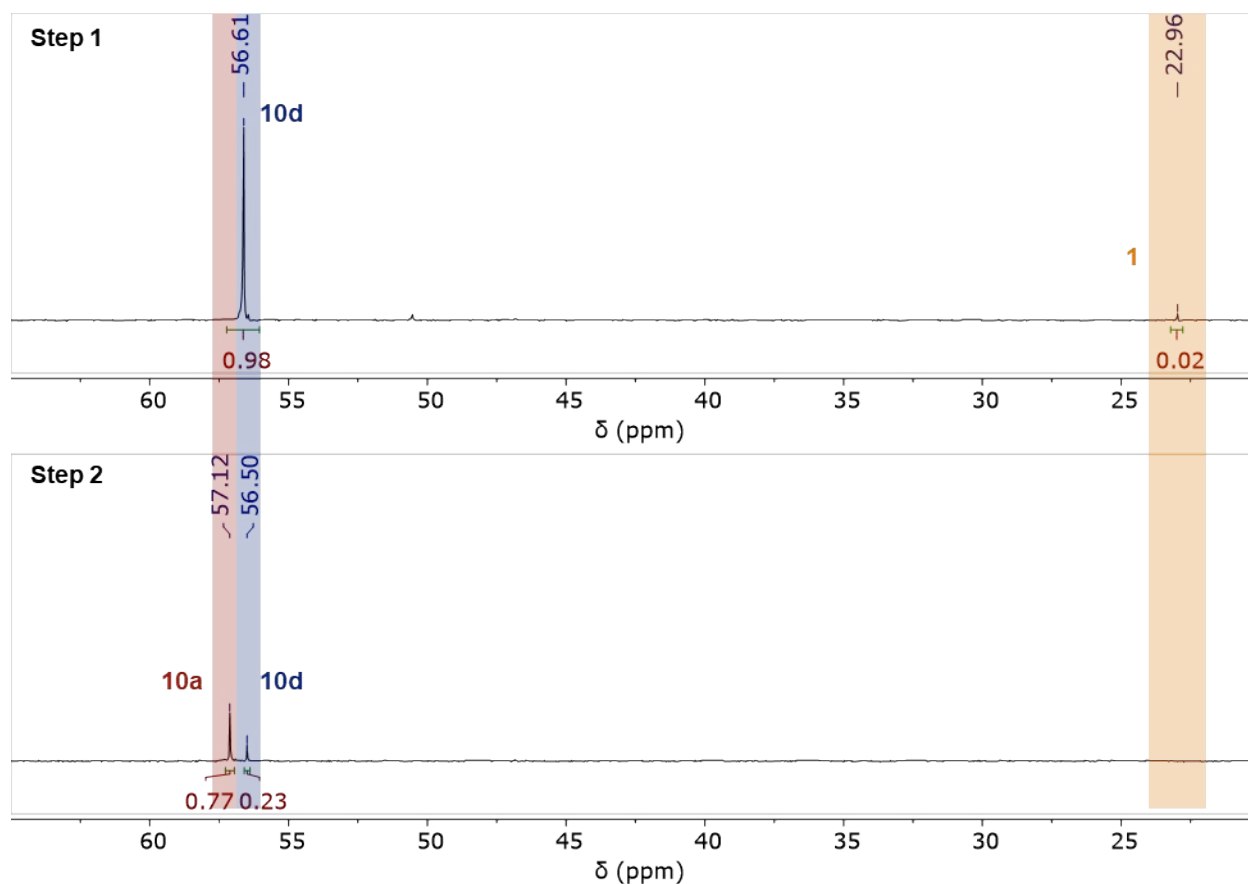


**Figure S11.**  $^{31}\text{P}\{^1\text{H}\}$  NMR spectra of conversions to **10d** and **10a** when **5d** was added first.

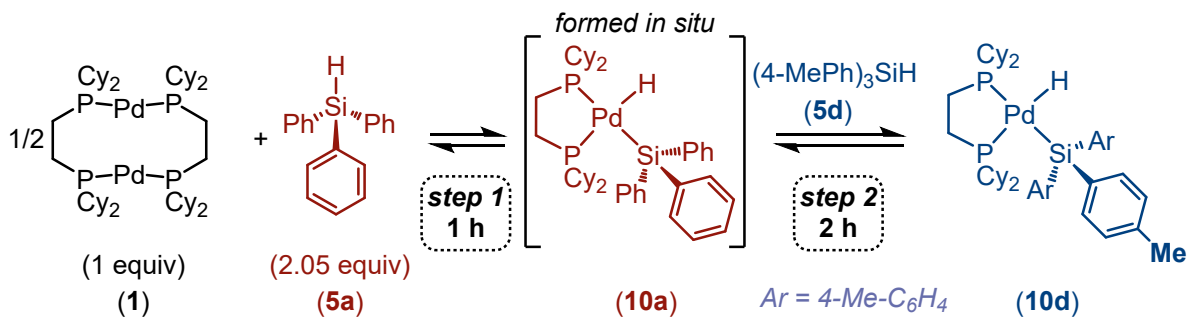


**Table S14.** Equilibrium conversions to **10f** and **10a** when **5a** was added first.

Step	Conversion to <b>10d</b>	Conversion to <b>10a</b>
1	---	100%
2	23%	77%

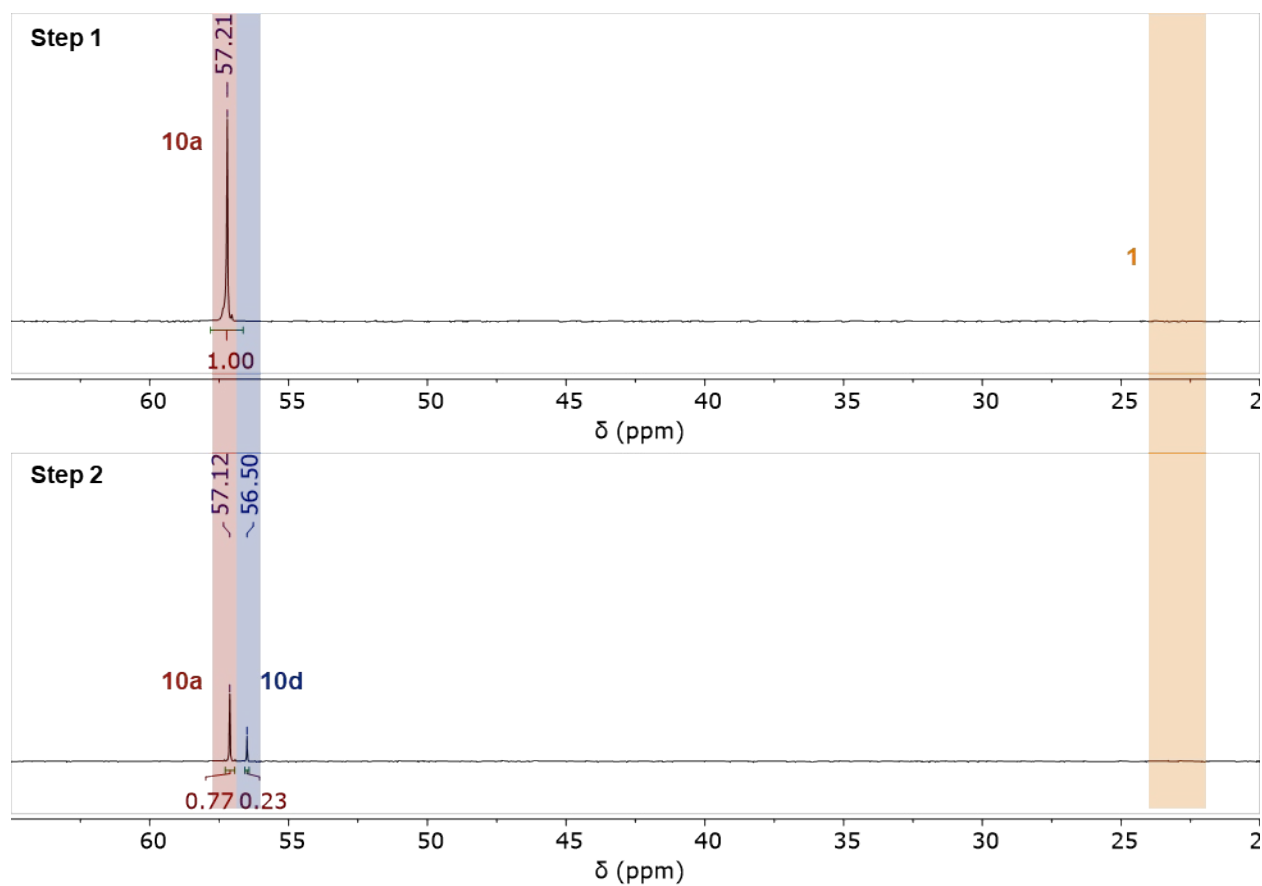


**Figure S12.**  $^{31}\text{P}\{^1\text{H}\}$  NMR spectra of conversions to **10d** and **10a** when **5a** was added first.

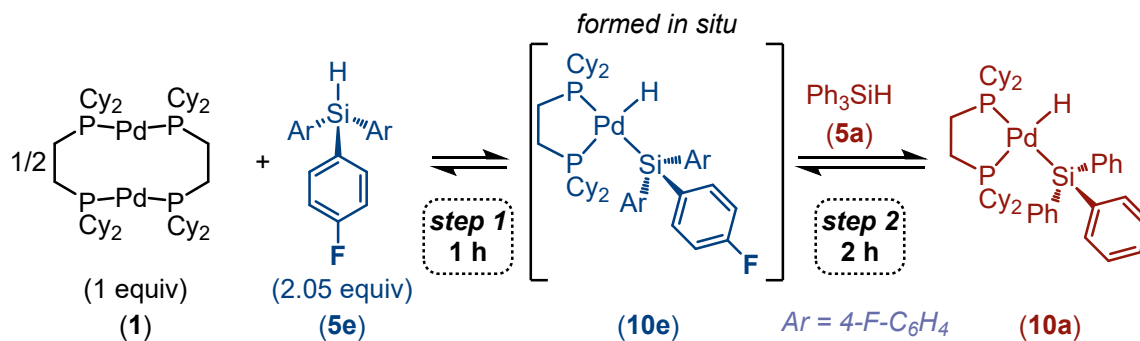


**Table S15.** Equilibrium conversions to **10e** and **10a** when **5e** was added first.

Step	Conversion to <b>10e</b>	Conversion to <b>10a</b>
1	100%	---
2	74%	26%

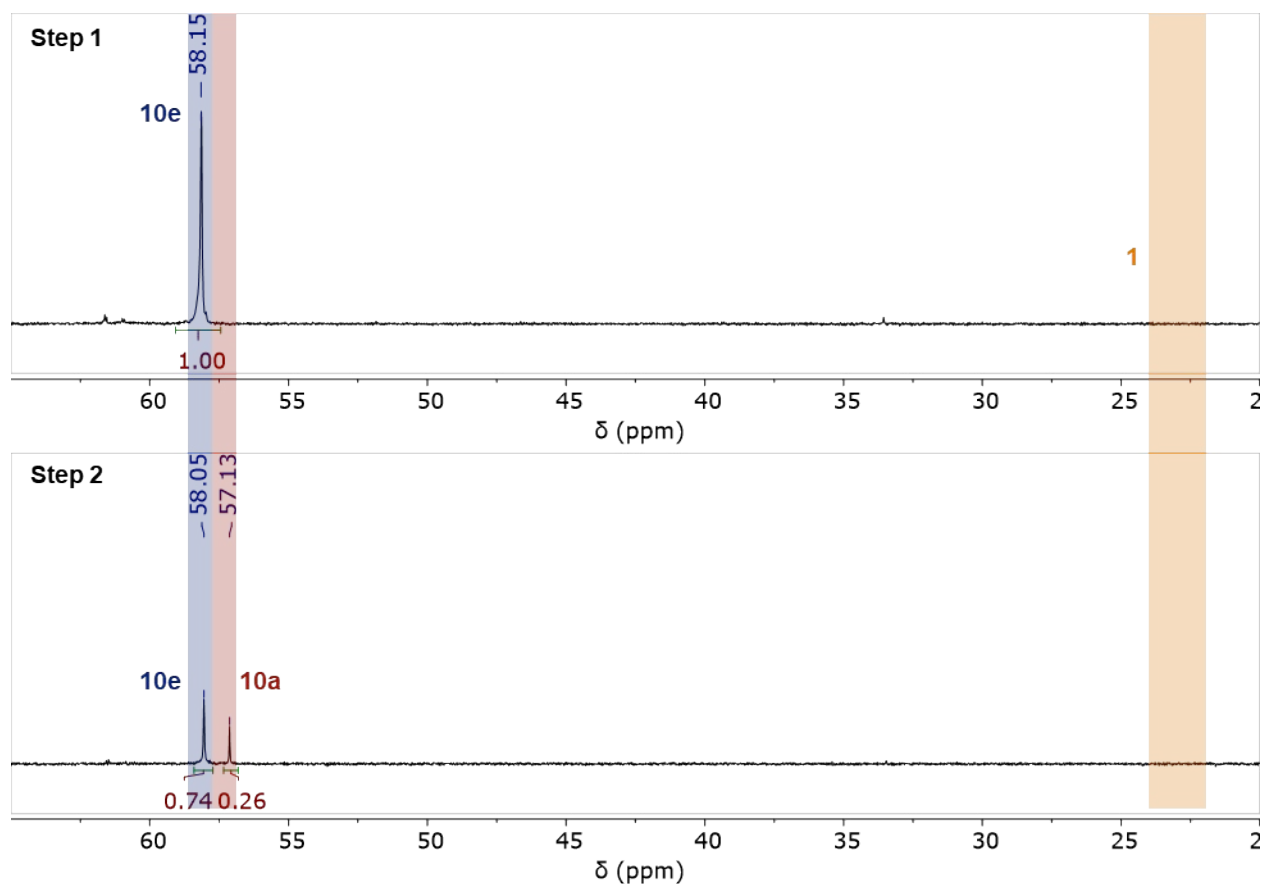


**Figure S13.** <sup>31</sup>P{<sup>1</sup>H} NMR spectra of conversions to **10e** and **10a** when **5e** was added first.

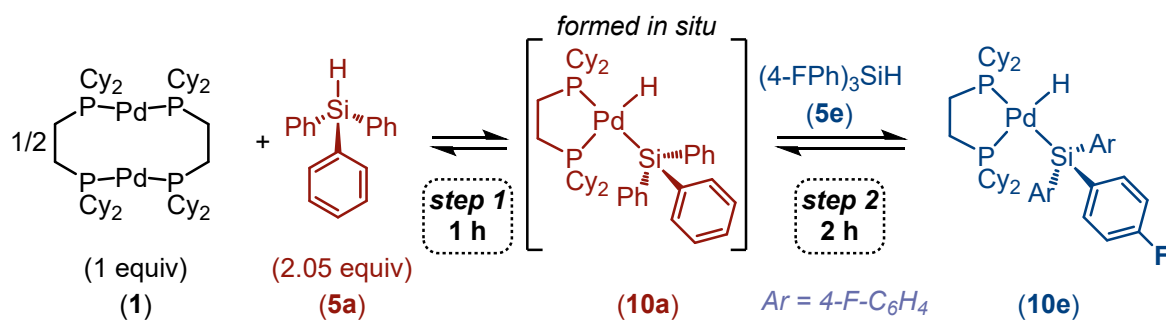


**Table S16.** Equilibrium conversions to **10a** and **10e** when **5a** was added first.

Step	Conversion to <b>10e</b>	Conversion to <b>10a</b>
1	---	100%
2	70%	30%

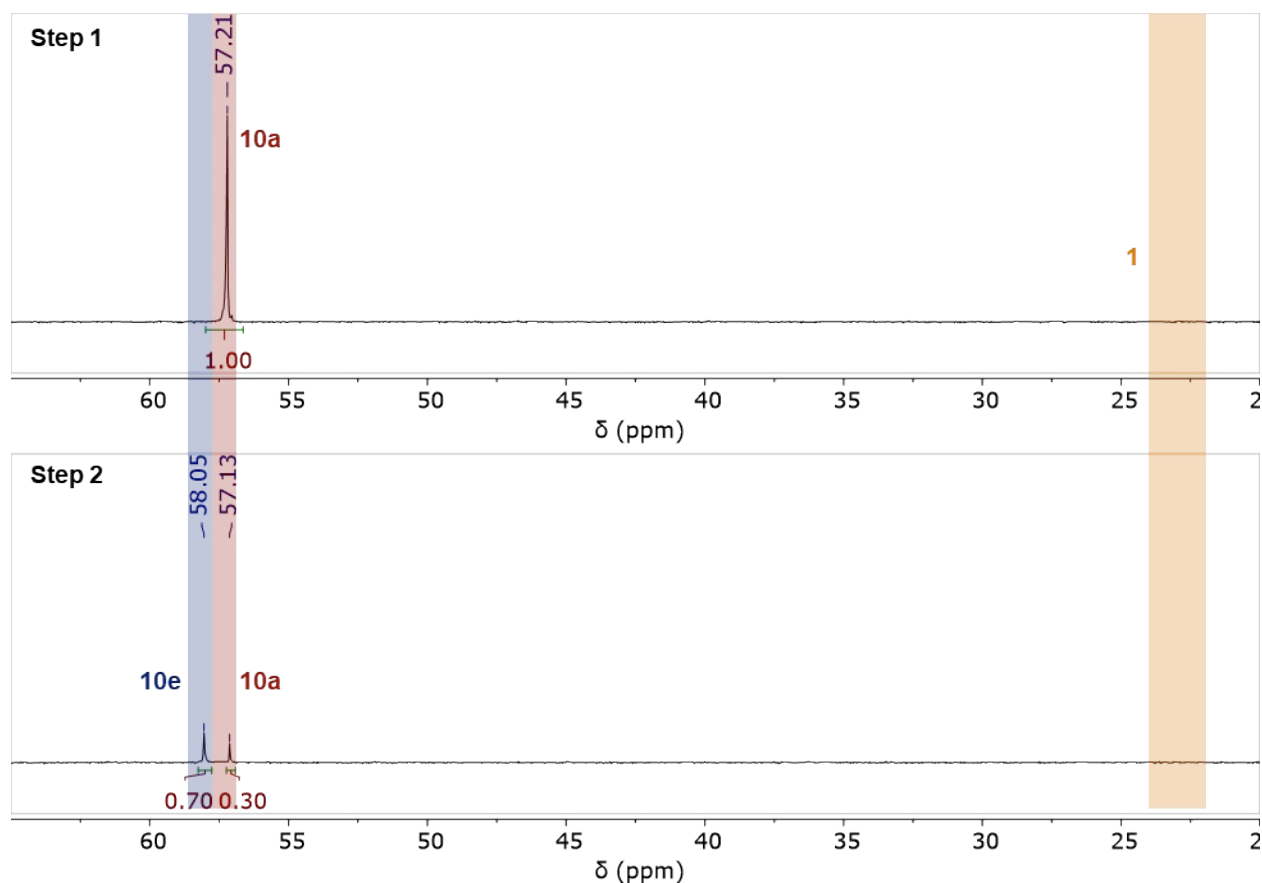
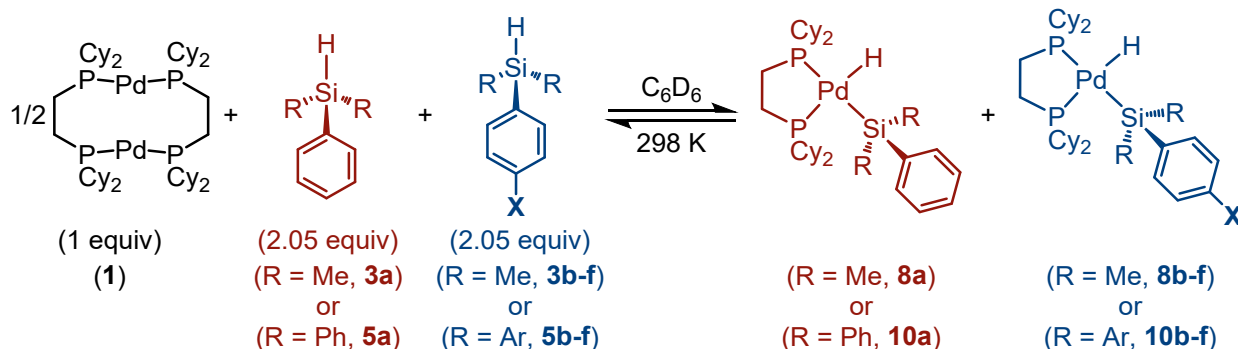


**Figure S14.** <sup>31</sup>P{<sup>1</sup>H} NMR spectra of conversions to **10e** and **10a** when **5a** was added first.

## 8. Competition Studies

### a. General procedure C



In a nitrogen-filled glovebox, stock solutions of **1** (13.3 mM), the parent silane (**3a** or **5a**, 54.7 mM), and the 4-substituted silane (**3b-f**, **5b-f**; 54.7 mM) were prepared by weighing out the reagents and diluting with C<sub>6</sub>D<sub>6</sub>. **1** (0.30 mL of stock solution, 0.004 mmol, 1.0 equiv), parent silane (0.15 mL of stock solution, 0.0082 mmol, 2.05 equiv), and the 4-substituted silane (0.15 mL of stock solution, 0.0082 mmol, 2.05 equiv) were added to a screw-top NMR tube using disposable 1-mL syringes. The NMR tube was capped and the reaction was allowed to react at room temperature for 4-6 h. Then, the NMR tube was removed from the glovebox for analysis by NMR. The integrations of the peaks corresponding to **1**, **10a** or **8a**, and **8b-f** or **10b-f** by <sup>31</sup>P{<sup>1</sup>H} NMR were used to determine conversion.

To construct the Hammett plot for competition between **3a** and **3b-f** or **5a** and **5b-f**, values for σ<sub>p</sub> were taken from reference 8. The values of log(K<sub>X</sub>/K<sub>H</sub>) for X = NMe<sub>2</sub>, OMe, Me, F, and CF<sub>3</sub> were plotted as a function of σ<sub>p</sub>. Using Microsoft Excel, the data were fit to a curve for the function y = mx + b, where y = log(K<sub>X</sub>/K<sub>H</sub>) input, m = sensitivity constant ρ output, x = σ<sub>p</sub> input, and b = intercept output. Using the competition between **3a** and **3e** (X = F) as an example, K<sub>X</sub>/K<sub>H</sub> was determined as follows:

$$\frac{K_X}{K_H} = \frac{\frac{[8e]^2}{[1][3e]^2}}{\frac{[8a]^2}{[1][3a]^2}} = \frac{[8e]^2 * [3a]^2}{[3e]^2 * [8a]^2}$$

## b. Results of competition between 5a and 5b-f

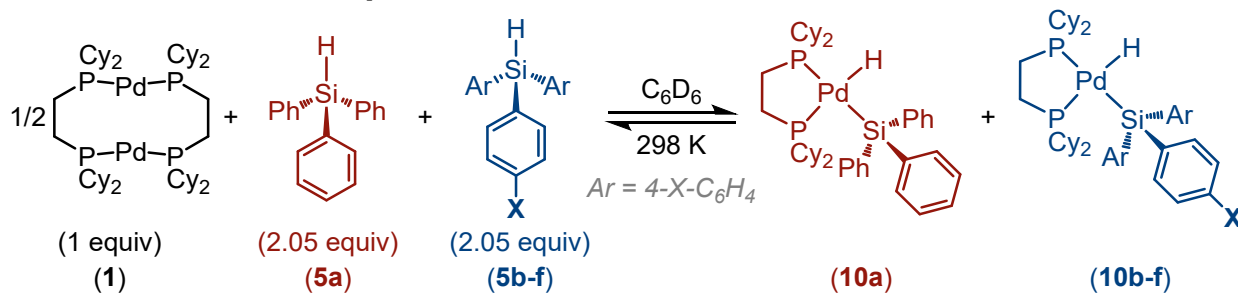


**Table S17.** Results of competition between **5a** and substituted silanes **5b-f**.

X-group	Silane (5b-f)	Trial	Conversion to 10a	Conversion to 10b-f	Average conversion to 10a	Average conversion to 10b-f	log(K <sub>X</sub> /K <sub>H</sub> )
-NMe <sub>2</sub>	<b>5b</b>	1	99%	1%	99%	2%	-6.4
		2	98%	2%			
-OMe	<b>5c</b>	1	87%	13%	84%	17%	-2.7
		2	80%	20%			
-Me	<b>5d</b>	1	76%	24%	77%	24%	-2.0
		2	78%	22%			
		3	75%	26%			
		4	77%	23%			
-F	<b>5e</b>	1	30%	70%	28%	72%	1.6
		2	25%	75%			
		3	30%	70%			
-CF <sub>3</sub>	<b>5f</b>	1	0%	100%	2%	99%	6.4
		2	3%	97%			

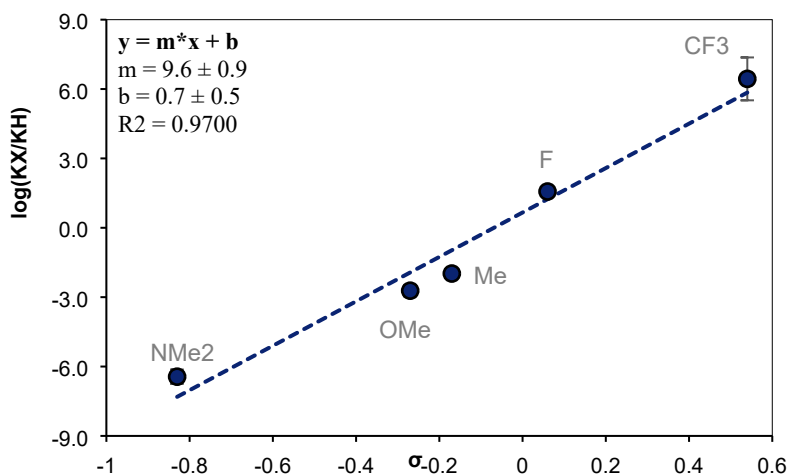


**Figure S15.** Hammett plot of competition between **5a** and **5b-f**.

### c. Results of competition between 3a and 3b-f

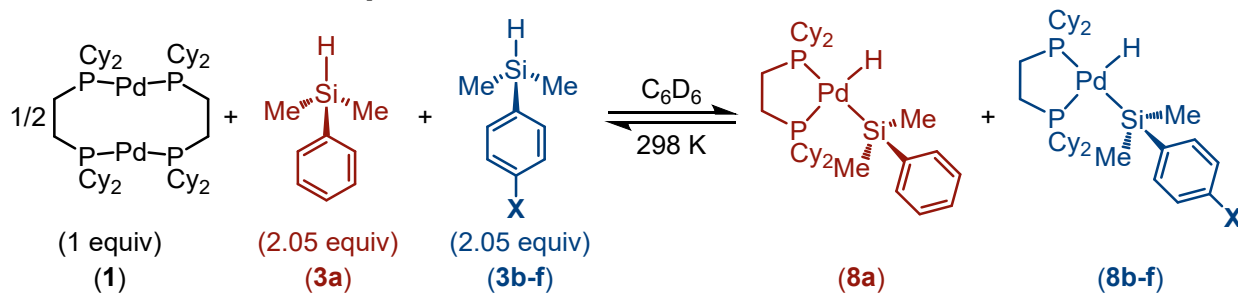


**Table S18.** Results of competition between **3a** and substituted silanes **3b-f**.

X-group	Silane ( <b>3b-f</b> )	Trial	Conversion to <b>8a</b>	Conversion to <b>8b-f</b>	Average conversion to <b>8a</b>	Average conversion to <b>8b-f</b>	$\log(K_X/K_H)$
-NMe <sub>2</sub>	<b>3b</b>	1	39%	5%	40%	6%	$-2.11 \pm 0.08$
		2	41%	6%			
-OMe	<b>3c</b>	1	35%	19%	36%	19%	$-0.78 \pm 0.04$
		2	37%	18%			
-Me	<b>3d</b>	1	37%	26%	38%	26%	$-0.48 \pm 0.02$
		2	38%	25%			
-F	<b>3e</b>	1	30%	45%	30%	46%	$0.61 \pm 0.03$
		2	29%	47%			
-CF <sub>3</sub>	<b>3f</b>	1	15%	82%	18%	81%	$2.5 \pm 0.1$
		2	20%	80%			

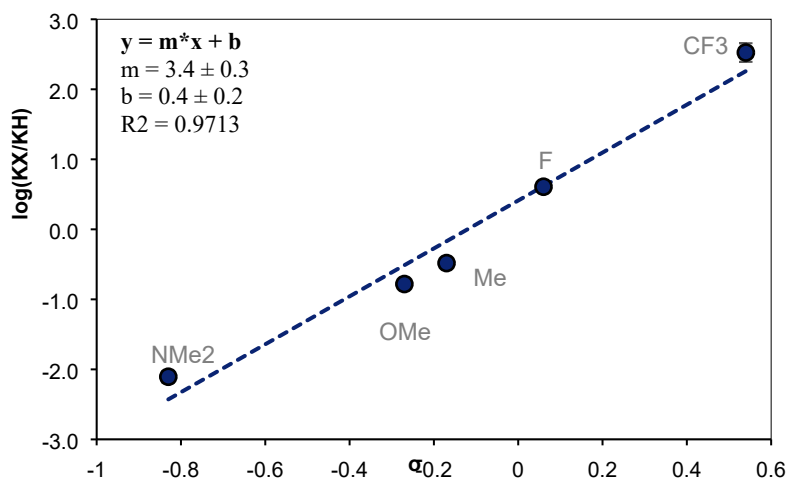
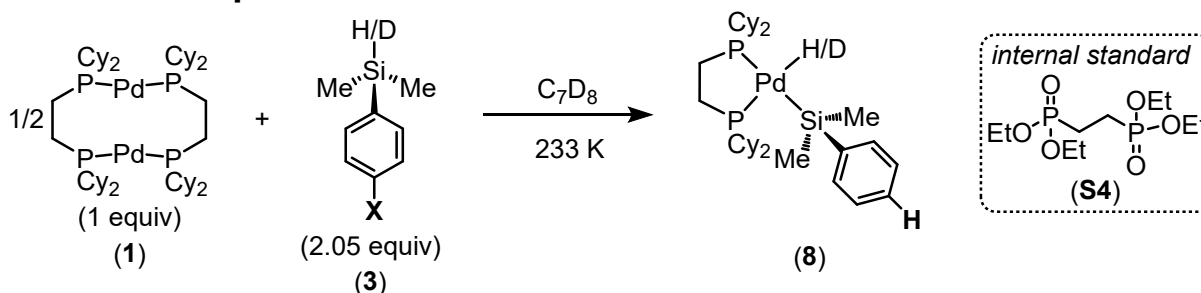


**Figure S16.** Hammett plot of competition between **3a** and **3b-f**.

## 9. Kinetic Studies

### a. General procedure D



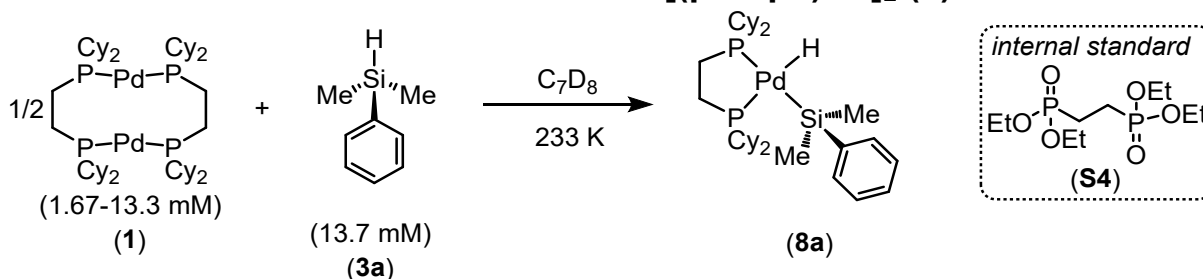
In a nitrogen-filled glovebox, stock solutions of **1** (13.3 mM), silane (54.7 mM), and internal standard (**S4**; tetraethyl(ethylene)bisphosphonate, 26.67 mM) were prepared by weighing out the reagents and diluting with  $C_7D_8$ . **1** (0.30 mL of stock solution, 0.0040 mmol, 1.0 equiv) and **S4** (0.15 mL of stock solution, 0.0040 mmol, 1.0 equiv) were added to a screw-top NMR tube using disposable 1-mL syringes. The NMR tube was capped with a septum cap and then removed from glovebox. The tube was then cooled to  $-78\text{ }^{\circ}\text{C}$  in a dry ice/acetone bath. In the glovebox, 0.15 mL of the silane solution (0.0082 mmol, 2.05 equiv) was pulled into a 1.0 mL plastic syringe, which was inverted, and the plunger pulled back completely to collect ample head space of nitrogen. The syringe was removed from the glovebox and injected quickly into the NMR tube while it is still submerged in the dry ice/acetone bath. The NMR tube was then briefly shaken to homogenize the solutions, and then quickly frozen in a liquid nitrogen bath. The samples were stored in the liquid nitrogen bath until analysis.

The NMR probe was pre-cooled to  $-40\text{ }^{\circ}\text{C}$  and was locked, tuned, and shimmed at temperature to a dummy sample of  $C_7D_8$ . The experimental sample was removed from liquid nitrogen dewar and quickly inserted into the instrument, and  $^{31}\text{P}\{^1\text{H}\}$  NMR scans were collected immediately upon the sample lock. Product concentration was determined by relative peak integrations against **S4**.

Kinetics data was analyzed using MestreNova v14.0. Integrations **8** and **S4** were used to determine concentrations of **8** as a function of time. The method of initial rates was used to determine the rate of reaction. We chose this method to prevent complications from the backwards reaction (conversion of **8** into **1** and **3**) interfering with analysis and interpretation of data. At least two separate trials were run, and all the data points from each trial were used collectively to determine the rate of the reaction.

Using Microsoft Excel, the concentration of product was plotted against time, and the data were fit to a curve for the function  $y = mx$ , where  $y$  = concentration of product input,  $m$  = observed rate (expressed in terms of  $\Delta[\mathbf{8}]/\Delta t$ ) output, and  $x$  = time input.

## b. Kinetics to measure the order in $[(\mu\text{-dcpe})\text{Pd}]_2$ (**1**)



General procedure D was followed using **3a** to form **8a** with the following differences:

- 26.7 mM stock solution of **1** was used, and the following amounts were added to each NMR tube:

**Table S19.** Amounts and concentrations of **1** used to collect rate data.

Final [ <b>1</b> ] (mM)	Volume of stock solution of <b>1</b> added	mmol <b>1</b> added	Volume of extra $\text{C}_7\text{D}_8$ added
1.67	38 $\mu\text{L}$	0.0010	0.26 mL
3.33	75 $\mu\text{L}$	0.0020	0.23 mL
6.67	150 $\mu\text{L}$	0.0040	0.15 mL
13.3	300 $\mu\text{L}$	0.0080	0 mL

- Only one trial for each concentration was run.

**Table S20.** Concentration of **8a** formed over time at differing initial concentrations of **1**.

[ <b>1</b> ] = 1.67 mM		[ <b>1</b> ] = 3.33 mM		[ <b>1</b> ] = 6.67 mM		[ <b>1</b> ] = 13.3 mM	
Time (s)	[ <b>8a</b> ] (mM)	Time (s)	[ <b>8a</b> ] (mM)	Time (s)	[ <b>8a</b> ] (mM)	Time (s)	[ <b>8a</b> ] (mM)
56	0.0482	56	0.1914	38	0.2415	38	0.2211
111	0.1417	112	0.3230	74	0.3444	76	0.3982
167	0.2846	168	0.4817	112	0.4166	113	0.5951
223	0.2960	224	0.5259	168	0.5226	151	0.8097
278	0.4259	281	0.6714	224	0.6818	188	1.0060
334	0.3496	336	0.9097	281	0.7620	225	1.1415
390	0.4662	392	0.8798	336	0.8998	262	1.1647
445	0.5721	448	0.9394	392	0.9893	319	1.4820
				449	1.1346	376	1.6773
						432	1.9192
						488	2.1106

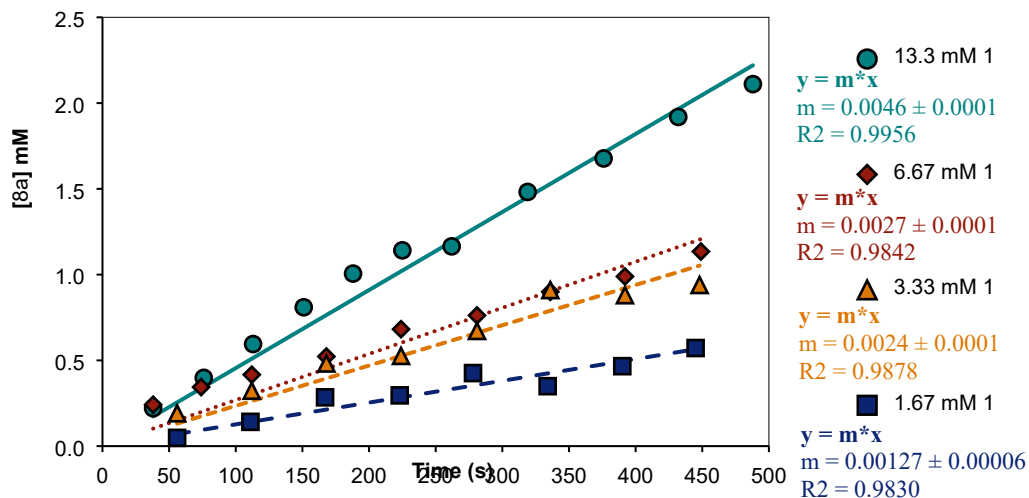


**Figure S17.** Rates of formation of **8a** at varying initial concentrations of **1**.

**Table S21.** Rates of formation of **8a** at varying initial concentrations of **1**.

[ <b>1</b> ] (mM)	$\Delta[8a]/\Delta t$ (mM/s)
1.67	$0.00127 \pm 0.00006$
3.33	$0.0024 \pm 0.0001$
6.67	$0.0027 \pm 0.0001$
13.3	$0.0046 \pm 0.0001$

The rates obtained were plotted as a function of the initial concentration of **1**. Using Microsoft Excel, the data were fit to a curve for the function  $y = Ax^b$ , where  $y$  = rate input,  $A = k_{\text{obs}}$  output,  $x = [\mathbf{1}]$  input, and  $b$  = order in **1**.

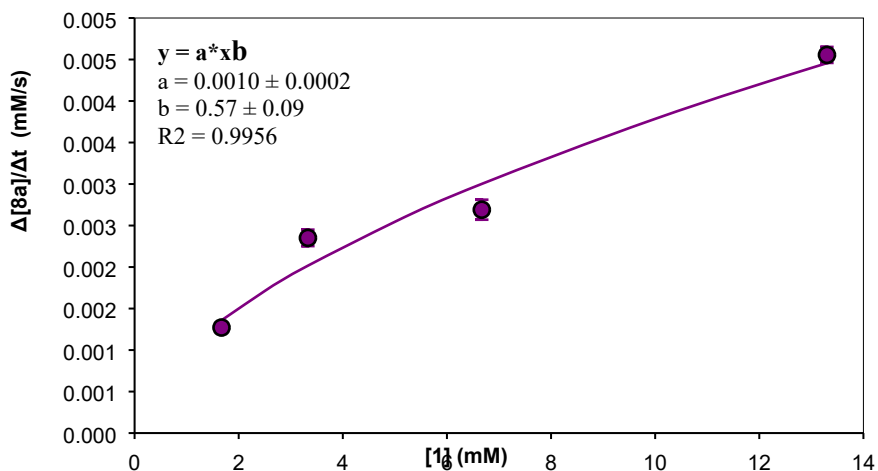
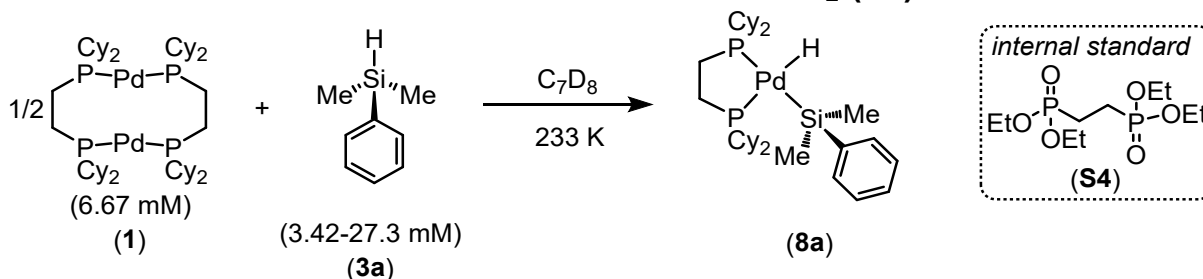


**Figure S18.** Order plot for **1**.

### c. Kinetics to measure the order in HSiPhMe<sub>2</sub> (**3a**)



General procedure D was followed using **3a** to form **8a** with the following differences:

- Four different stock solutions of **3a** were prepared, as detailed in Table S22 below and the following amounts were added to each NMR tube:

**Table S22.** Amounts and concentrations of **3a** used to collect rate data.

Final [ <b>3a</b> ] (mM)	Concentration of stock solution of <b>3a</b>	Volume of stock solution of <b>3a</b> added	mmol <b>3a</b> added
3.42 mM	13.7 mM	0.15 mL	0.0020
6.83 mM	27.3 mM	0.15 mL	0.0041
13.7 mM	54.7 mM	0.15 mL	0.0082
27.3 mM	109.3 mM	0.15 mL	0.0016

- Only one trial for each concentration was run.

**Table S23.** Concentration of **8a** formed over time at differing initial concentrations of **3a**.

[ <b>3a</b> ] = 3.42 mM		[ <b>3a</b> ] = 6.83 mM		[ <b>3a</b> ] = 13.7 mM		[ <b>3a</b> ] = 27.3 mM	
Time (s)	[ <b>8a</b> ] (mM)	Time (s)	[ <b>8a</b> ] (mM)	Time (s)	[ <b>8a</b> ] (mM)	Time (s)	[ <b>8a</b> ] (mM)
56	0.0797	56	0.0847	38	0.2415	36	0.5435
111	0.1290	112	0.1634	74	0.3444	73	0.7149
167	0.2506	168	0.1682	112	0.4166	111	1.1859
222	0.2206	224	0.3589	168	0.5226	149	1.3669
277	0.3356	280	0.4600	224	0.6818	187	1.8317
333	0.2475	336	0.5524	281	0.7620	242	1.8551
388	0.3264	393	0.6426	336	0.8998	299	2.2092
444	0.4135	449	0.7512	392	0.9893	355	2.5781
				449	1.1346	411	2.7020
						467	2.9994

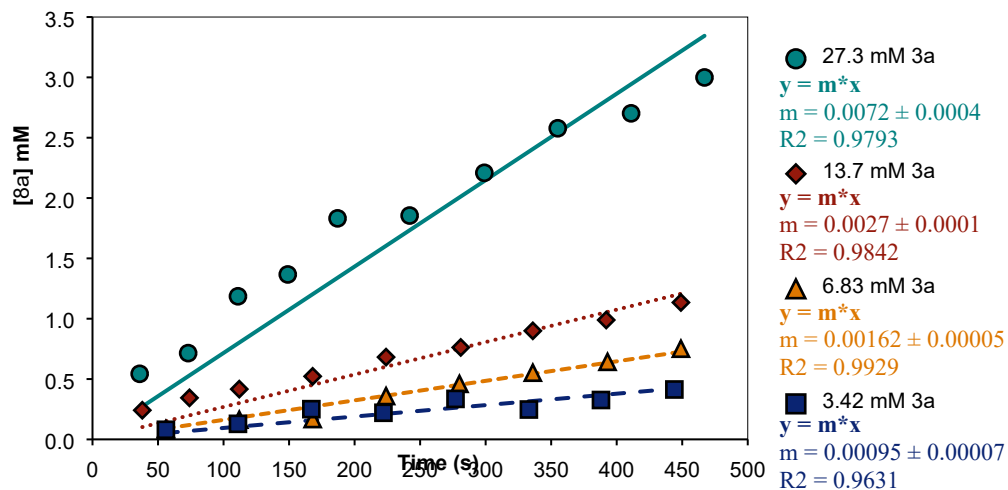


**Figure S19.** Rates of formation of **8a** at varying initial concentrations of **3a**.

**Table S24.** Rates of formation of **8a** at varying initial concentrations of **3a**.

[ <b>3a</b> ] (mM)	$\Delta[8a]/\Delta t$ (mM/s)
3.42	$0.00095 \pm 0.00007$
6.83	$0.00162 \pm 0.00005$
13.7	$0.0027 \pm 0.0001$
27.3	$0.0072 \pm 0.0004$

The rates obtained were plotted as a function of the initial concentration of **3a**. Using Microsoft Excel, the data were fit to a curve for the function  $y = Ax^b$ , where  $y$  = rate input,  $A = k_{\text{obs}}$  output,  $x = [\mathbf{3a}]$  input, and  $b$  = order in **3a**.

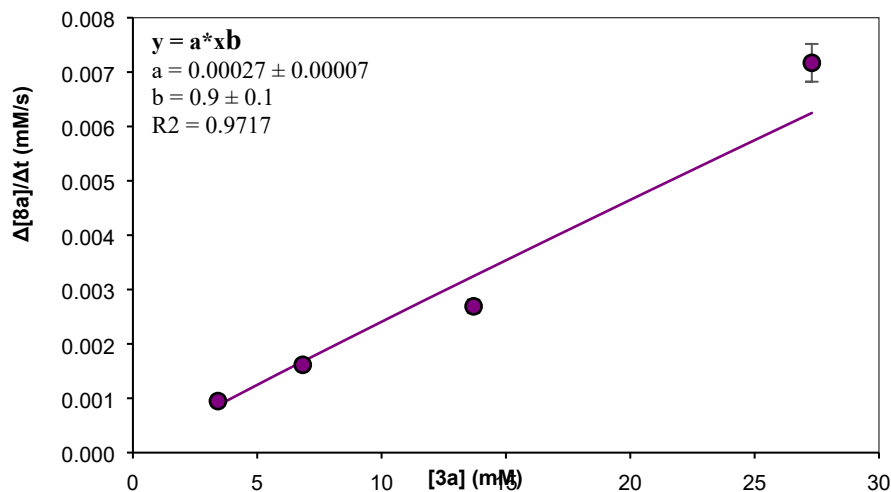
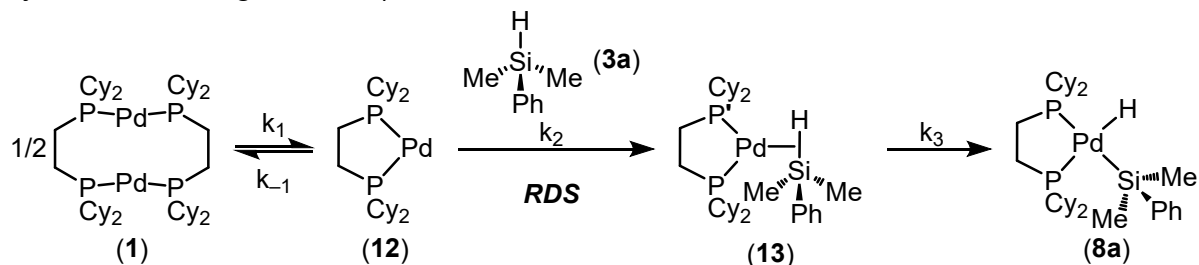


**Figure S20.** Order plot for **2**.

#### d. Derivation of the rate law

Using the results of the orders in **1** and **3a** (0.5<sup>th</sup> order and 1<sup>st</sup> order, respectively), and the proposal that formation of the  $\sigma$ -complex is rate-determining (as supported by dynamic exchange studies), we have derived the rate law.



$$\text{Rate} = k_2[3a][12]$$

Using the steady-state approximation:

$$\frac{d[12]}{dt} \approx 0 = k_1[1]^{0.5} - k_{-1}[12] - k_2[3a][12]$$

$$k_1[1]^{0.5} = (k_{-1} + k_2[3a])[12]$$

$$[12] = \frac{k_1[1]^{0.5}}{k_{-1} + k_2[3a]}$$

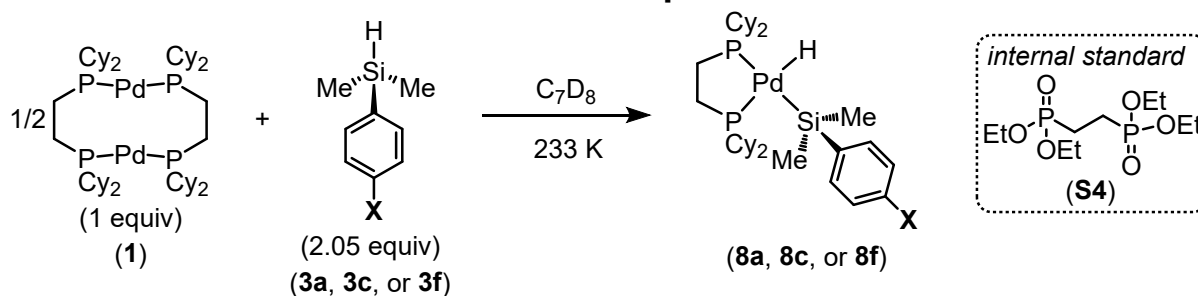
$$\text{Rate} = k_2[3a] \frac{k_1[1]^{0.5}}{k_{-1} + k_2[3a]}$$

Because  $k_2 \ll k_{-1}$ , the rate expression can be simplified to:

$$\text{Rate} = \frac{k_1 k_2}{k_{-1}} [3a][1]^{0.5}$$

This rate law is consistent with the proposed mechanism and the orders of **1** and **3a** obtained.

### e. Kinetics to construct a Hammett plot



General procedure D was followed using **3a**, **3c**, or **3f** to form **8a**, **8c**, or **8f**, respectively.

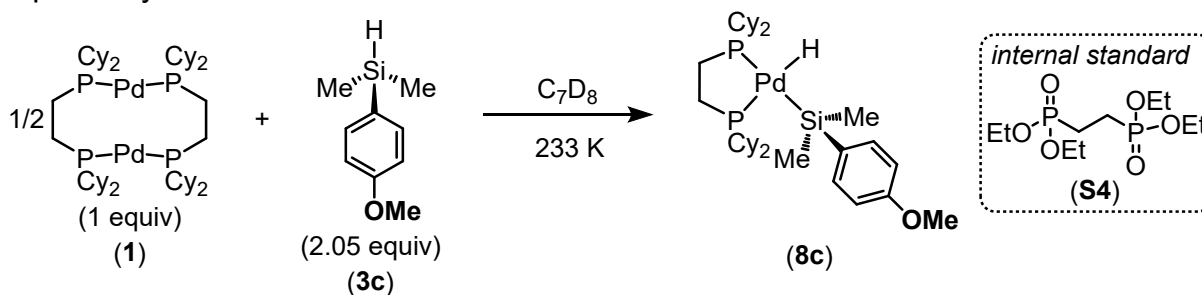


**Table S25.** Concentration of **8c** formed over time.

Trial 1		Trial 2	
Time (s)	[ <b>8c</b> ] (mM)	Time (s)	[ <b>8c</b> ] (mM)
56	0.0054	56	0.0191
112	0.0179	112	0.0525
166	0.0587	167	0.0166
222	0.0112	223	0.0089
277	0	315	0.0466
333	0.0444	435	0.0929
388	0	555	0.0662
444	0.0657	680	0.1050
499	0.0660	795	0.1468
555	0.1166	855	0.1246
610	0.0637	915	0.1063
665	0.1348	975	0.1391
721	0.0984	1035	0.1174
776	0.1508	1095	0.1678
832	0.1424	1155	0.2033
887	0.1101	1214	0.1819
942	0.0871	1275	0.1553
997	0.1202	1335	0.1626
1053	0.0965	1395	0.1980
1109	0.0846	1455	0.1724
1164	0.1259	1516	0.2265
1231	0.1757	1576	0.2162
1286	0.1850	1635	0.1872
1343	0.1344	1694	0.2458
1398	0.1493	1756	0.2192
1454	0.2011	1815	0.2079
1509	0.1772	1874	0.2713
1564	0.2159	1935	0.2237
1619	0.2011	1995	0.2652
1675	0.1544	2055	0.3155
1729	0.2326	2356	0.2598
1785	0.2356	2655	0.3055
1840	0.2197	2955	0.3492
1896	0.2635	3257	0.3831
1952	0.2368	3555	0.4059
2123	0.2437	3857	0.4187
		4158	0.4892
		4455	0.5089
		4764	0.5155
		5056	0.5457
		5357	0.5769

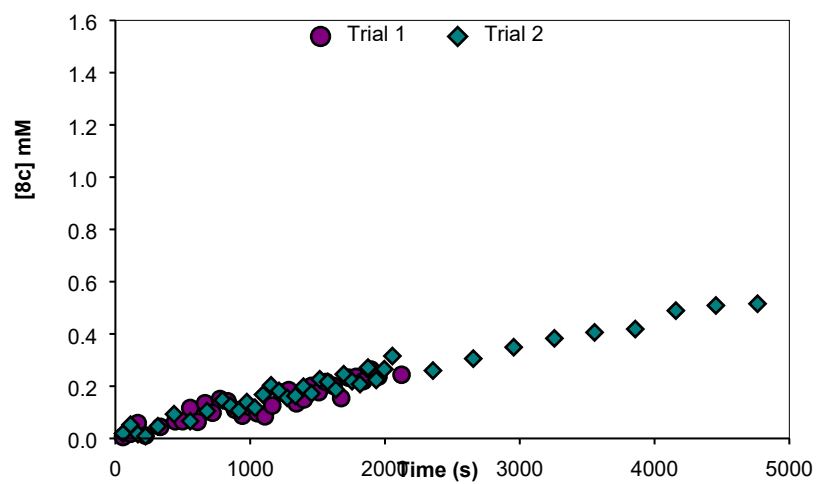


**Figure S21.** Rates of formation of **8c**.

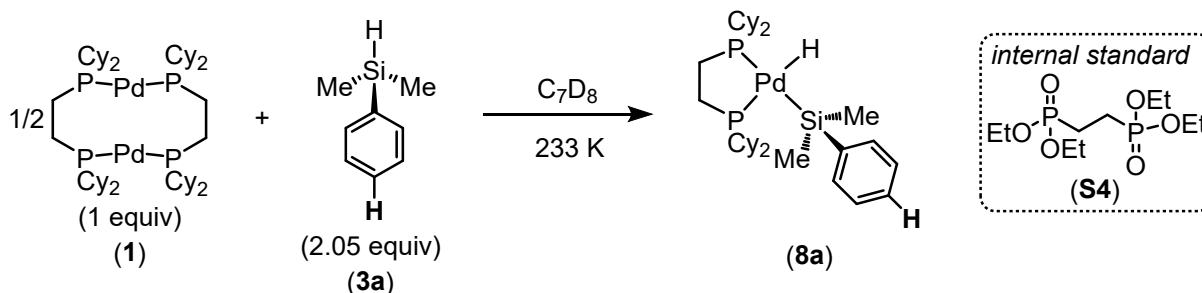


**Table S26.** Concentration of **8a** formed over time.

Trial 1		Trial 2		Trial 3	
Time (s)	[ <b>8a</b> ] (mM)	Time (s)	[ <b>8a</b> ] (mM)	Time (s)	[ <b>8a</b> ] (mM)
0	0.1088	0	0.0325	0	0.0778
57	0.2090	60	0.1591	38	0.2415
113	0.3863	118	0.2720	74	0.3444
170	0.5960	175	0.4790	112	0.4166
226	0.7661	232	0.4669	168	0.5226
282	0.9007	289	0.7464	224	0.6818
339	1.0294	345	0.9203	281	0.7620
397	1.2470	402	1.0393	336	0.8998
454	1.2398	458	1.1213	392	0.9893
509	1.3579	515	1.2794	449	1.1346
		571	1.4389	504	1.2262

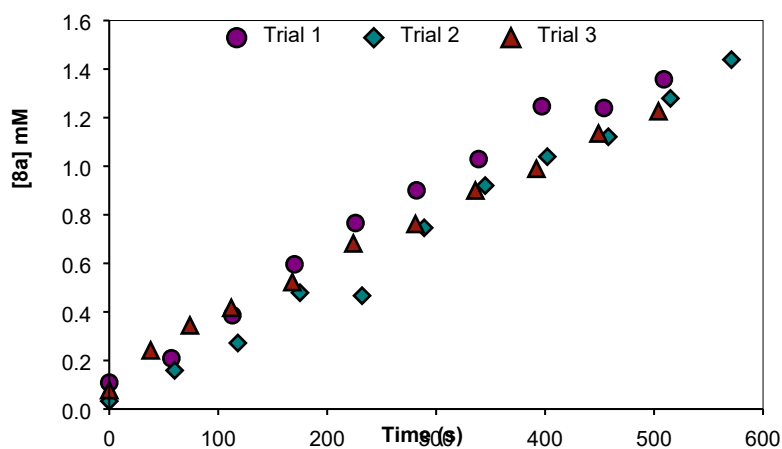


**Figure S22.** Rates of formation of **8a**.

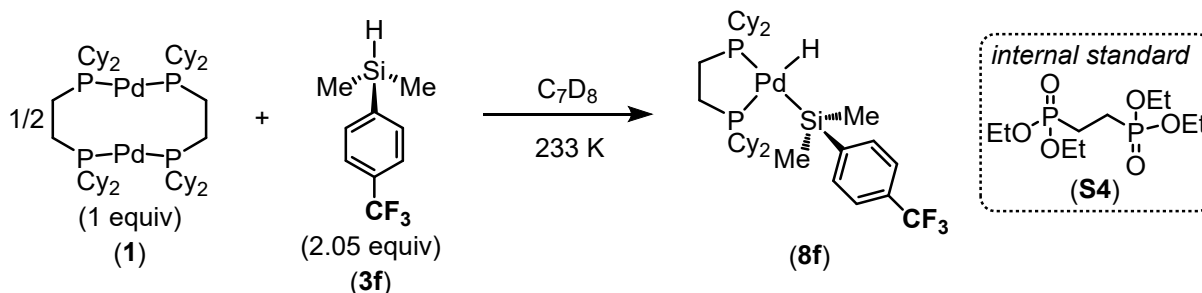


**Table S27.** Concentration of **8f** formed over time.

Trial 1		Trial 2		Trial 3	
Time (s)	[ <b>8f</b> ] (mM)	Time (s)	[ <b>8f</b> ] (mM)	Time (s)	[ <b>8f</b> ] (mM)
0	0.0306	0	0.1092	0	0.0158
38	0.1876	56	0.5301	56	0.3707
75	0.3414	112	0.6401	112	0.8267
112	0.4775	167	0.9010	168	0.9401
149	0.7208	223	1.0585	224	1.1622
186	0.9339	278	1.3505	280	1.3671
242	1.1145	334	1.6932	336	1.6690
298	1.4365	390	1.8090	393	1.7621
353	1.6156				
409	1.7155				

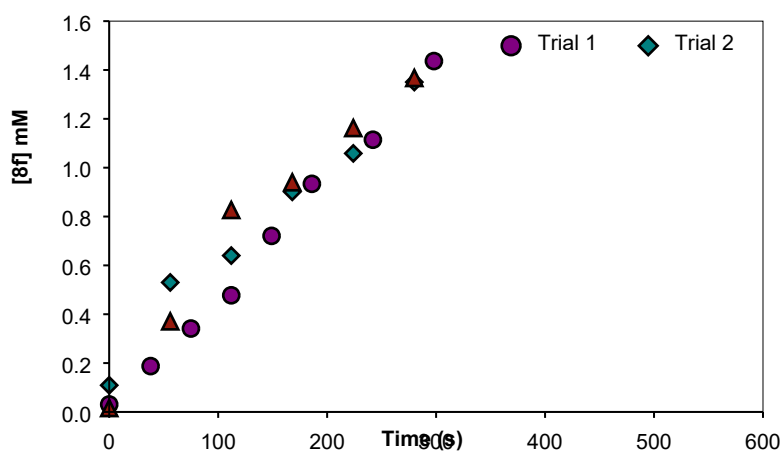


**Figure S23.** Rates of formation of **8f**.

To construct the kinetics Hammett plot for the aryl dimethyl silanes (**3**), values for  $\sigma_p$  were taken from reference 8. The values of  $\log(k_X/k_H)$  for X = OMe and CF<sub>3</sub> were plotted as a function of  $\sigma_p$ . Using Microsoft Excel, the data were fit to a curve for the function  $y = mx + b$ , where  $y = \log(k_X/k_H)$  input,  $m$  = sensitivity constant  $\rho$  output,  $x = \sigma_p$  input, and  $b$  = intercept output.

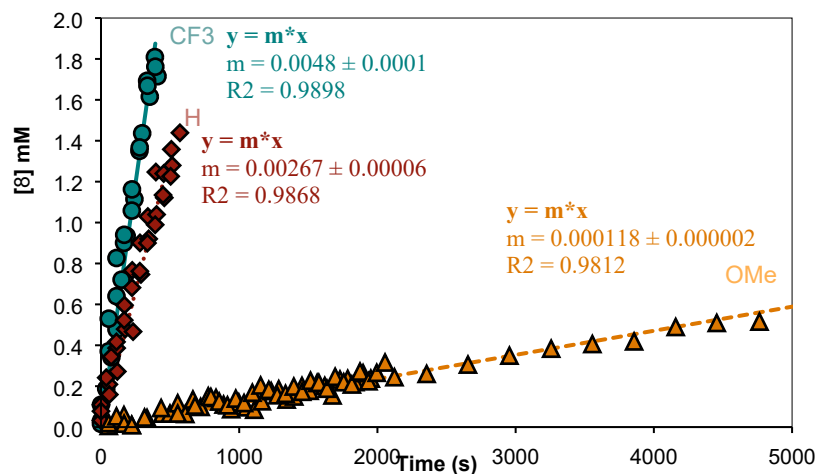


**Figure S24.** Combined rates of formation of **8a**, **8c**, and **8f**.

**Table S28.** Rates of formation of **8** as a function of electronic substitution.

X-group	Silane	$\sigma_p$	$\Delta[8]/\Delta t$ (mM/s)	$\log(k_X/k_H)$
-OMe	<b>3c</b>	-0.83	$0.000118 \pm 0.000002$	$-1.34 \pm 0.01$
-H	<b>3a</b>	0	$0.00267 \pm 0.00006$	0
-CF <sub>3</sub>	<b>3f</b>	0.54	$0.0048 \pm 0.0001$	$0.26 \pm 0.01$

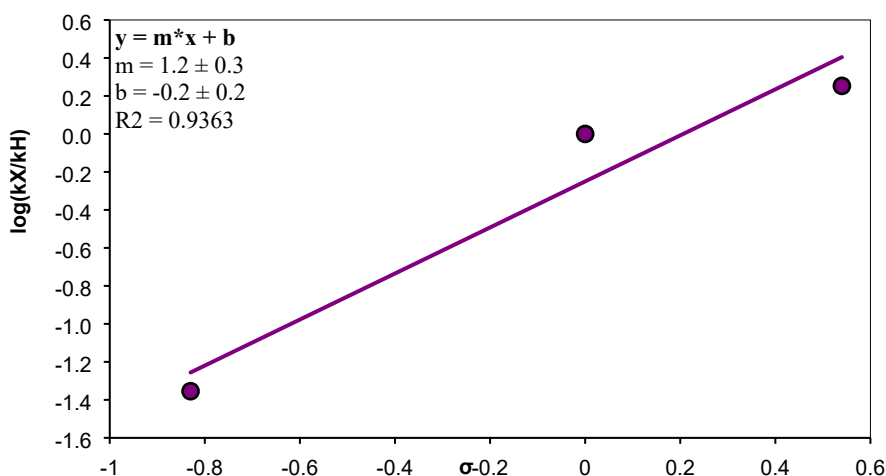
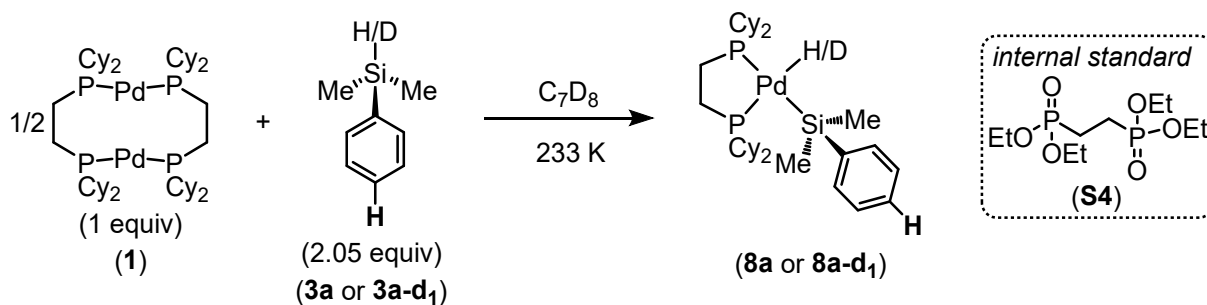


**Figure S25.** Rates Hammett plot using **3a**, **3c**, and **3f**.

## f. Kinetics to measure KIE



General procedure D was followed using **3a** or **3a-d<sub>1</sub>** to form **8a** or **8a-d<sub>1</sub>**, respectively.

**Table S29.** Formation of **8a** and **8a-d<sub>1</sub>** over time.

Silane	Trial 1		Trial 2		Trial 3	
	Time (s)	[ <b>8</b> ] (mM)	Time (s)	[ <b>8</b> ] (mM)	Time (s)	[ <b>8</b> ] (mM)
<b>3a</b>	0	0.1088	0	0.0325	0	0.0778
	57	0.2090	60	0.1591	38	0.2415
	113	0.3863	118	0.2720	74	0.3444
	170	0.5960	175	0.4790	112	0.4166
	226	0.7661	232	0.4669	168	0.5226
	282	0.9007	289	0.7464	224	0.6818
	339	1.0294	345	0.9203	281	0.7620
	397	1.2470	402	1.0393	336	0.8998
	454	1.2398	458	1.1213	392	0.9893
	509	1.3579	515	1.2794	449	1.1346
			571	1.4389	504	1.2262
<b>3a-d<sub>1</sub></b>	56	0.2859	56	0.1990		
	112	0.4918	112	0.1772		
	168	0.4858	168	0.4808		
	224	0.6662	224	0.6443		
	280	0.5858	279	0.6869		
	335	0.6832	334	0.7864		
	391	0.8585	390	0.9463		
	446	0.9203	446	1.0024		
	502	0.9660	502	1.1859		
	557	1.1495	558	1.2699		
	615	1.1952	616	1.3453		
	671	1.3905	672	1.5556		
			728	1.5565		

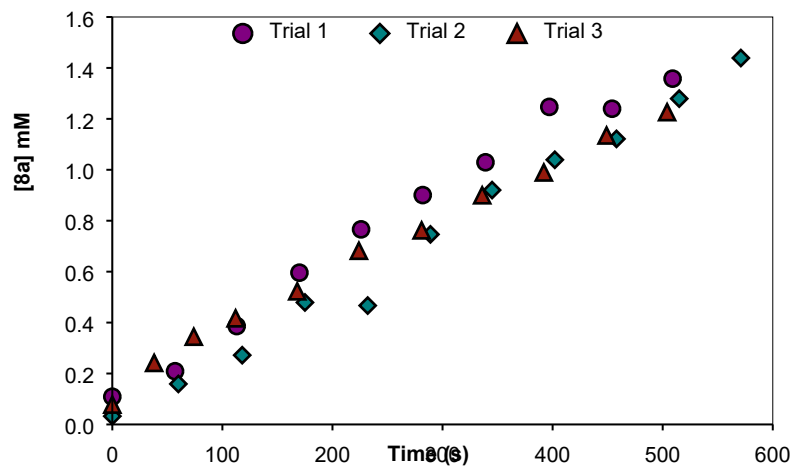


Figure S26. Rates of formation of 8a.

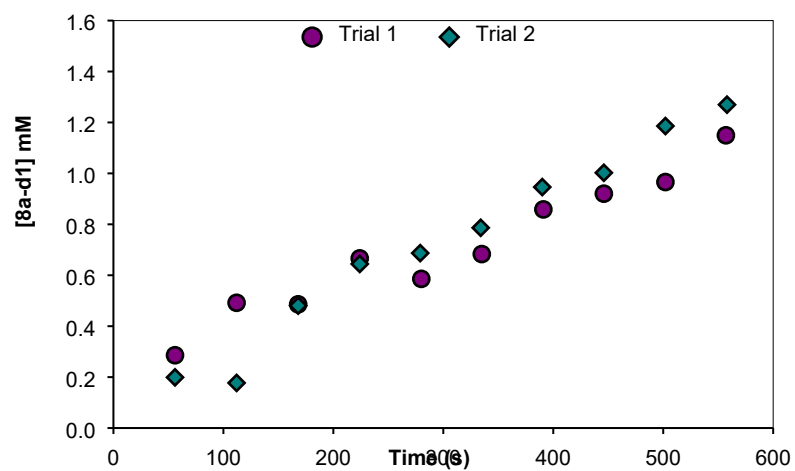


Figure S27. Rates of formation of 8a-d<sub>1</sub>.

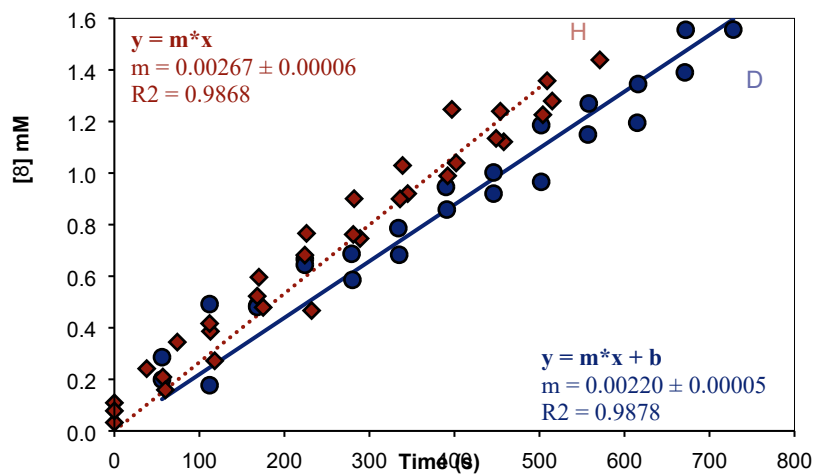


Figure S28. Combined rates of formation of 8a and 8a-d<sub>1</sub>.

The KIE was determined as follows:

$$KIE = \frac{k_H}{k_D} = \frac{Rate_H}{Rate_D} = \frac{0.00267 \pm 0.00006 \text{ mM} \cdot \text{s}^{-1}}{0.00220 \pm 0.00005 \text{ mM} \cdot \text{s}^{-1}} = 1.21 \pm 0.04$$

The assumption used above that:

$$\frac{k_H}{k_D} = \frac{Rate_H}{Rate_D}$$

is true if and only if the reactions with **3a** and **3a-d<sub>1</sub>** undergo the same mechanism, which we assume to be true.

The maximum KIE for Si-H/D without invoking tunneling was determined using the following equation:<sup>9</sup>

$$KIE_{max} = e^{\frac{h * c * \Delta\bar{\nu}}{k_B * T}}$$

Where...

$h = 6.63 \times 10^{-34} \text{ J} \cdot \text{s}$  (Planck's constant)

$c = 2.998 \times 10^{10} \text{ cm} \cdot \text{s}^{-1}$  (Speed of light)

$\Delta\bar{\nu} = \bar{\nu}_H - \bar{\nu}_D$

$\bar{\nu}_H =$  Stretching frequency of the Si-H bond ( $\text{cm}^{-1}$ )

$\bar{\nu}_D =$  Stretching frequency of the Si-D bond ( $\text{cm}^{-1}$ )

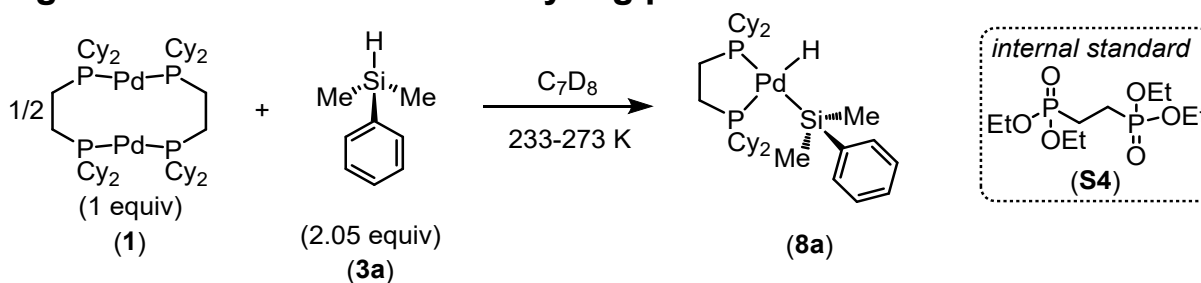
$k_B = 1.38 \times 10^{-23} \text{ J} \cdot \text{K}^{-1}$  (Boltzmann constant)

$T =$  Temperature (K)

For **3a**,  $\bar{\nu}_H = 2116 \text{ cm}^{-1}$ ; for **3a-d<sub>1</sub>**,  $\bar{\nu}_D = 1539 \text{ cm}^{-1}$ . Calculated at 298 K (the temperature at which the IR spectra were measured):

$$KIE_{max} = e^{\frac{(6.63 \times 10^{-34} \text{ J} \cdot \text{K}^{-1}) * (3.0 \times 10^{10} \text{ cm} \cdot \text{s}^{-1}) * (2118 \text{ cm}^{-1} - 1539 \text{ cm}^{-1})}{(1.38 \times 10^{-23} \text{ J} \cdot \text{K}^{-1}) * (298 \text{ K})}} = 4.0$$

### g. Kinetics to construct an Eyring plot



General procedure D was followed with the following exception:

- Only one trial was used for reactions run at 243 K, 253 K, and 273 K.

<b>Table S30.</b> Formation of <b>8a</b> over time at varying temperatures.						
Temperature	Trial 1		Trial 2		Trial 3	
	Time (s)	[ <b>8a</b> ] (mM)	Time (s)	[ <b>8a</b> ] (mM)	Time (s)	[ <b>8a</b> ] (mM)
233 K	0	0.1088	0	0.0325	0	0.0778
	57	0.2090	60	0.1591	38	0.2415
	113	0.3863	118	0.2720	74	0.3444
	170	0.5960	175	0.4790	112	0.4166
	226	0.7661	232	0.4669	168	0.5226
	282	0.9007	289	0.7464	224	0.6818
	339	1.0294	345	0.9203	281	0.7620
	397	1.2470	402	1.0393	336	0.8998
	454	1.2398	458	1.1213	392	0.9893
	509	1.3579	515	1.2794	449	1.1346
			571	1.4389	504	1.2262
243 K	0	0.2810				
	56	0.4321				
	111	0.8016				
	166	0.9961				
	222	1.3490				
	277	1.5313				
	332	1.9193				
	388	2.0927				
	443	2.2490				
	498	2.5314				
	554	2.4752				
	609	2.7544				
	666	3.0016				
253 K	0	0.1925				
	55	0.4346				
	110	0.9858				
	165	1.3520				
	221	1.8490				
	276	2.1120				
	332	2.4947				
	386	2.7399				
	442	3.0543				
273 K	0	0.1594				
	26	0.8862				
	63	1.6262				
	99	2.2059				
	154	3.0748				

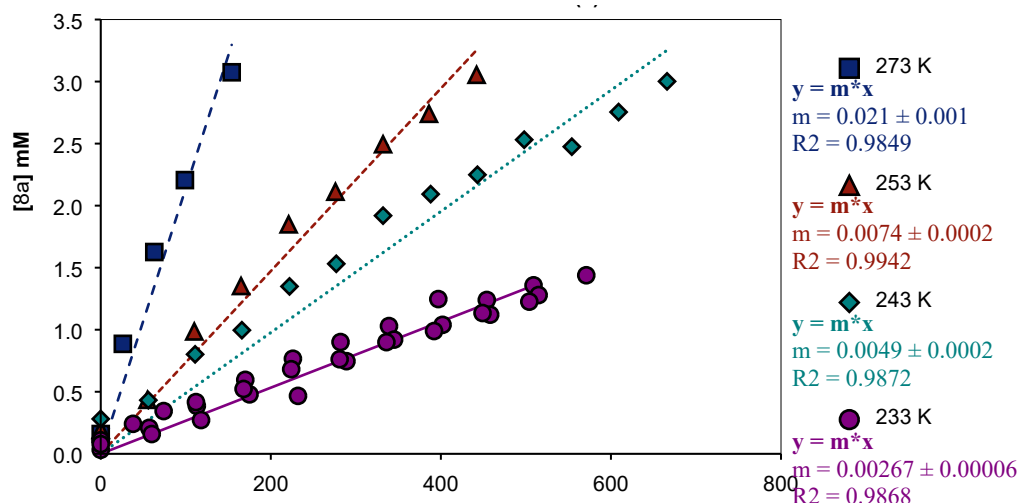


**Figure S29.** Rates of formation of **8a** at varying temperatures.

**Table S31.** Rates of formation of **8a** at varying temperatures.

Temperature	1/T (K <sup>-1</sup> )	Δ[8a]/Δt (mM/s)	ln(k/T)
233 K	0.00429	0.00267 ± 0.00005	-11.37 ± 0.02
243 K	0.00412	0.0049 ± 0.0002	-10.81 ± 0.03
253 K	0.00395	0.0074 ± 0.0002	-10.44 ± 0.03
273 K	0.00366	0.021 ± 0.001	-9.45 ± 0.06

To construct the Eyring plot,  $\ln(K_{eq})$  was plotted as a function of  $1/T$ . Using Microsoft Excel, the data were fit to a curve for the function  $y = mx + b$ , where  $y = \ln(K_{eq})$  input,  $m = -\Delta H \cdot R^{-1}$  output,  $x = T^{-1}$  input, and  $b = \Delta S \cdot R^{-1}$  output, as illustrated below.

$$\ln(K_{eq}) = \left( \frac{-\Delta H^\ddagger}{R} \right) \left( \frac{1}{T} \right) + \frac{\Delta S^\ddagger}{R} + \ln \left( \frac{k_B}{h} \right)$$

$$y = (m)(x) + b$$

Where...

$$\begin{aligned} R &= 0.001987 \text{ kcal} \cdot \text{mol}^{-1} \cdot \text{K}^{-1} && \text{(Ideal gas constant)} \\ k_B &= 1.38 \times 10^{-23} \text{ J} \cdot \text{K}^{-1} && \text{(Boltzmann constant)} \\ h &= 6.63 \times 10^{-34} \text{ J} \cdot \text{s} && \text{(Planck's constant)} \end{aligned}$$

Gibbs free energy of activation was determined using the following equation:

$$\Delta G^\ddagger = \Delta H^\ddagger - T\Delta S^\ddagger$$

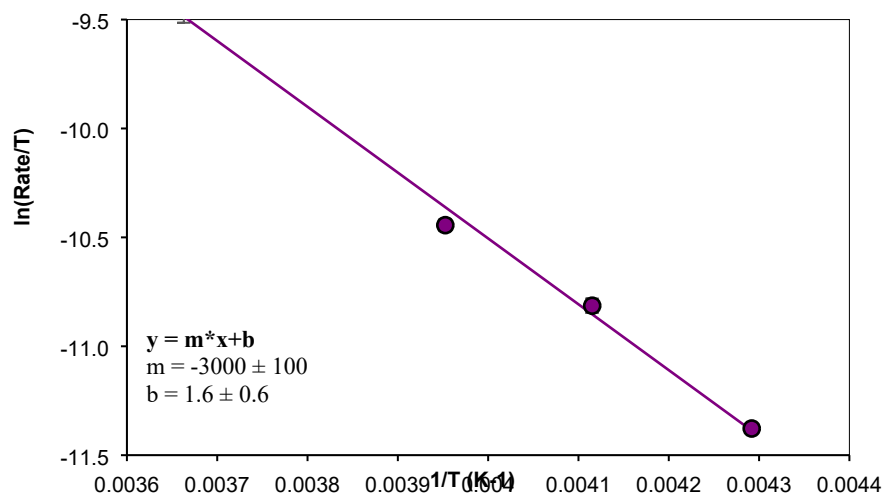


**Figure S30.** Eyring plot for **8a**.

$$\begin{aligned} \Delta H^\ddagger &= 6.0 \pm 0.3 && \text{kcal} \cdot \text{mol}^{-1} \\ \Delta S^\ddagger &= -40 \pm 20 && \text{cal} \cdot \text{mol}^{-1} \cdot \text{K}^{-1} \\ \Delta G^\ddagger_{298\text{K}} &= 19.1 \pm 0.3 && \text{kcal} \cdot \text{mol}^{-1} \\ \Delta G^\ddagger_{233\text{K}} &= 16.3 \pm 0.3 && \text{kcal} \cdot \text{mol}^{-1} \end{aligned}$$

## 10. Dynamic Behavior

### a. Reaction setup, data, spectra, and analysis

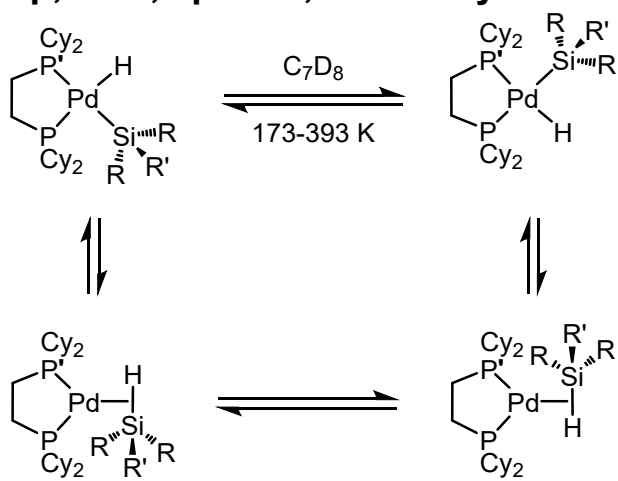


**Figure S31.** Proposed mechanism of dynamic exchange.

General procedure B was followed to generate the (silyl)Pd(H) species in solution with the exception that larger temperature ranges were examined. Activation parameters were estimated by the bandwidth method.<sup>10, 11</sup>

At cold temperatures, the exchange of ligand environments is slow on the NMR timescale, and two distinct peaks can be observed in  $^{31}\text{P}\{^1\text{H}\}$  NMR spectra. The rate of such slow exchange can be approximated as:

$$k = \pi[(\Delta v_e)_{1/2} - (\Delta v_0)_{1/2}]$$

Where  $(\Delta v_e)_{1/2}$  is the width at half-height (WHH) of a peak that is broadened as a consequence of exchange at low temperatures, and  $(\Delta v_0)_{1/2}$  is the WHH of the same peak at a temperature where broadening due to exchange is negligible.

At slightly warmer temperatures, the rate of exchange begins to transition from slow on the NMR timescale to fast on the NMR timescale. Between those two regimes is the point of coalescence, at which  $^{31}\text{P}\{^1\text{H}\}$  NMR spectra changes from two distinct peaks to one broad, ill-defined peak that is not resolved from the baseline. At this temperature, which varies based on the silane examined, rate can be approximated:

$$k = \frac{\pi \Delta v_0}{\sqrt{2}}$$

Where  $\Delta v_0$  is the separation (in Hz) between the two distinct peaks present in NMR spectra of a system in slow exchange. At temperatures above coalescence, exchange enters a regime that is fast on the NMR timescale and spectra show only a single peak. Within this regime, rate can be approximated:

$$k = \frac{\pi \Delta v_0^2}{2} [(\Delta v_e)_{1/2} - (\Delta v_0)_{1/2}]^{-1}$$

At a temperature within the fast regime, the peak of interest will be the least broadened due to exchange. At this temperature, the rate is simplified and can be approximated as:

$$k = \frac{\pi \Delta \nu_0^2}{2}$$

Using these equations in analysis of  $^{31}\text{P}\{^1\text{H}\}$  NMR spectra, the rate of exchange was determined for a range of temperatures, and Eyring plots were constructed to determine the activation parameters for this dynamic exchange process. See above section on the method for data analysis for Eyring plots.

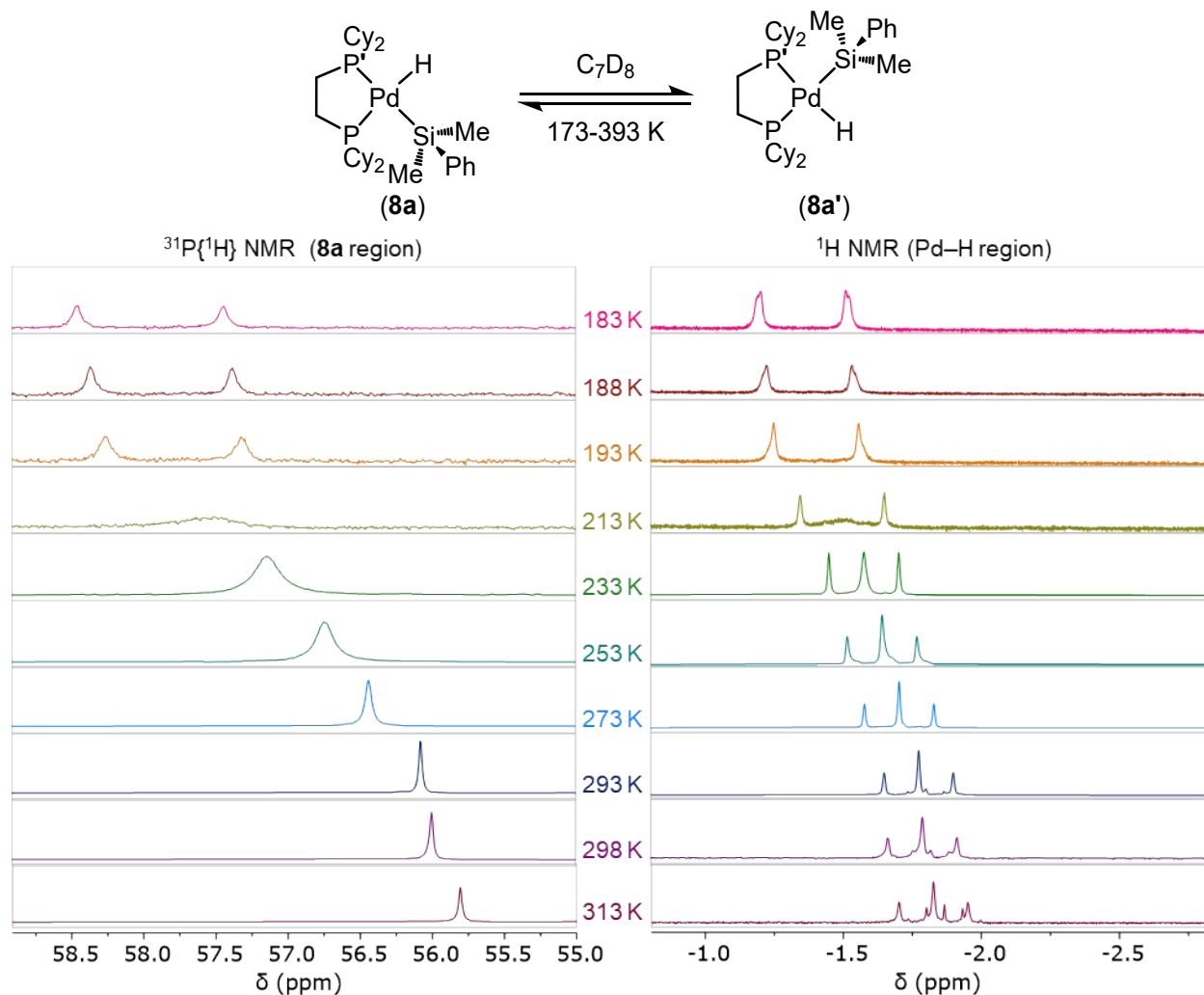


**Figure S32.**  $^{31}P\{^1H\}$  NMR spectra of **8a** at variable temperature.

**Table S32.** Rates of dynamic exchange of **8a/8a'** at varying temperatures.

Temperature (K)	1/T (K <sup>-1</sup> )	k (rate)	ln(k/T)
188	0.00532	21.1	-2.19
193	0.00518	42.7	-1.51
213	0.00470	245	0.142
233	0.00429	1460	1.84
253	0.00395	2300	2.21
273	0.00366	9680	3.57
293	0.00341	66200	5.42
298	0.00336	63700	5.36
313	0.00320	221000	6.56

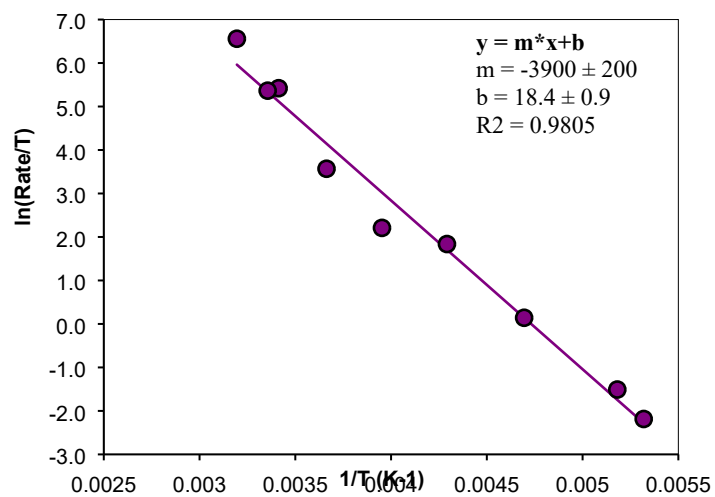


**Figure S33.** Eyring plot for dynamic exchange of **8a**.

$$\begin{aligned} \Delta H_{\text{DE}}^{\ddagger} &= 7.7 \pm 0.4 \quad \text{kcal} \cdot \text{mol}^{-1} \\ \Delta S_{\text{DE}}^{\ddagger} &= -10.7 \pm 0.5 \quad \text{cal} \cdot \text{mol}^{-1} \cdot \text{K}^{-1} \\ \Delta G_{\text{DE}(298\text{K})}^{\ddagger} &= 10.9 \pm 0.4 \quad \text{kcal} \cdot \text{mol}^{-1} \\ \Delta G_{\text{DE}(233\text{K})}^{\ddagger} &= 10.2 \pm 0.4 \quad \text{kcal} \cdot \text{mol}^{-1} \end{aligned}$$

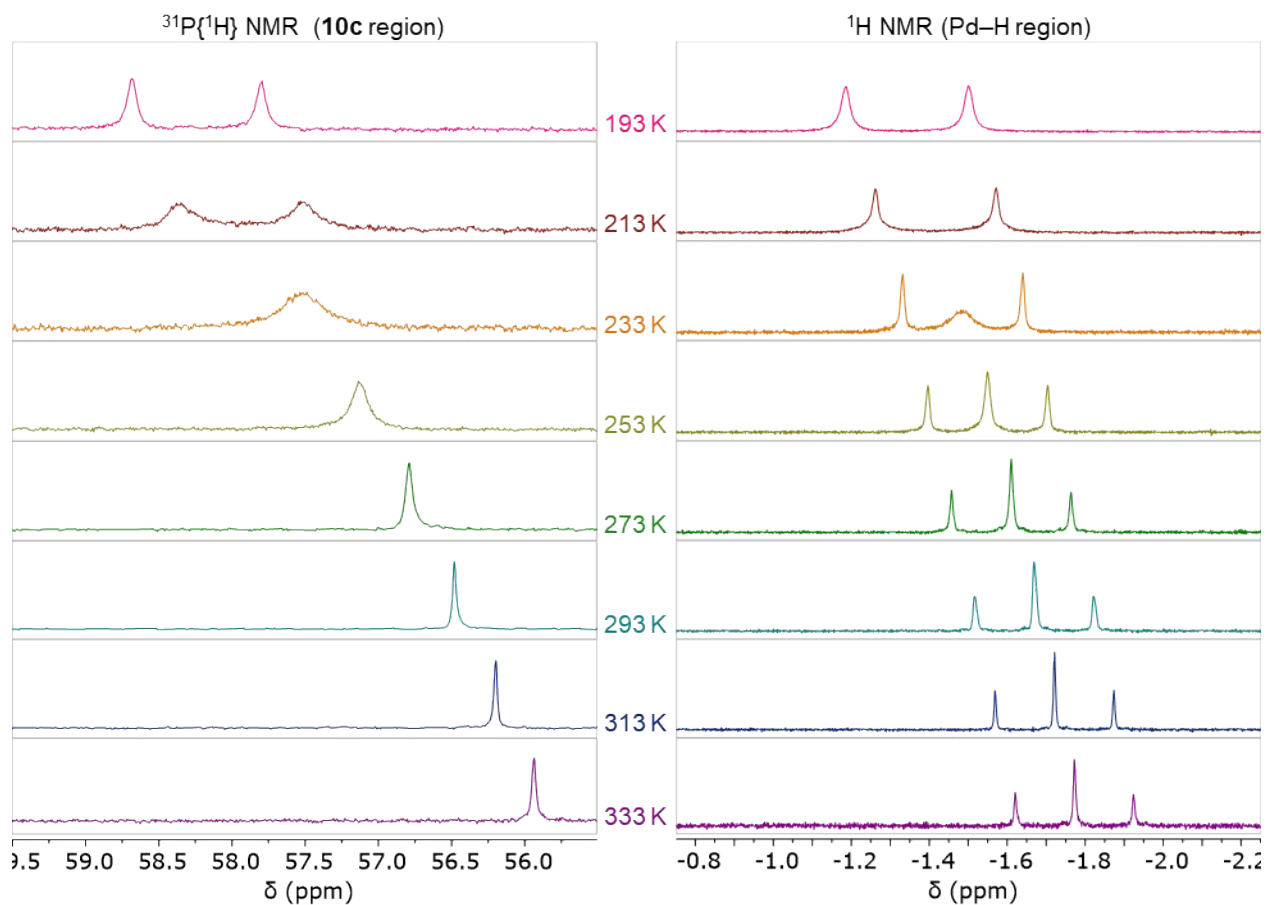
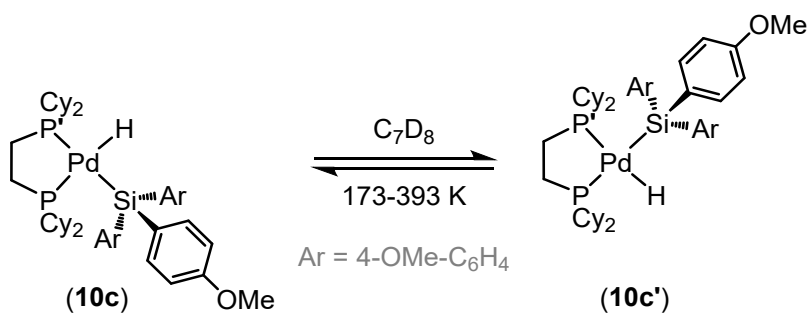


**Figure S34.**  $^{31}\text{P}\{^1\text{H}\}$  NMR spectra of **10c** at variable temperature.

**Table S33.** Rates of dynamic exchange of **10c/10c'** at varying temperatures.

Temperature (K)	1/T (K <sup>-1</sup> )	k (rate)	ln(k/T)
233	0.00429	414	0.576
253	0.00395	2500	2.29
273	0.00366	9430	3.54
293	0.00341	54700	5.23
313	0.00320	133000	6.05

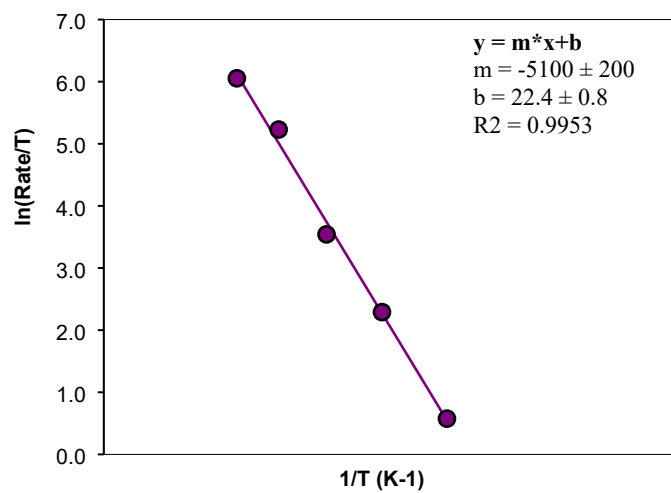


**Figure S35.** Eyring plot for dynamic exchange of **10c**.

$$\begin{aligned}
 \Delta H_{\text{DE}}^{\ddagger} &= 10.1 \pm 0.4 && \text{kcal} \cdot \text{mol}^{-1} \\
 \Delta S_{\text{DE}}^{\ddagger} &= -2.80 \pm 0.09 && \text{cal} \cdot \text{mol}^{-1} \cdot \text{K}^{-1} \\
 \Delta G_{\text{DE}(298\text{K})}^{\ddagger} &= 10.9 \pm 0.4 && \text{kcal} \cdot \text{mol}^{-1} \\
 \Delta G_{\text{DE}(233\text{K})}^{\ddagger} &= 10.7 \pm 0.4 && \text{kcal} \cdot \text{mol}^{-1}
 \end{aligned}$$

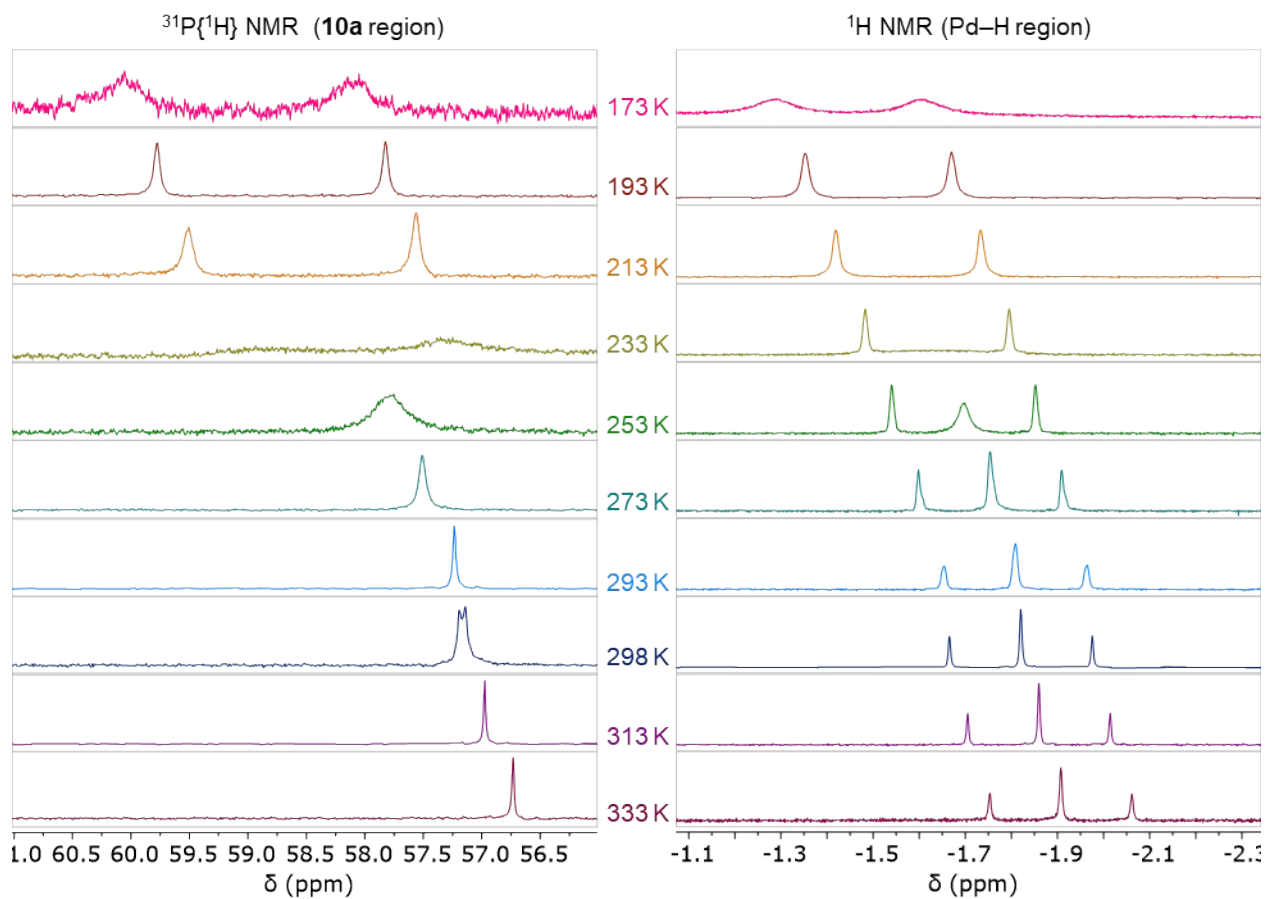
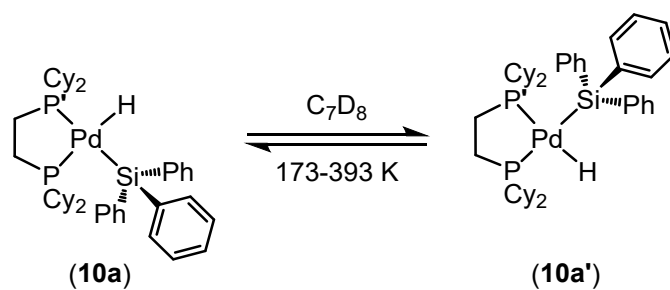


**Figure S36.**  $^{31}\text{P}\{^1\text{H}\}$  NMR spectra of **10a** at variable temperature.

**Table S34.** Rates of dynamic exchange of **10a/10a'** at varying temperatures.

Temperature (K)	1/T (K <sup>-1</sup> )	k (rate)	ln(k/T)
213	0.00470	45.8	-1.54
233	0.00429	355	0.421
253	0.00395	895	1.26
273	0.00366	24700	4.50
293	0.00341	127000	6.07
313	0.00320	255000	6.70

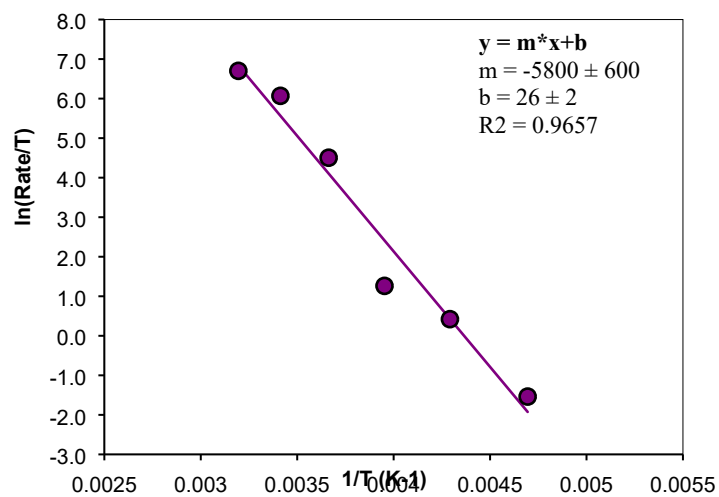


**Figure S37.** Eyring plot for dynamic exchange of **10a**.

$$\begin{aligned} \Delta H^\ddagger_{\text{DE}} &= 12 \pm 1 && \text{kcal} \cdot \text{mol}^{-1} \\ \Delta S^\ddagger_{\text{DE}} &= 3.5 \pm 0.3 && \text{cal} \cdot \text{mol}^{-1} \cdot \text{K}^{-1} \\ \Delta G^\ddagger_{\text{DE}(298\text{K})} &= 11 \pm 1 && \text{kcal} \cdot \text{mol}^{-1} \\ \Delta G^\ddagger_{\text{DE}(233\text{K})} &= 11 \pm 1 && \text{kcal} \cdot \text{mol}^{-1} \end{aligned}$$

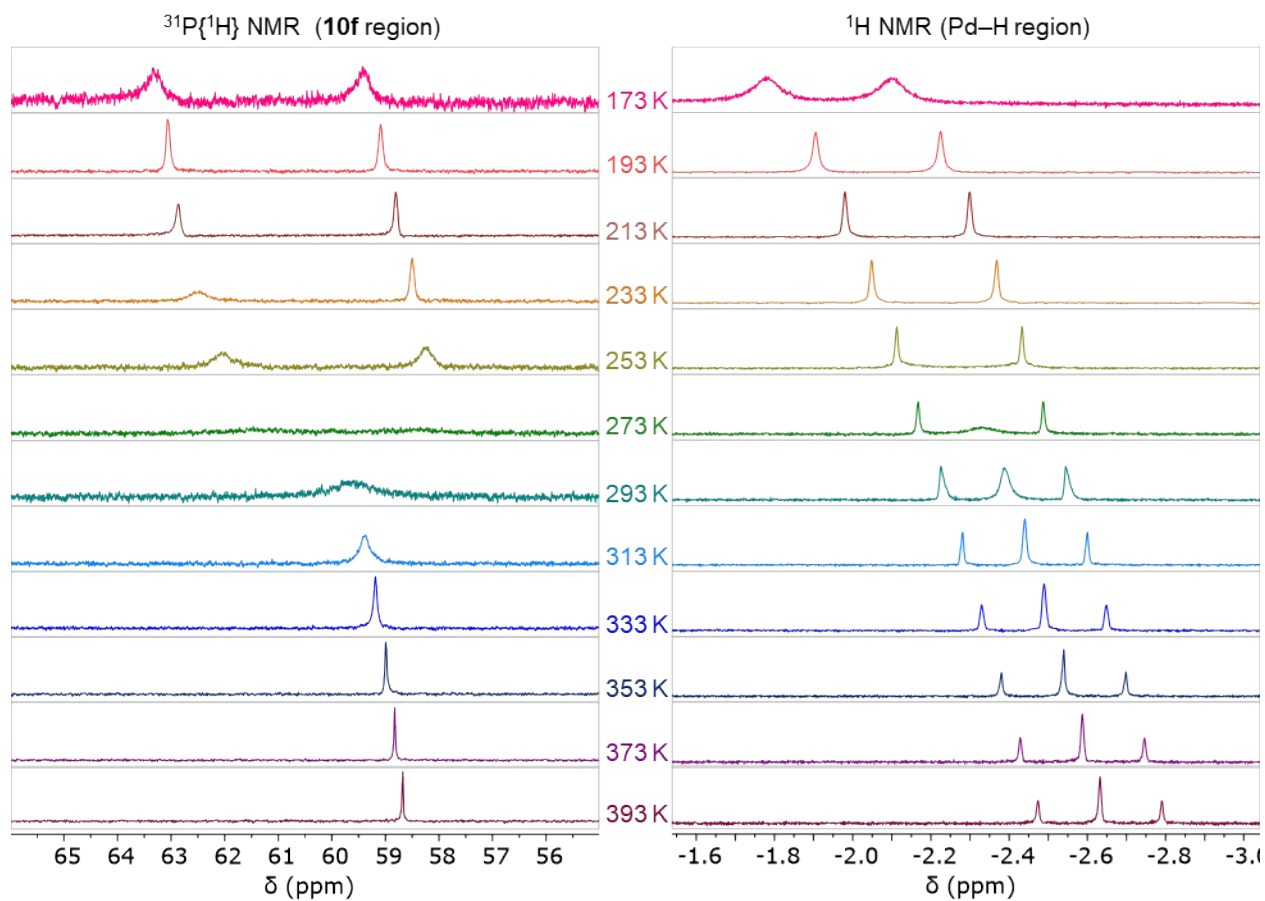
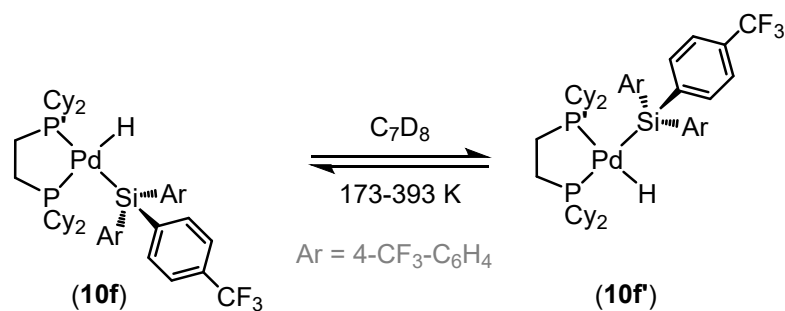


**Figure S38.**  $^{31}\text{P}\{^1\text{H}\}$  NMR spectra of **10f** at variable temperature.

**Table S35.** Rates of dynamic exchange of **10f/10f'** at varying temperatures.

Temperature (K)	1/T (K <sup>-1</sup> )	k (rate)	ln(k/T)
253	0.00395	151	-0.514
273	0.00366	653	0.873
313	0.00320	24100	4.34
333	0.00300	102000	5.73
353	0.00283	283000	6.69
373	0.00268	138000	8.21

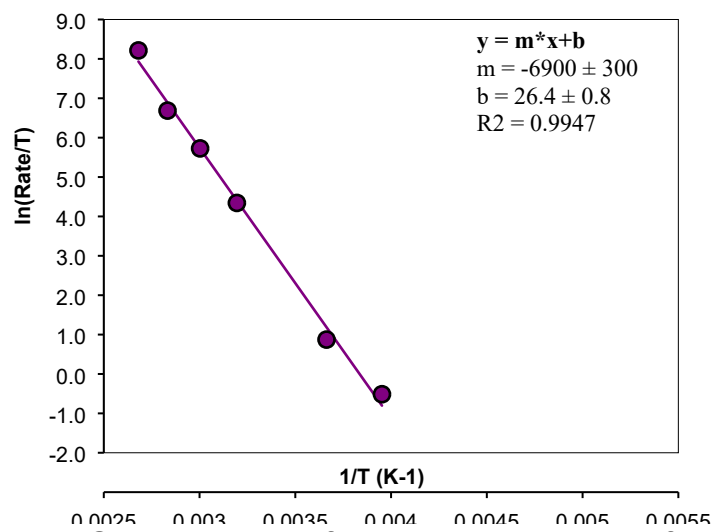


**Figure S39.** Eyring plot for dynamic exchange of **10f**.

$$\begin{aligned}
 \Delta H_{\text{DE}}^{\ddagger} &= 13.6 \pm 0.5 && \text{kcal} \cdot \text{mol}^{-1} \\
 \Delta S_{\text{DE}}^{\ddagger} &= 5.2 \pm 0.2 && \text{cal} \cdot \text{mol}^{-1} \cdot \text{K}^{-1} \\
 \Delta G_{\text{DE}(298\text{K})}^{\ddagger} &= 12.1 \pm 0.5 && \text{kcal} \cdot \text{mol}^{-1} \\
 \Delta G_{\text{DE}(233\text{K})}^{\ddagger} &= 12.5 \pm 0.5 && \text{kcal} \cdot \text{mol}^{-1}
 \end{aligned}$$

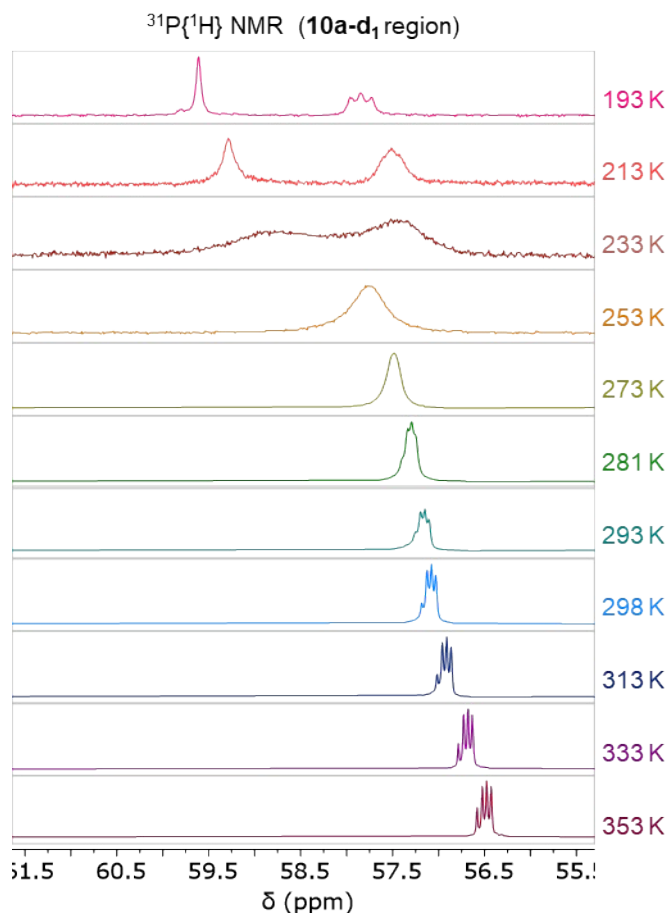
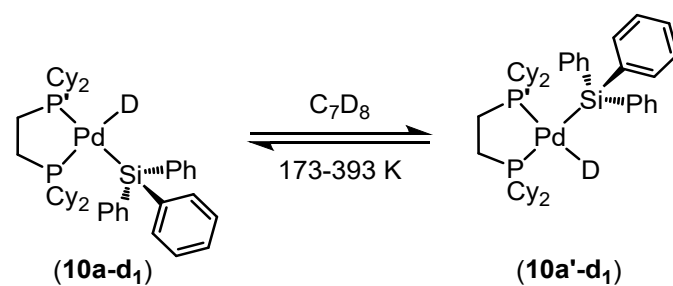


**Figure S40.** <sup>31</sup>P{<sup>1</sup>H} NMR spectra of **10a-d<sub>1</sub>** at variable temperature.

**Table S36.** Rates of dynamic exchange of **10a-d<sub>1</sub>/10a-d<sub>1</sub>'** at varying temperatures.

Temperature (K)	1/T (K <sup>-1</sup> )	k (rate)	ln(k/T)
213	0.00470	101	-0.747
233	0.00429	570	0.895
253	0.00395	2550	2.31
273	0.00366	12400	3.81
281	0.00356	31960	4.73
293	0.00341	39900	4.91
298	0.00336	108000	5.90
313	0.00320	199600	6.46
333	0.00300	814000	7.80

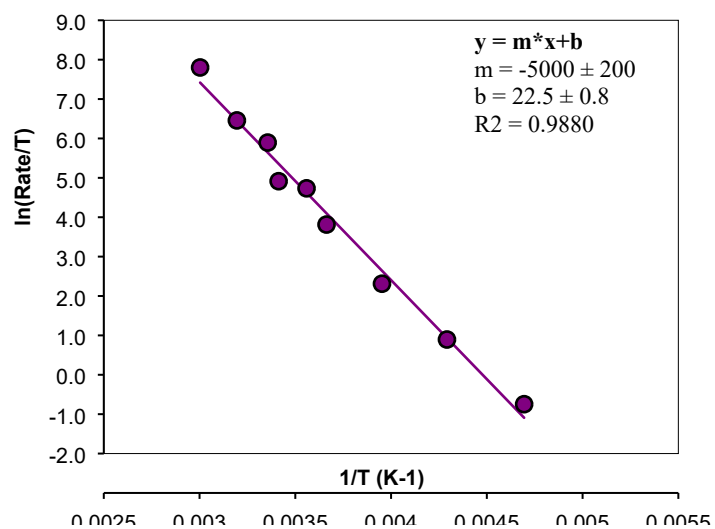


**Figure S41.** Eyring plot for dynamic exchange of **10a-d<sub>1</sub>**.

$$\begin{aligned}
 \Delta H_{\text{DE}}^{\ddagger} &= 10.0 \pm 0.4 && \text{kcal} \cdot \text{mol}^{-1} \\
 \Delta S_{\text{DE}}^{\ddagger} &= -2.46 \pm 0.09 && \text{cal} \cdot \text{mol}^{-1} \cdot \text{K}^{-1} \\
 \Delta G_{\text{DE}(298\text{K})}^{\ddagger} &= 10.7 \pm 0.4 && \text{kcal} \cdot \text{mol}^{-1} \\
 \Delta G_{\text{DE}(233\text{K})}^{\ddagger} &= 10.6 \pm 0.4 && \text{kcal} \cdot \text{mol}^{-1}
 \end{aligned}$$

## b. Rates of dynamic exchange as a function of concentration

General procedure B was followed to generate **10f** in solution with the exception that larger temperature ranges were examined, and different concentrations were used. For the final concentration of 6.67 mM **10f**, 0.15 mL of a 13.33 mM stock solution of **1** was used (0.002 mmol, 1.0 equiv), 0.15 mL of a 27.33 mM stock solution of **5f** was used (0.0041 mmol, 2.05 equiv), and 0.3 mL of additional C<sub>7</sub>D<sub>8</sub> was added to achieve the final desired concentration. For the final concentration of 26.7 mM **10f**, 0.3 mL of a 26.67 mM stock solution of **1** was used (0.008 mmol, 1.0 equiv) and 0.3 mL of a 54.67 mM stock solution of **5f** was used (0.0164 mmol, 2.05 equiv) to achieve the final desired concentration.

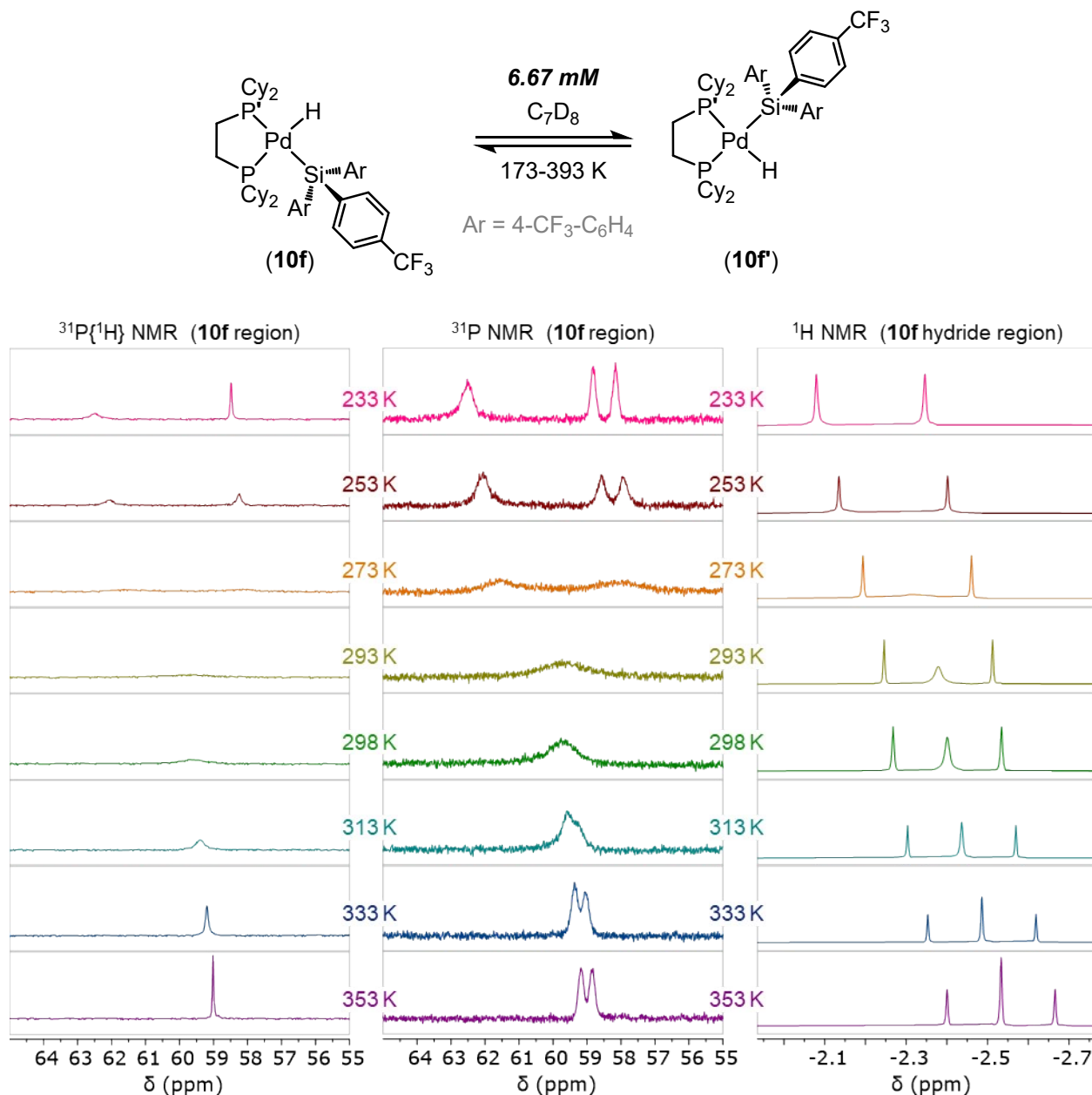
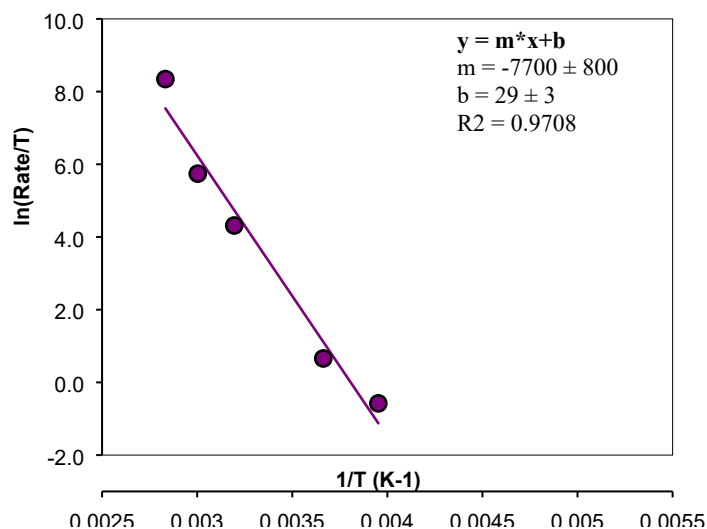


Figure S42. <sup>31</sup>P{<sup>1</sup>H}, <sup>31</sup>P, and <sup>1</sup>H NMR spectra of **10f** (6.67 mM) at variable temperature.

**Table S37.** Rates of dynamic exchange of **10f/10f'** (6.67 mM) at varying temperatures.

Temperature (K)	1/T (K <sup>-1</sup> )	k (rate)	ln(k/T)
253	0.00395	142	-0.577
273	0.00366	527	0.658
313	0.00320	23400	4.316
333	0.00300	104000	5.74
353	0.00283	1490000	8.34



**Figure S43.** Eyring plot for dynamic exchange of **10f/10f'** (6.67 mM).

$$\begin{aligned}\Delta H^\ddagger_{\text{DE}} &= 15 \pm 2 \text{ kcal} \cdot \text{mol}^{-1} \\ \Delta S^\ddagger_{\text{DE}} &= 11 \pm 1 \text{ cal} \cdot \text{mol}^{-1} \cdot \text{K}^{-1} \\ \Delta G^\ddagger_{\text{DE}(298\text{K})} &= 12 \pm 2 \text{ kcal} \cdot \text{mol}^{-1} \\ \Delta G^\ddagger_{\text{DE}(233\text{K})} &= 13 \pm 2 \text{ kcal} \cdot \text{mol}^{-1}\end{aligned}$$

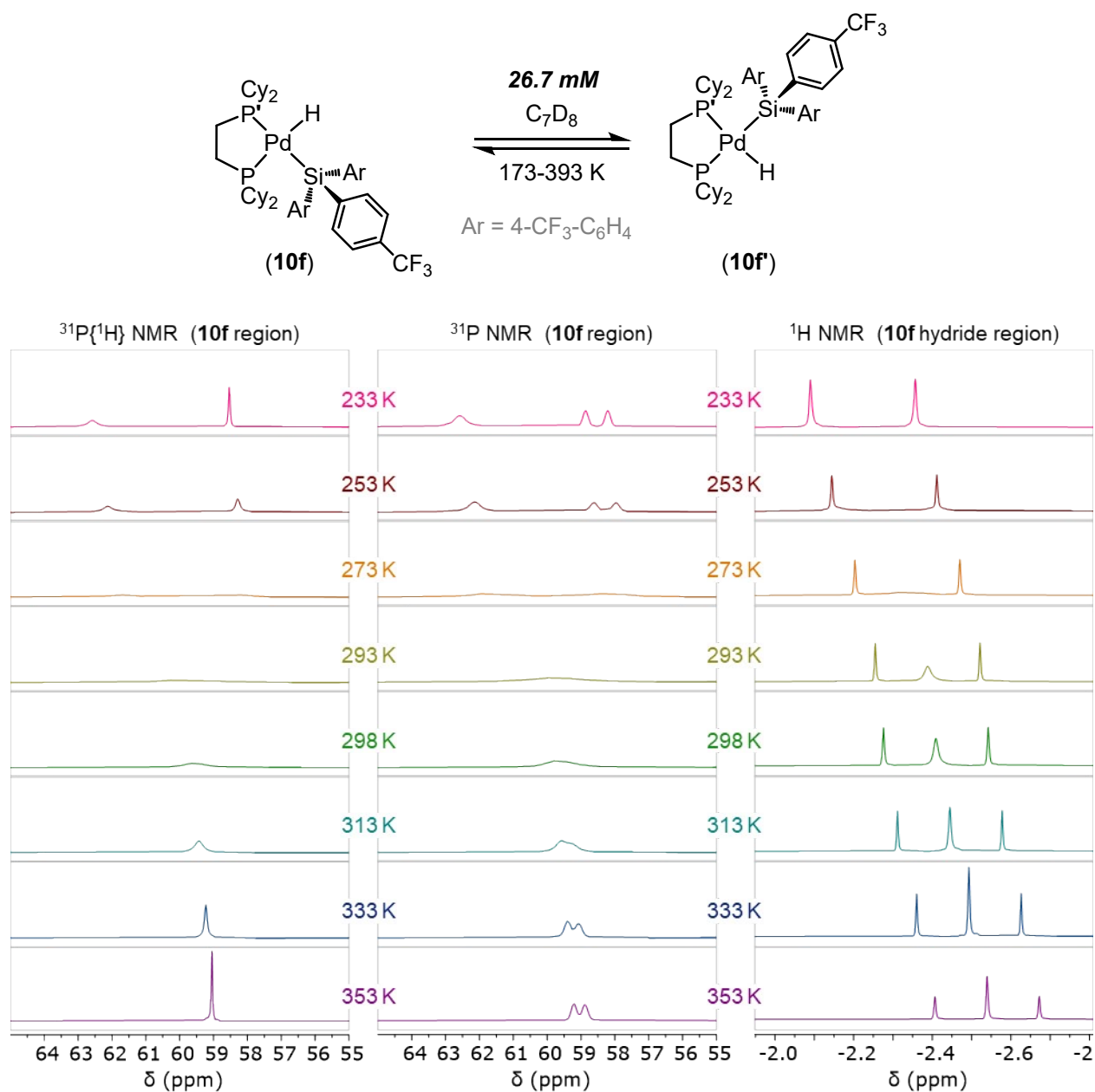


**Figure S44.**  $^{31}\text{P}\{^1\text{H}\}$ ,  $^{31}\text{P}$ , and  $^1\text{H}$  NMR spectra of **10f** (26.7 mM) at variable temperature.

**Table S38.** Rates of dynamic exchange of **10f/10f'** (26.7 mM) at varying temperatures.

Temperature (K)	1/T (K <sup>-1</sup> )	k (rate)	ln(k/T)
253	0.00395	135	-0.627
273	0.00366	708	0.953
313	0.00320	29000	4.53
333	0.00300	110000	5.80
353	0.00283	1520000	8.37

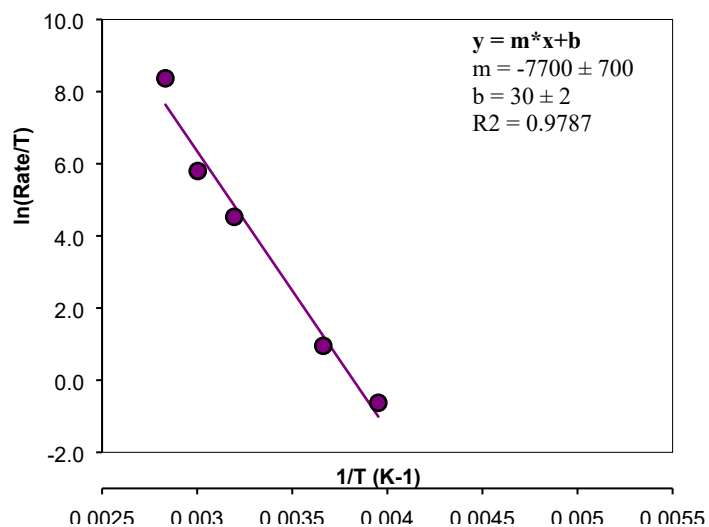
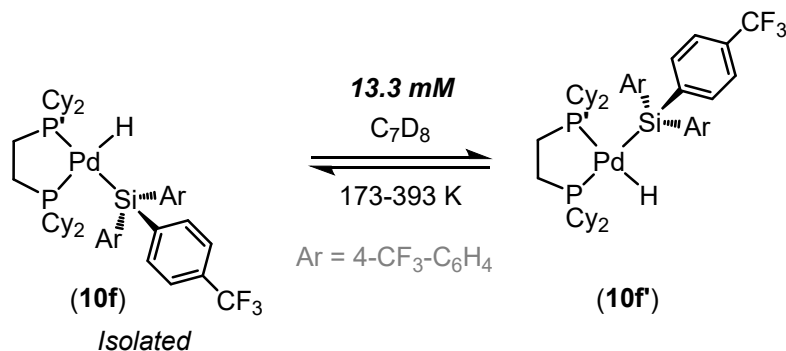


**Figure S45.** Eyring plot for dynamic exchange of **10f/10f'** (26.7 mM).

$$\begin{aligned}
 \Delta H^\ddagger_{\text{DE}} &= 15 \pm 1 && \text{kcal} \cdot \text{mol}^{-1} \\
 \Delta S^\ddagger_{\text{DE}} &= 11.5 \pm 0.9 && \text{cal} \cdot \text{mol}^{-1} \cdot \text{K}^{-1} \\
 \Delta G^\ddagger_{\text{DE}(298\text{K})} &= 12 \pm 1 && \text{kcal} \cdot \text{mol}^{-1} \\
 \Delta G^\ddagger_{\text{DE}(233\text{K})} &= 13 \pm 1 && \text{kcal} \cdot \text{mol}^{-1}
 \end{aligned}$$



**10f** was added to the NMR tube as a solid, isolated by filtration from a reaction mixture generated as described in General Procedure B.

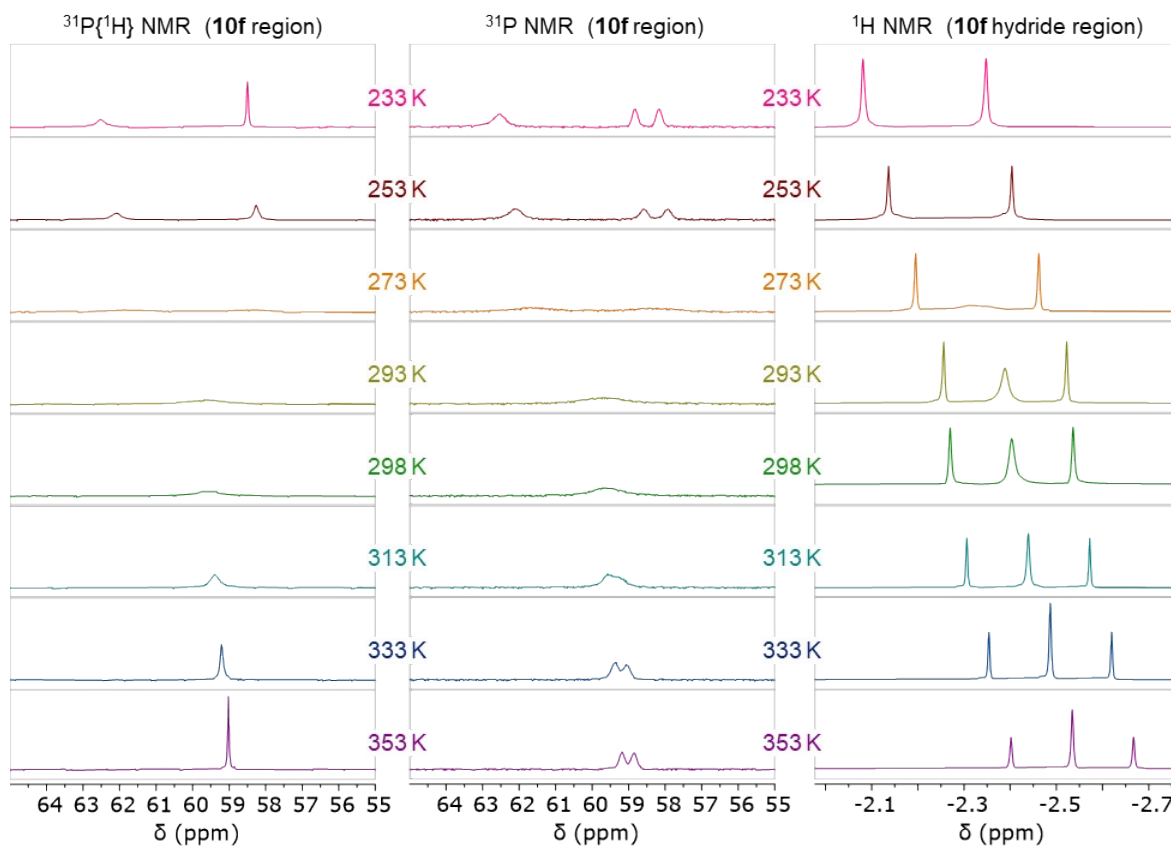


**Figure S46.**  $^{31}\text{P}\{^1\text{H}\}$ ,  $^{31}\text{P}$ , and  $^1\text{H}$  NMR spectra of **10f** (13.3 mM, isolated) at variable temperature.

**Table S39.** Rates of dynamic exchange of **10f/10f'** (13.3 mM) at varying temperatures.

Temperature (K)	1/T (K <sup>-1</sup> )	k (rate)	ln(k/T)
253	0.00395	127	-0.687
273	0.00366	641	0.853
313	0.00320	23500	4.32
333	0.00300	106000	5.76
353	0.00283	1500000	8.35

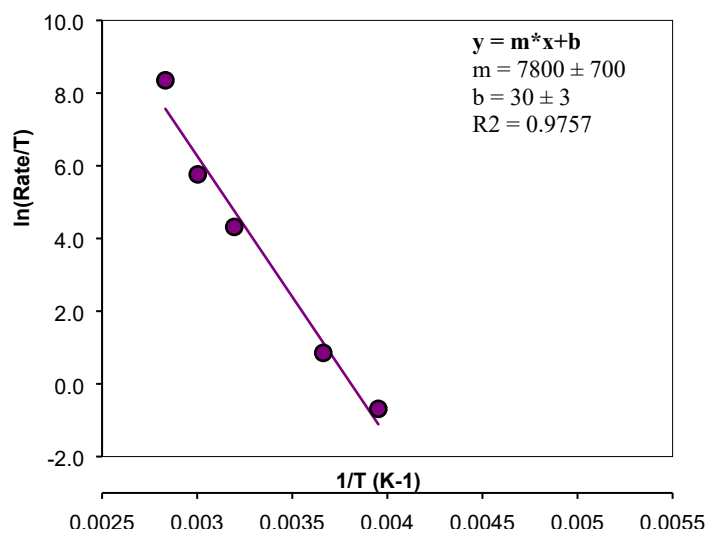
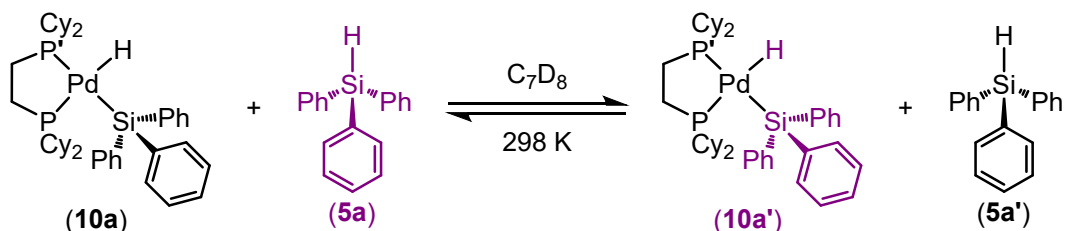


**Figure S47.** Eyring plot for dynamic exchange of **10f/10f'** (13.6 mM, isolated).

$$\begin{aligned}
 \Delta H^\ddagger_{\text{DE}} &= 15 \pm 1 && \text{kcal} \cdot \text{mol}^{-1} \\
 \Delta S^\ddagger_{\text{DE}} &= 11.5 \pm 0.9 && \text{cal} \cdot \text{mol}^{-1} \cdot \text{K}^{-1} \\
 \Delta G^\ddagger_{\text{DE}(298\text{K})} &= 12 \pm 1 && \text{kcal} \cdot \text{mol}^{-1} \\
 \Delta G^\ddagger_{\text{DE}(233\text{K})} &= 13 \pm 1 && \text{kcal} \cdot \text{mol}^{-1}
 \end{aligned}$$

### c. ROESY NMR spectrum of 10a/5a mixture



In a nitrogen-filled glovebox, stock solutions of **1** (13.3 mM) and **5a** (54.7 mM) were prepared by weighing out the reagents and diluting with  $C_6D_6$ . **1** (0.30 mL of stock solution, 0.0040 mmol, 1.0 equiv) and **5a** (0.15 mL of stock solution, 0.0082 mmol, 2.05 equiv) were added to an NMR tube using disposable 1-mL syringes. Then, the NMR tube was capped and the reaction was allowed to react for 4 hours in the glovebox, after which it was further sealed with Teflon tape to prevent exposure to air and moisture and removed from the glovebox for analysis by NMR. The ROESY was recorded at 298 K using a 400 ms mixing time.

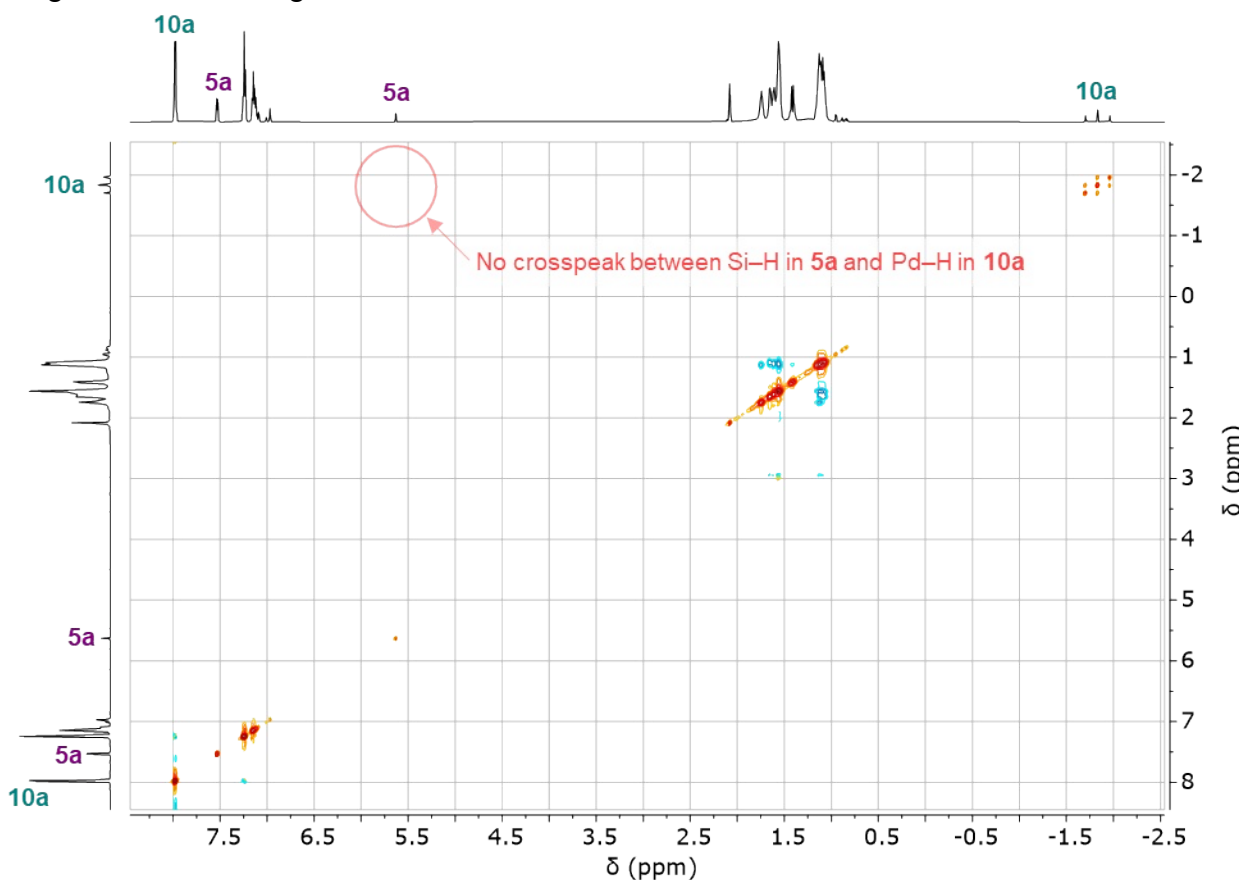


**Figure S48.** ROESY NMR spectra of a mixture of **5a** and **10a**.

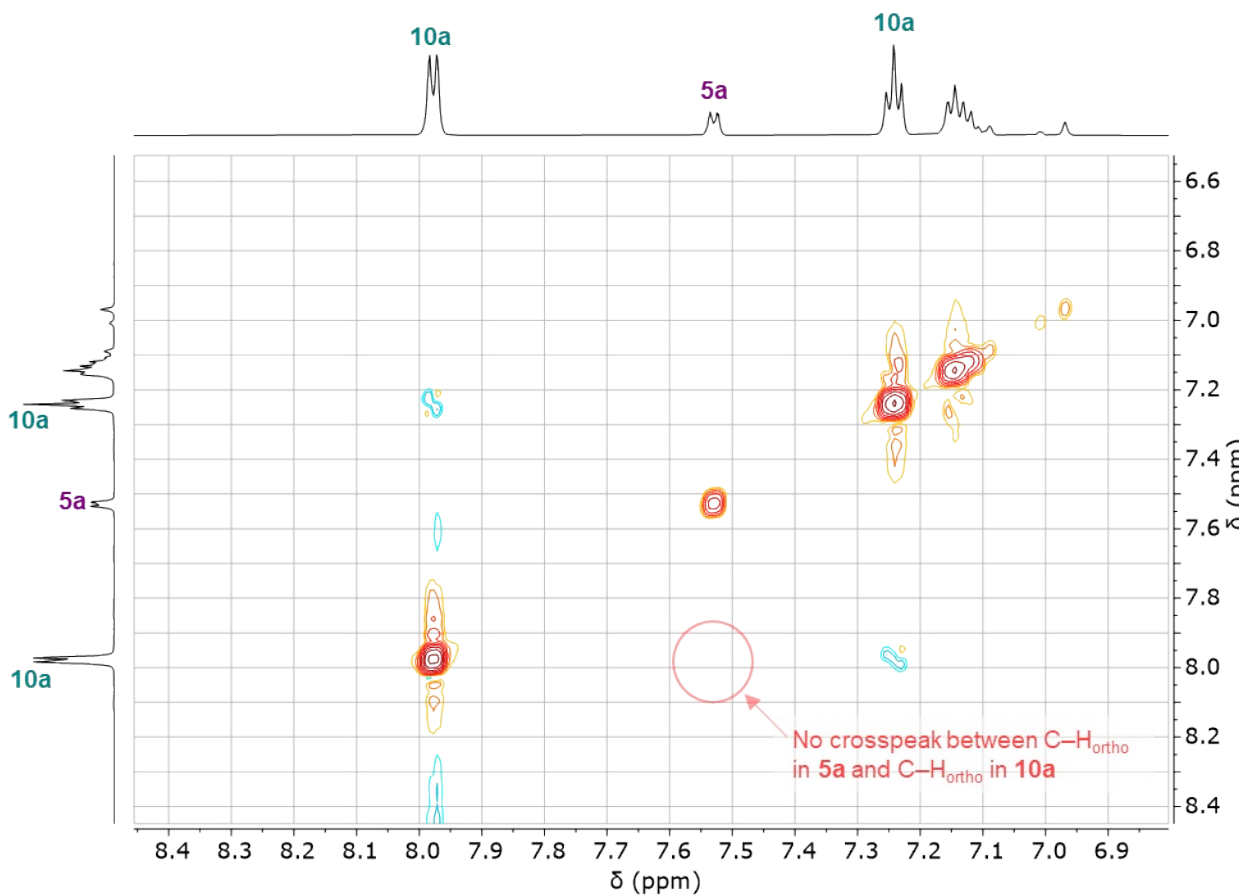
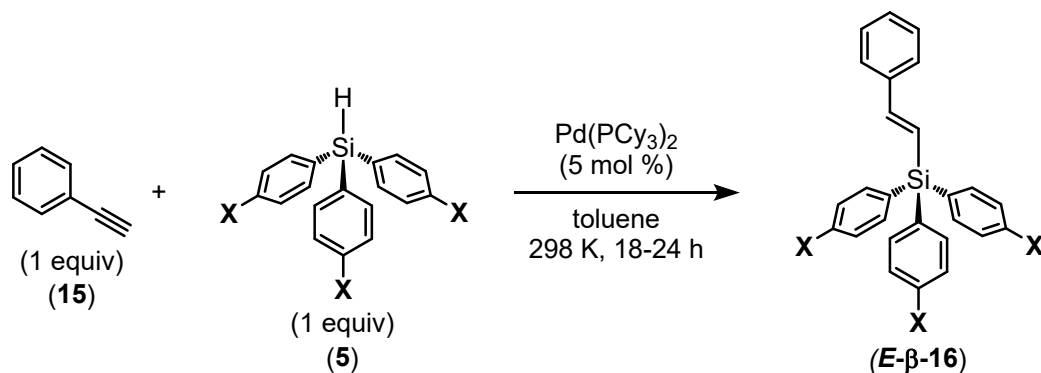


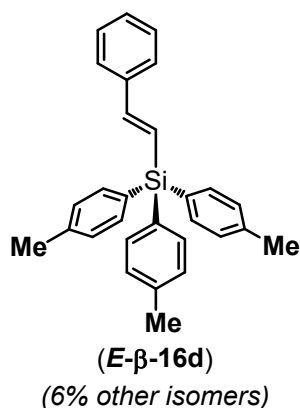
**Figure S49.** Zoom in of the aryl region of the ROESY NMR spectra of a mixture of **5a** and **10a**.

## 11. Catalysis

### a. Synthesis of hydrosilylation products using an independent method



Hydrosilylation products were synthesized using a modified procedure from the literature:<sup>12</sup> Pd(PCy<sub>3</sub>)<sub>2</sub> (6.7 mg, 0.010 mmol, 0.050 equiv.) and silane (0.20 mmol, 1.0 equiv.) were weighed out into a 20 mL scintillation vial in the glovebox. Phenylacetylene (20 mg, 0.20 mmol, 1.0 equiv.), was weighed out into a separate vial and dissolved in toluene (10 mL), and the resulting solution was added to solid reagents while stirring. The reaction vial was sealed and removed from the glovebox, where it was allowed to stir overnight (18-24 hours) at room temperature. The vial was opened and water added to quench the reaction. The organic phase was separated and filtered through a plug of silica/MgSO<sub>4</sub> (approximately 10:1 by volume) which was flushed thoroughly with dichloromethane. The filtrate was dried under vacuum to give the crude products as a viscous yellow oil or oily solid. Purification was conducted via column chromatography, as described below for each product.



(*E*)-1-phenyl-2-[tris(4-methylphenyl)silyl]ethene (**E-β-16d**)

Synthesis details: Tris(4-methylphenyl)silane (**5d**) (60.5 mg) was used. (42 mg, 0.10 mmol, 52% yield).

Purification details: Column chromatography was performed using a gradient eluent 5-20% DCM/hexanes to give the product as a white solid.  $R_f$  = 0.56, developed in 20% DCM/hexanes. Isolated as a mixture of isomers: branched/*E*-linear/*Z*-linear, 2:94:4 (**α-16d**, **E-β-16d**, and **Z-β-16d**, respectively).

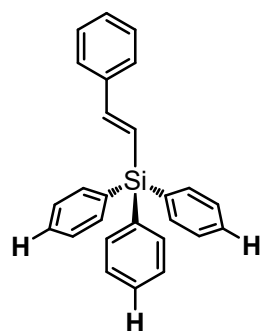
$^1\text{H}$  NMR (600 MHz,  $\text{CD}_3\text{CN}$ , 298 K):  $\delta$  7.50 (d,  $J$  = 7.6 Hz, 2H, *ortho* Ph-H), 7.44 (d,  $J$  = 7.8 Hz, 6H, *ortho* Ar-H), 7.35 (t,  $J$  = 7.6 Hz, 2H, *meta* Ph-H), 7.32-7.28 (m, 1H, *para* Ph-H), 7.23 (d,  $J$  = 7.8 Hz, 6H, *meta* Ar-H), 7.05 (d,  $J$  = 19.1 Hz, 1H, Ph-C-H), 6.93 (d,  $J$  = 19.1 Hz, 1H, Si-C-H), 2.35 (s, 9H, CAr-CH<sub>3</sub>)

$^{13}\text{C}\{^1\text{H}\}$  NMR (151 MHz,  $\text{CD}_3\text{CN}$ , 298 K):  $\delta$  149.3 (Si-C-H), 140.7 (*ipso* C<sub>Ar</sub>), 138.9 (*ipso* C<sub>Ph</sub>), 136.7 (*ortho* C<sub>Ar</sub>), 132.1 (C<sub>Ar</sub>-CH<sub>3</sub>), 129.7 (*meta* C<sub>Ar</sub>), 129.6 (*meta* C<sub>Ph</sub>), 129.5 (*para* C<sub>Ph</sub>), 127.6 (*ortho* C<sub>Ph</sub>), 124.4 (Ph-C-H), 21.5 (CAr-CH<sub>3</sub>)

$^{29}\text{Si}\{^1\text{H}\}$  NMR (119 MHz,  $\text{CD}_3\text{CN}$ , 298 K):  $\delta$  -17.55

IR (neat)  $\nu$  1597  $\text{cm}^{-1}$  (medium), 1107  $\text{cm}^{-1}$  (strong), 994  $\text{cm}^{-1}$  (strong), 799  $\text{cm}^{-1}$  (strong), 734  $\text{cm}^{-1}$  (strong), 631  $\text{cm}^{-1}$  (strong)

ASAP/HRMS ( $m/z$ ):  $[\text{M}]^+$  calculated for  $\text{C}_{29}\text{H}_{28}\text{Si}$ : 404.1960; found 404.1952



(**E-β-16a**)  
(5% branched isomer)

(**E**)-1-phenyl-2-(triphenylsilyl)ethene (**E-β-16a**)

Synthesis details: Triphenylsilane (**5a**) (52.1 mg) was used. (58 mg, 0.16 mmol, 80% yield).

Purification details: Column chromatography was performed using a gradient eluent 5-20% DCM/hexanes to give the product as a white solid.  $R_f$  = 0.43, developed in 20% DCM/hexanes. Isolated as a mixture of isomers: branched/*E*-linear/*Z*-linear, 5:95:0 (**α-16a**, **E-β-16a**, and **Z-β-16a**, respectively). NMR and IR spectra matches values previously reported.<sup>13</sup>

<sup>1</sup>H NMR (600 MHz, CDCl<sub>3</sub>, 298 K): δ 7.59 (d,  $J$  = 7.2 Hz, 6H), 7.48 (d,  $J$  = 7.6 Hz, 2H), 7.45-7.42 (m, 3H), 7.40-7.37 (m, 6H), 7.34 (t,  $J$  = 7.6 Hz, 2H), 7.29-7.28 (m, 1H), 7.01-6.94 (ms, 2H)

<sup>1</sup>H NMR (600 MHz, CD<sub>3</sub>CN, 298 K): δ 7.58 (d,  $J$  = 6.6 Hz, 6H), 7.53 (d,  $J$  = 7.6 Hz, 2H), 7.49-7.45 (m, 3H), 7.44-7.40 (m, 6H), 7.37 (t,  $J$  = 7.6 Hz, 2H), 7.34-7.30 (m, 1H), 7.10 (d,  $J$  = 19.1 Hz, 1H), 6.98 (d,  $J$  = 19.1 Hz, 1H)

<sup>13</sup>C{<sup>1</sup>H} NMR (151 MHz, CDCl<sub>3</sub>, 298 K): δ 148.9, 138.0, 136.0, 134.5, 129.6, 128.6, 128.5, 127.9, 126.8, 122.9

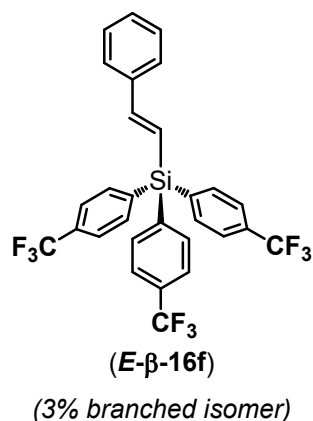
<sup>13</sup>C{<sup>1</sup>H} NMR (151 MHz, CD<sub>3</sub>CN, 298 K): δ 149.9, 138.8, 136.7, 135.4, 130.7, 129.7, 129.6, 129.0, 127.6, 123.6

<sup>29</sup>Si{<sup>1</sup>H} NMR (119 MHz, CDCl<sub>3</sub>, 298 K): δ -16.71

<sup>29</sup>Si{<sup>1</sup>H} NMR (119 MHz, CD<sub>3</sub>CN, 298 K): δ -17.23

IR (neat) ν 1426 cm<sup>-1</sup> (medium), 1107 cm<sup>-1</sup> (medium), 990 cm<sup>-1</sup> (medium), 733 cm<sup>-1</sup> (strong), 697 cm<sup>-1</sup> (strong)

ASAP/HRMS (m/z): [M]<sup>+</sup> calculated for C<sub>26</sub>H<sub>22</sub>Si: 362.1491; found 362.1462



(*E*)-1-phenyl-2-[tris(4-trifluoromethylphenyl)silyl]ethene  
(**E-β-16f**)

Synthesis details: Tris[4-(trifluoromethyl)phenyl]silane (**5f**) (92.9 mg) was used. (60 mg, 0.11 mmol, 53% yield).

Purification details: Column chromatography was performed using a gradient eluent 1-10% DCM/hexanes to give the product as a white solid.  $R_f$  = 0.41, developed in 5% DCM/hexanes. Isolated as a mixture of isomers: branched/*E*-linear/*Z*-linear, 3:97:0 (**α-16f**, **E-β-16f**, and **Z-β-16f**, respectively).

$^1\text{H}$  NMR (600 MHz,  $\text{CD}_3\text{CN}$ , 298 K):  $\delta$  7.78-7.72 (ms, 12H, *ortho/meta* Ar-H), 7.56 (d,  $J$  = 7.2 Hz, 2H, *ortho* Ph-H), 7.39 (t,  $J$  = 7.4 Hz, 2H, *meta* Ph-H), 7.36-7.33 (m, 1H, *para* Ph-H), 7.10 (d,  $J$  = 19.2 Hz, 1H, Ph-C-H), 7.04 (d,  $J$  = 19.2 Hz, 1H, Si-C-H)

$^{13}\text{C}\{^1\text{H}\}$  NMR (151 MHz,  $\text{CD}_3\text{CN}$ , 298 K):  $\delta$  151.8 (Si-C-H), 139.4 (*ipso*  $\text{C}_{\text{Ar}}$ ), 138.5 (*ipso*  $\text{C}_{\text{Ph}}$ ), 137.5 (*ortho*  $\text{C}_{\text{Ar}}$ ), 132.4 (q,  $J$  = 32.2 Hz,  $\text{C}_{\text{Ar}}-\text{CF}_3$ ), 130.2 (*para*  $\text{C}_{\text{Ph}}$ ), 129.8 (*meta*  $\text{C}_{\text{Ph}}$ ), 127.9 (*ortho*  $\text{C}_{\text{Ph}}$ ), 125.7 (q,  $J$  = 3.9 Hz, *meta*  $\text{C}_{\text{Ar}}$ ), 125.3 (q,  $J$  = 271.2 Hz,  $\text{C}_{\text{Ar}}-\text{CF}_3$ ), 120.6 (Ph-C-H)

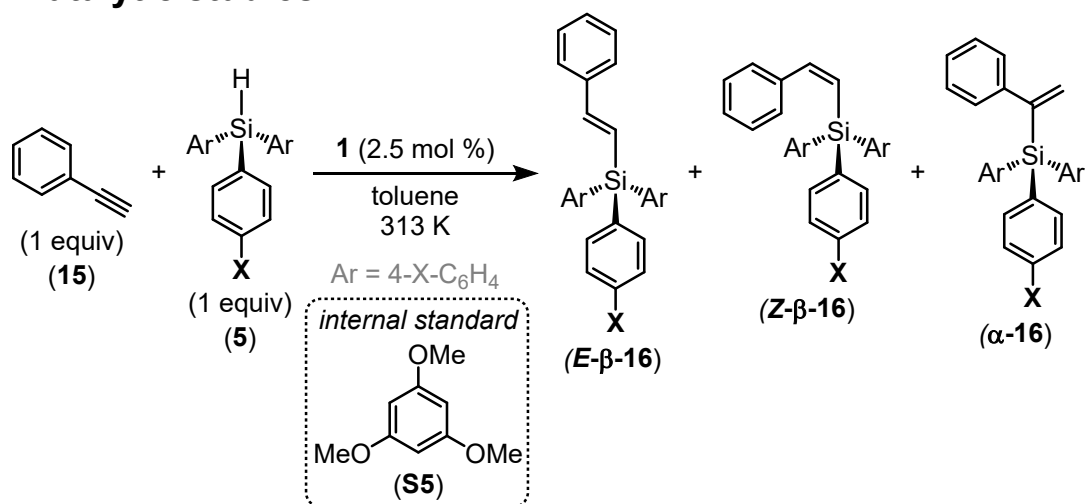
$^{19}\text{F}$  NMR (565 MHz,  $\text{CD}_3\text{CN}$ , 298 K):  $\delta$  -63.56

$^{29}\text{Si}\{^1\text{H}\}$  NMR (119 MHz,  $\text{CD}_3\text{CN}$ , 298 K):  $\delta$  -16.85

IR (neat)  $\nu$  1607  $\text{cm}^{-1}$  (weak), 1391  $\text{cm}^{-1}$  (medium), 1319  $\text{cm}^{-1}$  (strong), 1119  $\text{cm}^{-1}$  (strong), 1056  $\text{cm}^{-1}$  (strong), 1017  $\text{cm}^{-1}$  (strong), 702  $\text{cm}^{-1}$  (strong)

ASAP/HRMS ( $m/z$ ):  $[\text{M}]^+$  calculated for  $\text{C}_{29}\text{H}_{19}\text{F}_9\text{Si}$ : 566.1112; found 566.1114

## b. Catalytic studies



Prior to conducting catalytic studies, **1** was further purified. In the glovebox, cold diethyl ether (-30 °C) was added to **1** in a scintillation vial. The resulting dark red solution was immediately filtered through celite, and the collected filtrate was concentrated to dryness under vacuum to give a deep red, microcrystalline powder.

A 4 mM solution of **1** was prepared by dissolving **1** (1.1 mg, 0.0010 mmol, 0.025 equiv.) in 0.25 mL toluene. 160 mM stock solutions of the silanes (0.040 mmol, 1.0 equiv.), phenylacetylene (**15**; 4.1 mg, 0.040 mmol, 1.0 equiv.), and 1,3,5-trimethoxybenzene (**S5**; internal standard; 6.7 mg, 0.040 mmol, 1.0 equiv.) were similarly prepared. To a 4 mL scintillation vial was added 0.25 mL of the stock solution of **1**, followed by 0.25 mL of the silane solution, 0.25 mL phenylacetylene solution, and finally 0.25 mL TMB solution, for a total volume of 1.0 mL. The reaction vial was sealed with a septum-adapted lid, then removed from glovebox and placed onto a vial block preheated to 40 °C. At determined timepoints, a 25 µL syringe was used to remove 10 µL aliquots, which were filtered through silica and then flushed thoroughly with dichloromethane into a GCMS vial of 1.5 mL total volume. The product concentration was determined via relative integration (by GCMS) of the product peaks against **S5**, in accordance with calibration curves prepared independently using the isolated products. All trials reported were run in duplicate.

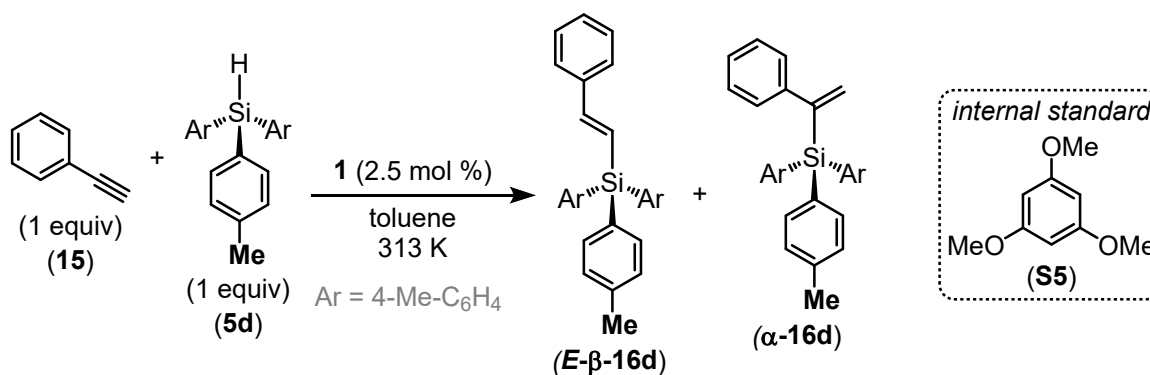


**Table S40.** Results of Hydrosilylation with silane 5d

Time (min)	Trial 1		Trial 2	
	Yield <i>E</i> -β-16d	Yield α-16d	Yield <i>E</i> -β-16d	Yield α-16d
0	n.d.	n.d.	n.d.	n.d.
30	n.d.	n.d.	n.d.	n.d.
60	n.d.	n.d.	n.d.	n.d.
90	5.6%	n.d.	4.6%	n.d.
120	8.6%	n.d.	6.1%	n.d.
150	10%	n.d.	7.0%	n.d.
180	13%	2.2%	8.3%	2.7%
240	15%	3.0%	14%	3.2%
300	22%	3.6%	17%	4.1%
360	25%	4.0%	28%	4.8%
420	29%	5.0%	30%	4.9%
480	34%	5.7%	32%	5.0%
540	35%	5.6%	33%	6.7%

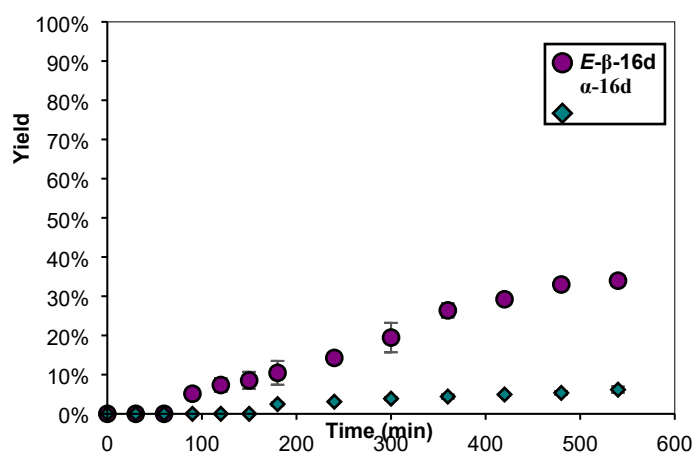


**Figure S50.** Plot of yield of *E*-β-16d and α-16d versus time.

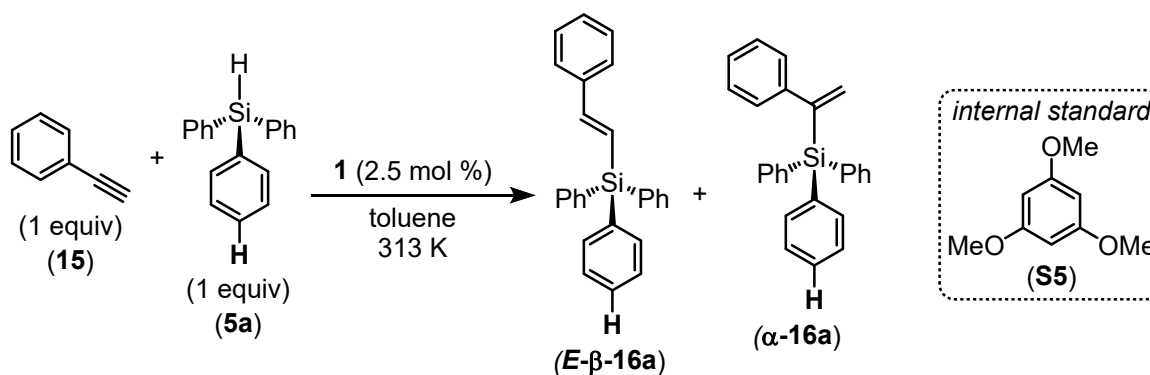


**Table S41.** Results of Hydrosilylation with silane **5a**

Time (min)	Trial 1		Trial 2	
	Yield <i>E</i> - $\beta$ - <b>16a</b>	Yield $\alpha$ - <b>16a</b>	Yield <i>E</i> - $\beta$ - <b>16a</b>	Yield $\alpha$ - <b>16a</b>
0	n.d.	n.d.	n.d.	n.d.
30	9.4%	n.d.	7.9%	n.d.
60	20%	2.7%	17%	2.2%
90	28%	3.1%	26%	2.3%
120	39%	4.3%	38%	3.9%
150	42%	5.3%	41%	3.9%
180	50%	6.6%	44%	4.4%
240	54%	7.6%	48%	4.7%
300	57%	6.9%	51%	6.4%
360	59%	7.1%	53%	6.6%
420	62%	7.6%	57%	6.7%

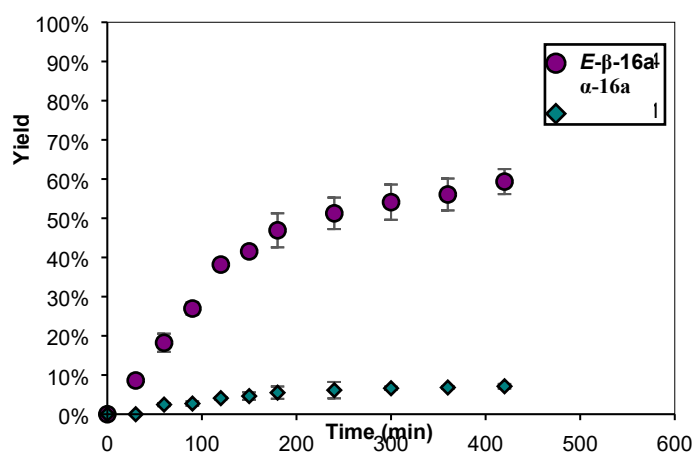


**Figure S51.** Plot of yield of *E*- $\beta$ -**16a** and  $\alpha$ -**16a** versus time.

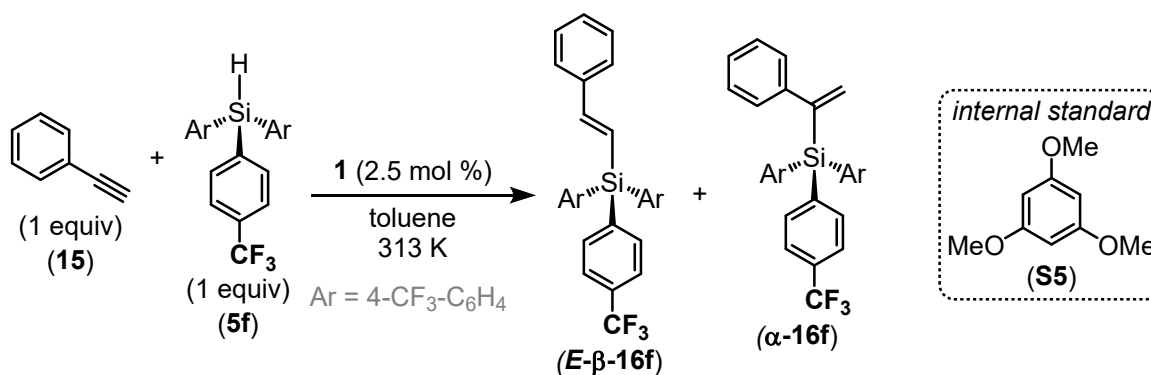


**Table S42.** Results of Hydrosilylation with silane **5f**

Time (min)	Trial 1		Trial 2	
	Yield <i>E</i> -β-16f	Yield α-16f	Yield <i>E</i> -β-16f	Yield α-16f
0	13%	1.9%	17%	n.d.
10	60%	2.5%	69%	2.0%
20	79%	2.5%	81%	1.9%
30	88%	2.4%	85%	2.4%
40	91%	2.5%	91%	1.7%
50	92%	2.6%	94%	1.8%
60	93%	3.1%	94%	2.3%
90	93%	2.6%	95%	2.3%
120	93%	2.3%	96%	2.1%
180	94%	3.1%	96%	2.1%
240	96%	3.2%	97%	2.1%
300	95%	2.9%	95%	2.1%
360	94%	2.9%	97%	2.6%

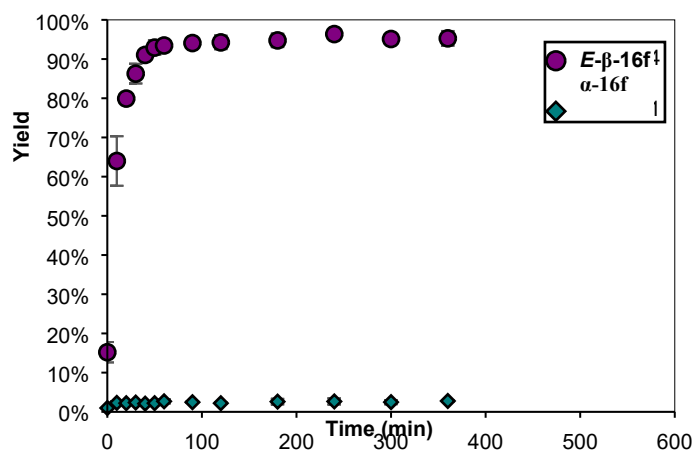
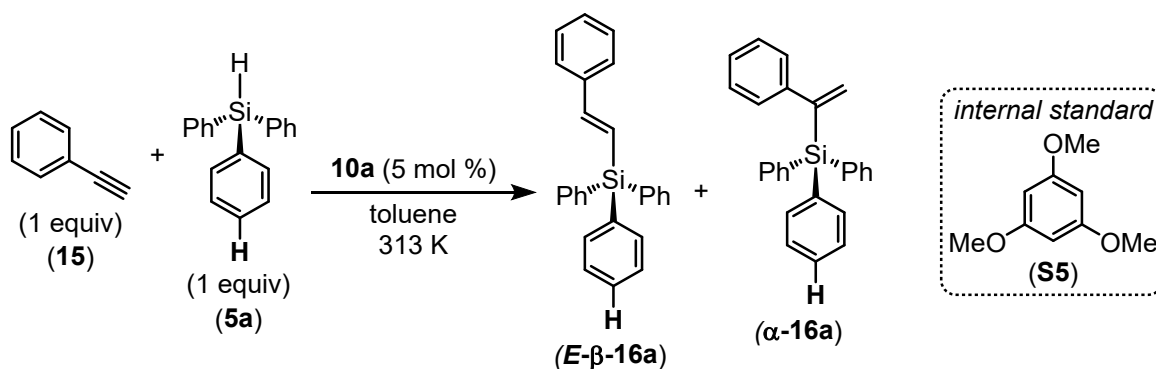


**Figure S52.** Plot of yield of **E**-β-16f and α-16f versus time.



Hydrosilylation was also evaluated using the isolated complex **10a** as a catalyst. The catalysis procedure above was used, with the following modification: complex **1** was replaced with **10a**. An 8.0 mM solution of **10a** was prepared by dissolving **10a** (1.6 mg, 0.0020 mmol, 0.050 equiv.) in 0.25 mL toluene.

**Table S43.** Results of Hydrosilylation with silane **5a** using **10a** as the catalyst.

Time (min)	Trial 1		Trial 2	
	Yield <i>E</i> -β- <b>16a</b>	Yield α- <b>16a</b>	Yield <i>E</i> -β- <b>16a</b>	Yield α- <b>16a</b>
0	n.d.	n.d.	n.d.	n.d.
30	6.2%	n.d.	4.6%	n.d.
60	10%	n.d.	5.5%	0.8%
90	15%	2.3%	13%	2.6%
120	24%	3.7%	19%	3.2%
150	30%	4.0%	26%	2.9%
180	36%	3.9%	38%	3.5%
240	45%	5.2%	44%	4.8%
300	51%	5.9%	50%	5.8%
360	54%	5.9%	53%	4.9%
420	56%	6.0%	60%	6.4%

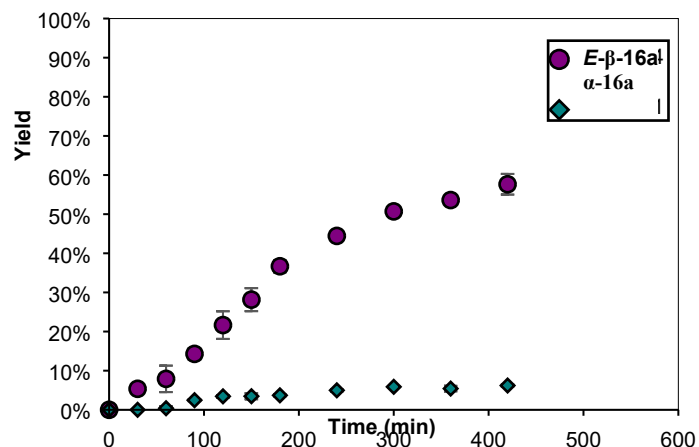


**Figure S53.** Plot of yield of *E*-β-**16a** and α-**16a** versus time.

## 12. Crystallographic information of **10f**

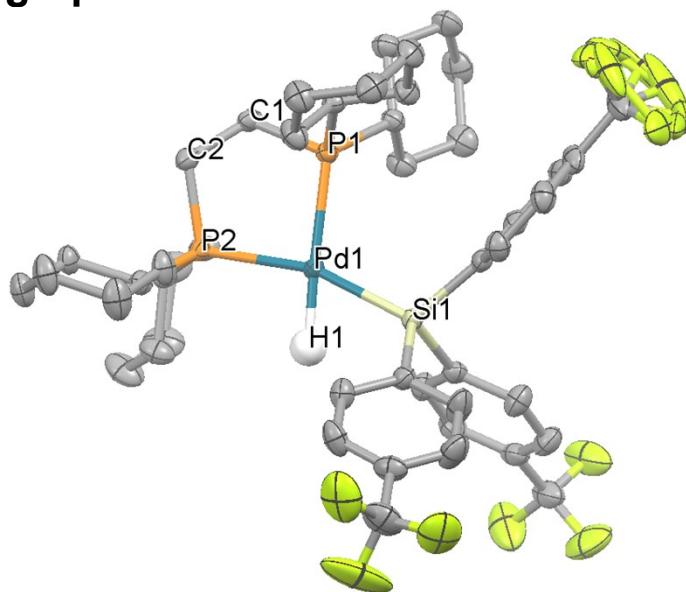


**Figure S54.** Molecular structure of (dcpe)Pd(H)[Si(4-CF<sub>3</sub>Ph)<sub>3</sub>] (**10f**). Thermal ellipsoids are drawn at 50% probability level. Hydrogen atoms except for Pd–H are omitted for clarity.

Diffraction intensities for **10f** were collected at 173 K on a Bruker Apex2 CCD diffractometer using CuK $\alpha$  radiation,  $\lambda = 1.54178$  Å. Space group was determined based on systematic absences. Absorption correction was applied by SADABS.<sup>14</sup> Structure was solved by direct methods and Fourier techniques and refined on  $F^2$  using full matrix least-squares procedures. All non-H atoms were refined with anisotropic thermal parameters. All H atoms were refined in calculated positions in a rigid group model except the H atom bonded to the Pd atom. This H atom was found from the difference map and refined without restrictions with isotropic thermal parameter. The terminal –CF<sub>3</sub> groups seem to be slightly disordered. The thermal parameters for some F atoms in these groups are elongated. These groups were refined with restrictions; the standard C–F distances were used in the refinement as the targets for corresponding bond distances. All calculations were performed by the Bruker SHELXL-2014 package.<sup>15</sup>

Crystallographic Data for **10f**: C<sub>47</sub>H<sub>61</sub>F<sub>9</sub>P<sub>2</sub>PdSi,  $M = 993.38$ ,  $0.13 \times 0.02 \times 0.02$  mm,  $T = 173(2)$  K, Orthorhombic, space group  $Pbca$ ,  $a = 18.3966(6)$  Å,  $b = 21.9565(7)$  Å,  $c = 22.9636(7)$  Å,  $V = 9275.6(5)$  Å<sup>3</sup>,  $Z = 8$ ,  $D_c = 1.423$  Mg/m<sup>3</sup>,  $\mu(\text{Cu}) = 4.716$  mm<sup>-1</sup>,  $F(000) = 4112$ ,  $2\theta_{\text{max}} = 133.27^\circ$ , 54242 reflections, 8175 independent reflections [ $R_{\text{int}} = 0.0491$ ],  $R1 = 0.0274$ ,  $wR2 = 0.0690$  and  $\text{GOF} = 1.033$  for 8175 reflections (600 parameters) with  $I > 2s(I)$ ,  $R1 = 0.0314$ ,  $wR2 = 0.0715$  and  $\text{GOF} = 1.044$  for all reflections, max/min residual electron density  $+0.511/-0.467$  eÅ<sup>-3</sup>.

### 13. Calculation of $\tau_4$ Structural Parameter of 10f

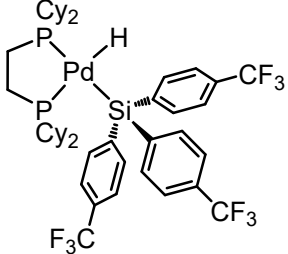
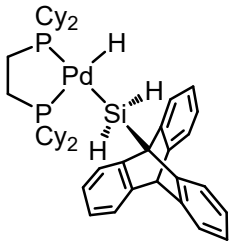
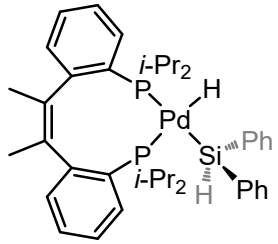
The structural parameter  $\tau_4$  is a quantitative measure of structural distortion in 4-coordinate complexes from tetrahedral or square planar geometries. The  $\tau_4$  value for a complex is derived from bond angles determined from its structure determined by single crystal diffraction. The description of complexes using  $\tau_4$  was first introduced by Houser and co-workers<sup>16</sup> and was further developed by Becker and co-workers<sup>17</sup> to distinguish between the larger and smaller bond angles (termed  $\tau_4'$ ).  $\tau_4$  and  $\tau_4'$  can be described:

$$\tau_4 = \frac{(360^\circ - (\alpha + \beta))}{(360^\circ - 2\theta)}$$

$$\tau_4' = \frac{\beta - \alpha}{360^\circ - \theta} + \frac{180^\circ - \beta}{180^\circ - \theta}$$

Where  $\theta = 109.5^\circ$  and  $\alpha$  and  $\beta$  are the greatest bond angles around the metal center, where  $\beta > \alpha$ . These values describe a structure with increasing square planar character as the value  $\rightarrow 0$ , and a structure with increasing tetrahedral character as the value  $\rightarrow 1$ .

**Table S44.**  $\tau_4$  values for known (silyl)Pd(H) complexes.

<div style="display: flex; justify-content: space-around; align-items: flex-end;"> <div style="text-align: center;">  <p>(10f)</p> </div> <div style="text-align: center;">  <p>Ishii<sup>18</sup></p> </div> <div style="text-align: center;">  <p>Iluc<sup>19</sup></p> </div> </div>				
$\alpha$	161.97°	170.44°	146.66°	
$\beta$	176.35°	174.71°	158.86°	
$\tau_4$	0.154	0.105	0.386	
$\tau_4'$	0.109	0.0921	0.349	

## 14. NMR and IR Spectra

### a. Palladium(0) complexes

$[(\mu\text{-dcpe})\text{Pd}]_2$  (**1**)

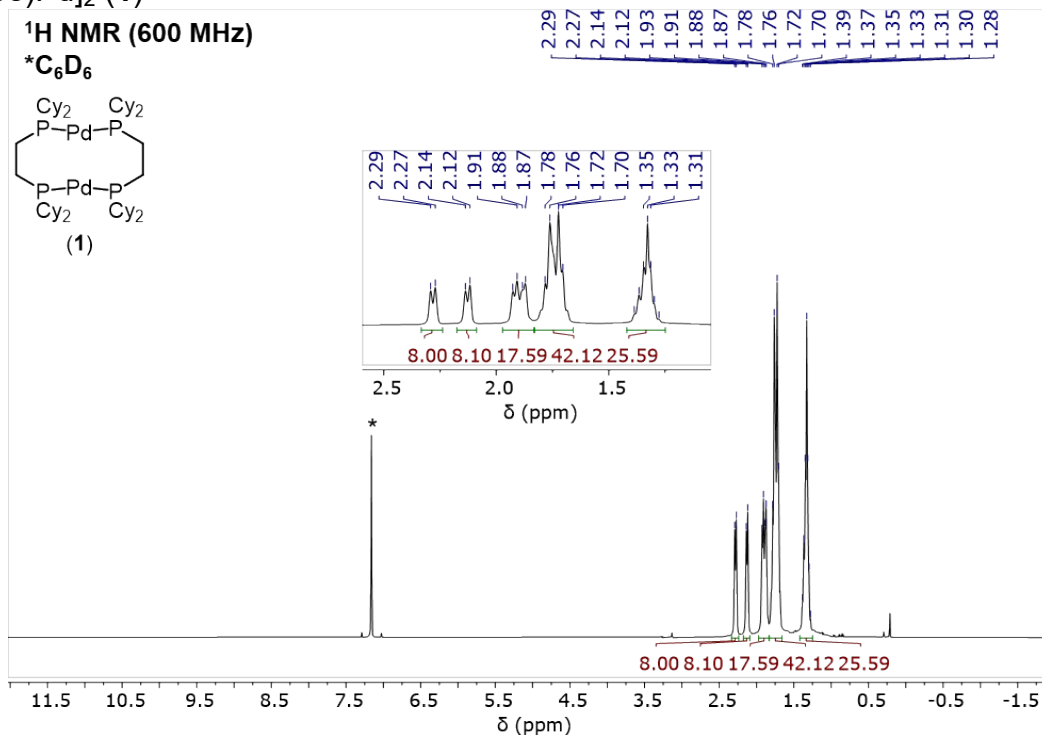


**Figure S55.**  $^1\text{H}$  NMR spectrum of **1** recorded in  $\text{C}_6\text{D}_6$  at room temperature.

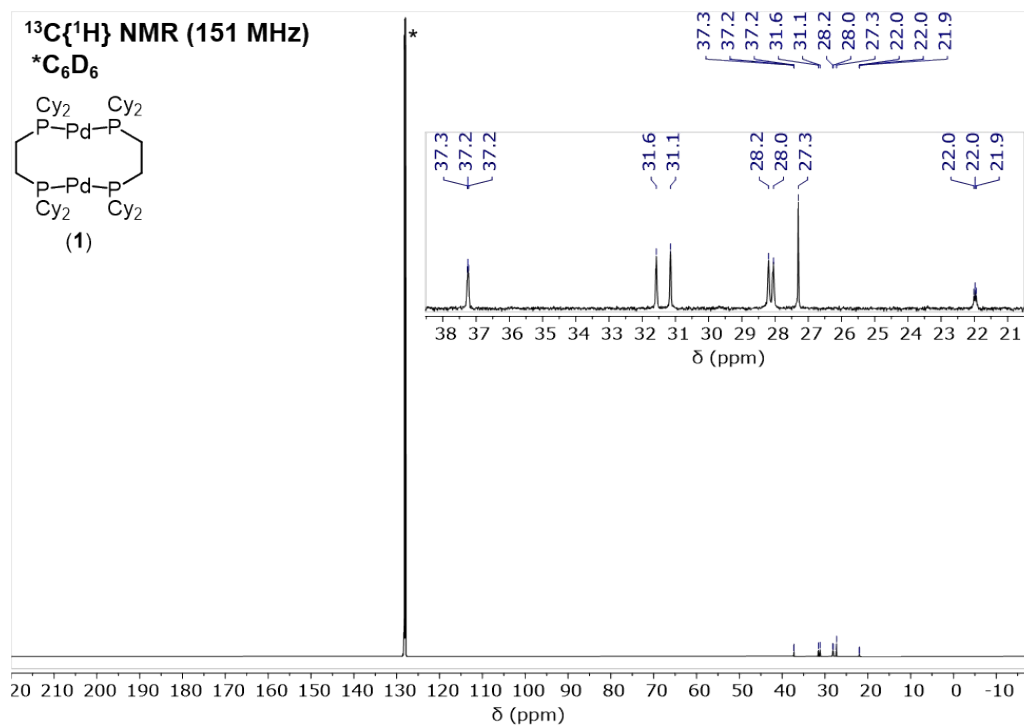


**Figure S56.**  $^{13}\text{C}\{^1\text{H}\}$  NMR spectrum of **1** recorded in  $\text{C}_6\text{D}_6$  at room temperature.

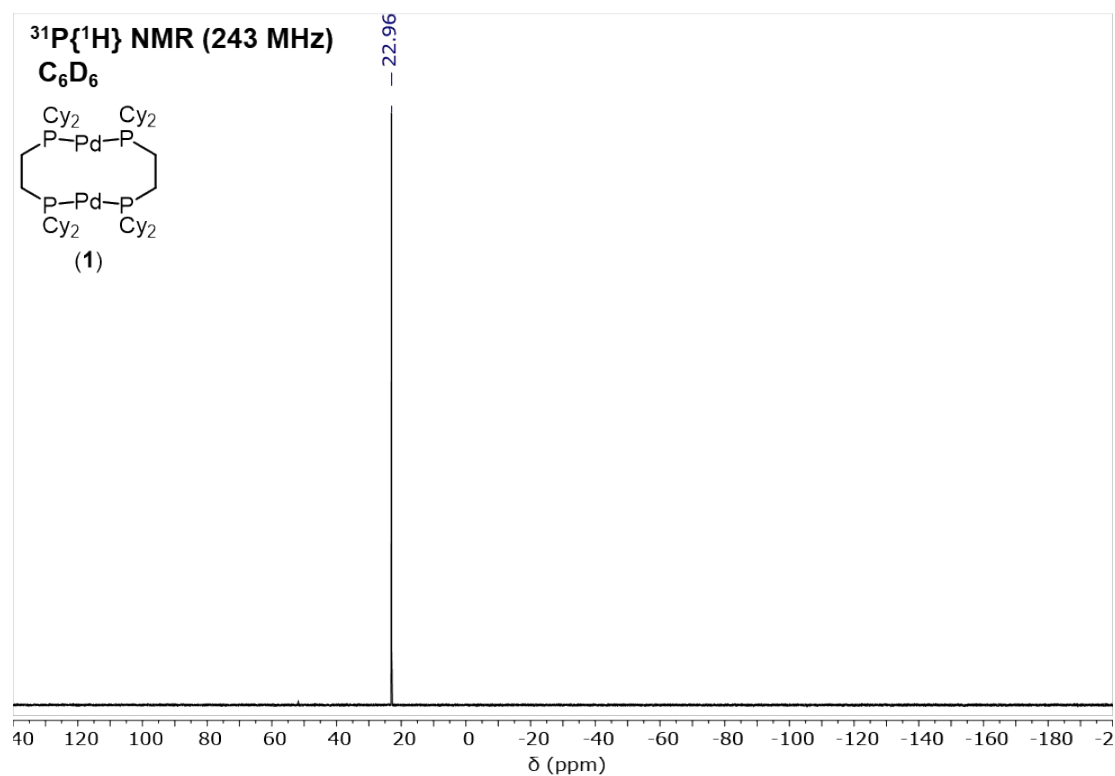


**Figure S57.**  $^{31}\text{P}\{^1\text{H}\}$  NMR spectrum of **1** recorded in  $\text{C}_6\text{D}_6$  at room temperature.

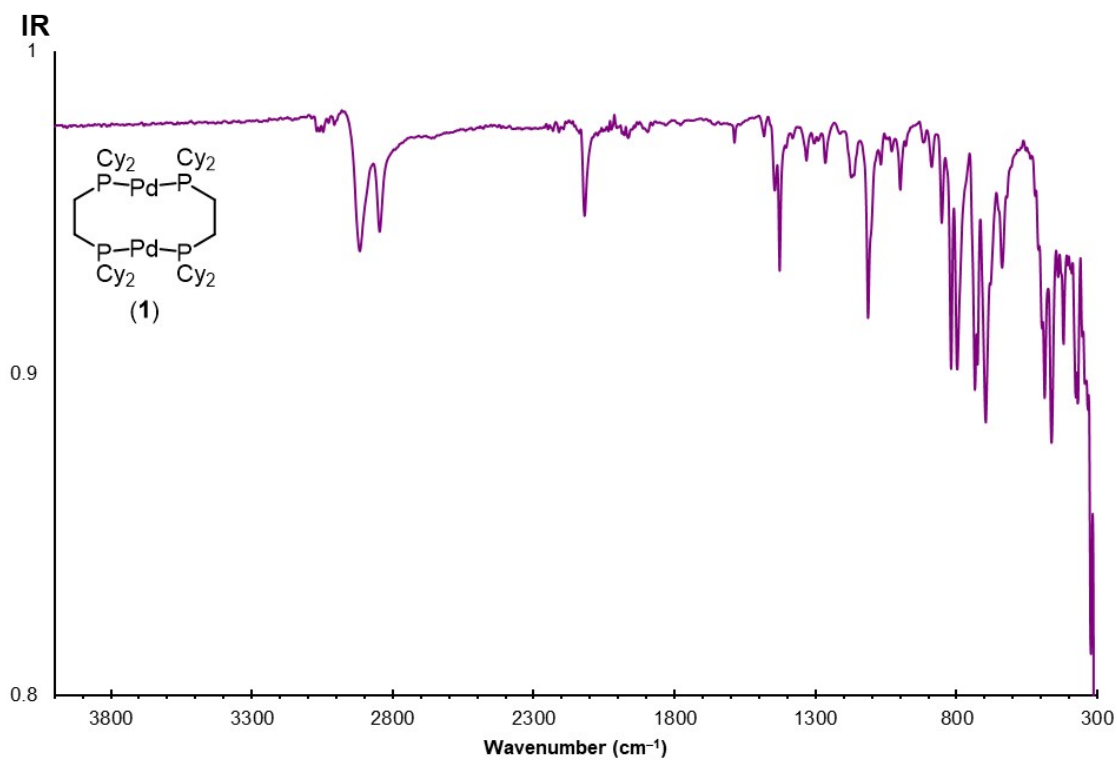


**Figure S58.** IR spectrum of **1** recorded neat at room temperature.

## b. Triaryl silanes

Tris[4-(*N,N*-dimethylamino)phenyl]silane (**5b**)

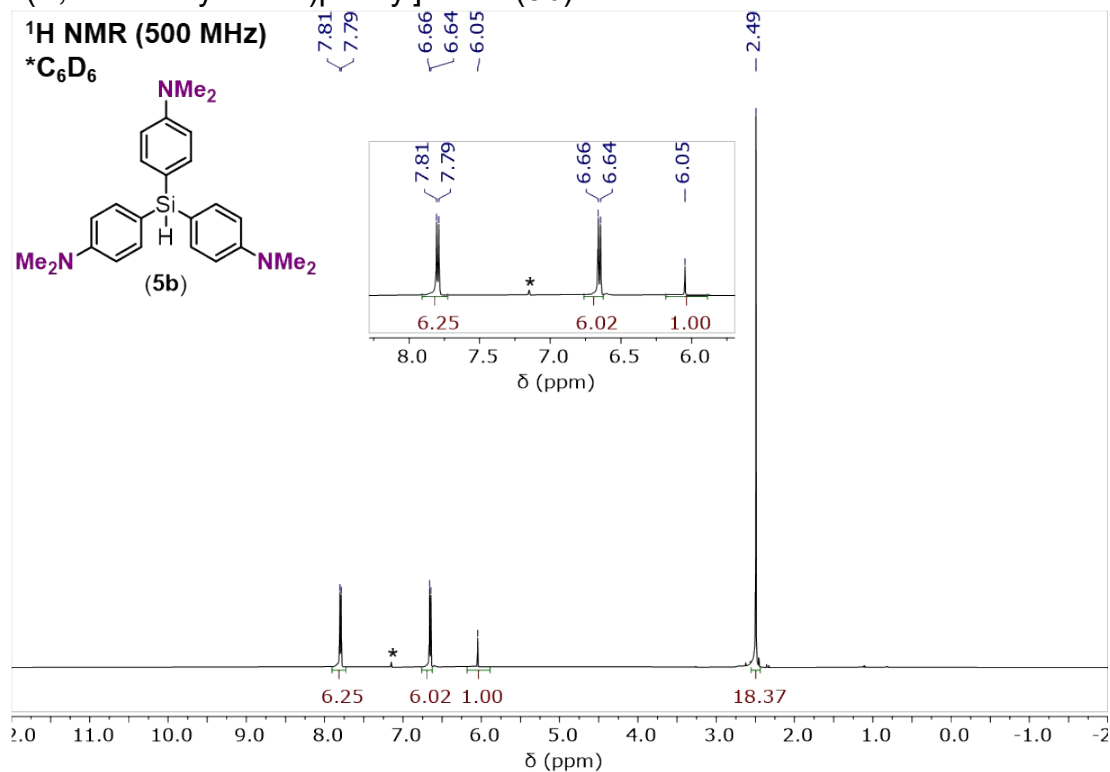


Figure S59. <sup>1</sup>H NMR spectrum of **5b** recorded in C<sub>6</sub>D<sub>6</sub> at room temperature.

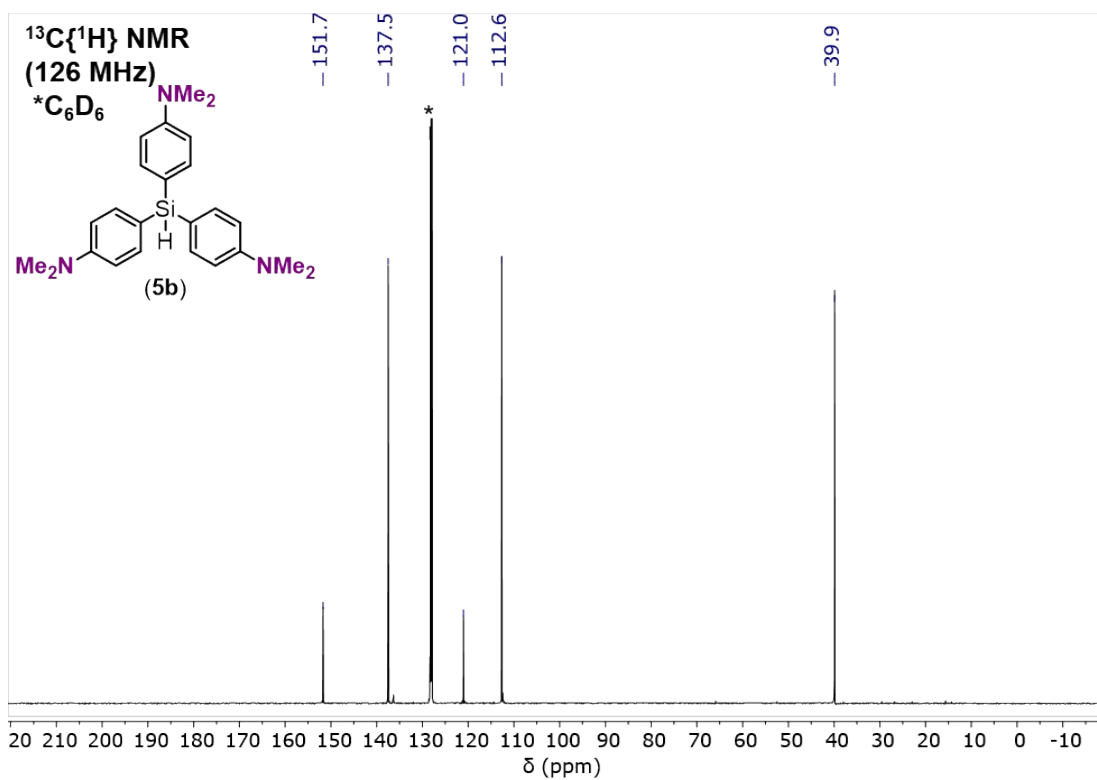
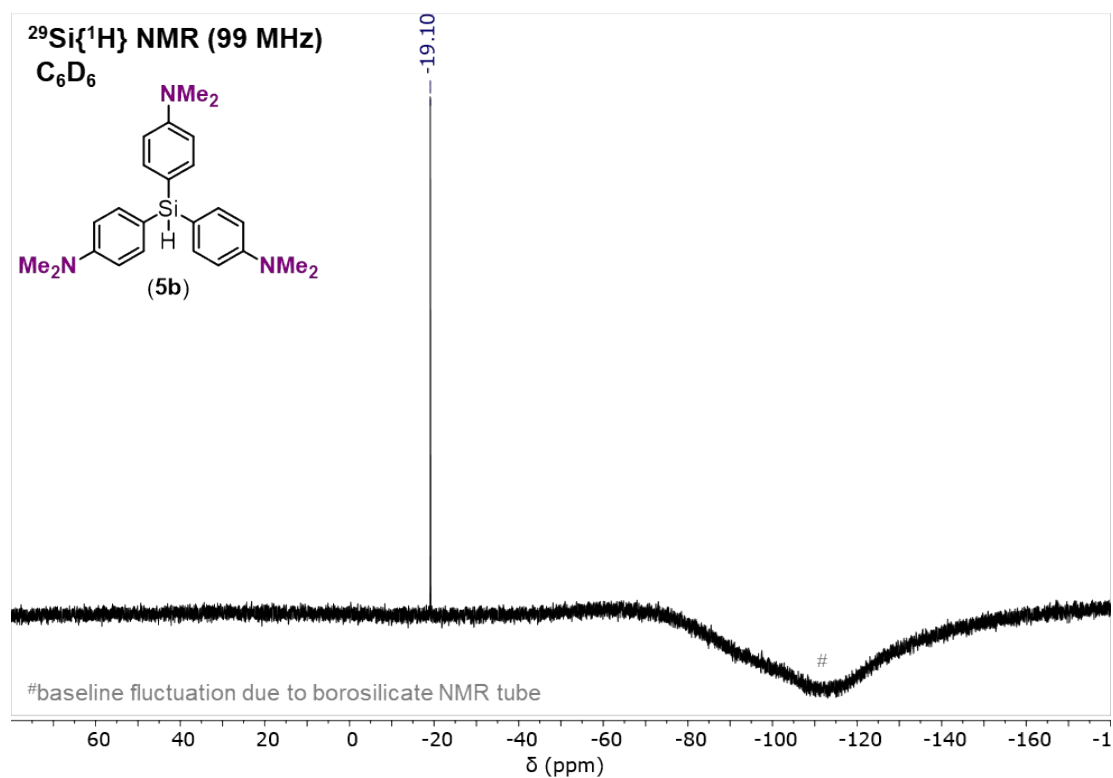
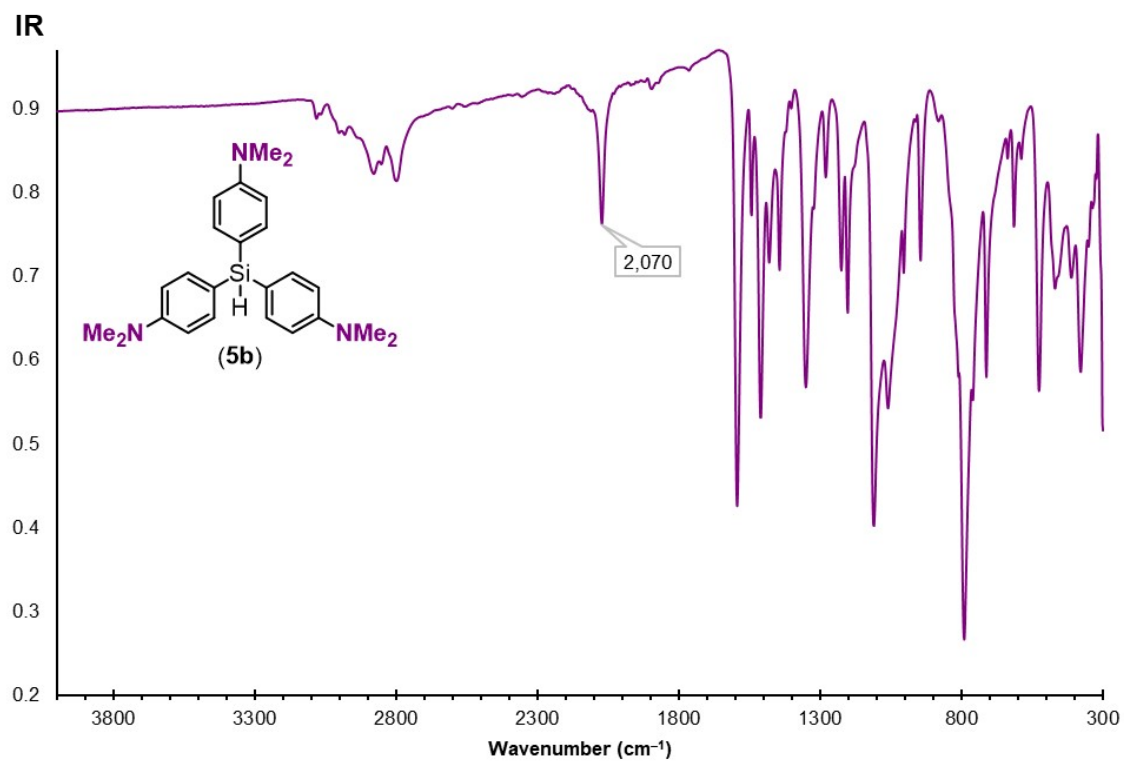


Figure S60. <sup>13</sup>C{<sup>1</sup>H} NMR spectrum of **5b** recorded in C<sub>6</sub>D<sub>6</sub> at room temperature.



**Figure S61.** <sup>29</sup>Si{<sup>1</sup>H} NMR spectrum of **5b** recorded in C<sub>6</sub>D<sub>6</sub> at room temperature.



**Figure S62.** IR spectrum of **5b** recorded neat at room temperature.

Tris(4-methoxyphenyl)silane (**5c**)

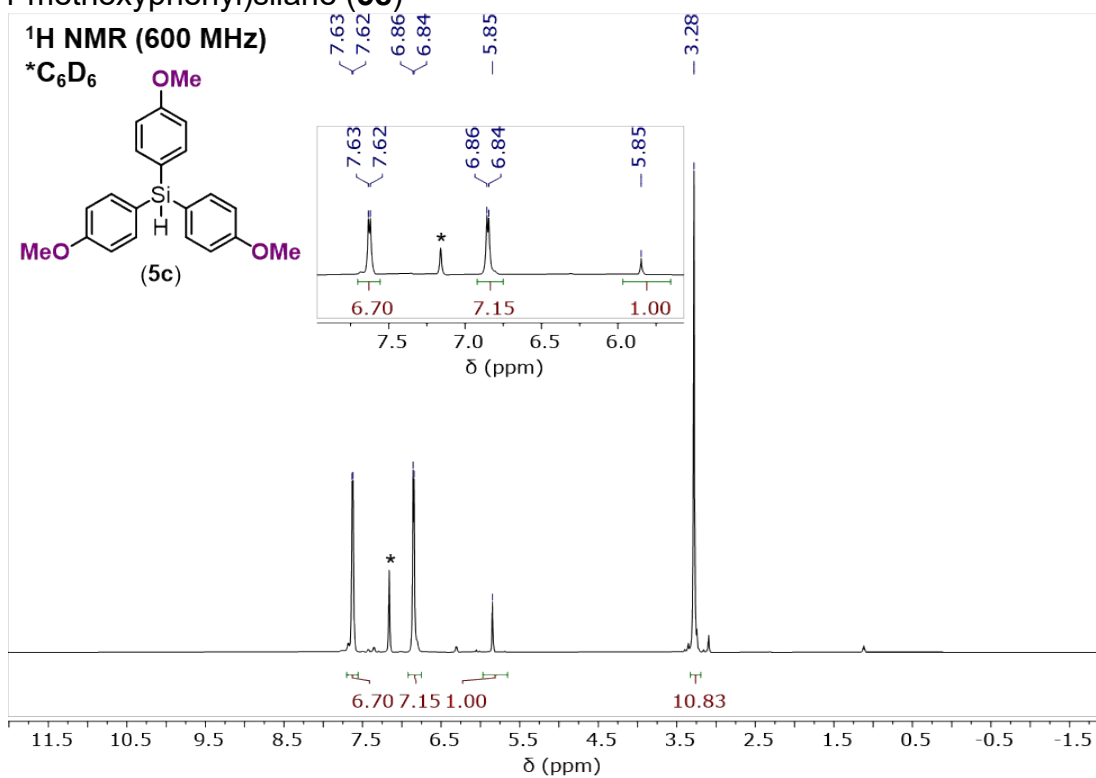


Figure S63. <sup>1</sup>H NMR spectrum of **5c** recorded in C<sub>6</sub>D<sub>6</sub> at room temperature.

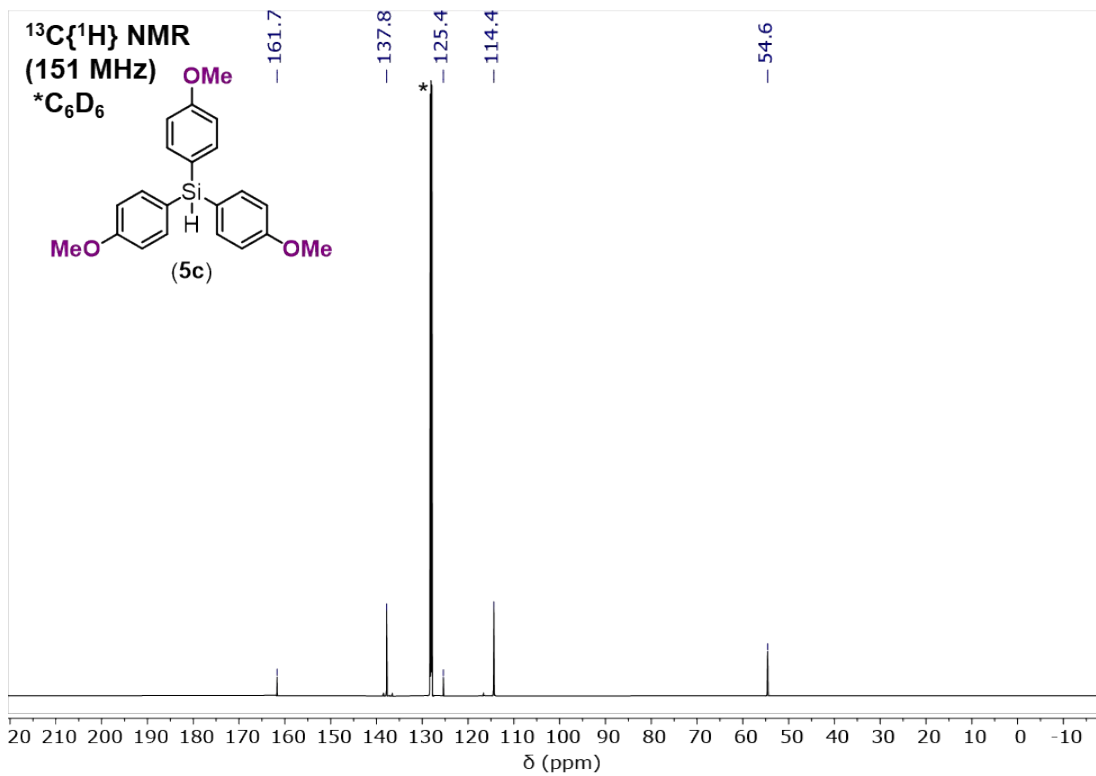
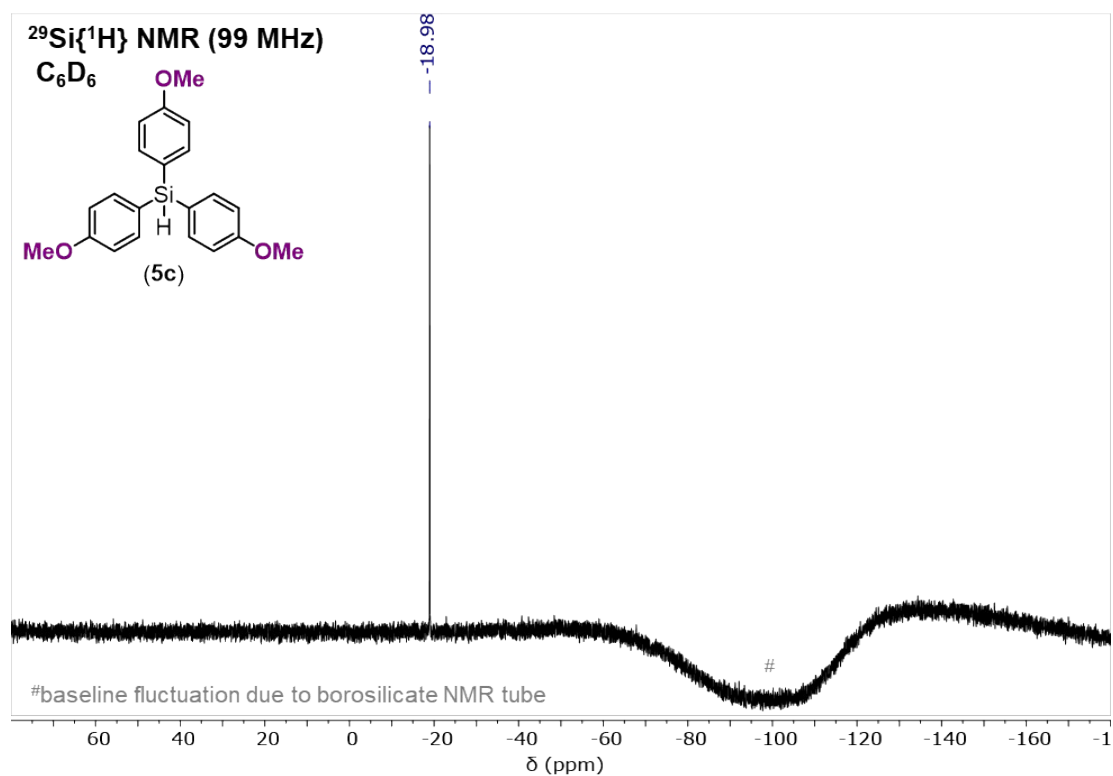
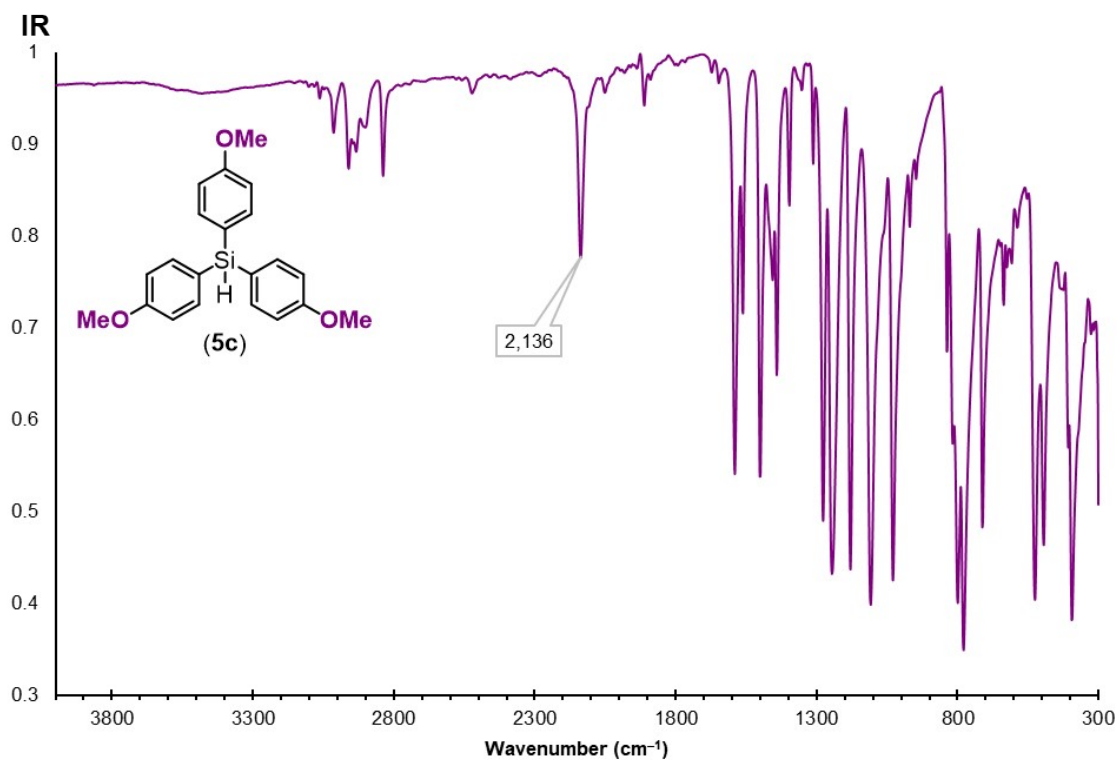


Figure S64. <sup>13</sup>C{<sup>1</sup>H} NMR spectrum of **5c** recorded in C<sub>6</sub>D<sub>6</sub> at room temperature.



**Figure S65.** <sup>29</sup>Si{<sup>1</sup>H} NMR spectrum of **5c** recorded in C<sub>6</sub>D<sub>6</sub> at room temperature.



**Figure S66.** IR spectrum of **5c** recorded neat at room temperature.

Tris(4-methylphenyl)silane (**5d**)

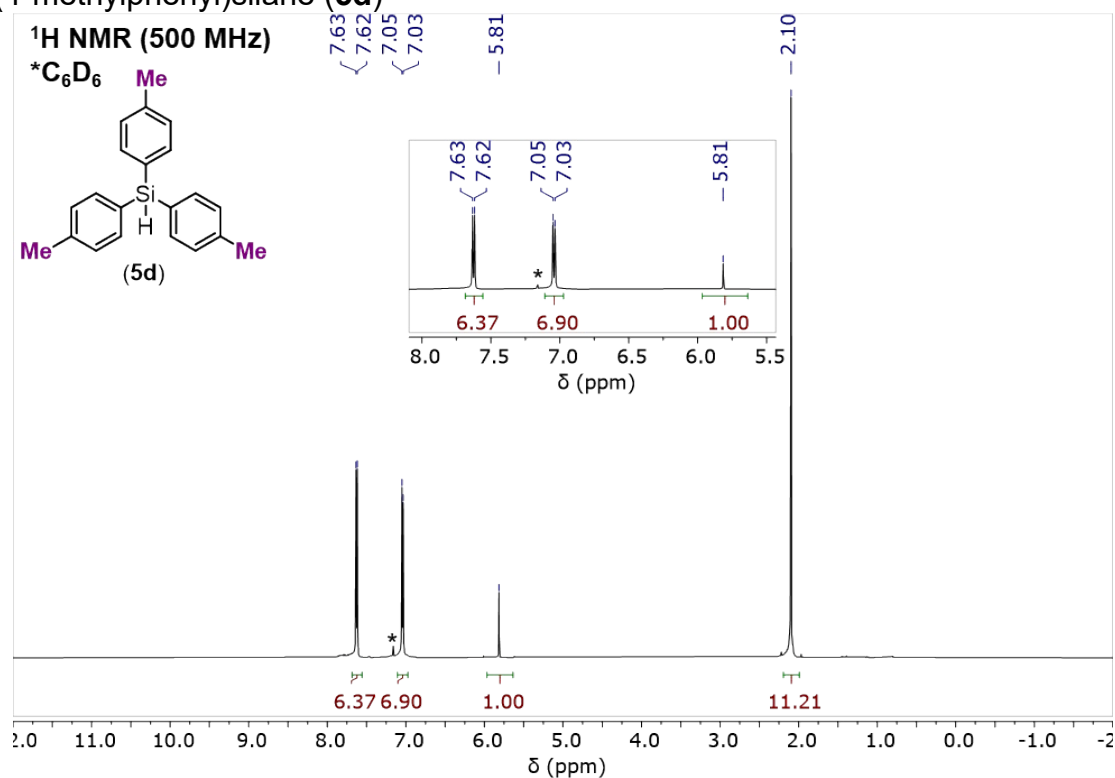


Figure S67. <sup>1</sup>H NMR spectrum of **5d** recorded in C<sub>6</sub>D<sub>6</sub> at room temperature.

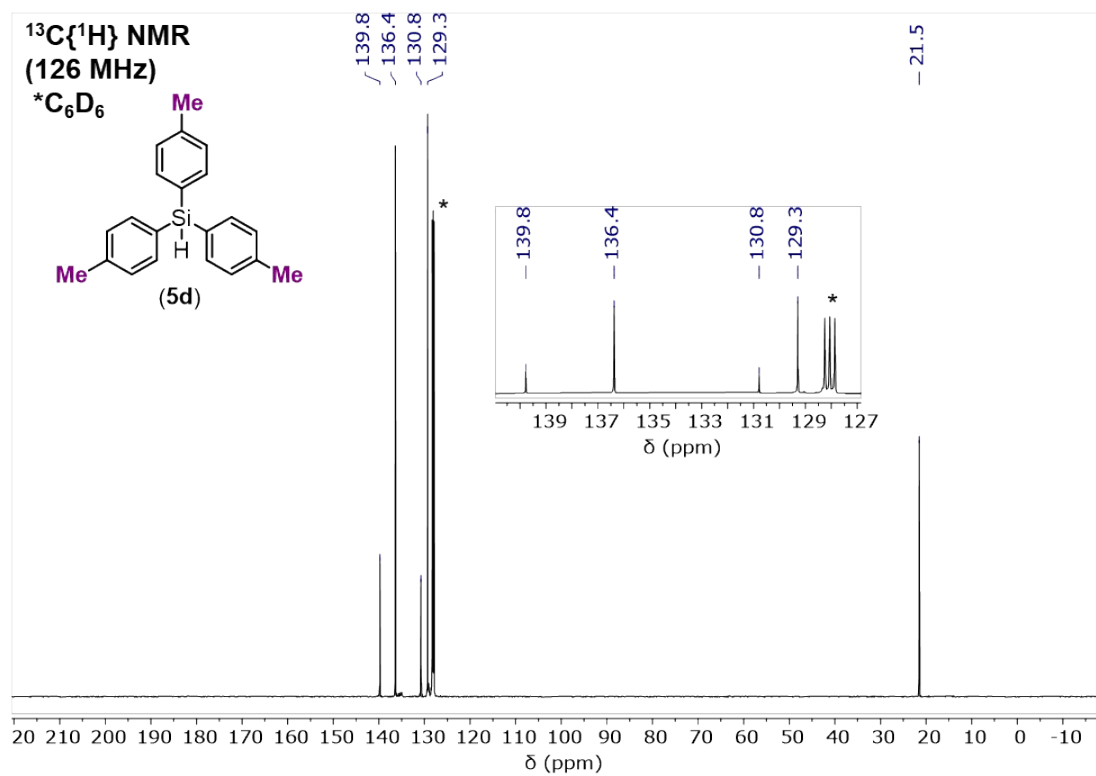
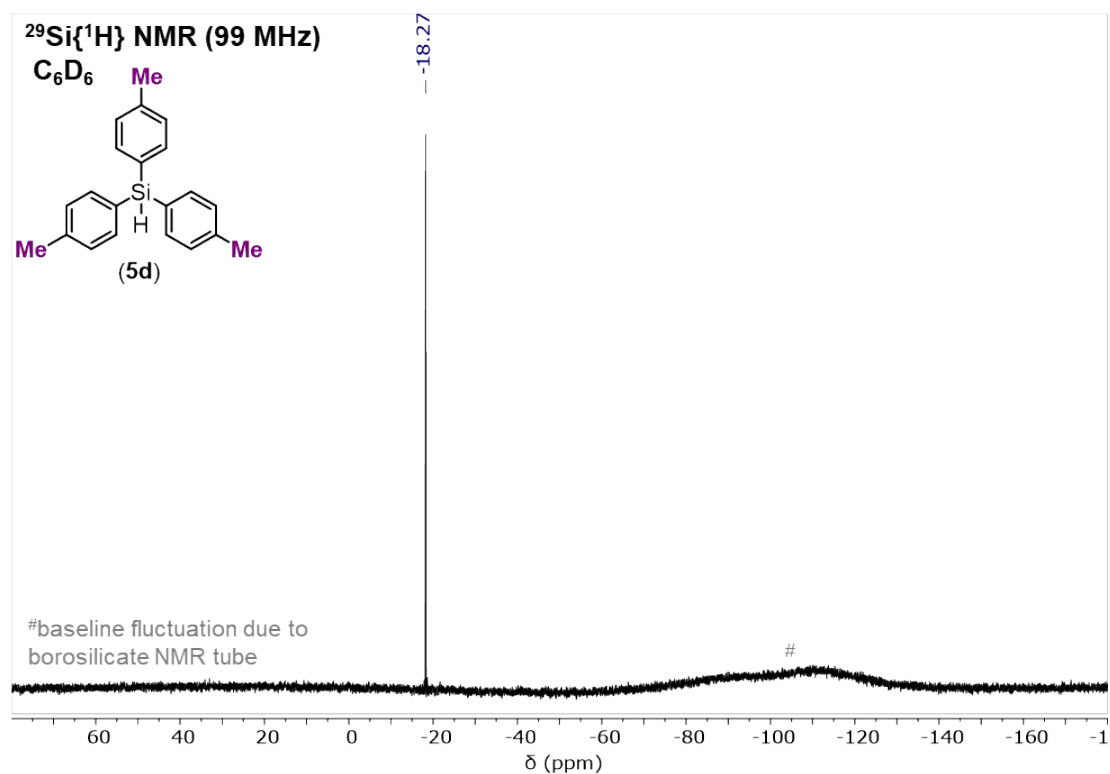
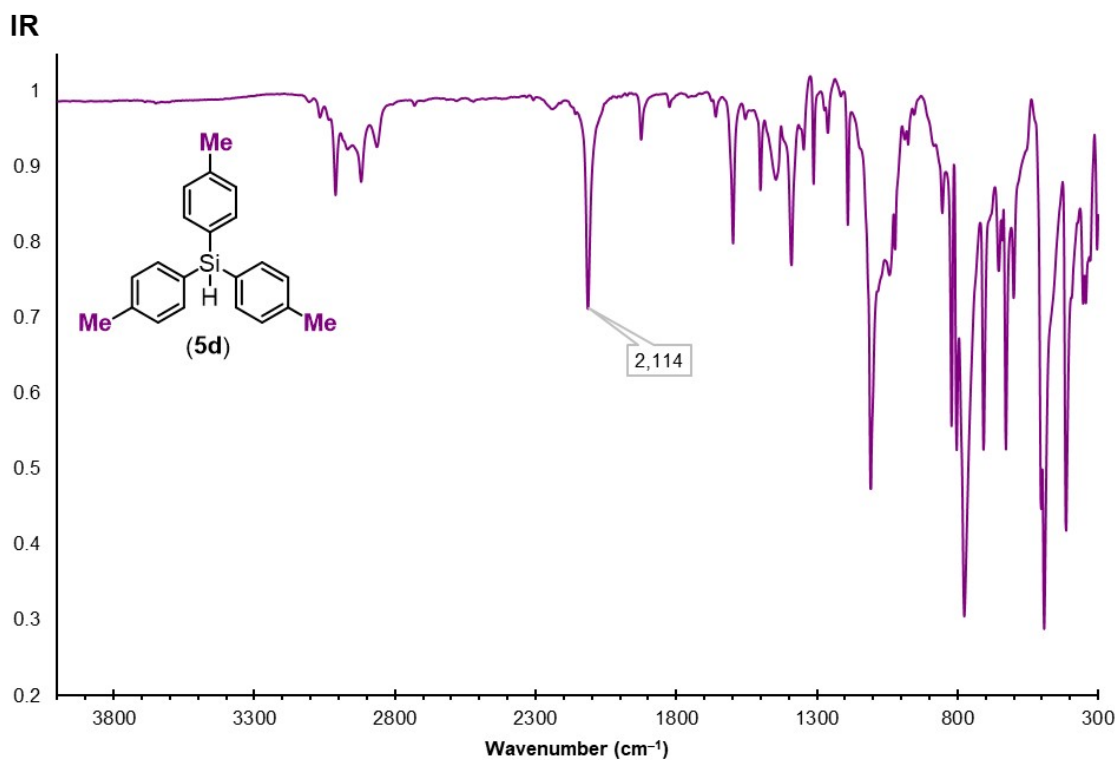


Figure S68. <sup>13</sup>C{<sup>1</sup>H} NMR spectrum of **5d** recorded in C<sub>6</sub>D<sub>6</sub> at room temperature.



**Figure S69.** <sup>29</sup>Si{<sup>1</sup>H} NMR spectrum of **5d** recorded in C<sub>6</sub>D<sub>6</sub> at room temperature.



**Figure S70.** IR spectrum of **5d** recorded neat at room temperature.

Triphenylsilane (**5a**)

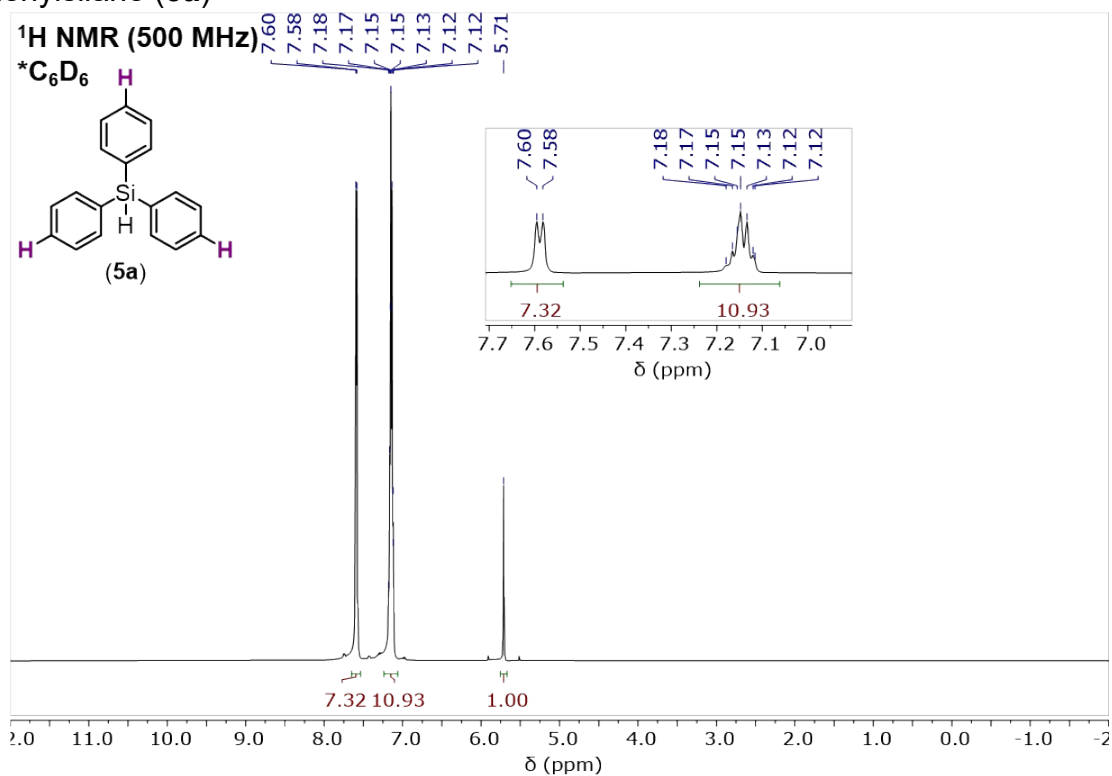


Figure S71. <sup>1</sup>H NMR spectrum of **5a** recorded in C<sub>6</sub>D<sub>6</sub> at room temperature.

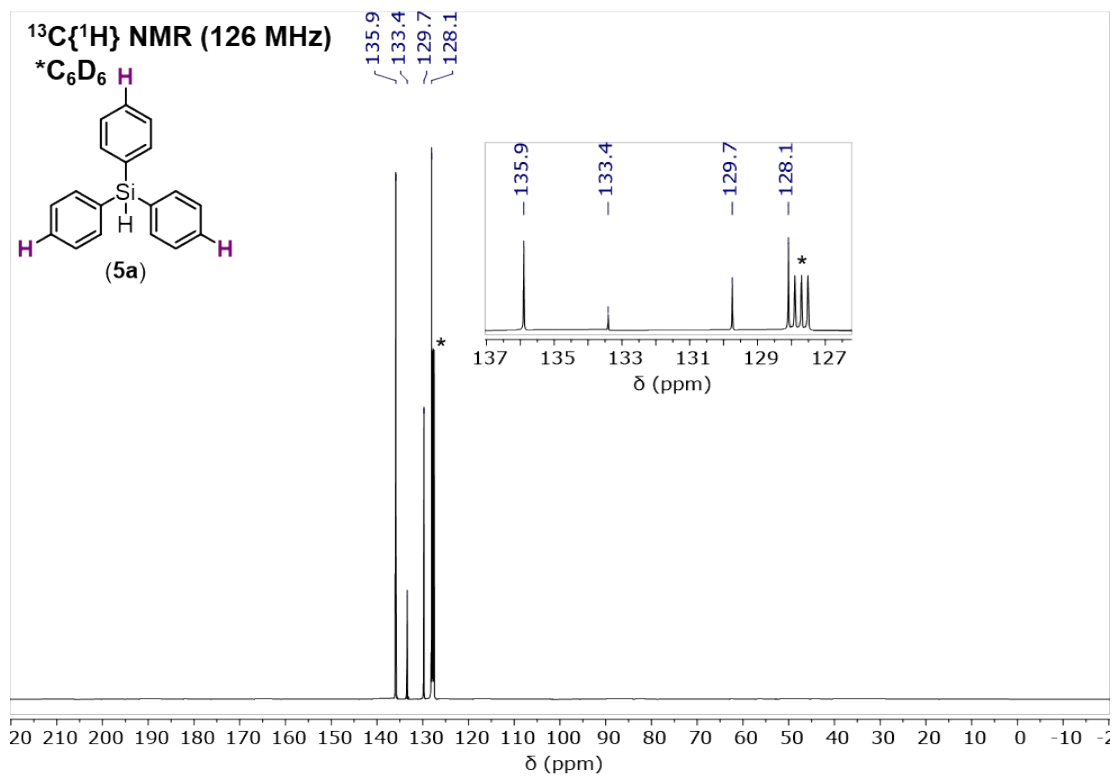
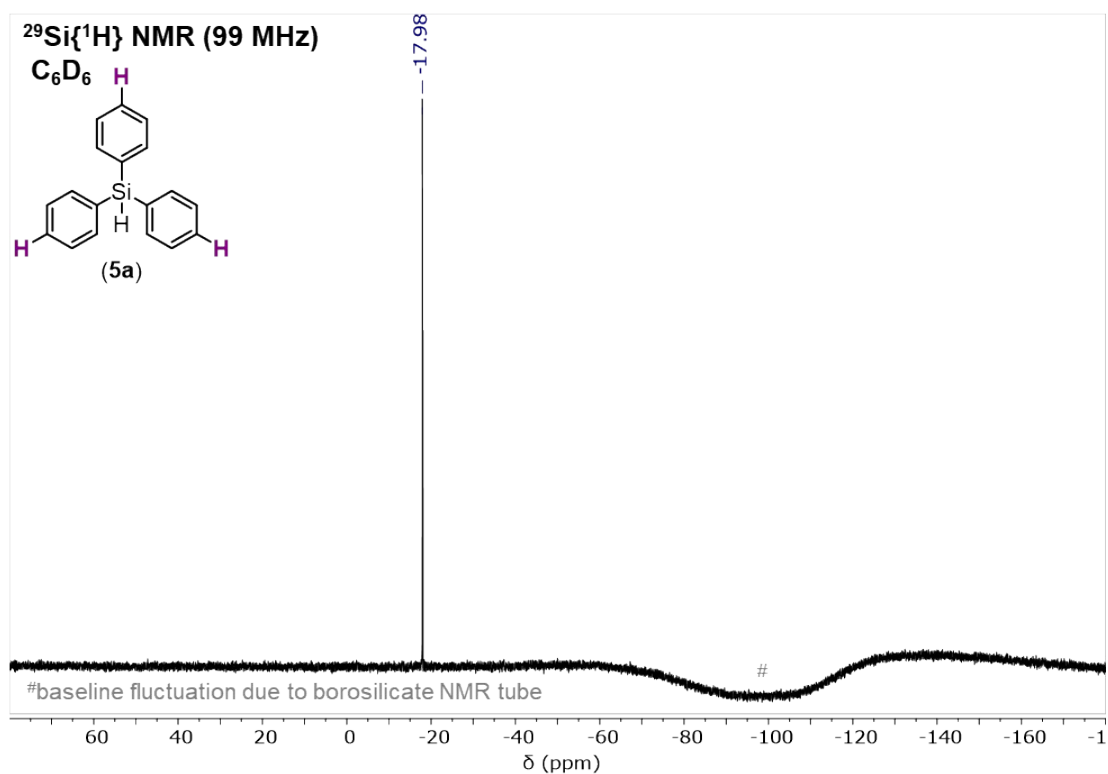
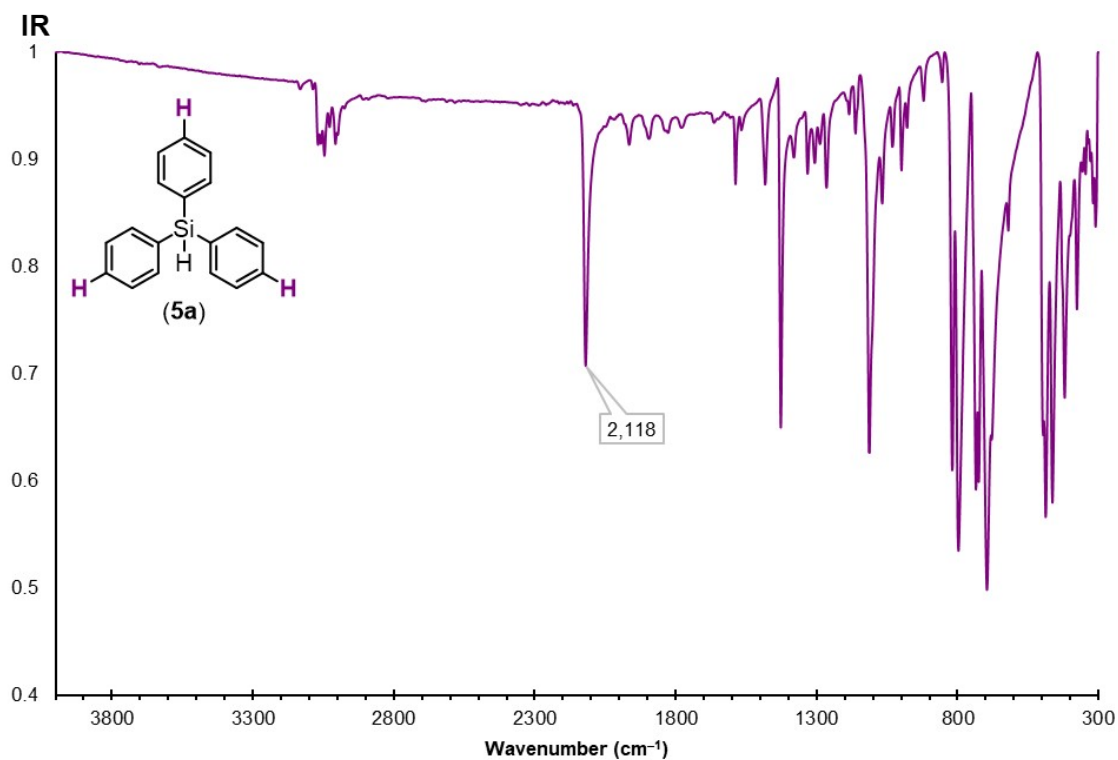


Figure S72. <sup>13</sup>C{<sup>1</sup>H} NMR spectrum of **5a** recorded in C<sub>6</sub>D<sub>6</sub> at room temperature.



**Figure S73.** <sup>29</sup>Si{<sup>1</sup>H} NMR spectrum of **5a** recorded in C<sub>6</sub>D<sub>6</sub> at room temperature.



**Figure S74.** IR spectrum of **5a** recorded neat at room temperature.

Tris(4-fluorophenyl)silane (**5e**)

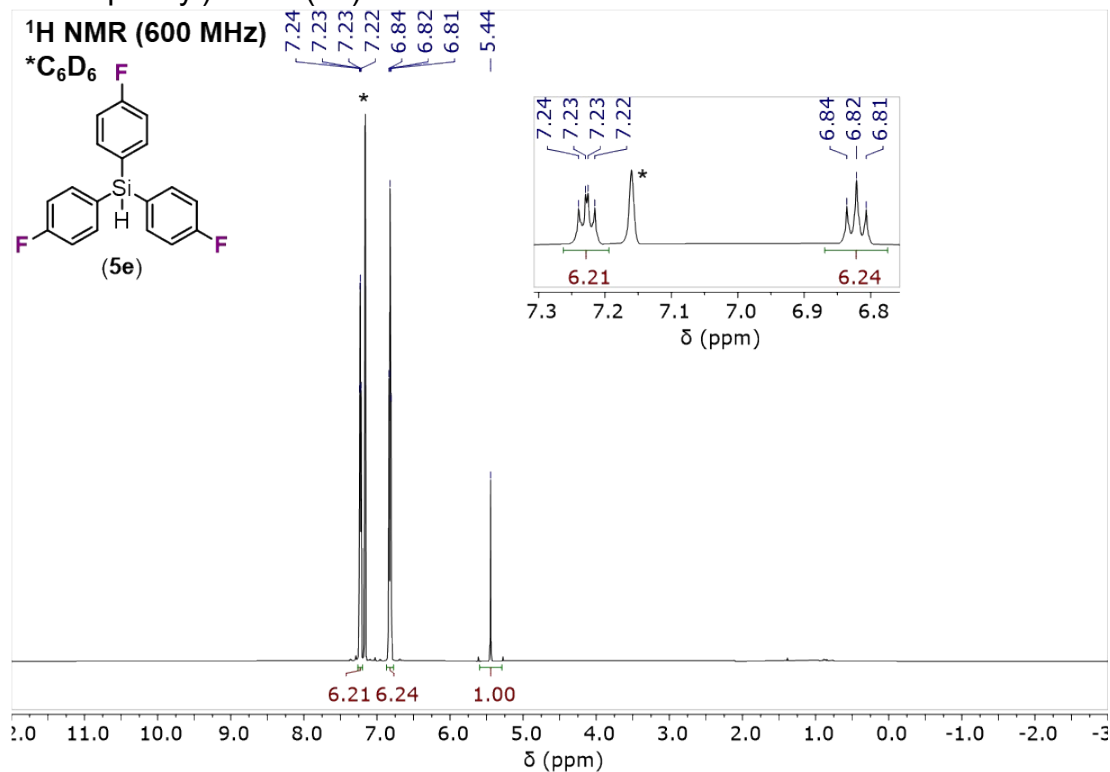


Figure S75. <sup>1</sup>H NMR spectrum of **5e** recorded in C<sub>6</sub>D<sub>6</sub> at room temperature.

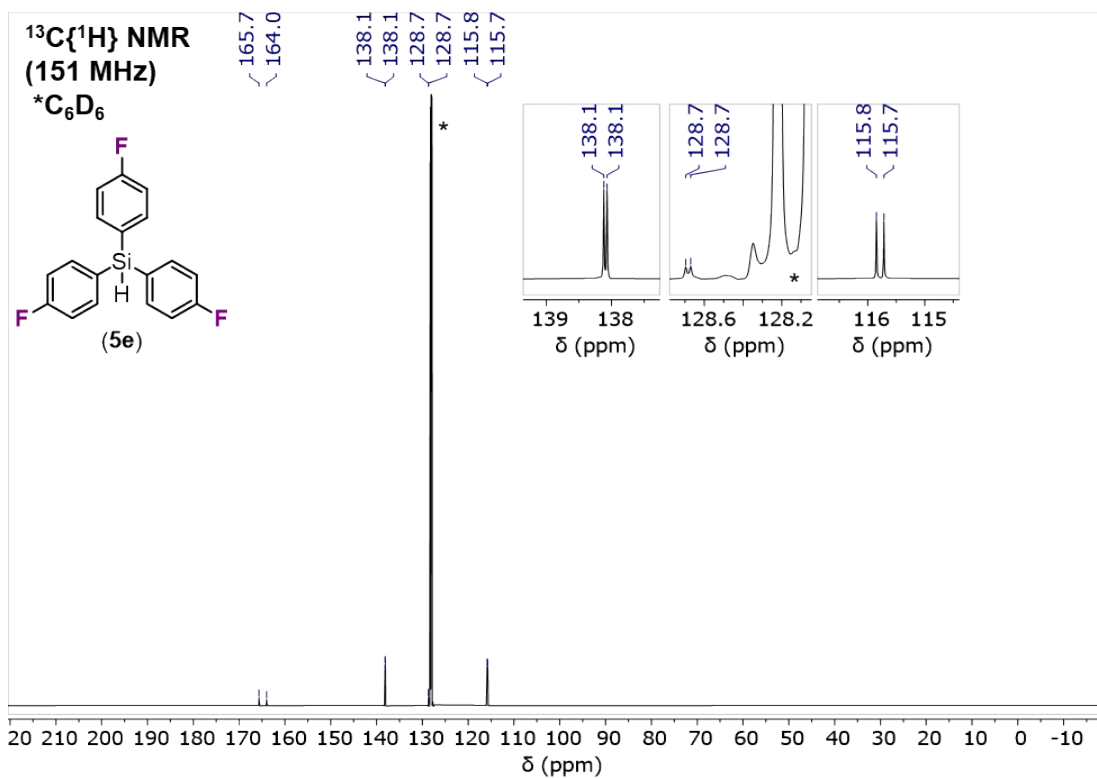
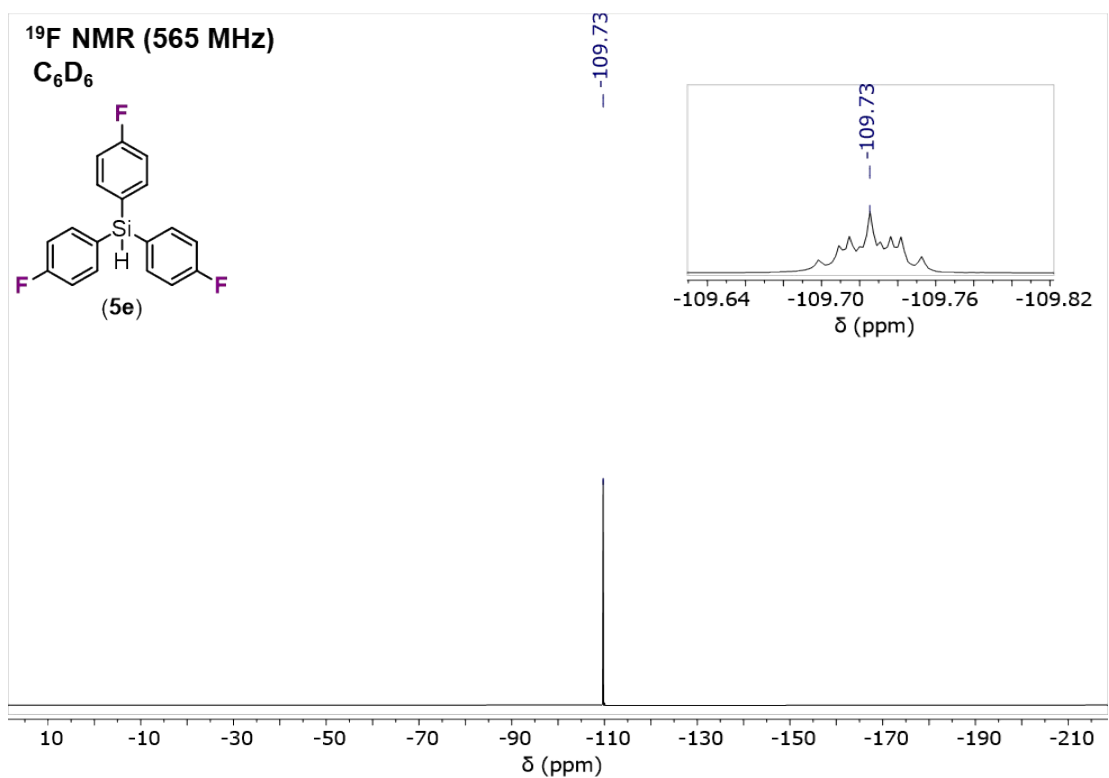
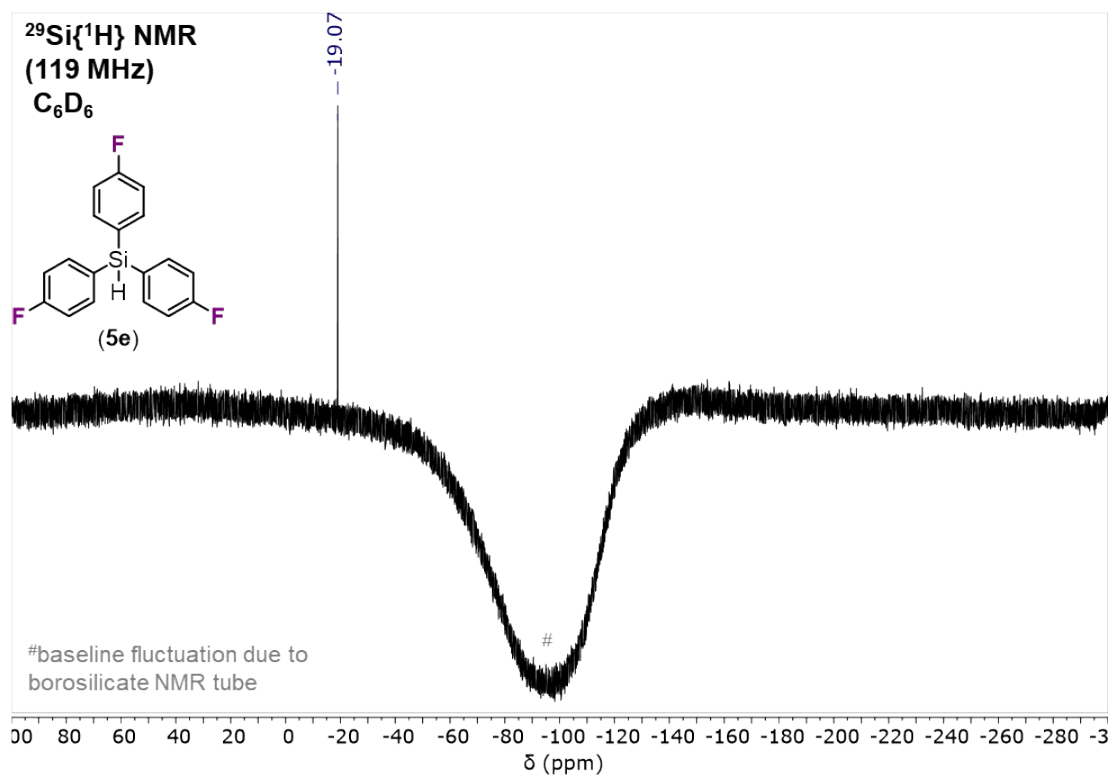


Figure S76. <sup>13</sup>C{<sup>1</sup>H} NMR spectrum of **5e** recorded in C<sub>6</sub>D<sub>6</sub> at room temperature.



**Figure S77.**  $^{19}\text{F}$  NMR spectrum of **5e** recorded in  $\text{C}_6\text{D}_6$  at room temperature.



**Figure S78.**  $^{29}\text{Si}\{^1\text{H}\}$  NMR spectrum of **5e** recorded in  $\text{C}_6\text{D}_6$  at room temperature.

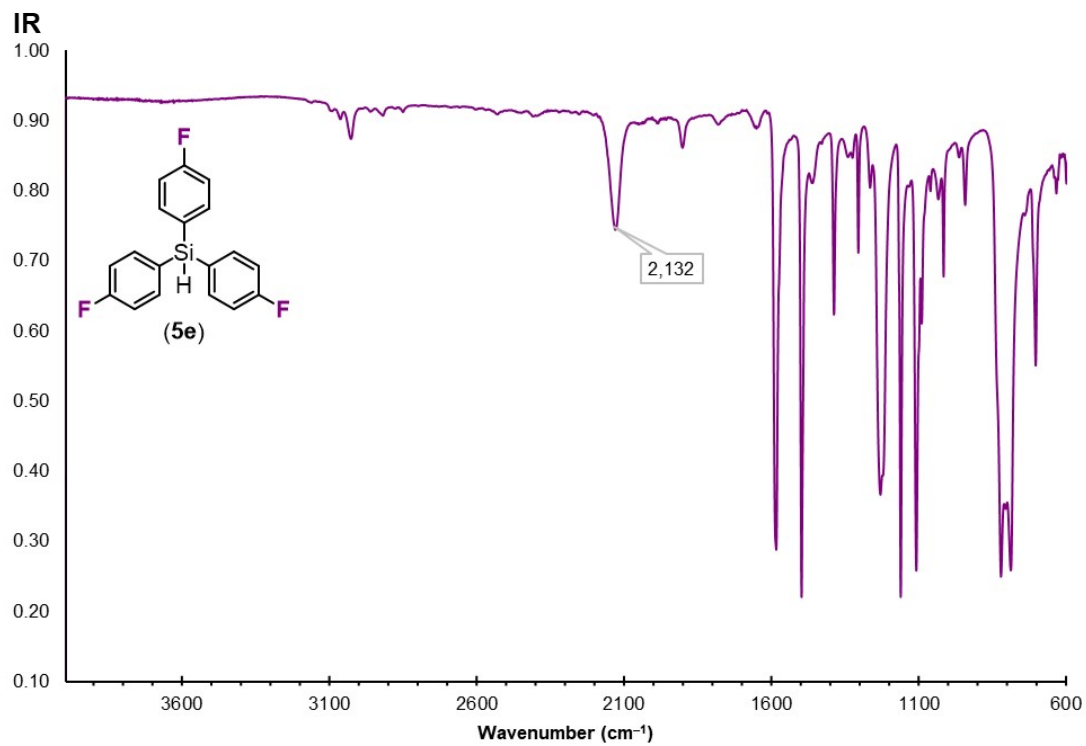


**Figure S79.** IR spectrum of **5e** recorded neat at room temperature.

Tris[4-(trifluoromethyl)phenyl]silane (**5f**)

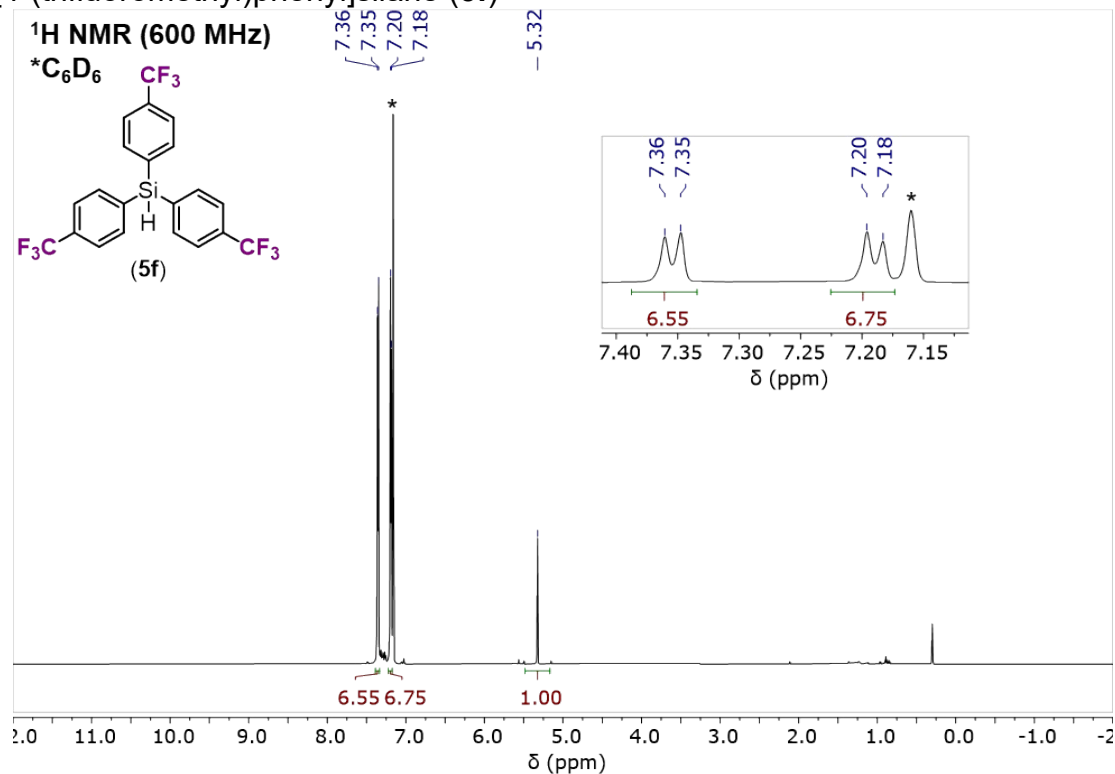


Figure S80. <sup>1</sup>H NMR spectrum of **5f** recorded in C<sub>6</sub>D<sub>6</sub> at room temperature.

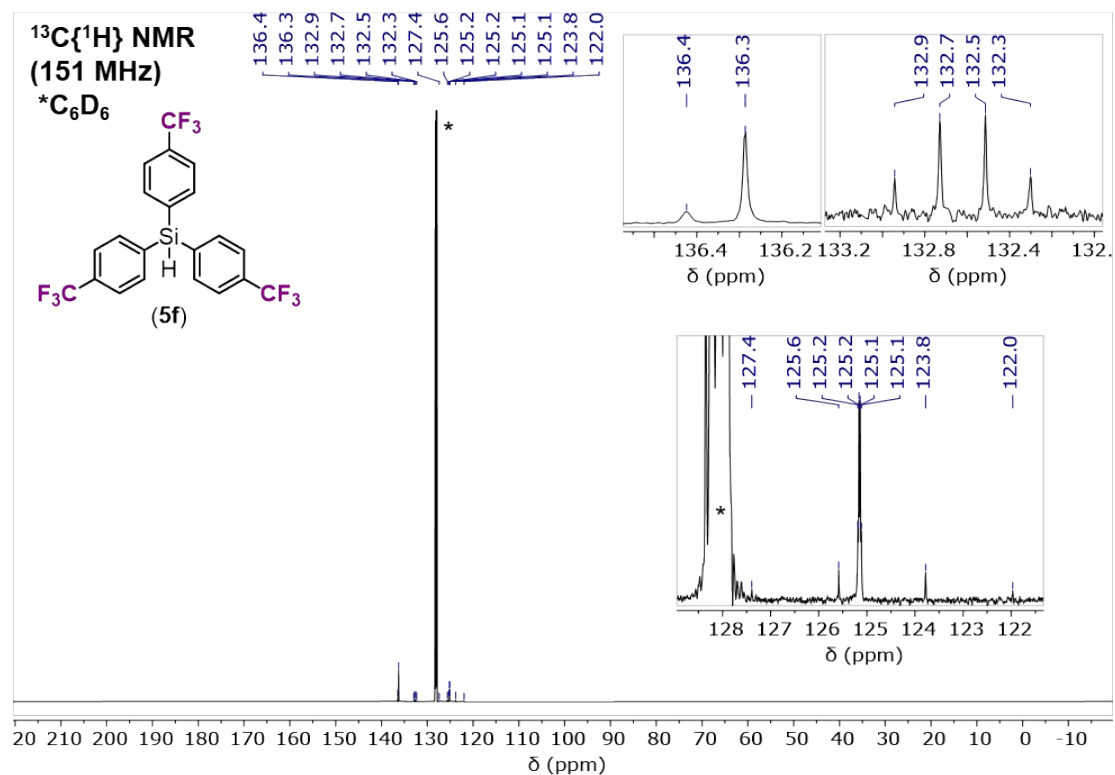
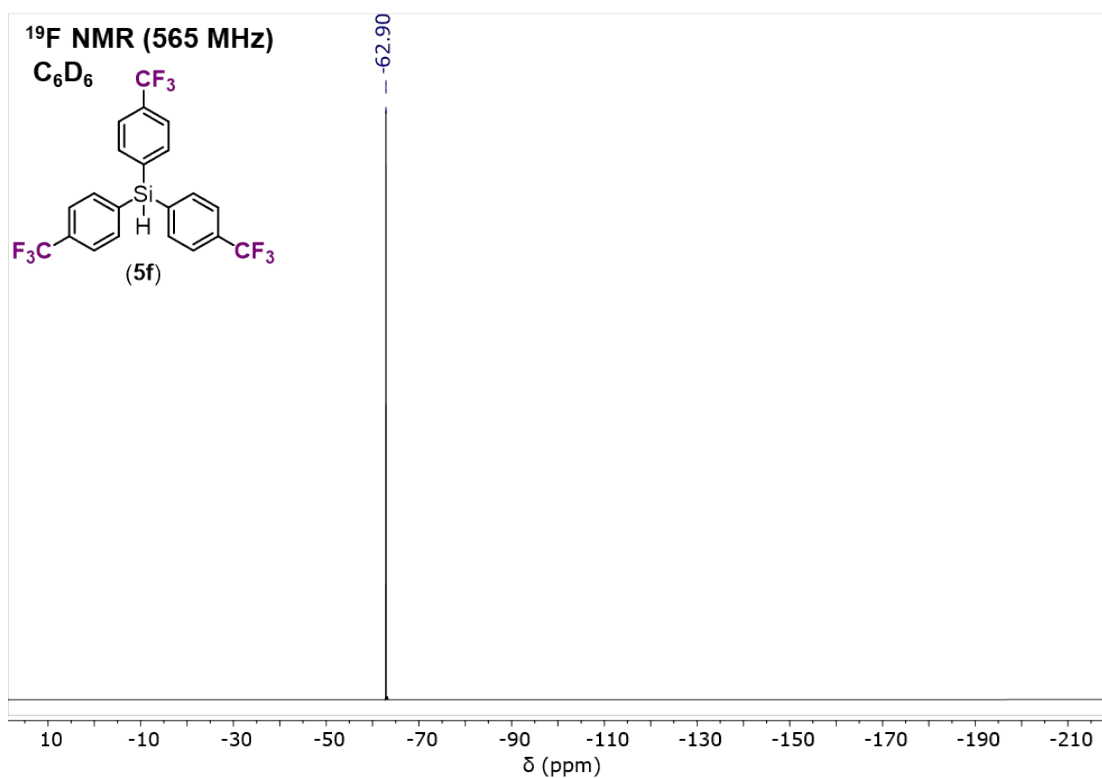
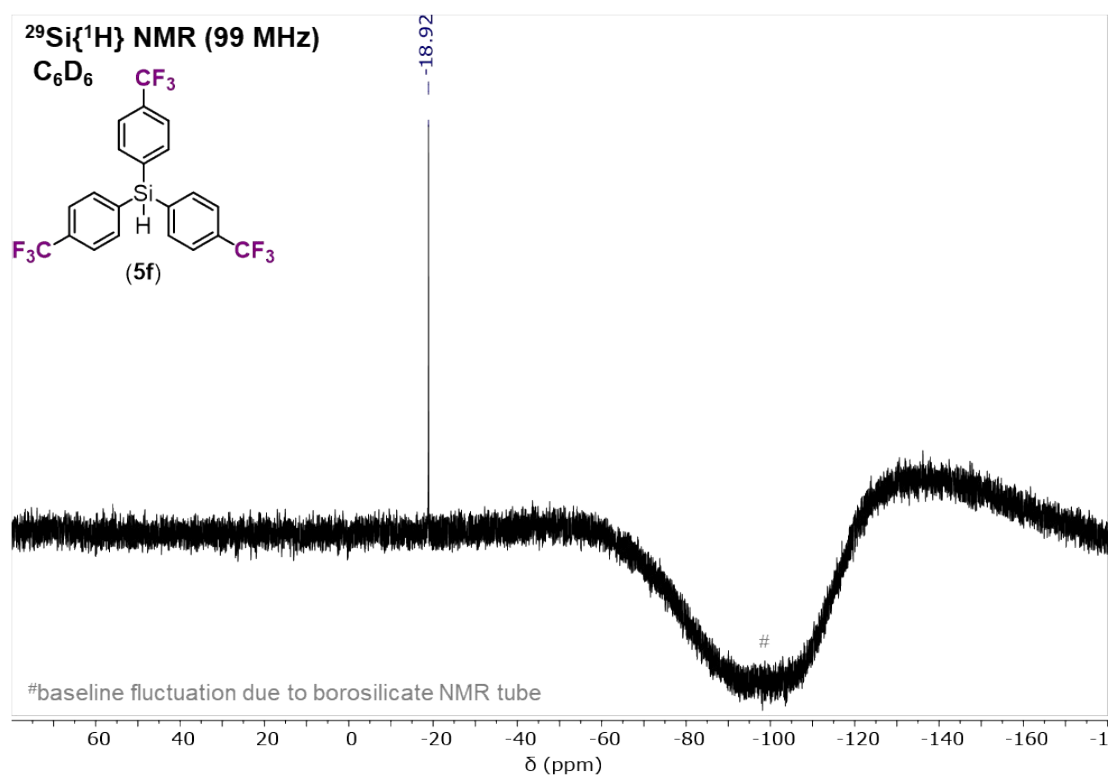


Figure S81. <sup>13</sup>C{<sup>1</sup>H} NMR spectrum of **5f** recorded in C<sub>6</sub>D<sub>6</sub> at room temperature.



**Figure S82.**  $^{19}\text{F}$  NMR spectrum of **5f** recorded in  $\text{C}_6\text{D}_6$  at room temperature.



**Figure S83.**  $^{29}\text{Si}\{^1\text{H}\}$  NMR spectrum of **5f** recorded in  $\text{C}_6\text{D}_6$  at room temperature.

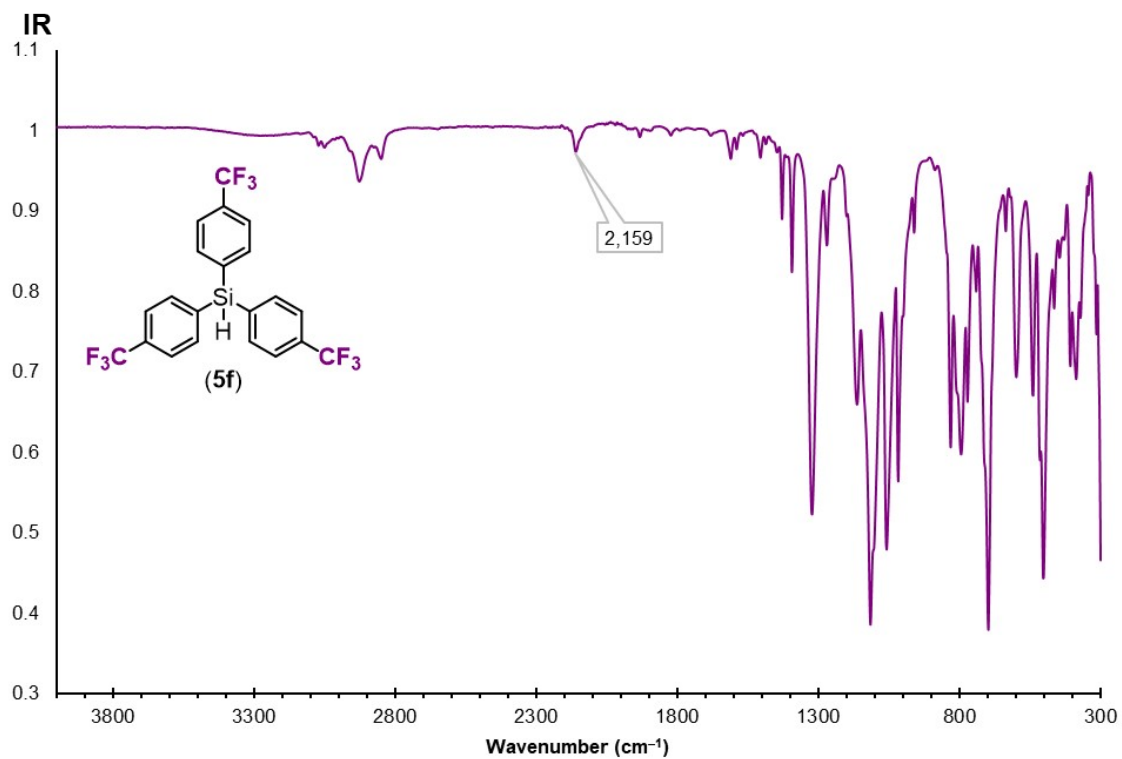


**Figure S84.** IR spectrum of **5f** recorded neat at room temperature.

### c. Aryl dimethyl silanes

[4-(*N,N*-dimethylamino)phenyl]dimethylsilane (**3b**)

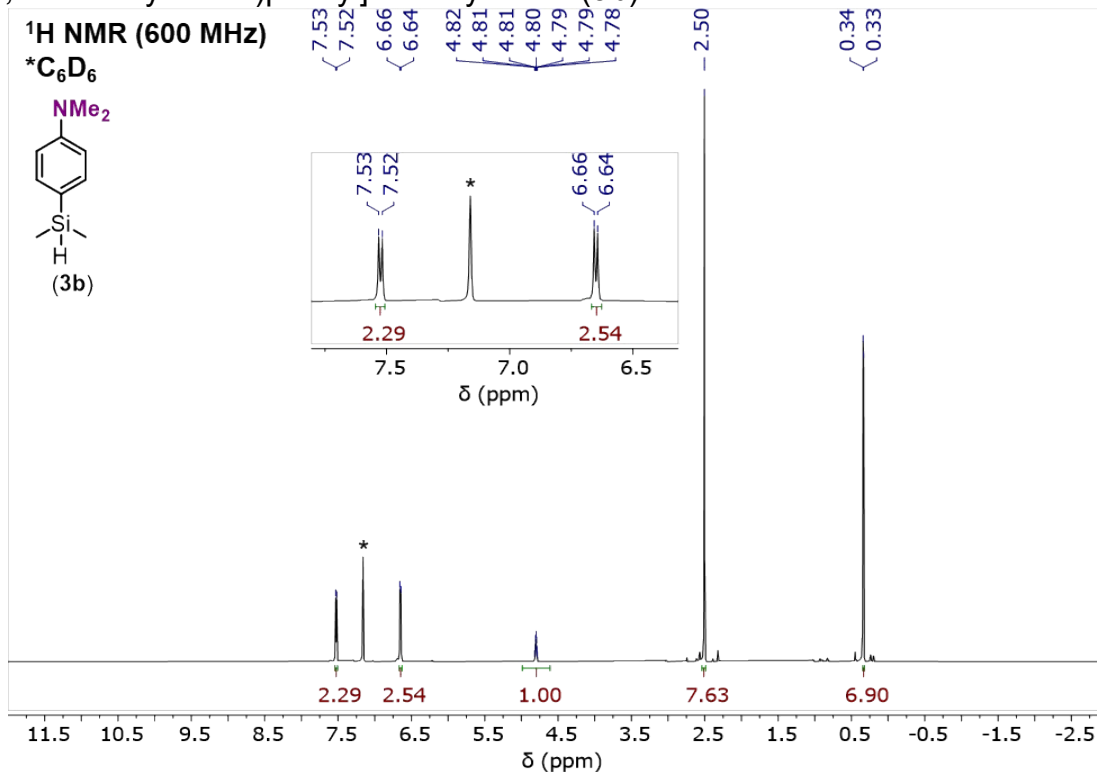


Figure S85. <sup>1</sup>H NMR spectrum of **3b** recorded in C<sub>6</sub>D<sub>6</sub> at room temperature.

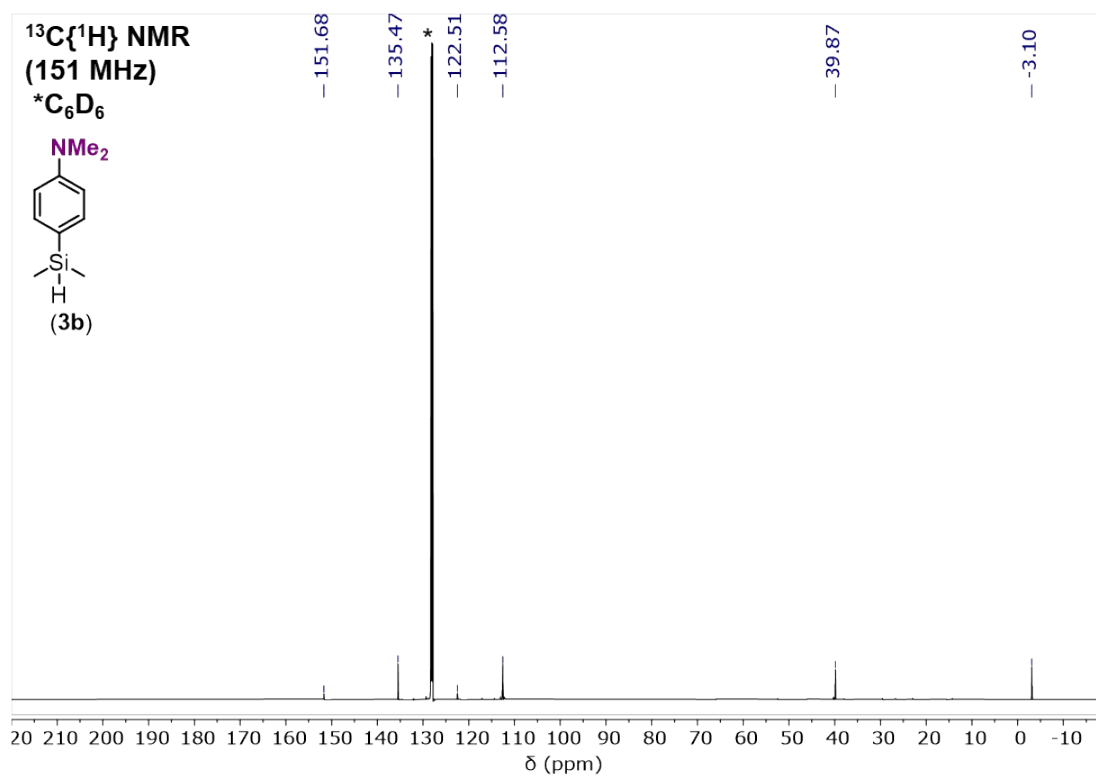
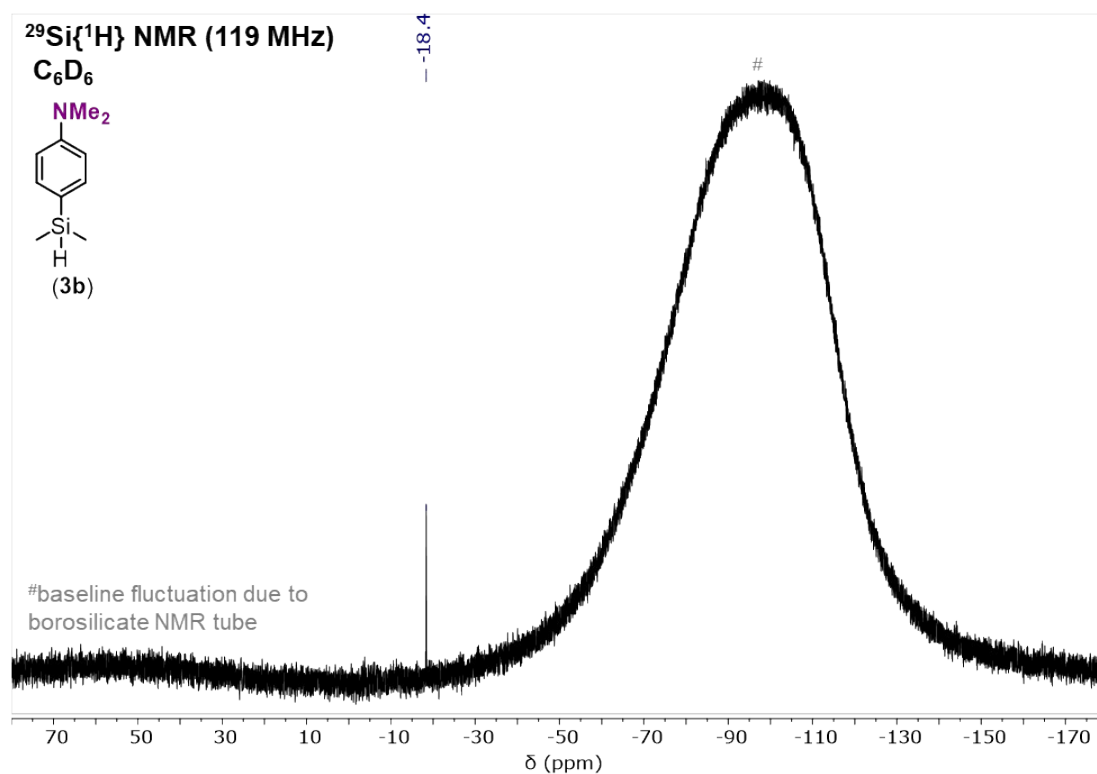
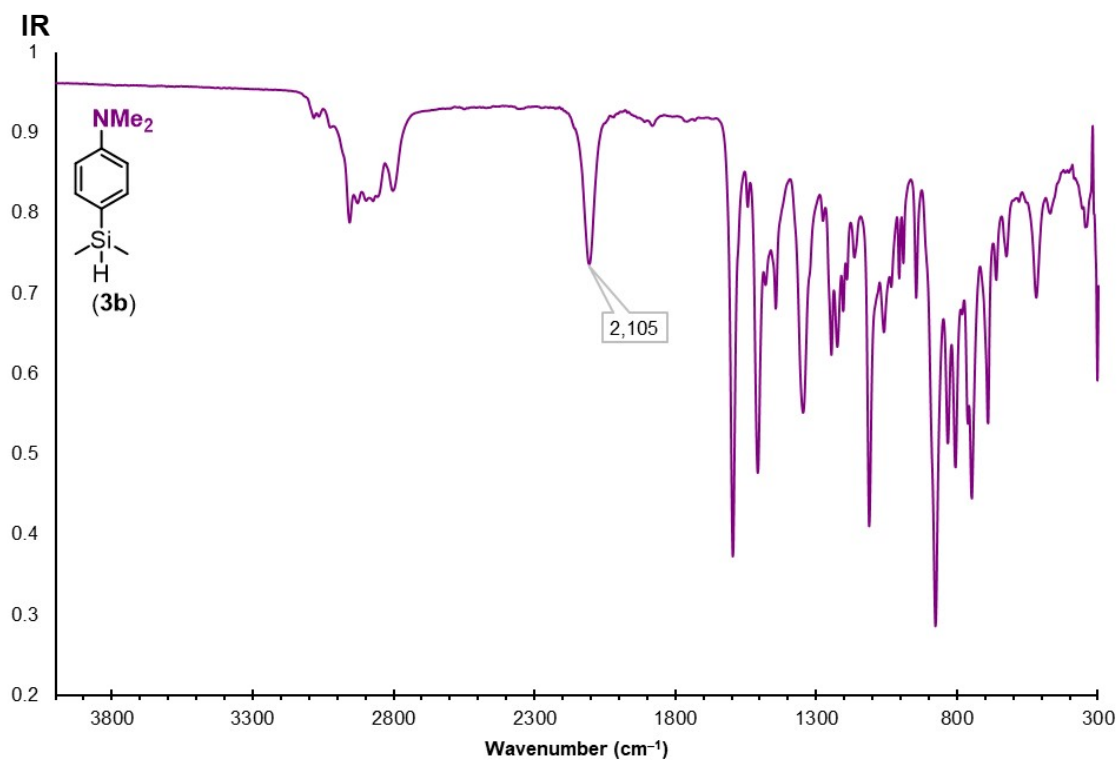


Figure S86. <sup>13</sup>C{<sup>1</sup>H} NMR spectrum of **3b** recorded in C<sub>6</sub>D<sub>6</sub> at room temperature.



**Figure S87.** <sup>29</sup>Si{<sup>1</sup>H} NMR spectrum of **3b** recorded in C<sub>6</sub>D<sub>6</sub> at room temperature.



**Figure S88.** IR spectrum of **3b** recorded neat at room temperature.

(4-methoxyphenyl)dimethylsilane (**3c**)

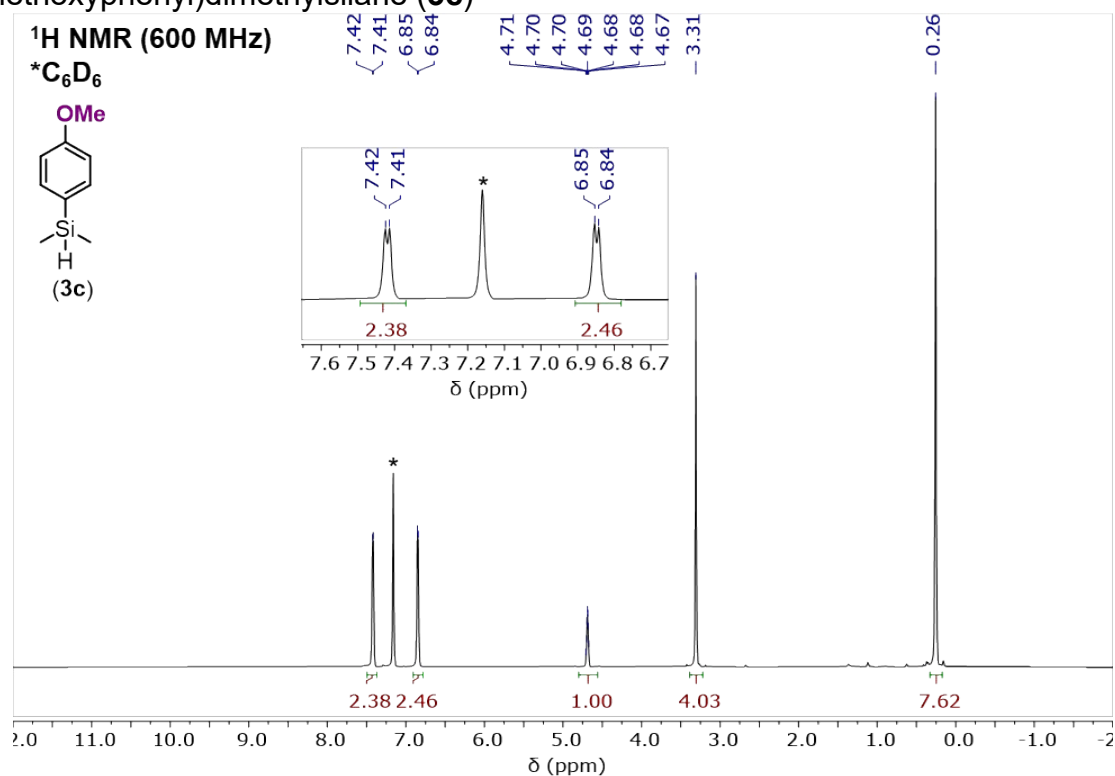


Figure S89. <sup>1</sup>H NMR spectrum of **3c** recorded in C<sub>6</sub>D<sub>6</sub> at room temperature.

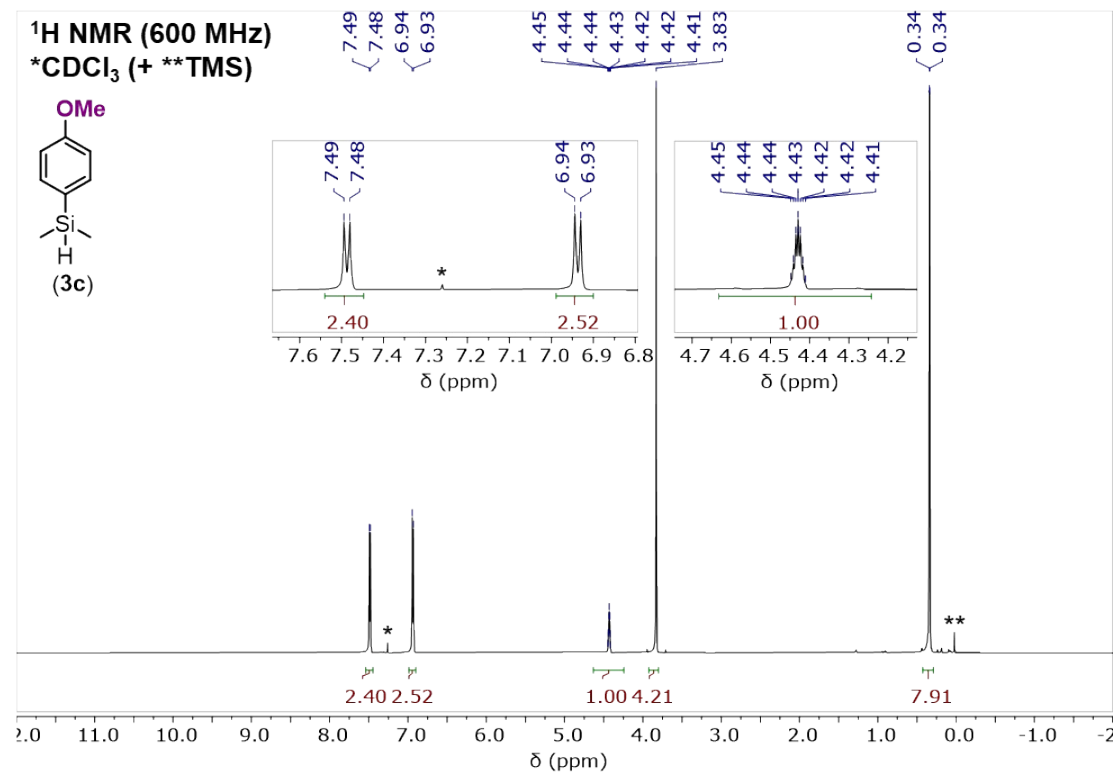
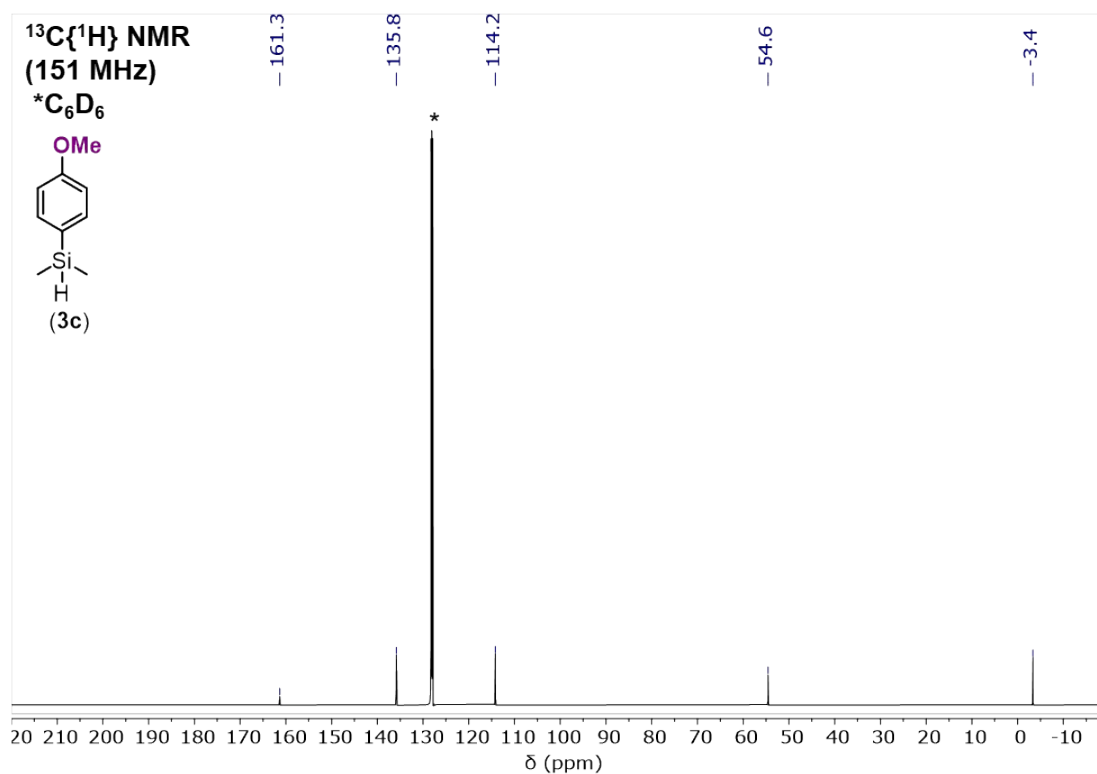
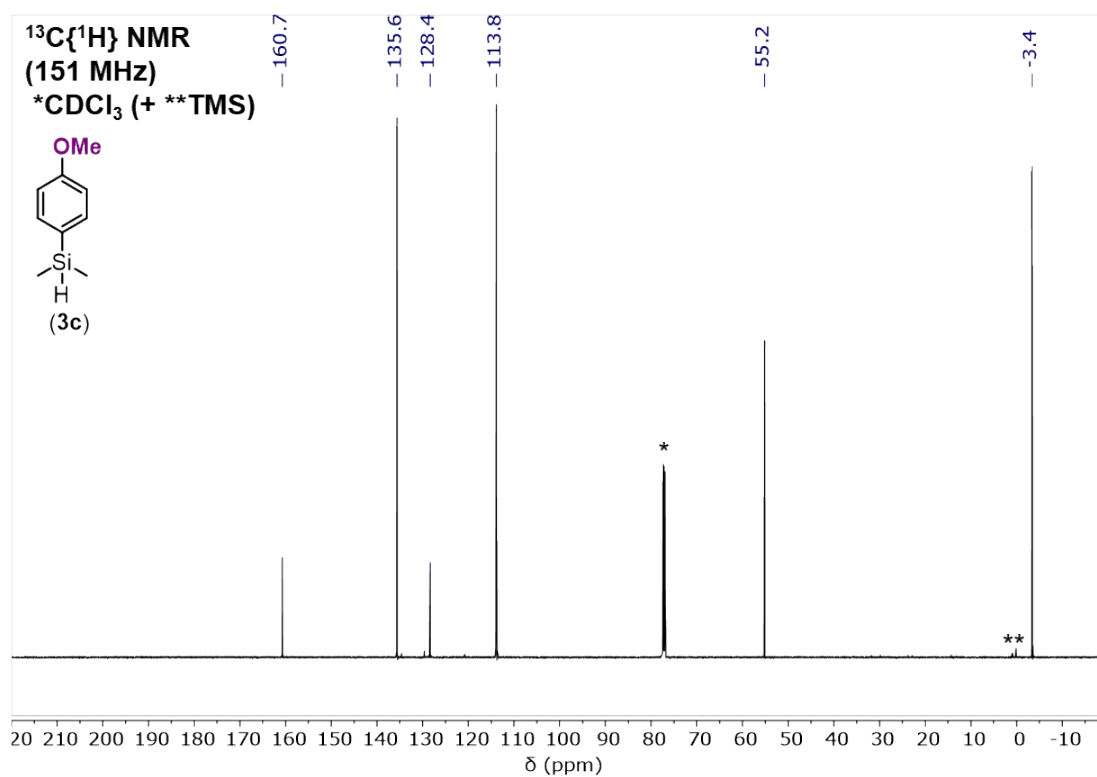


Figure S90. <sup>1</sup>H NMR spectrum of **3c** recorded in CDCl<sub>3</sub> at room temperature.



**Figure S91.**  $^{13}\text{C}\{^1\text{H}\}$  NMR spectrum of **3c** recorded in  $\text{C}_6\text{D}_6$  at room temperature.



**Figure S92.**  $^{13}\text{C}\{^1\text{H}\}$  NMR spectrum of **3c** recorded in  $\text{CDCl}_3$  at room temperature.

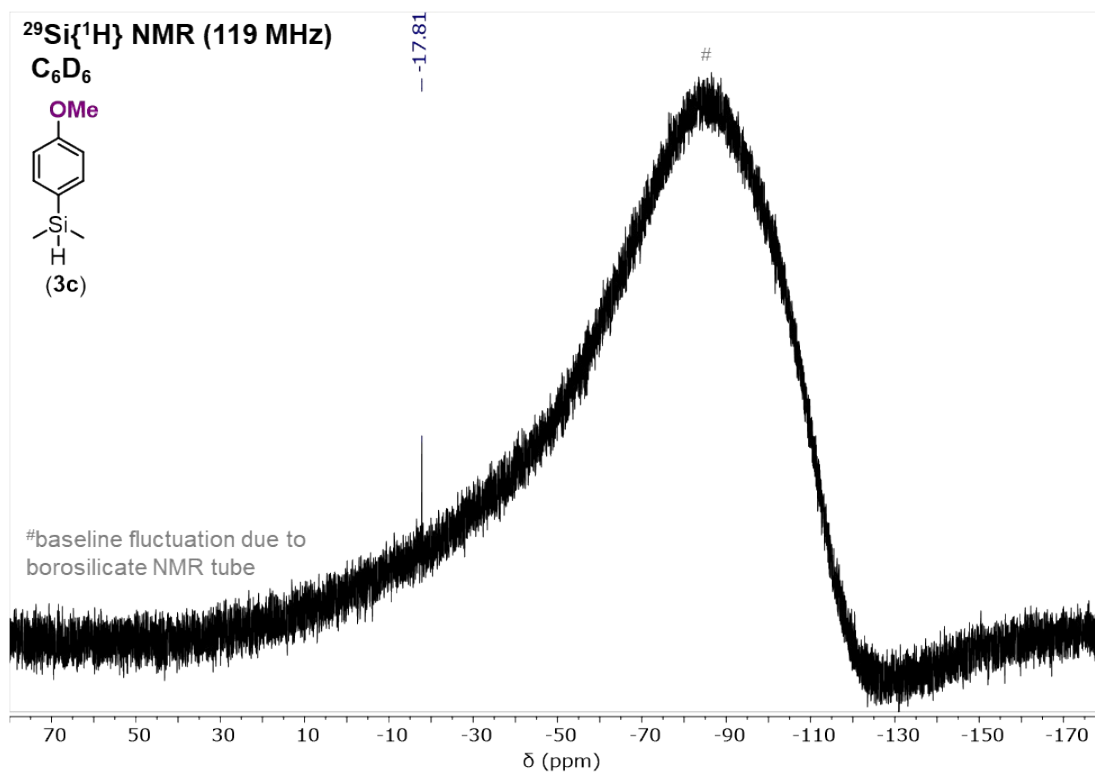


**Figure S93.**  $^{29}\text{Si}\{^1\text{H}\}$  NMR spectrum of **3c** recorded in  $\text{C}_6\text{D}_6$  at room temperature.

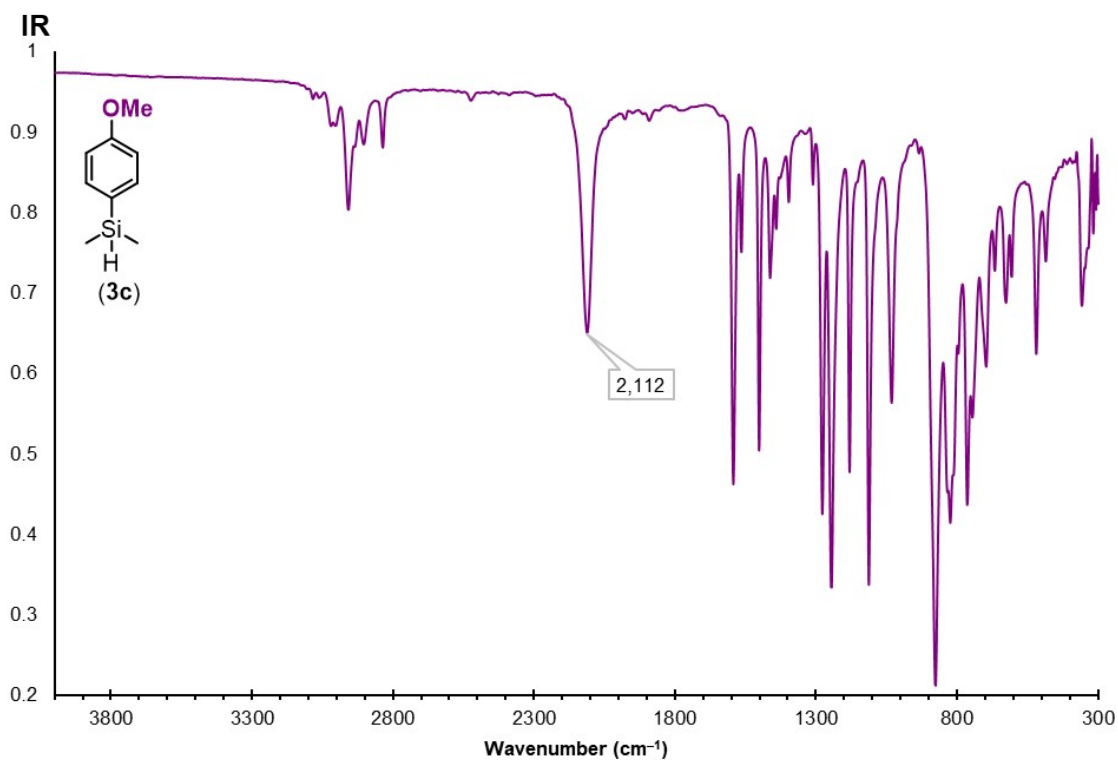


**Figure S94.** IR spectrum of **3c** recorded neat at room temperature.

(4-methylphenyl)dimethylsilane (**3d**)

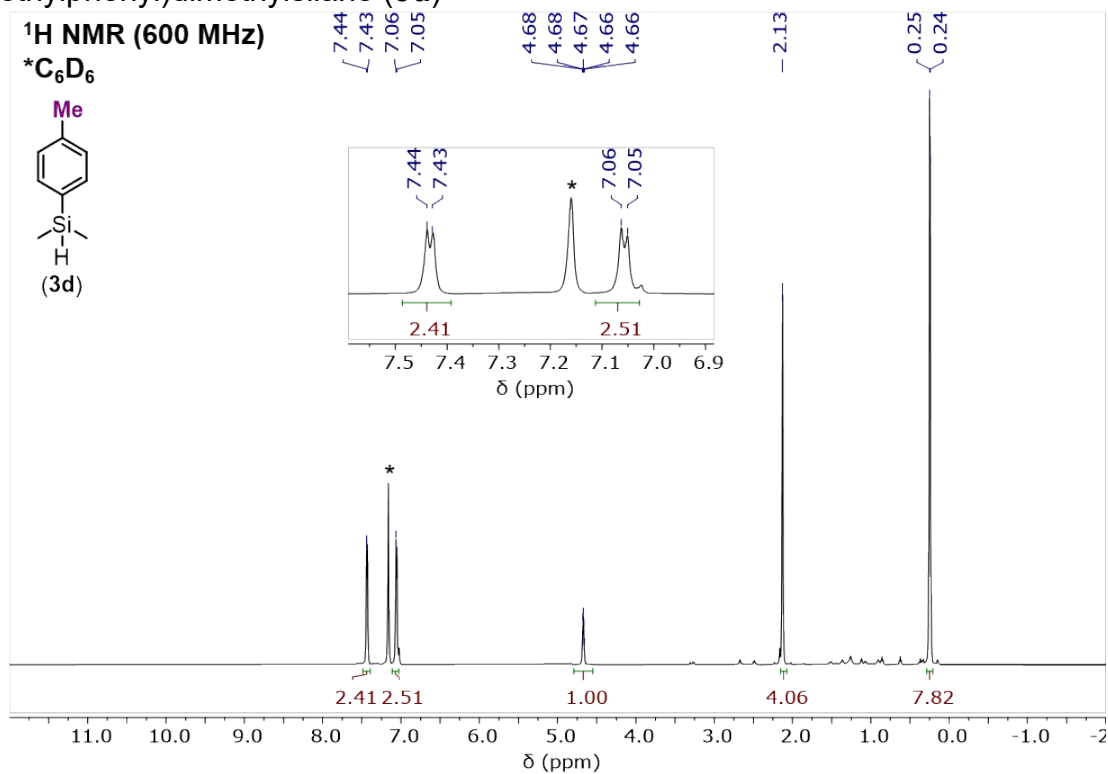


Figure S95. <sup>1</sup>H NMR spectrum of **3d** recorded in C<sub>6</sub>D<sub>6</sub> at room temperature.

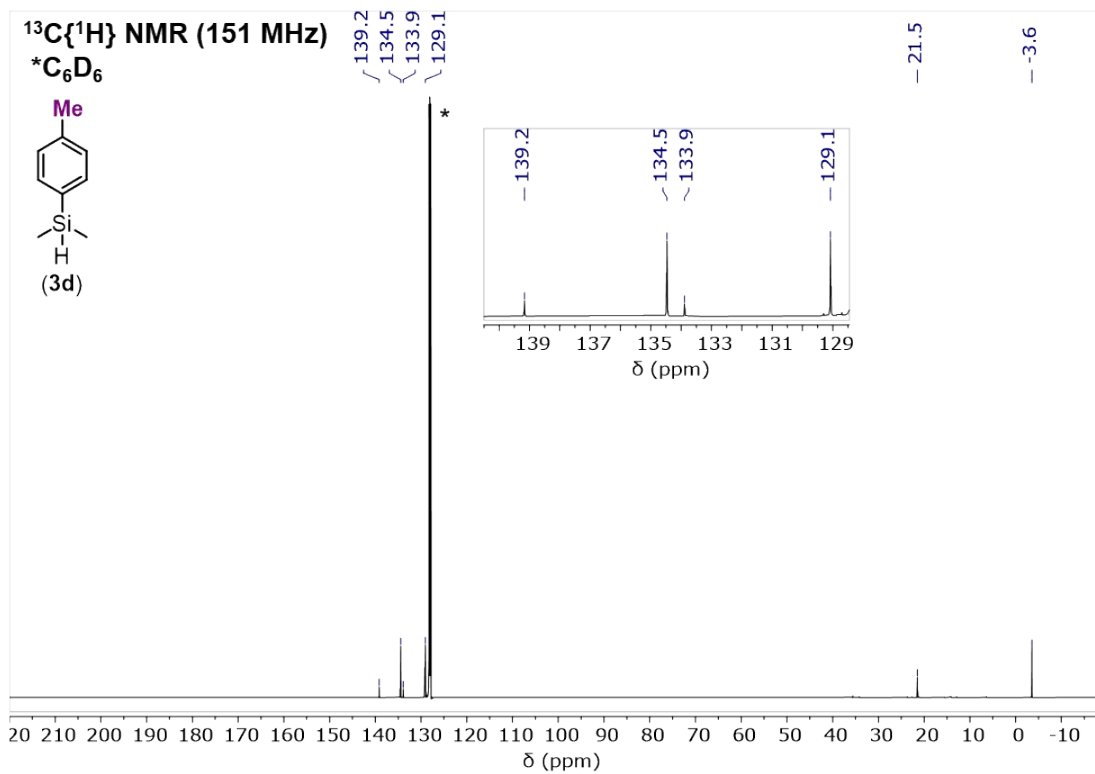
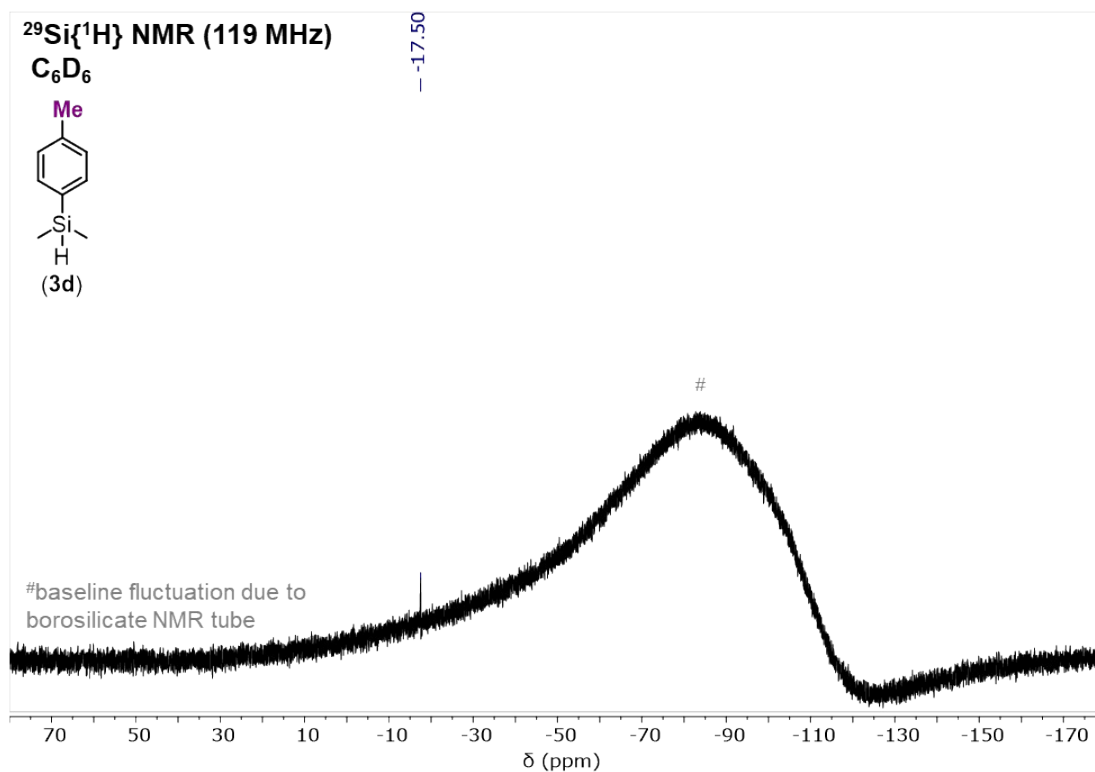
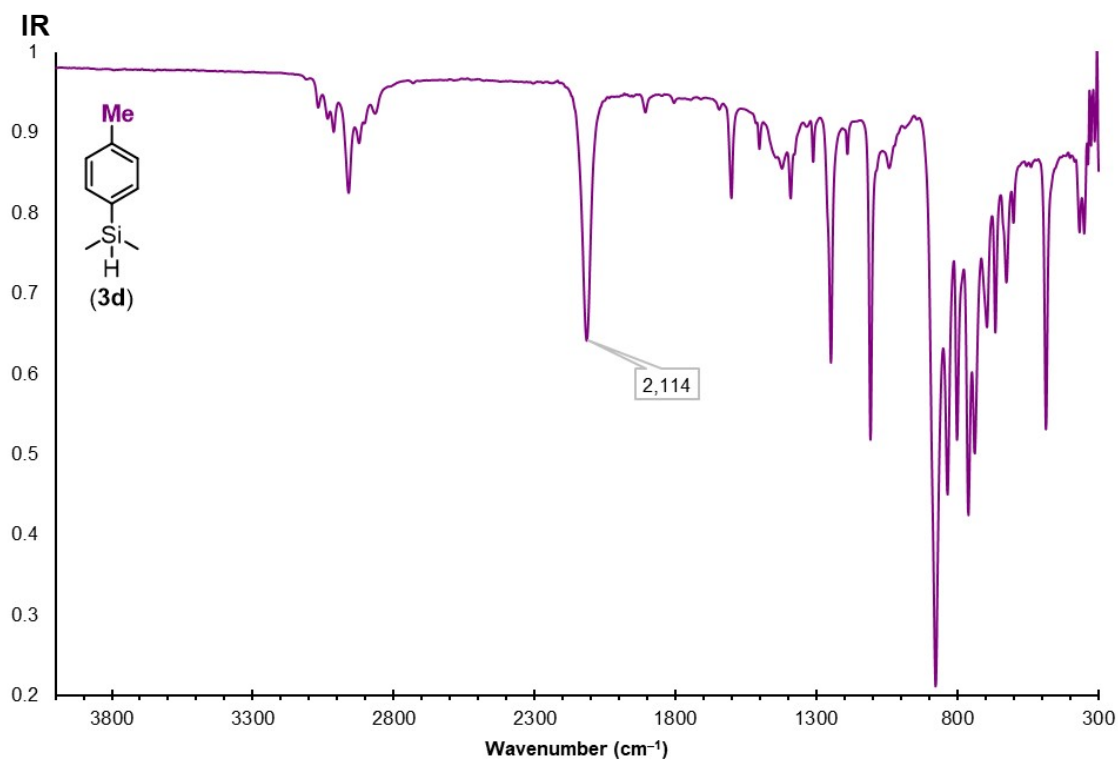


Figure S96. <sup>13</sup>C{<sup>1</sup>H} NMR spectrum of **3d** recorded in C<sub>6</sub>D<sub>6</sub> at room temperature.



**Figure S97.**  $^{29}\text{Si}\{^1\text{H}\}$  NMR spectrum of **3d** recorded in  $\text{C}_6\text{D}_6$  at room temperature.



**Figure S98.** IR spectrum of **3d** recorded neat at room temperature.

Phenyldimethylsilane (**3a**)

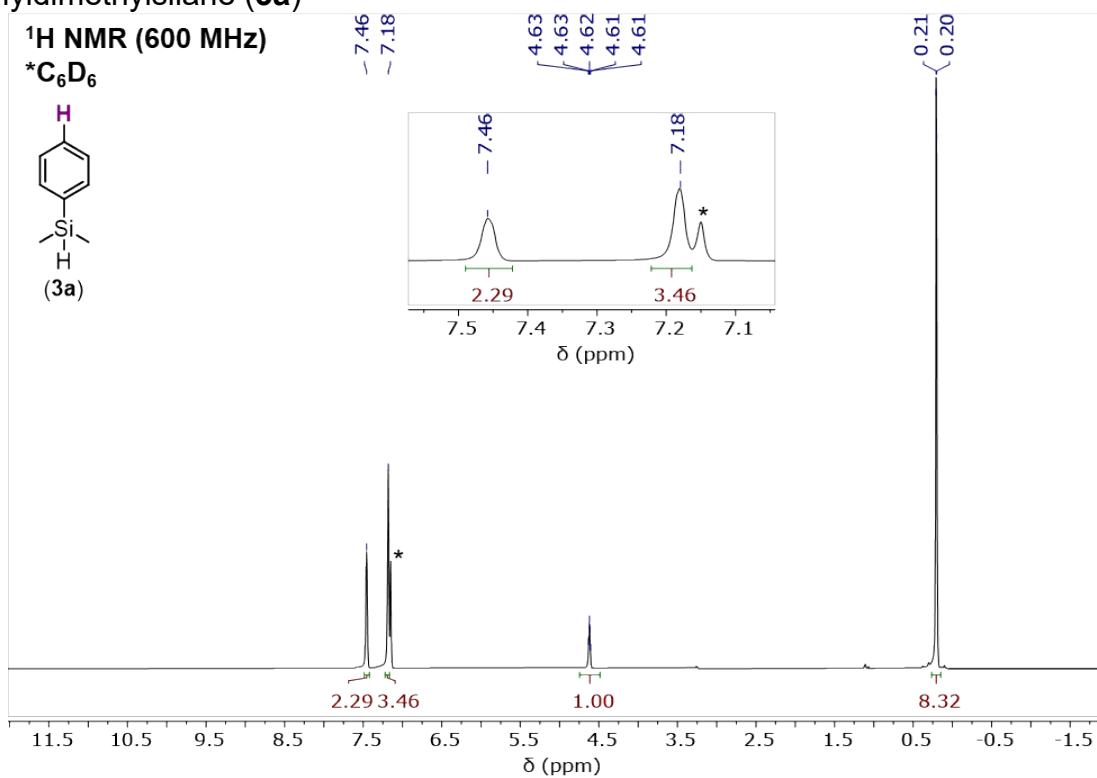


Figure S99. <sup>1</sup>H NMR spectrum of **3a** recorded in C<sub>6</sub>D<sub>6</sub> at room temperature.

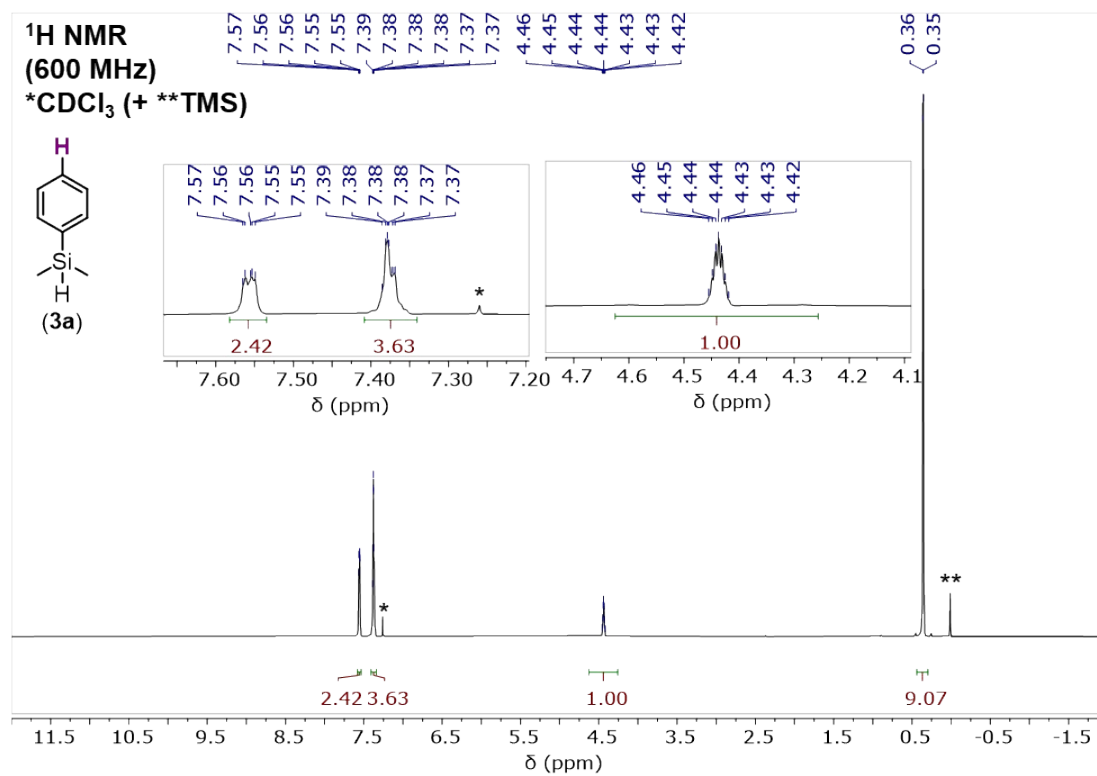
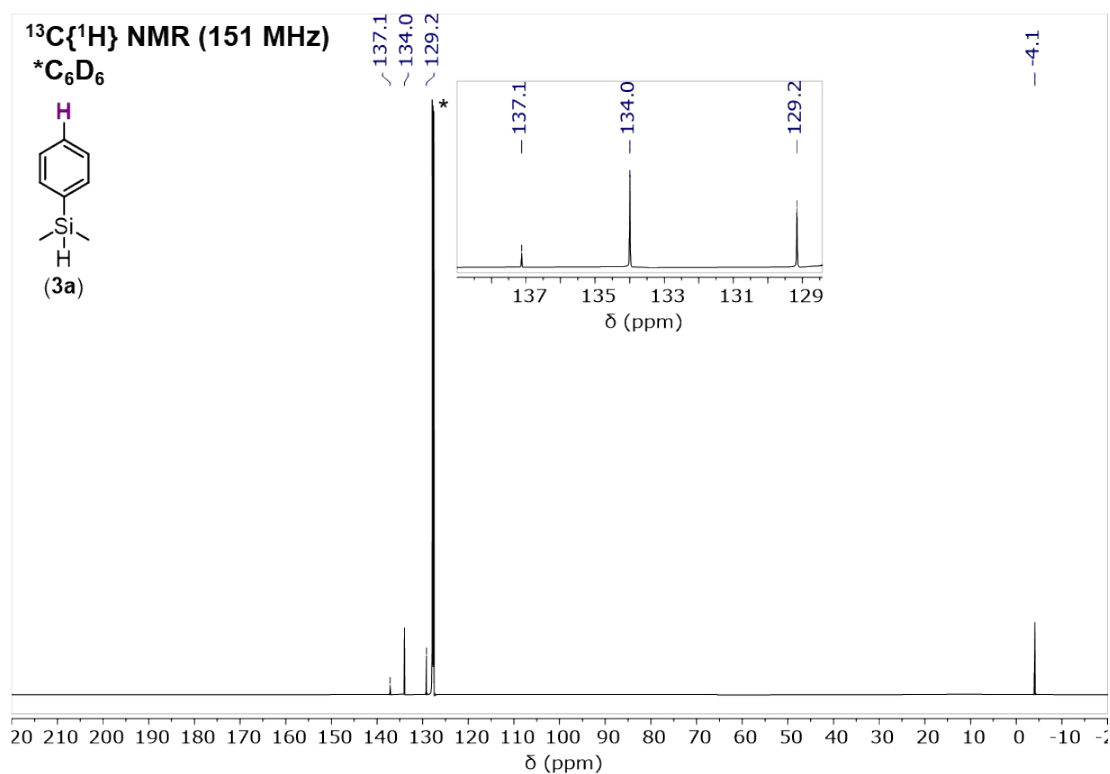
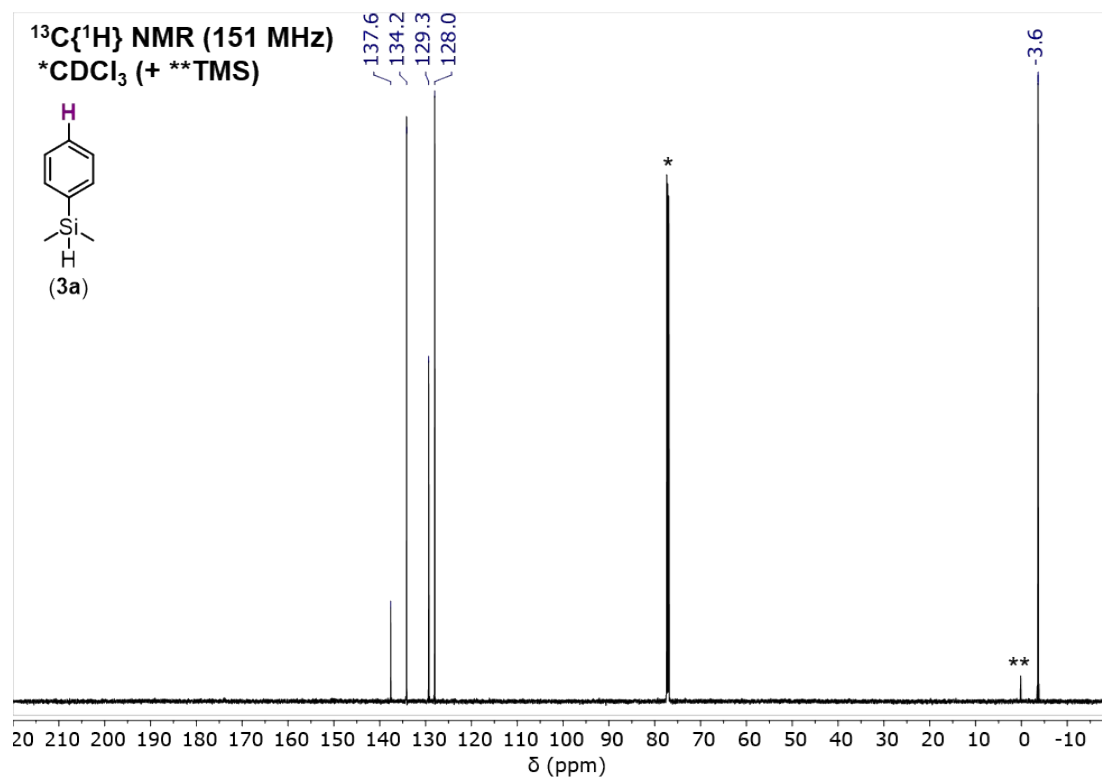


Figure S100. <sup>1</sup>H NMR spectrum of **3a** recorded in CDCl<sub>3</sub> at room temperature.



**Figure S101.**  $^{13}\text{C}\{^1\text{H}\}$  NMR spectrum of **3a** recorded in  $\text{C}_6\text{D}_6$  at room temperature.



**Figure S102.**  $^{13}\text{C}\{^1\text{H}\}$  NMR spectrum of **3a** recorded in  $\text{CDCl}_3$  at room temperature.

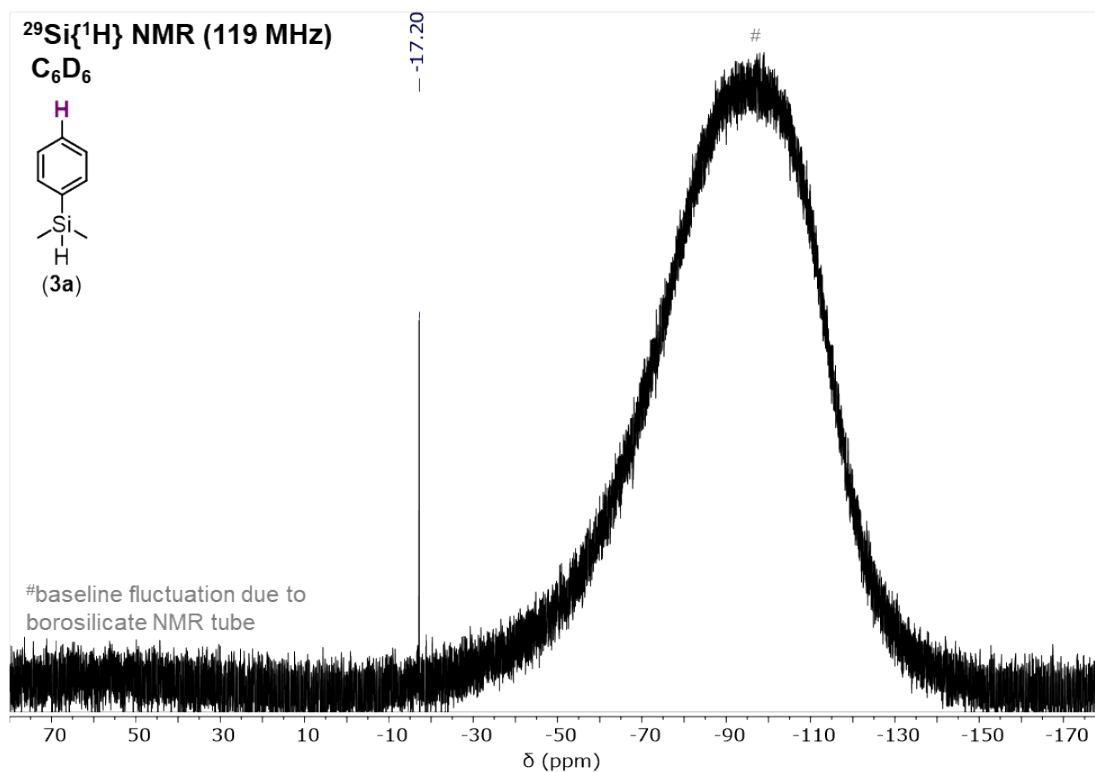


**Figure S103.** <sup>29</sup>Si{<sup>1</sup>H} NMR spectrum of **3a** recorded in C<sub>6</sub>D<sub>6</sub> at room temperature.

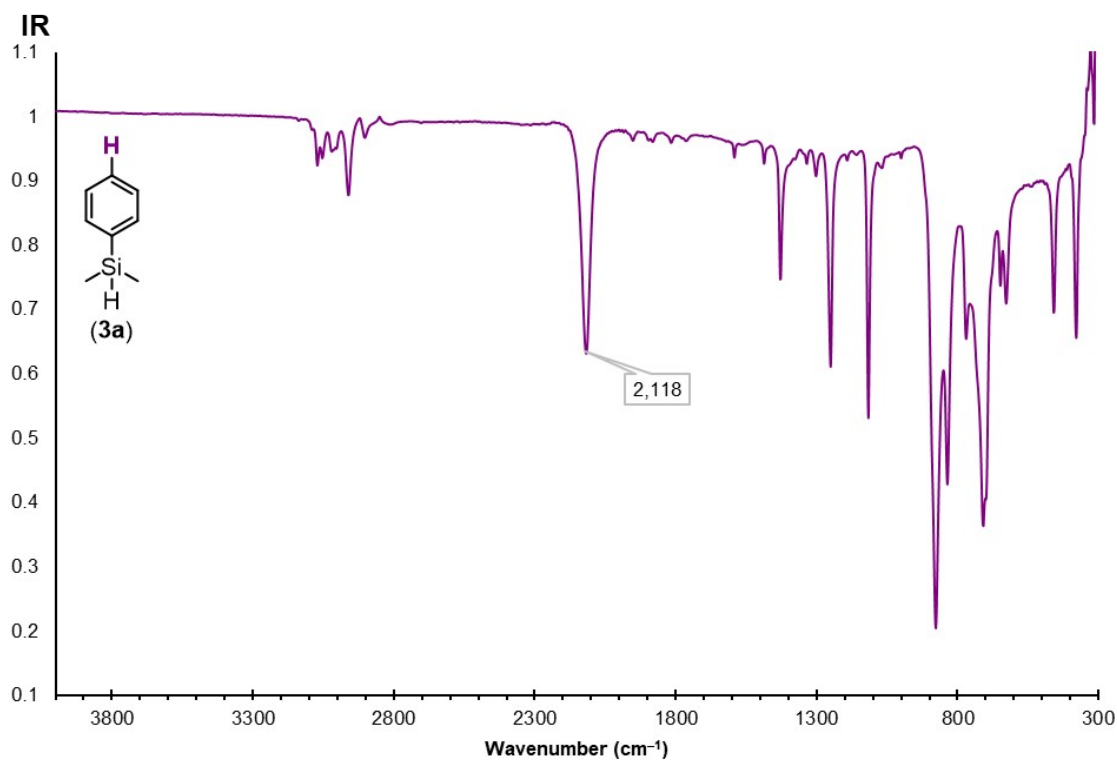


**Figure S104.** IR spectrum of **3a** recorded neat at room temperature.

(4-fluorophenyl)dimethylsilane (**3e**)

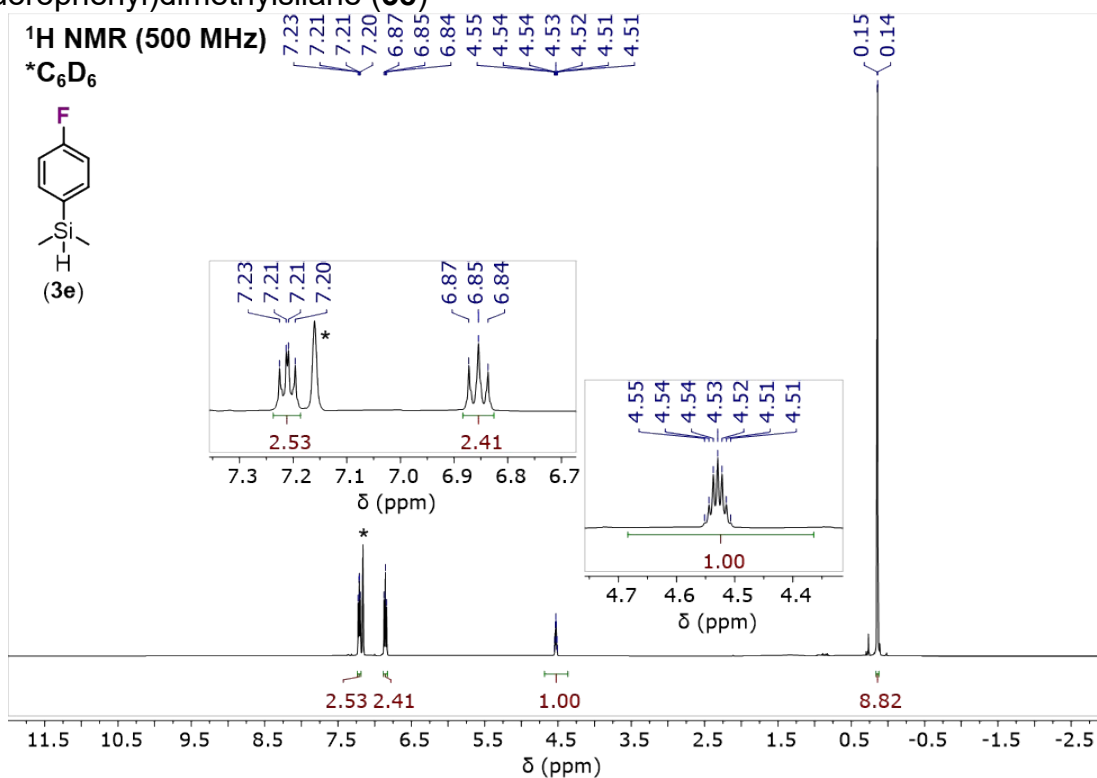


Figure S105. <sup>1</sup>H NMR spectrum of **3e** recorded in C<sub>6</sub>D<sub>6</sub> at room temperature.

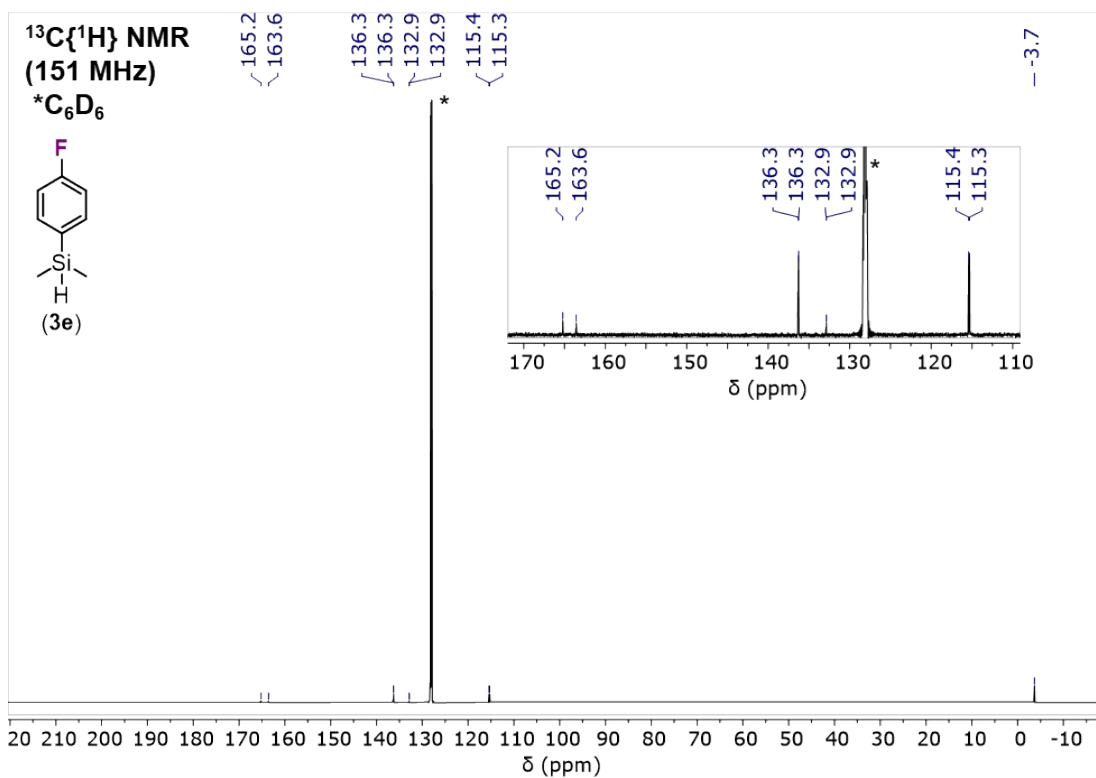
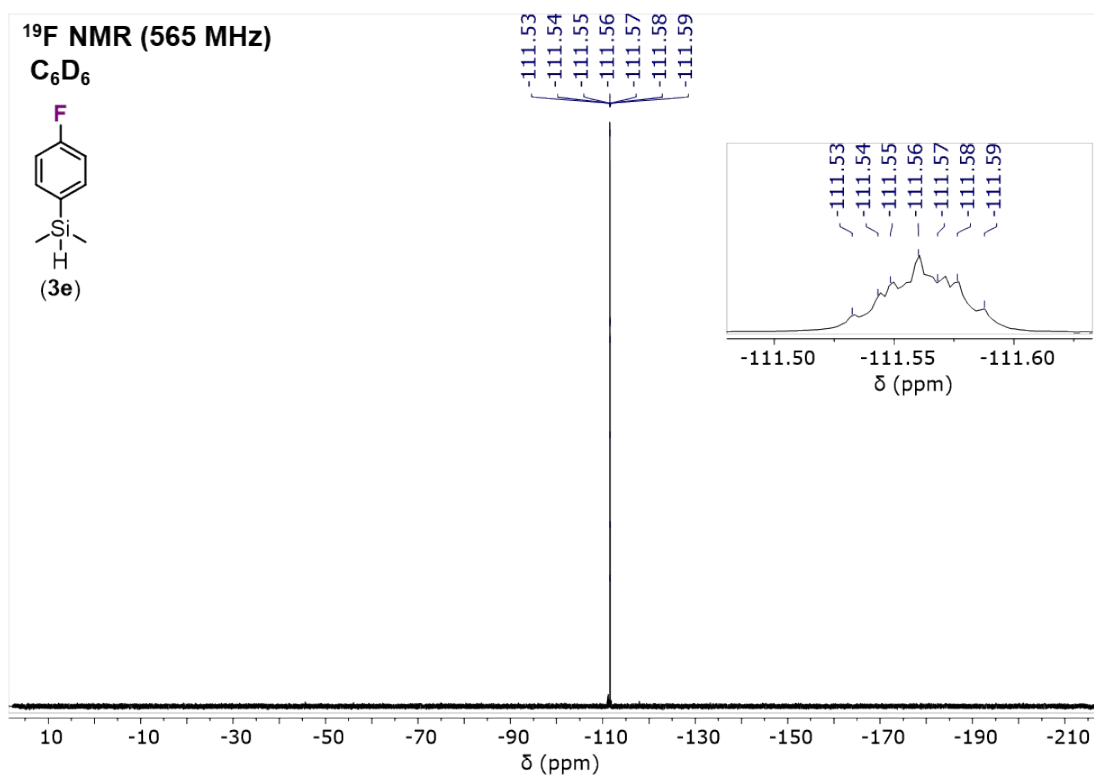
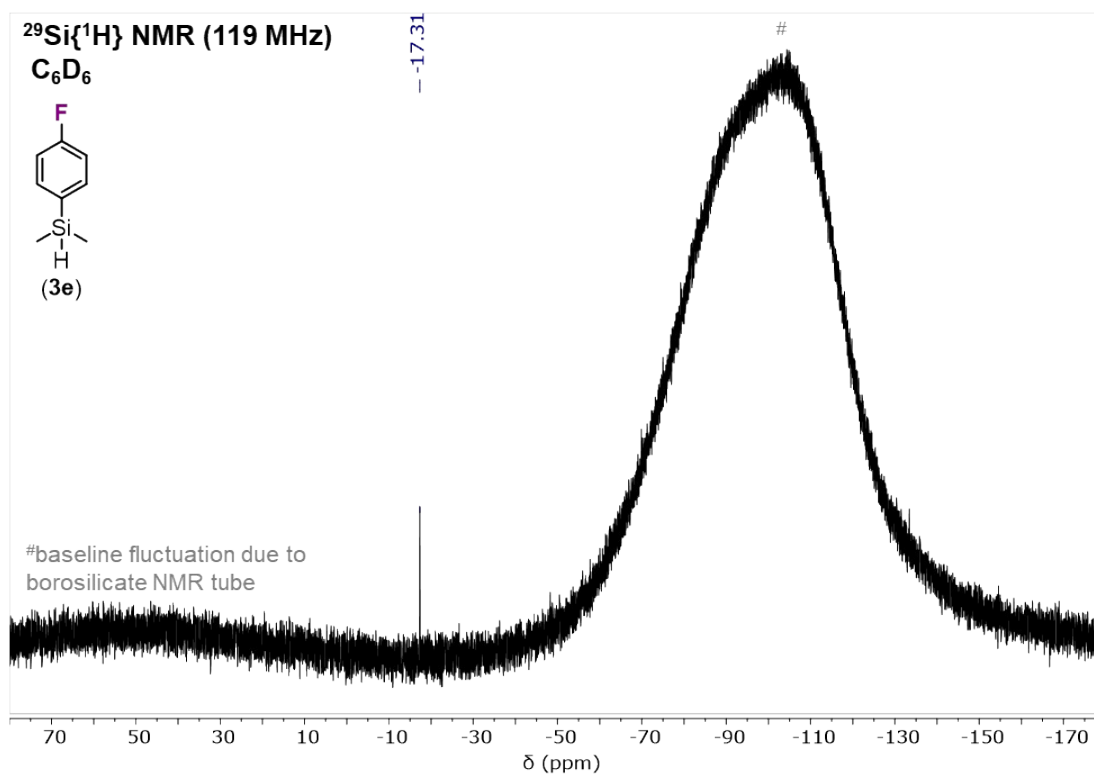


Figure S106. <sup>13</sup>C{<sup>1</sup>H} NMR spectrum of **3e** recorded in C<sub>6</sub>D<sub>6</sub> at room temperature.



**Figure S107.**  $^{19}\text{F}$  NMR spectrum of **3e** recorded in  $\text{C}_6\text{D}_6$  at room temperature.



**Figure S108.**  $^{29}\text{Si}\{^1\text{H}\}$  NMR spectrum of **3e** recorded in  $\text{C}_6\text{D}_6$  at room temperature.

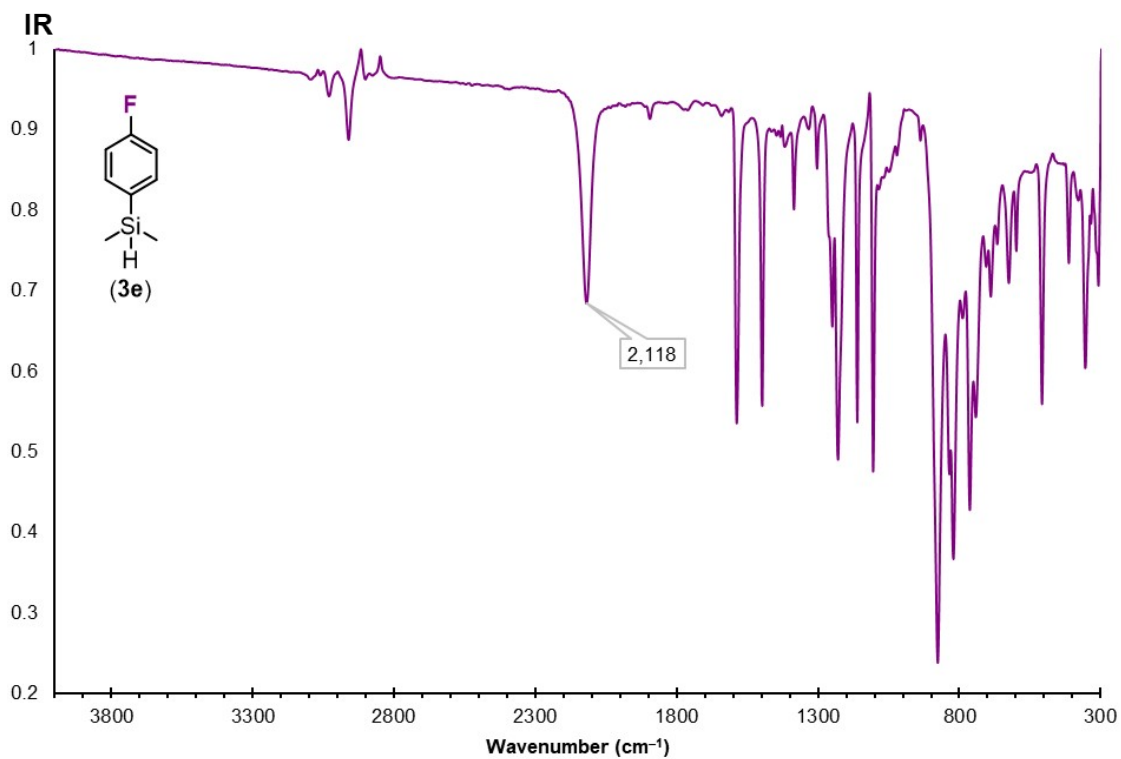


**Figure S109.** IR spectrum of **3e** recorded neat at room temperature.

[4-(trifluoromethyl)phenyl]dimethylsilane (**3f**)

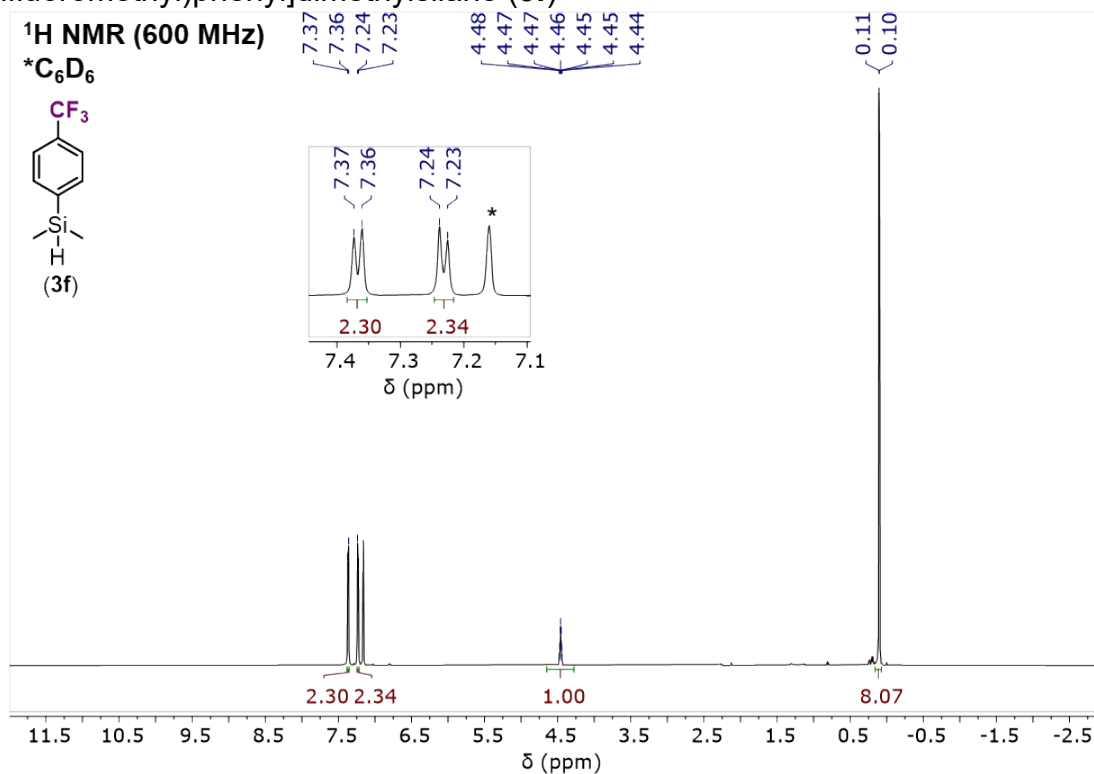


Figure S110. <sup>1</sup>H NMR spectrum of **3f** recorded in C<sub>6</sub>D<sub>6</sub> at room temperature.

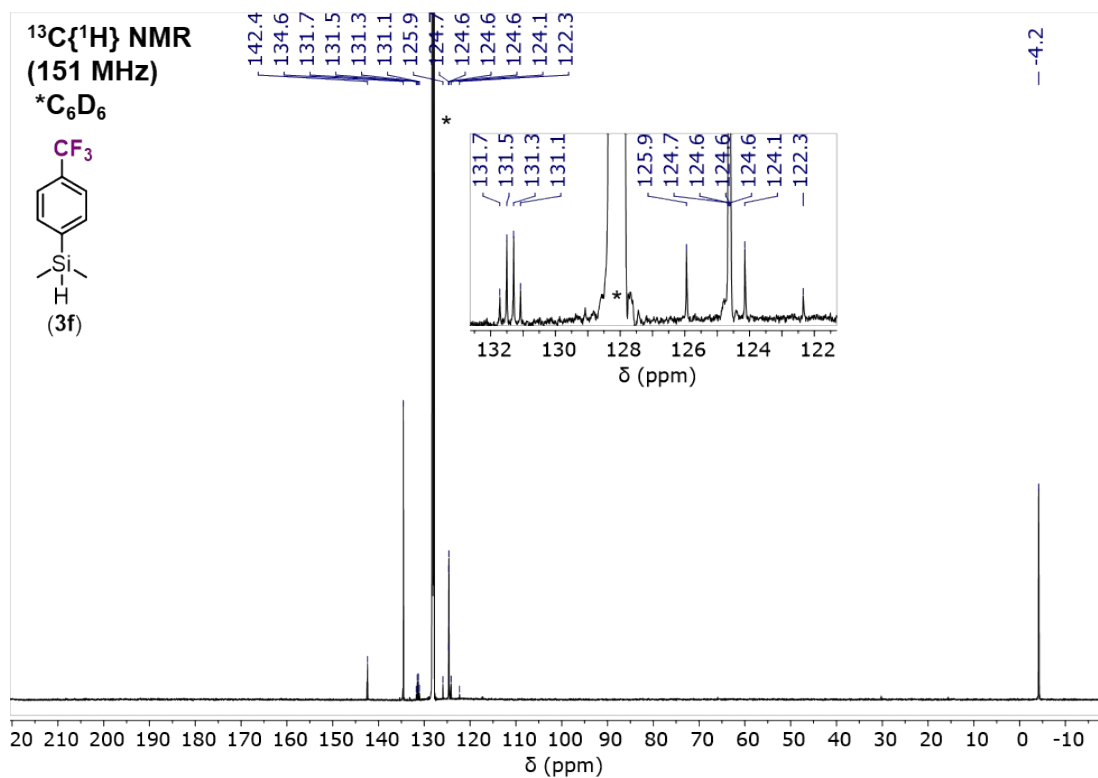
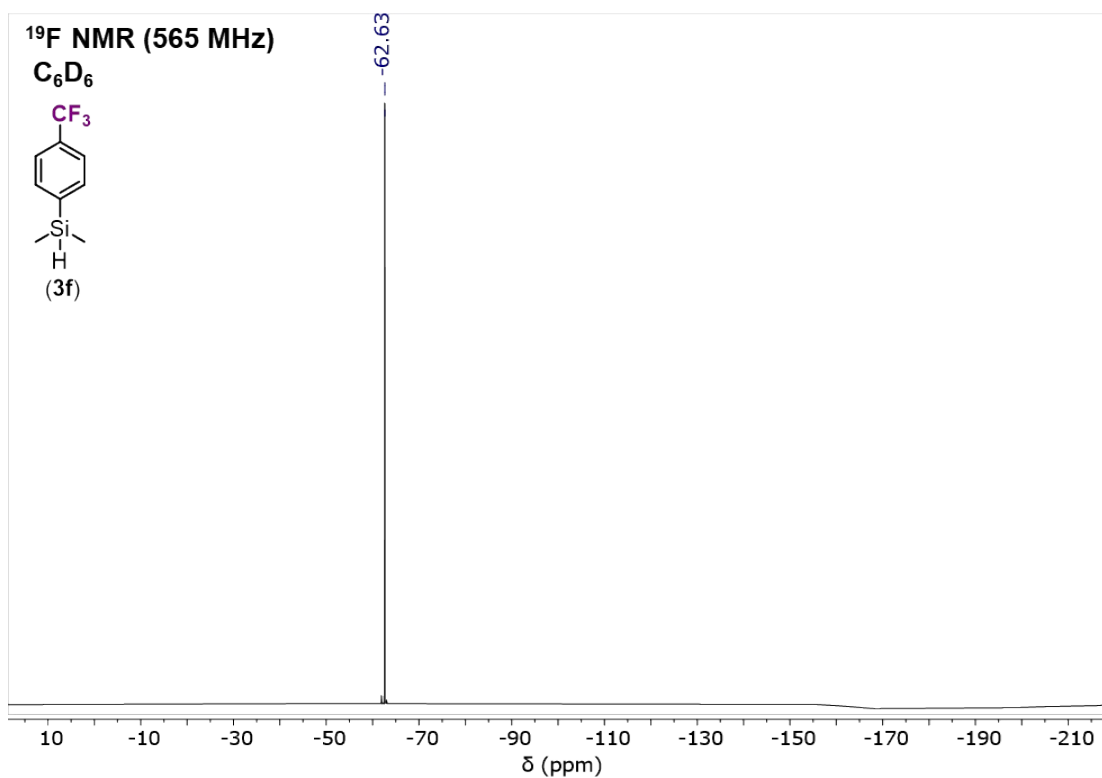
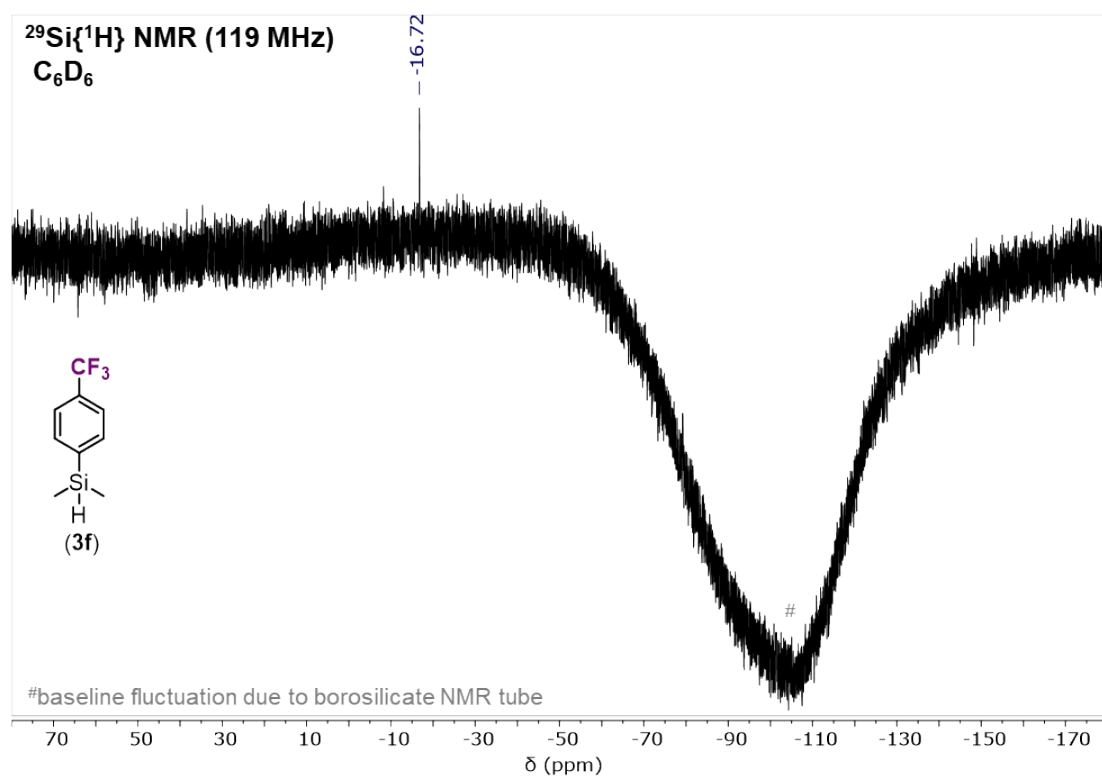


Figure S111. <sup>13</sup>C{<sup>1</sup>H} NMR spectrum of **3f** recorded in C<sub>6</sub>D<sub>6</sub> at room temperature.



**Figure S112.**  $^{19}\text{F}$  NMR spectrum of **3f** recorded in  $\text{C}_6\text{D}_6$  at room temperature.



**Figure S113.**  $^{29}\text{Si}\{^1\text{H}\}$  NMR spectrum of **3f** recorded in  $\text{C}_6\text{D}_6$  at room temperature.

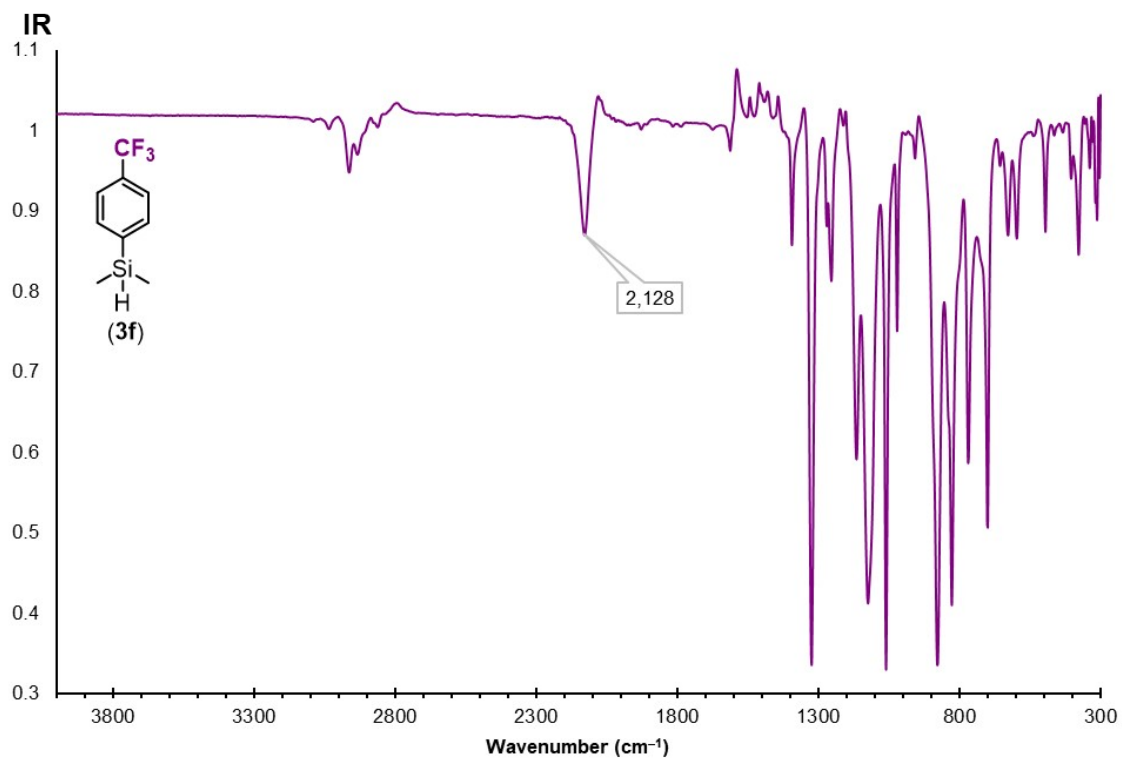


**Figure S114.** IR spectrum of **3f** recorded neat at room temperature.

### d. Deuterated silanes

Triphenylsilane- $d_1$  (**5a-d<sub>1</sub>**)

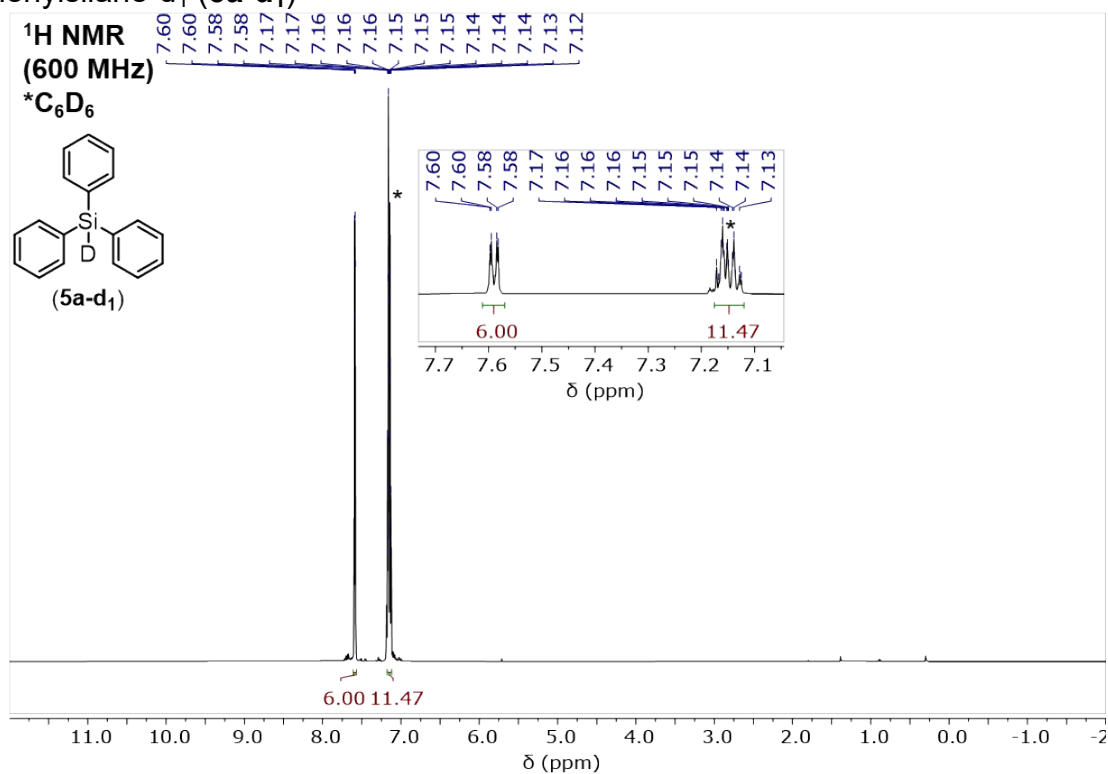


**Figure S115.**  $^1\text{H}$  NMR spectrum of **5a-d<sub>1</sub>** recorded in  $\text{C}_6\text{D}_6$  at room temperature.

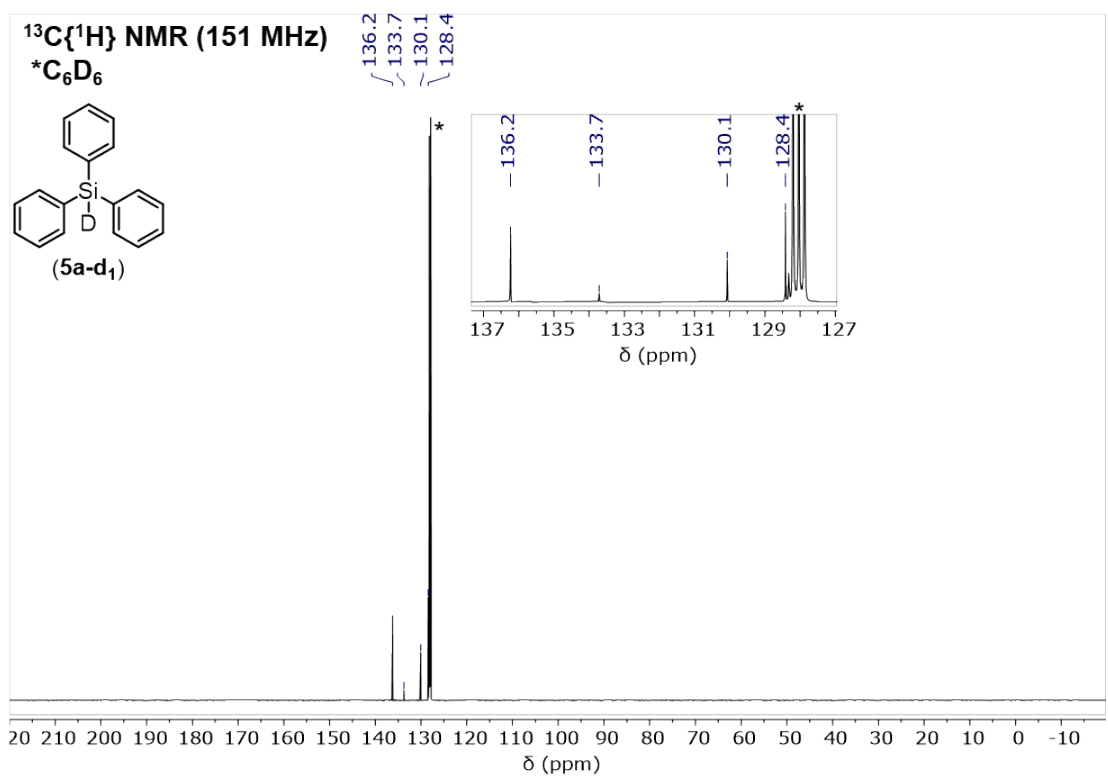


**Figure S116.**  $^{13}\text{C}\{^1\text{H}\}$  NMR spectrum of **5a-d<sub>1</sub>** recorded in  $\text{C}_6\text{D}_6$  at room temperature.

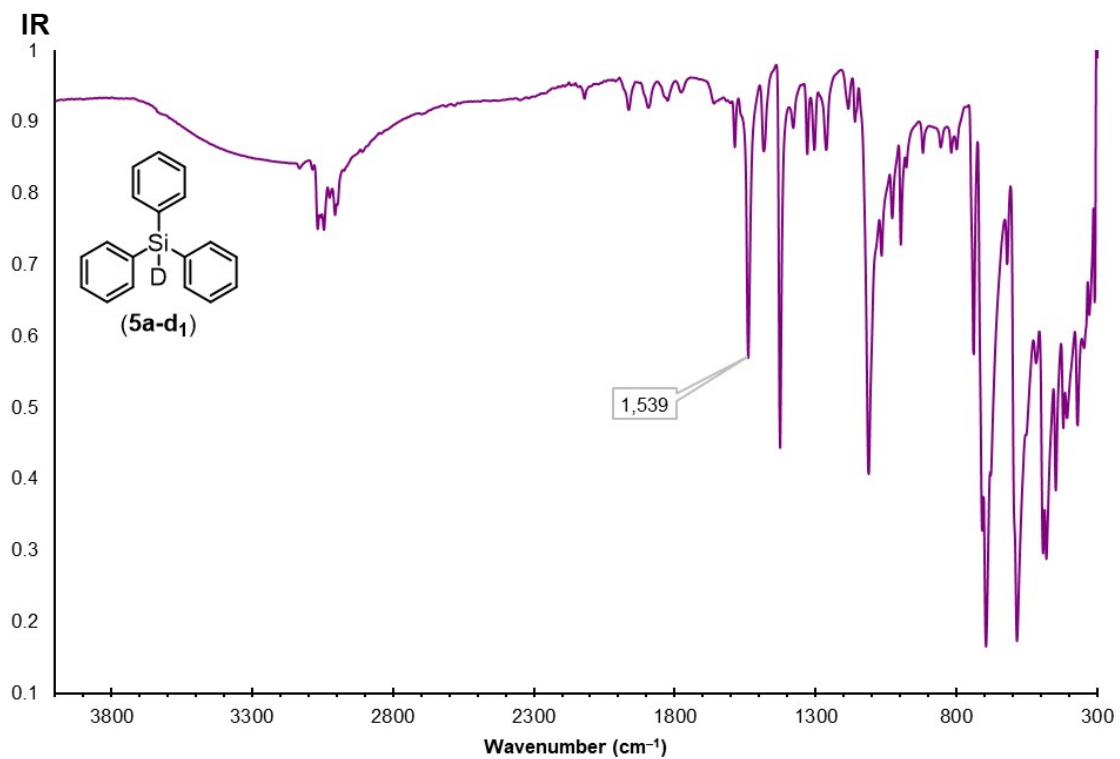


**Figure S117.** IR spectrum of **5a-d<sub>1</sub>** recorded neat at room temperature.

Phenyldimethylsilane-d<sub>1</sub> (**3a-d<sub>1</sub>**)

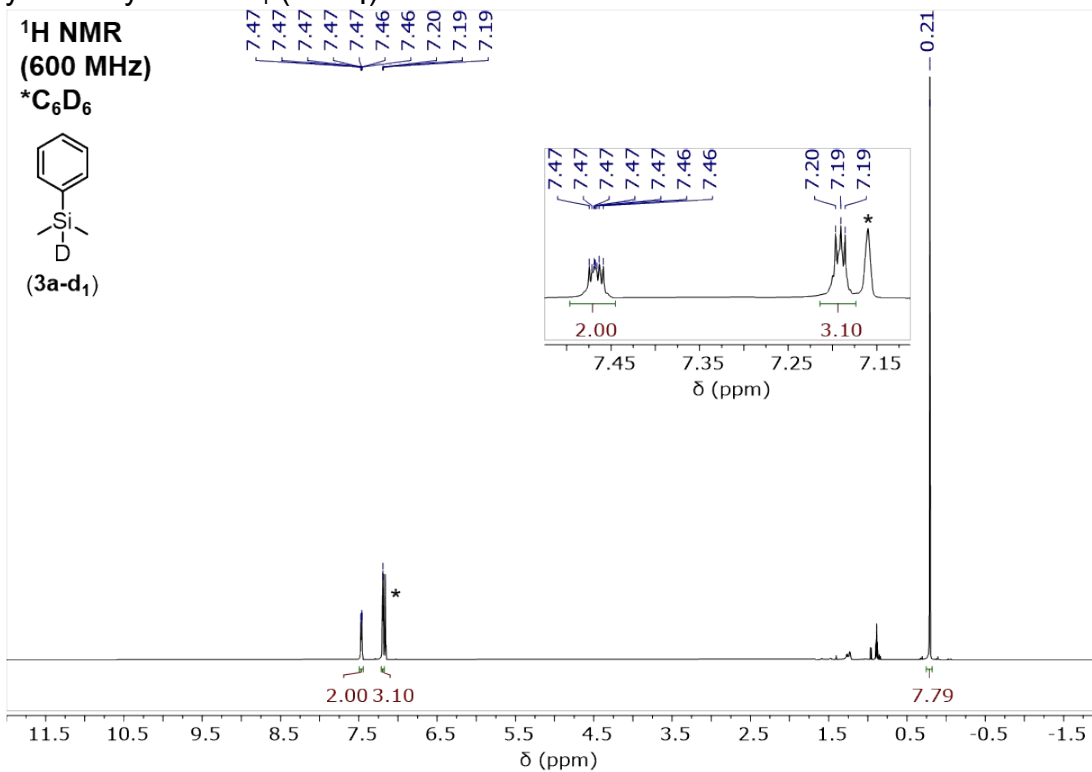


**Figure S118.** <sup>1</sup>H NMR spectrum of **3a-d<sub>1</sub>** recorded in C<sub>6</sub>D<sub>6</sub> at room temperature.

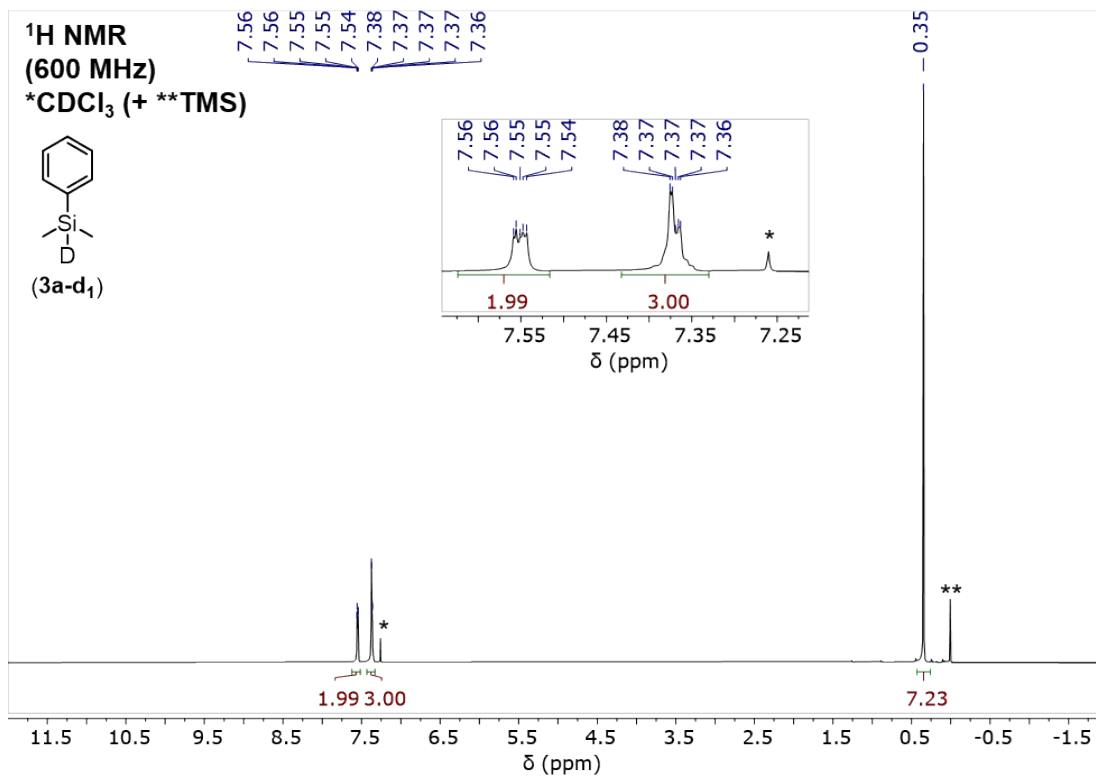


**Figure S119.** <sup>1</sup>H NMR spectrum of **3a-d<sub>1</sub>** recorded in CDCl<sub>3</sub> at room temperature.

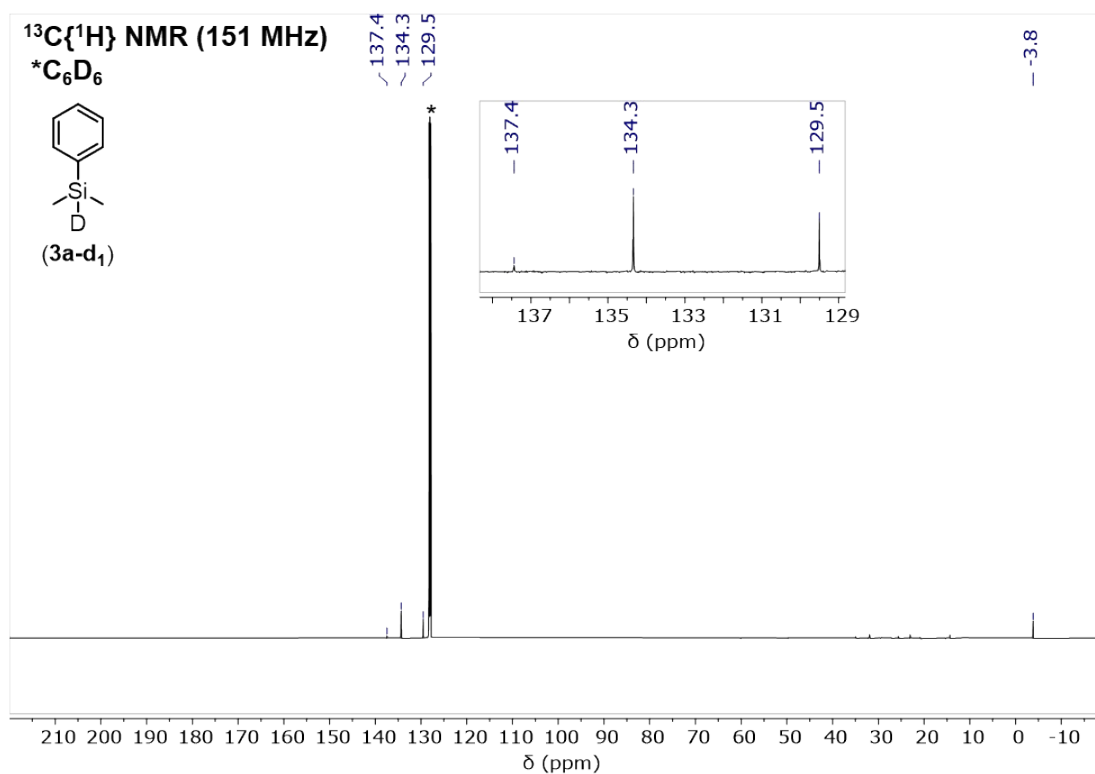


**Figure S120.**  $^{13}\text{C}\{^1\text{H}\}$  NMR spectrum of **3a-d<sub>1</sub>** recorded in  $\text{C}_6\text{D}_6$  at room temperature.

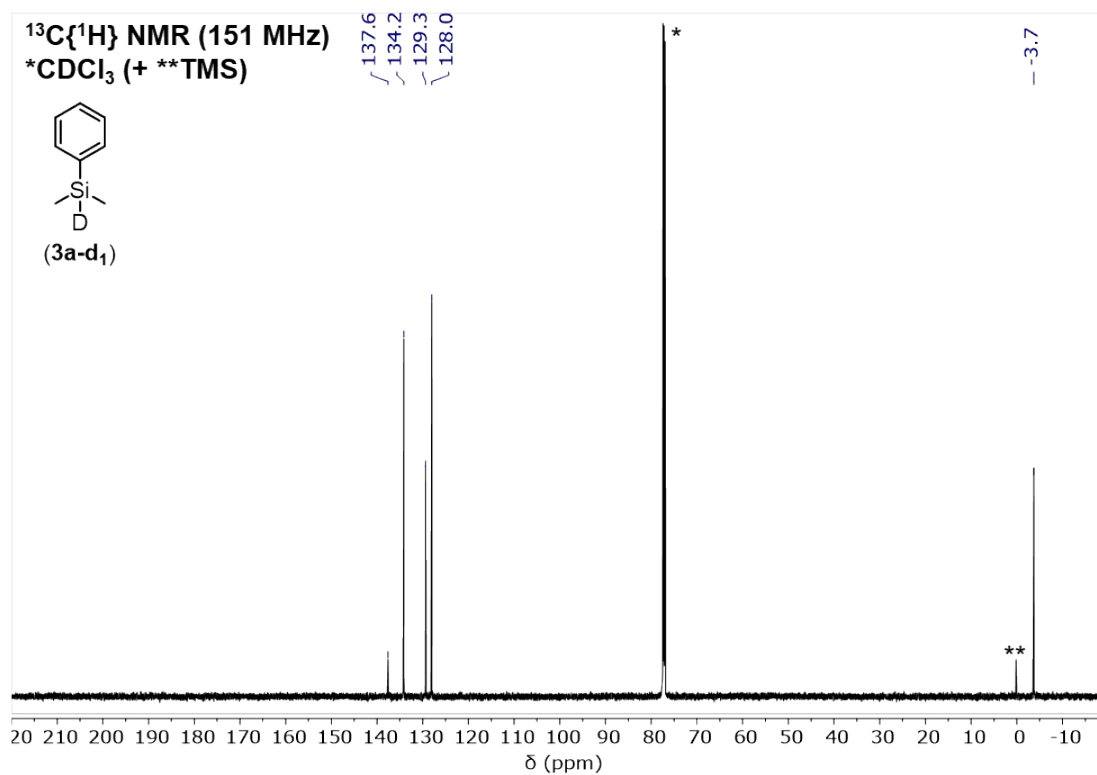


**Figure S121.**  $^{13}\text{C}\{^1\text{H}\}$  NMR spectrum of **3a-d<sub>1</sub>** recorded in  $\text{CDCl}_3$  at room temperature.

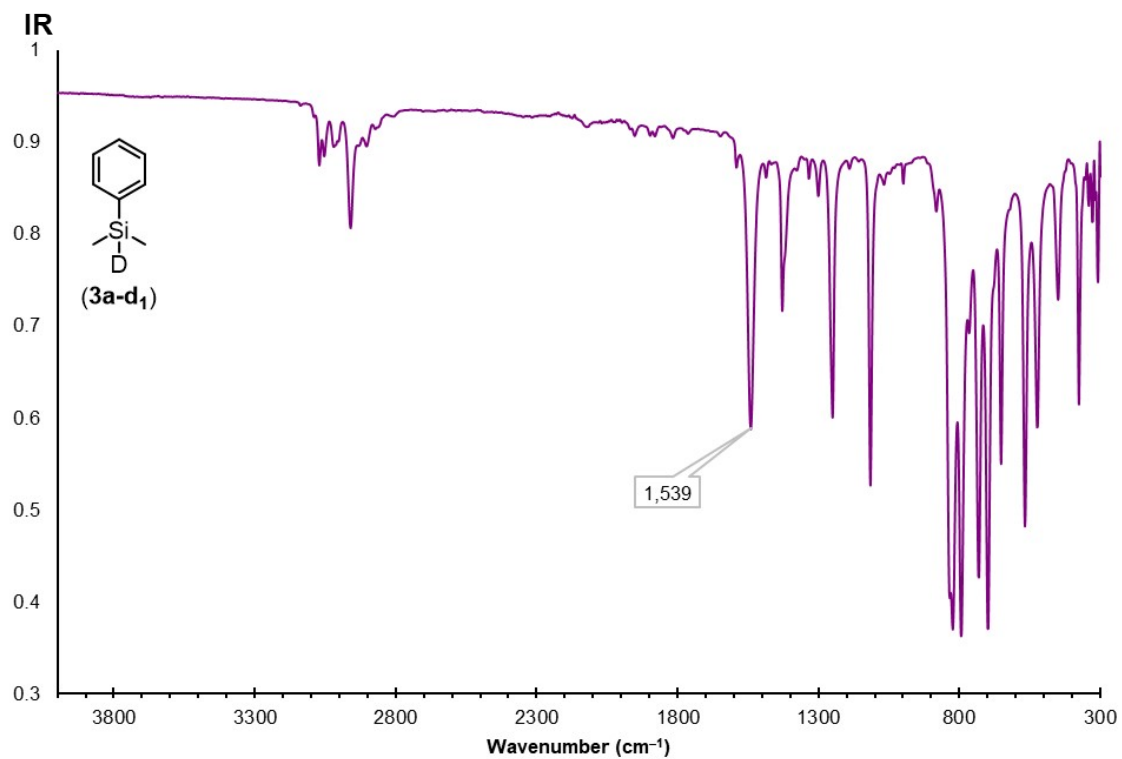


**Figure S122.** IR spectrum of **3a-d<sub>1</sub>** recorded neat at room temperature.

### e. Other silanes

Triethylsilane (**2**)

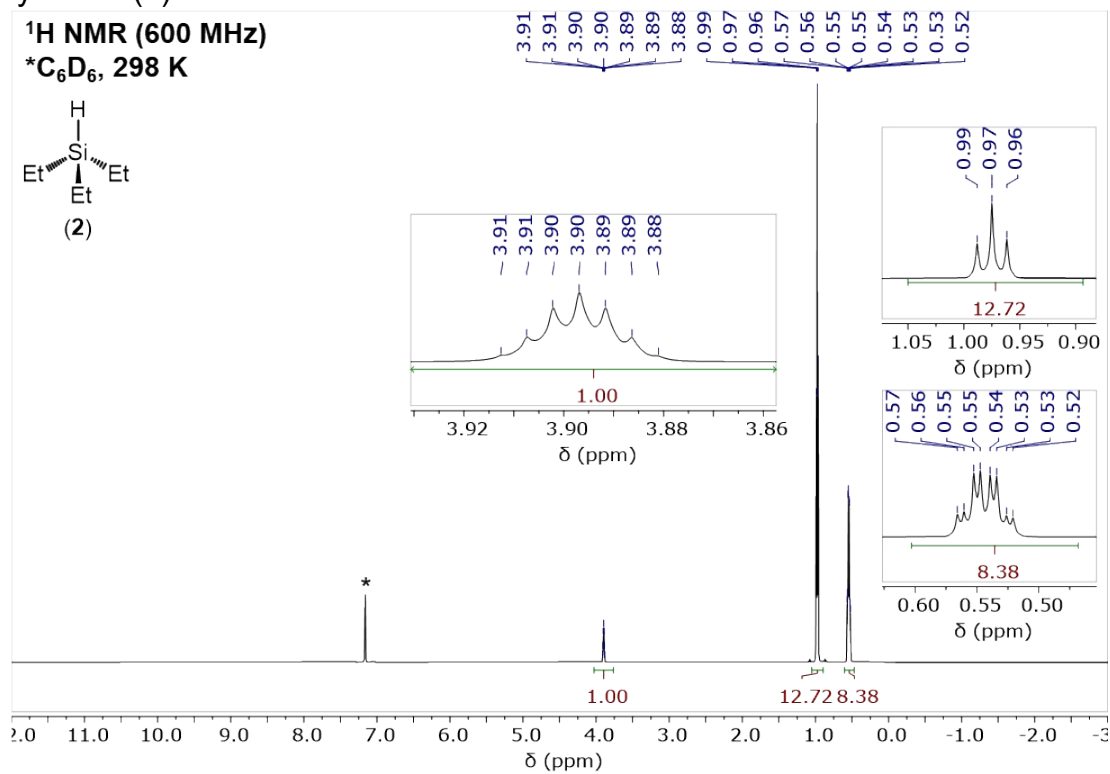


**Figure S123.** <sup>1</sup>H NMR spectrum of **2** recorded in C<sub>6</sub>D<sub>6</sub> at room temperature.

Methyldiphenylsilane (**4**)

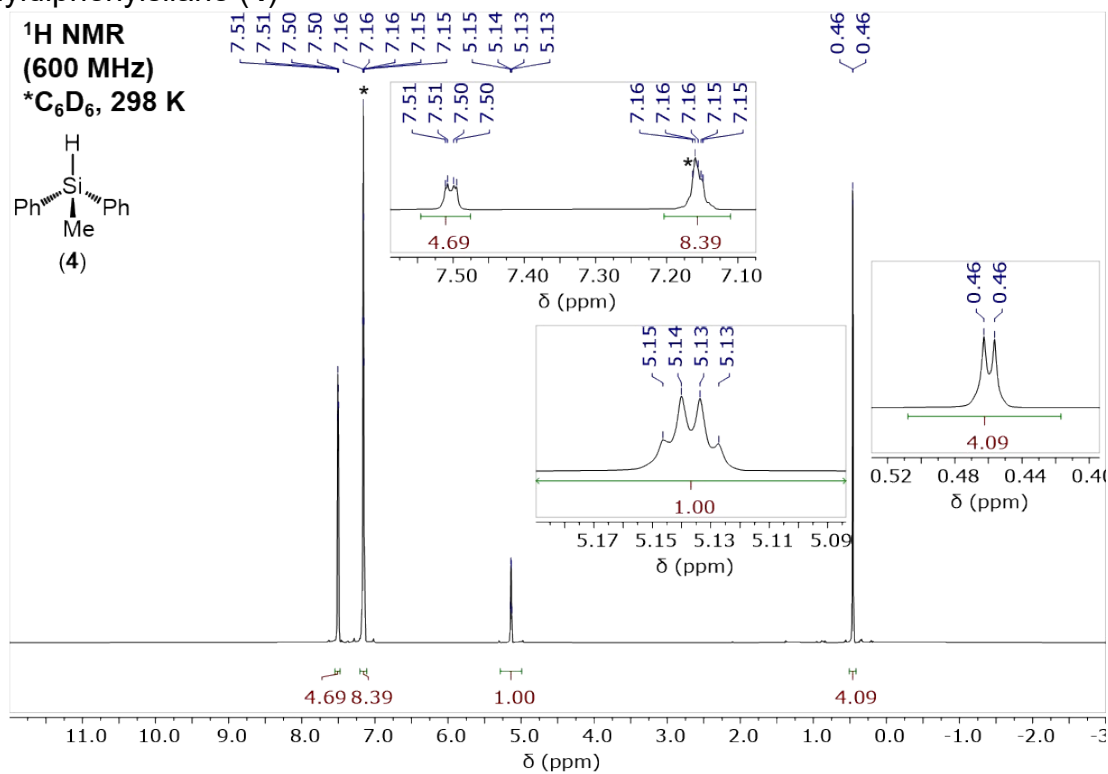


**Figure S124.**  $^1\text{H}$  NMR spectrum of **4** recorded in  $\text{C}_6\text{D}_6$  at room temperature.

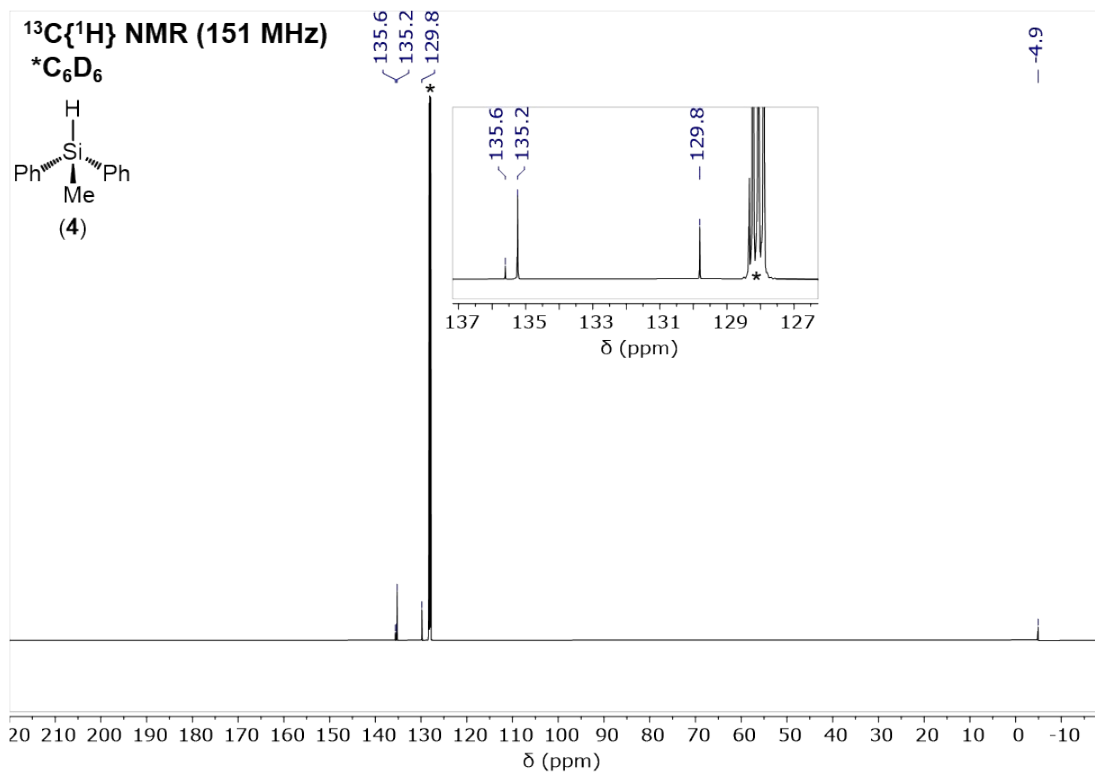


**Figure S125.**  $^{13}\text{C}\{^1\text{H}\}$  NMR spectrum of **4** recorded in  $\text{C}_6\text{D}_6$  at room temperature.

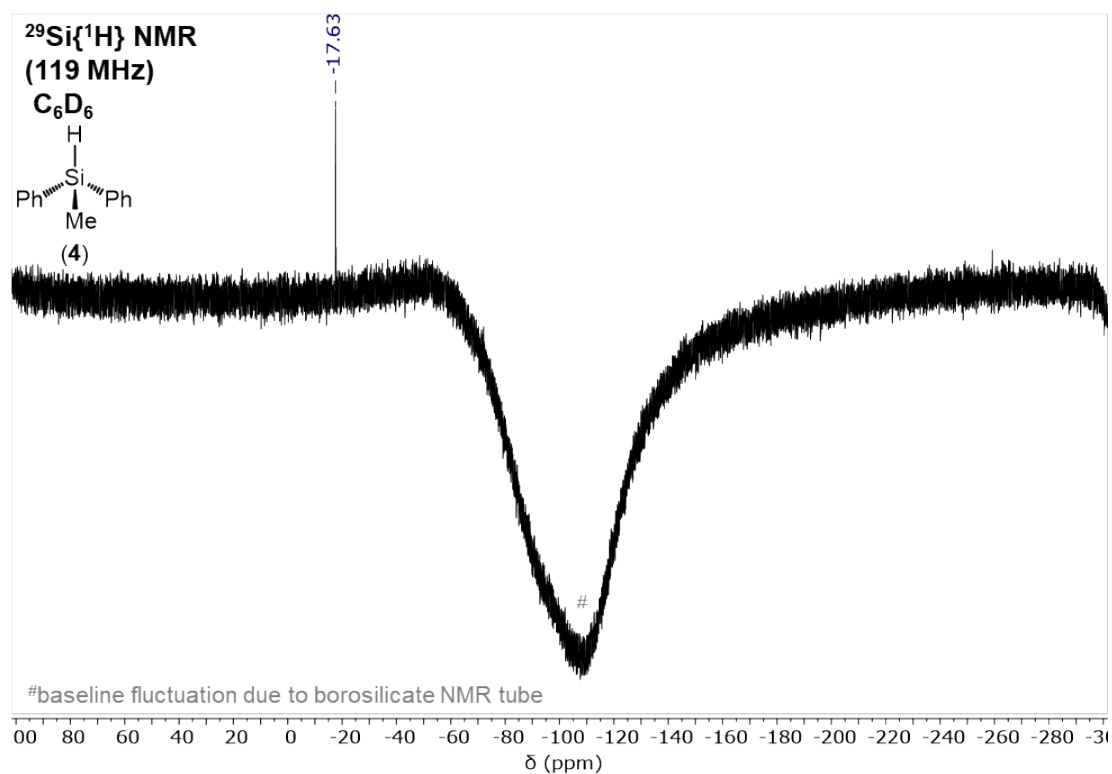


**Figure S126.**  $^{29}\text{Si}\{^1\text{H}\}$  NMR spectrum of **4** recorded in  $\text{C}_6\text{D}_6$  at room temperature.

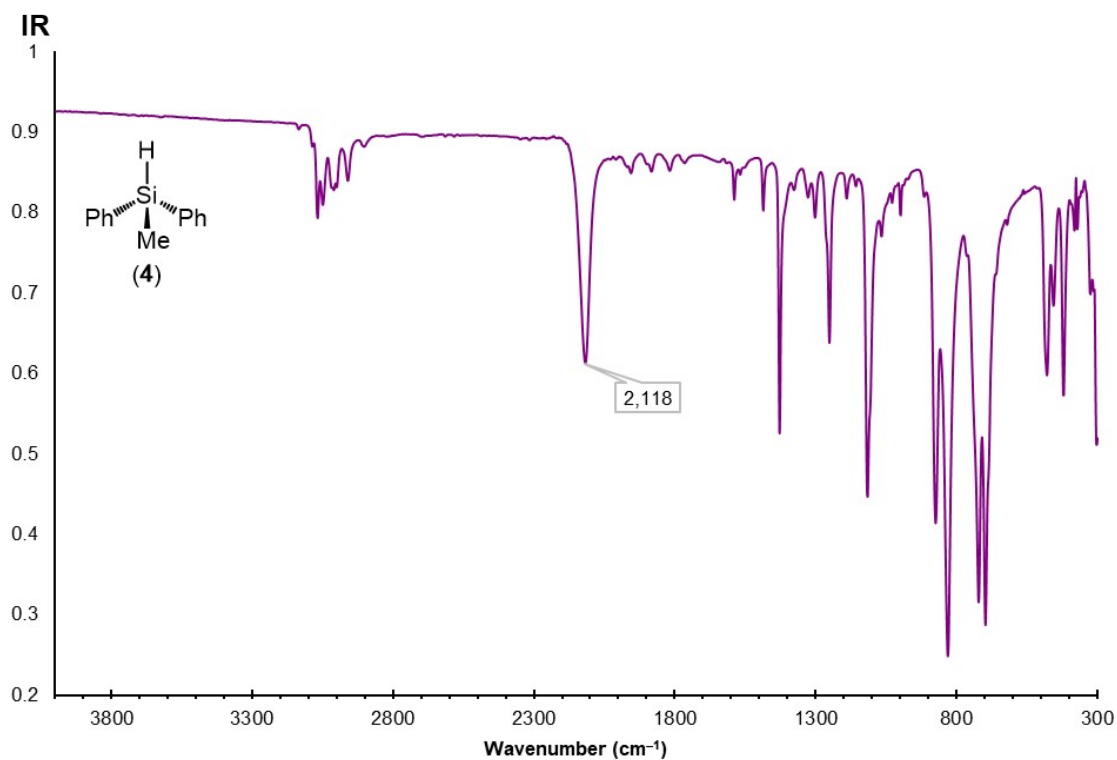


**Figure S127.** IR spectrum of **4** recorded neat at room temperature.

Triethoxysilane (**6**)

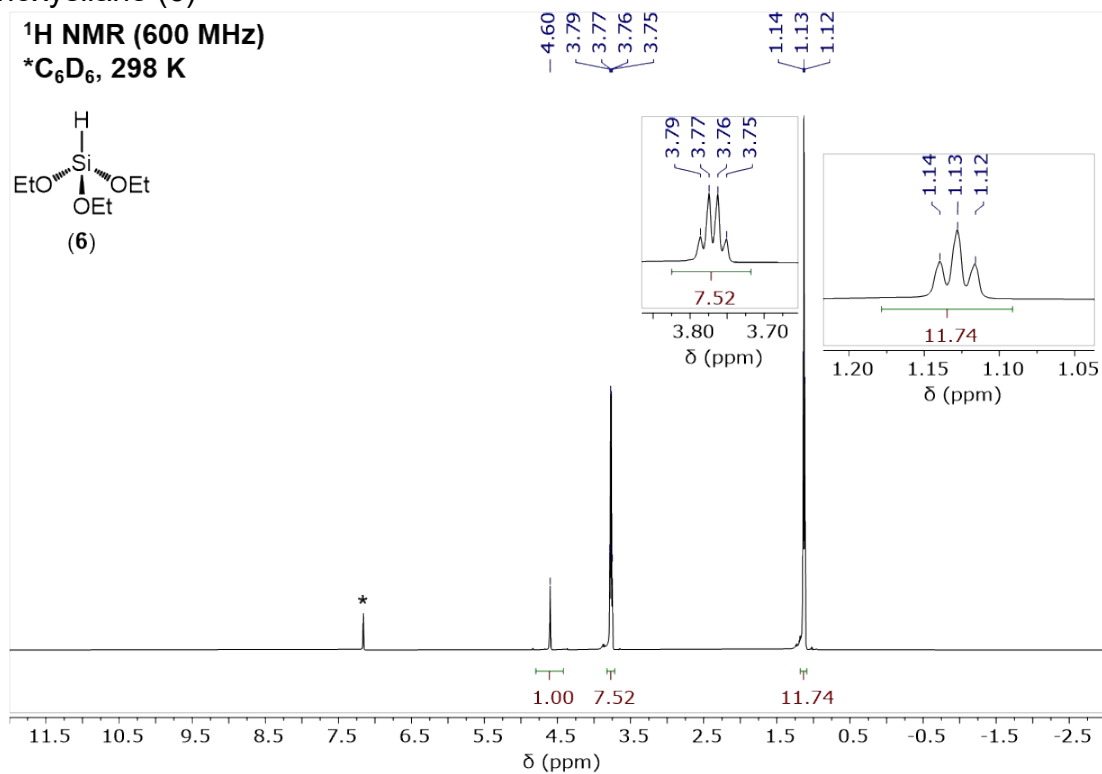


**Figure S128.**  $^1\text{H}$  NMR spectrum of **6** recorded in  $\text{C}_6\text{D}_6$  at room temperature.

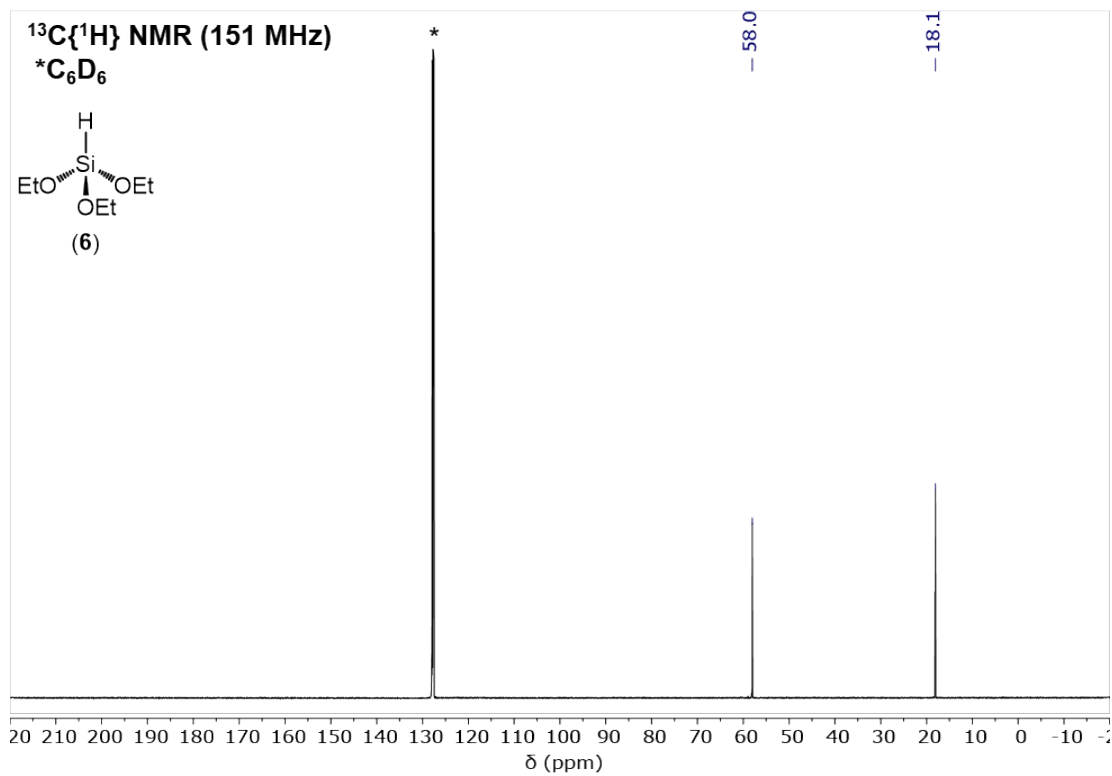


**Figure S129.**  $^{13}\text{C}\{^1\text{H}\}$  NMR spectrum of **6** recorded in  $\text{C}_6\text{D}_6$  at room temperature.

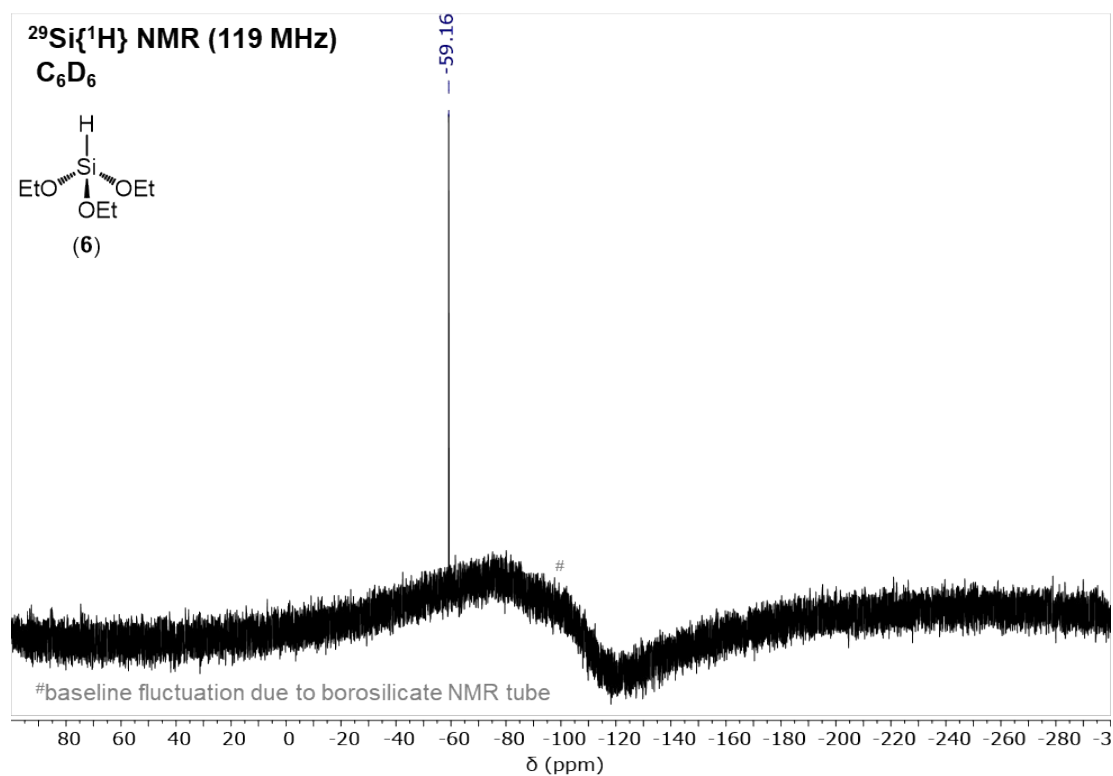


**Figure S130.**  $^{29}\text{Si}\{^1\text{H}\}$  NMR spectrum of **6** recorded in  $\text{C}_6\text{D}_6$  at room temperature.

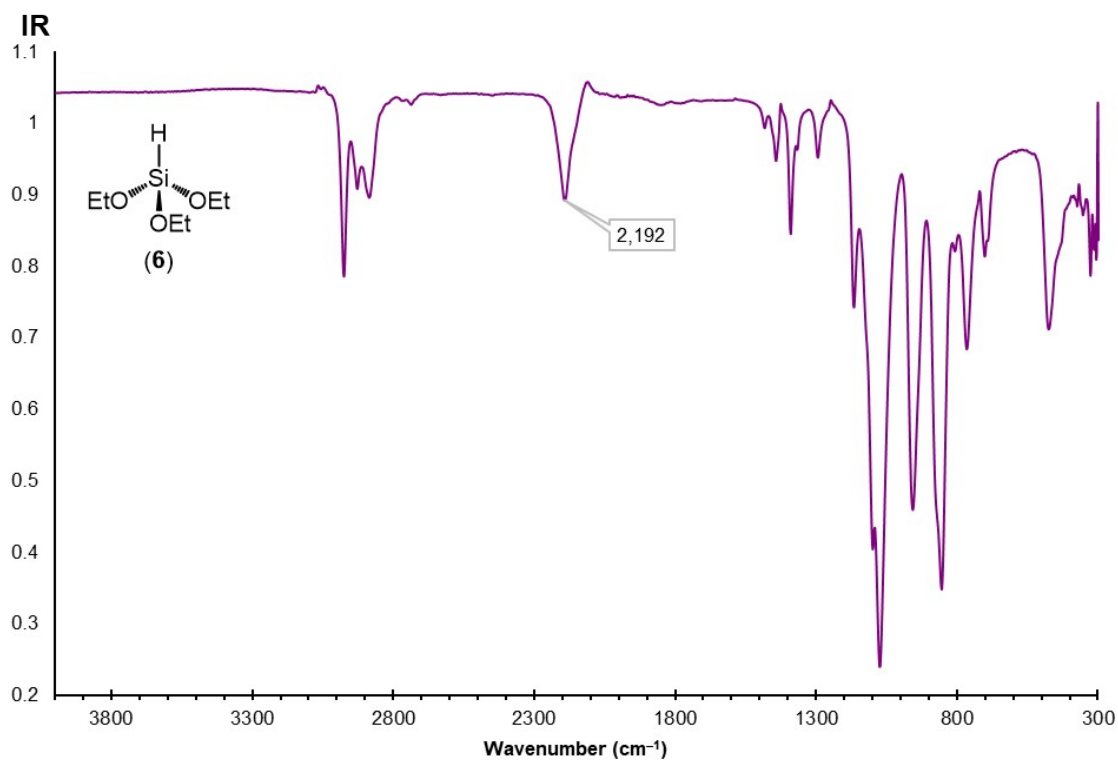


**Figure S131.** IR spectrum of **6** recorded neat at room temperature.

**f. Silyl Palladium Hydrides/Deuterides**  
 (dcpe)Pd(H)[Si(4-NMe<sub>2</sub>-Ph)<sub>3</sub>] (**10b**)

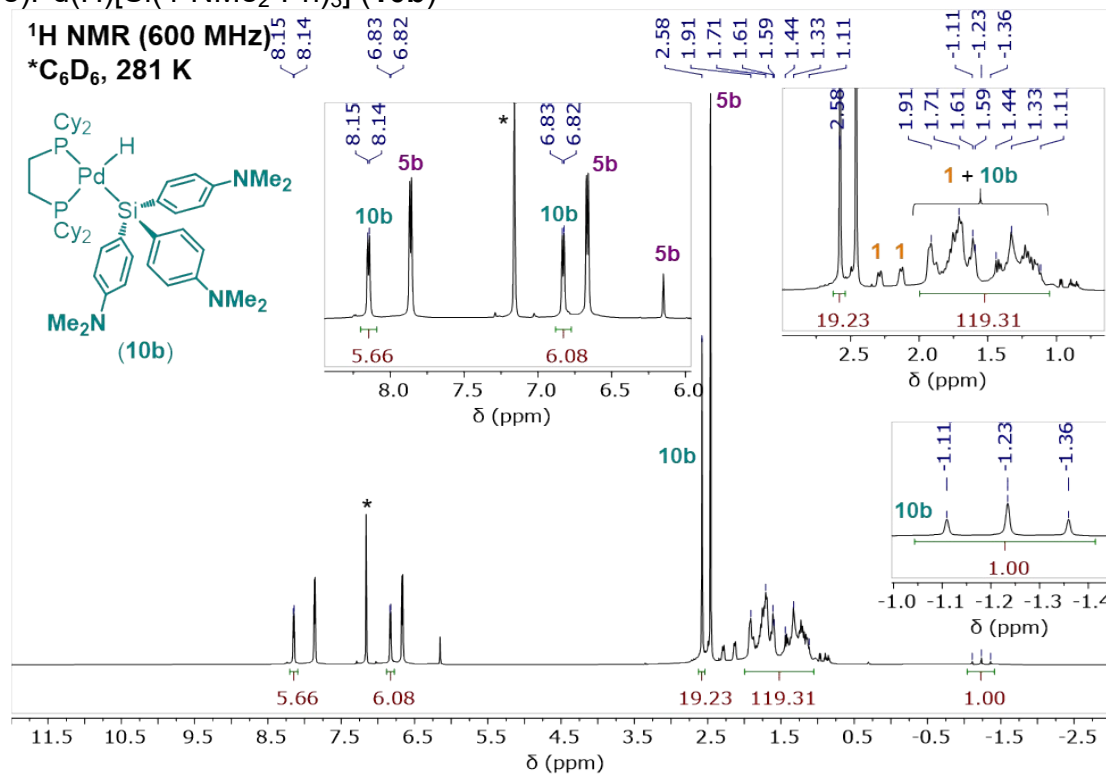


**Figure S132.** <sup>1</sup>H NMR spectrum of **10b** recorded in C<sub>6</sub>D<sub>6</sub> at 281 K.

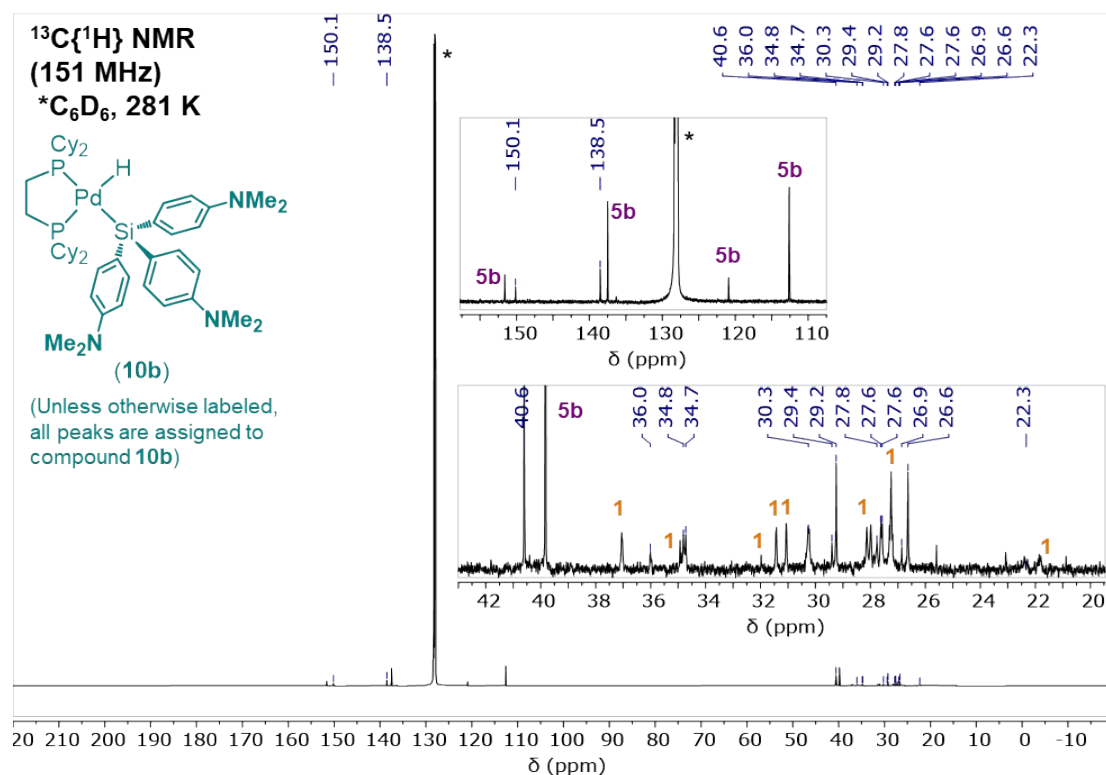


**Figure S133.** <sup>13</sup>C{<sup>1</sup>H} NMR spectrum of **10b** recorded in C<sub>6</sub>D<sub>6</sub> at 281 K.

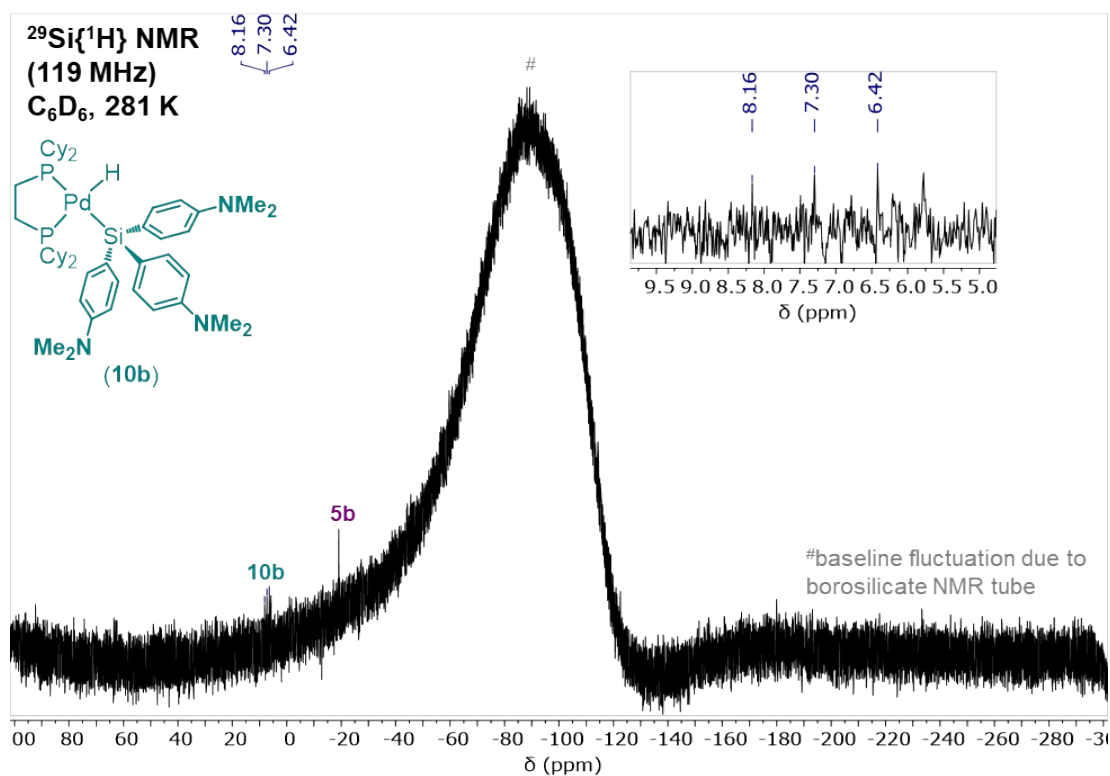


**Figure S134.**  $^{29}\text{Si}\{^1\text{H}\}$  NMR spectrum of **10b** recorded in  $\text{C}_6\text{D}_6$  at 281 K.

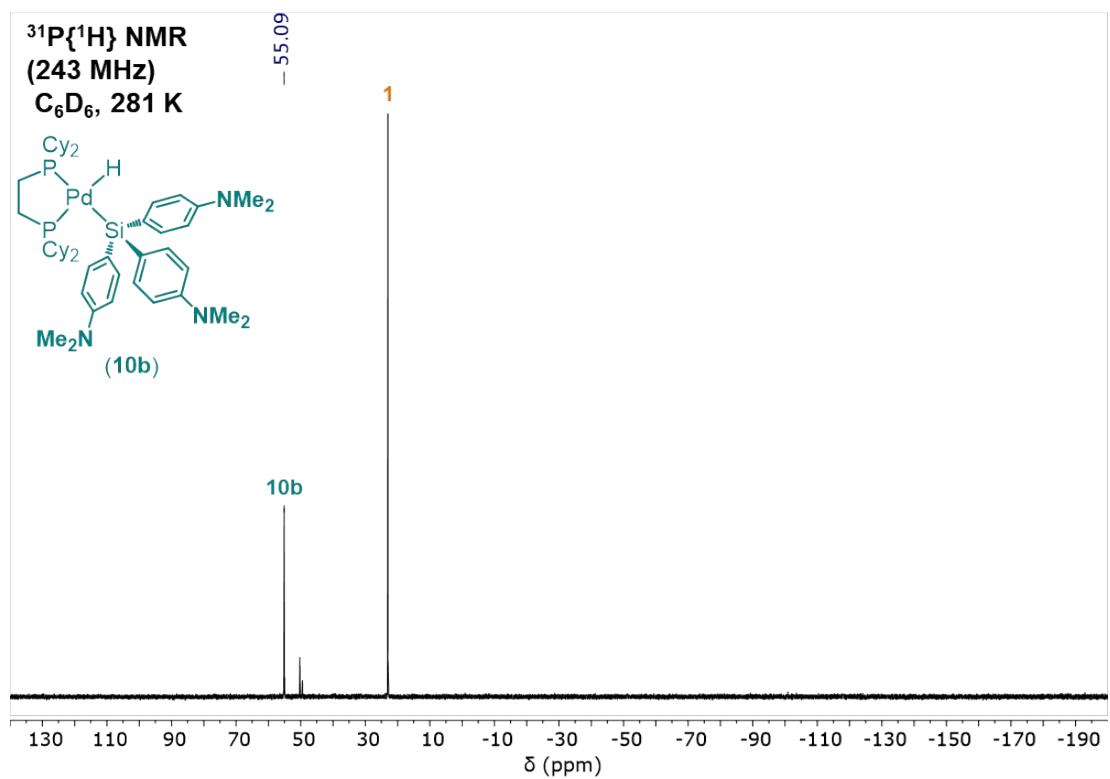


**Figure S135.**  $^{31}\text{P}\{^1\text{H}\}$  NMR spectrum of **10b** recorded in  $\text{C}_6\text{D}_6$  at 281 K.

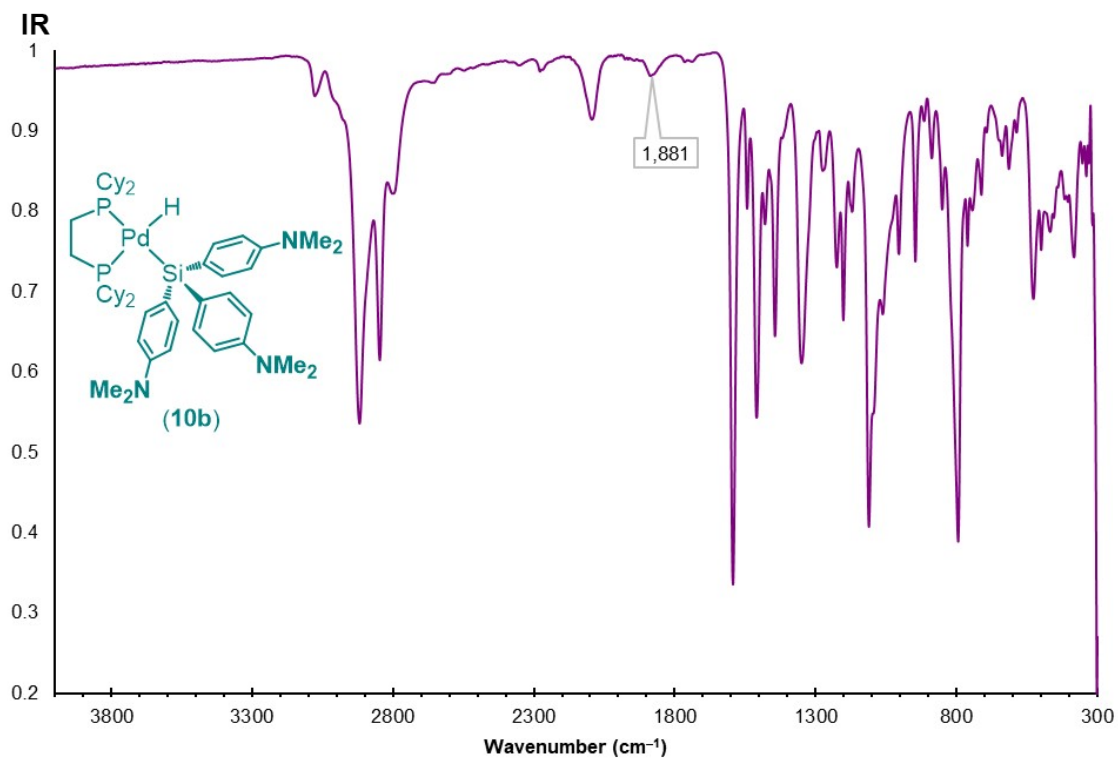


**Figure S136.** IR spectrum of **10b** recorded neat at room temperature.

(dcpe)Pd(H)[Si(4-OMe-Ph)<sub>3</sub>] (**10c**)

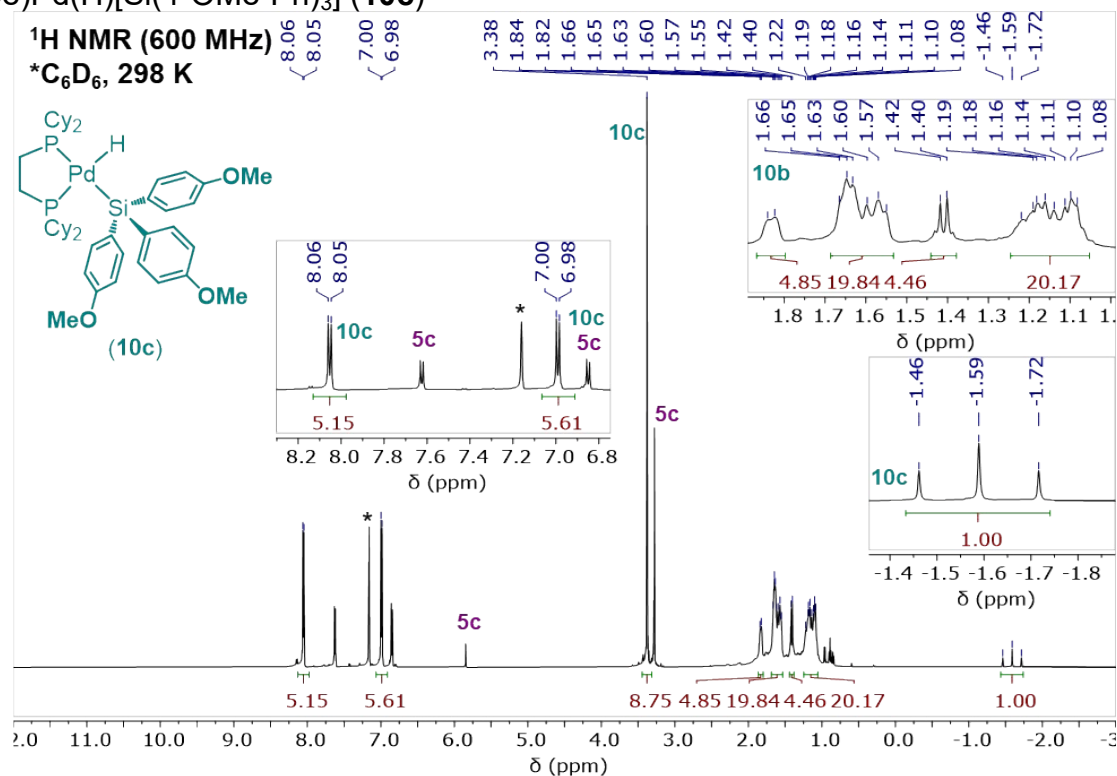


Figure S137. <sup>1</sup>H NMR spectrum of **10c** recorded in C<sub>6</sub>D<sub>6</sub> at 298 K.

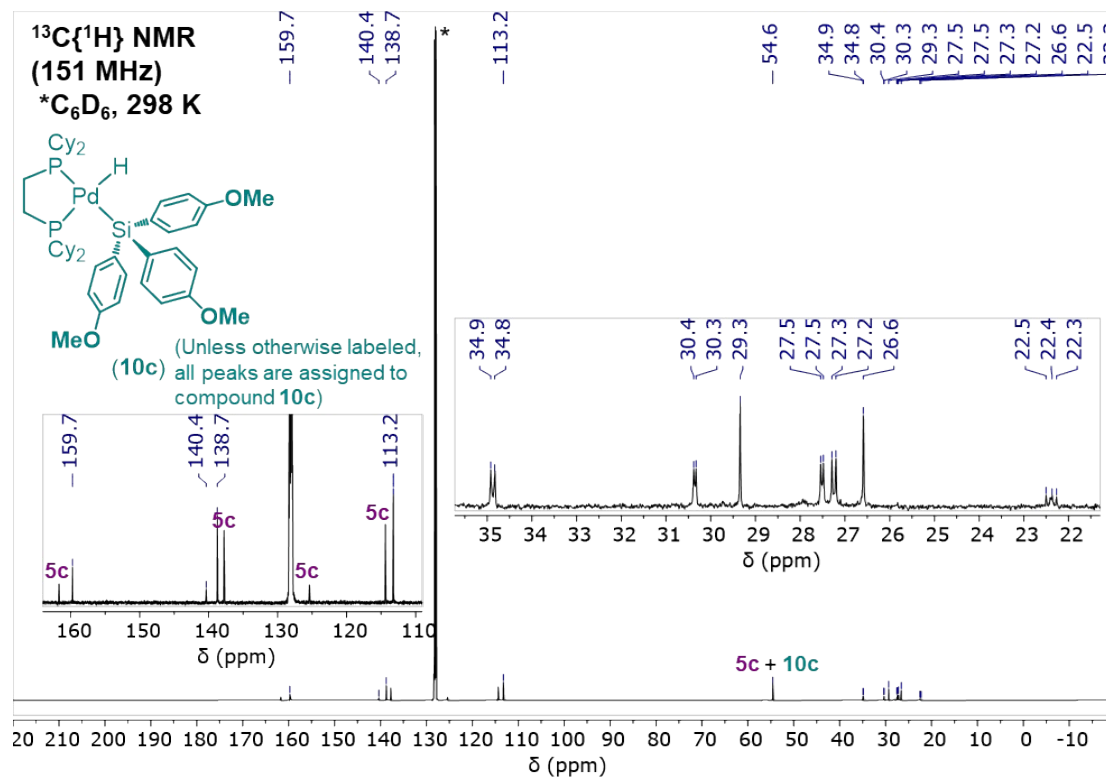
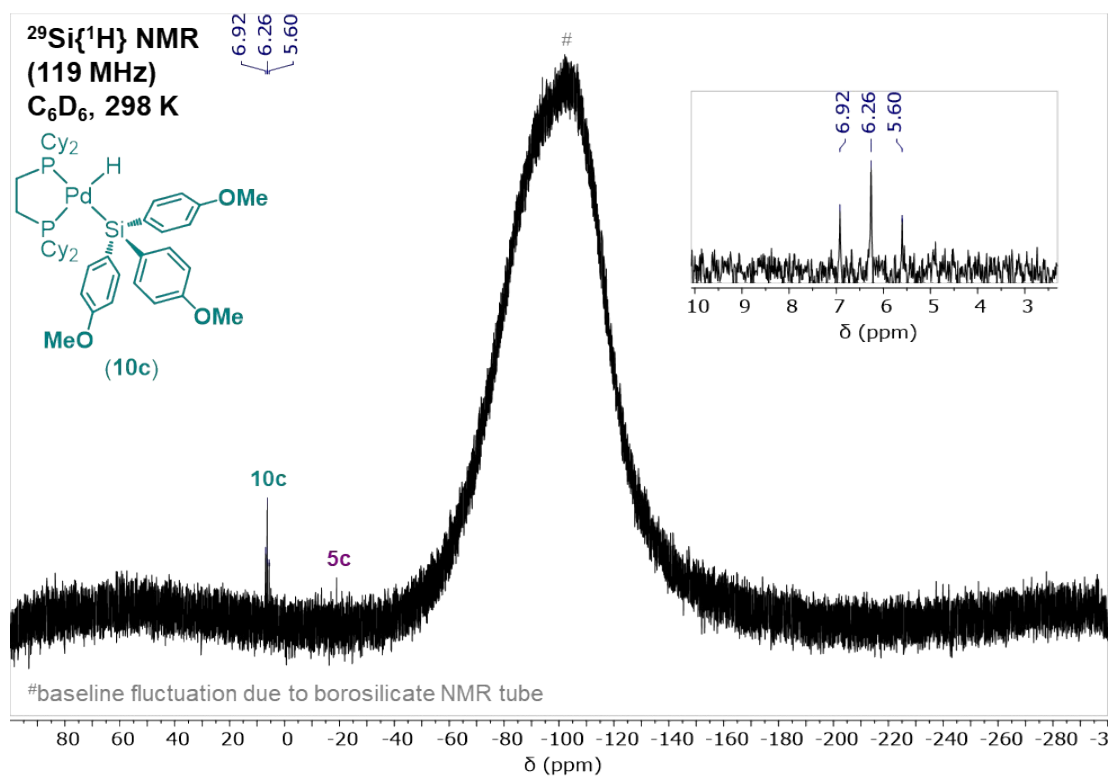
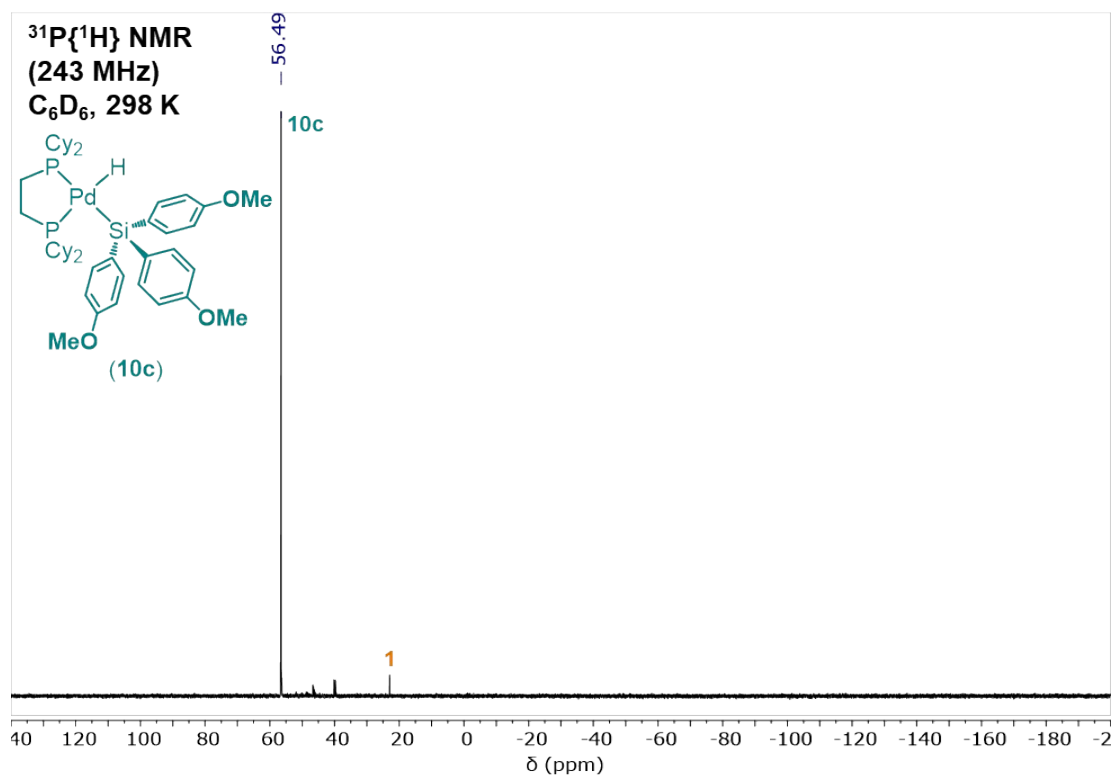


Figure S138. <sup>13</sup>C{<sup>1</sup>H} NMR spectrum of **10c** recorded in C<sub>6</sub>D<sub>6</sub> at 298 K.



**Figure S139.**  $^{29}\text{Si}\{^1\text{H}\}$  NMR spectrum of **10c** recorded in  $\text{C}_6\text{D}_6$  at 298 K.



**Figure S140.**  $^{31}\text{P}\{^1\text{H}\}$  NMR spectrum of **10c** recorded in  $\text{C}_6\text{D}_6$  at 298 K.

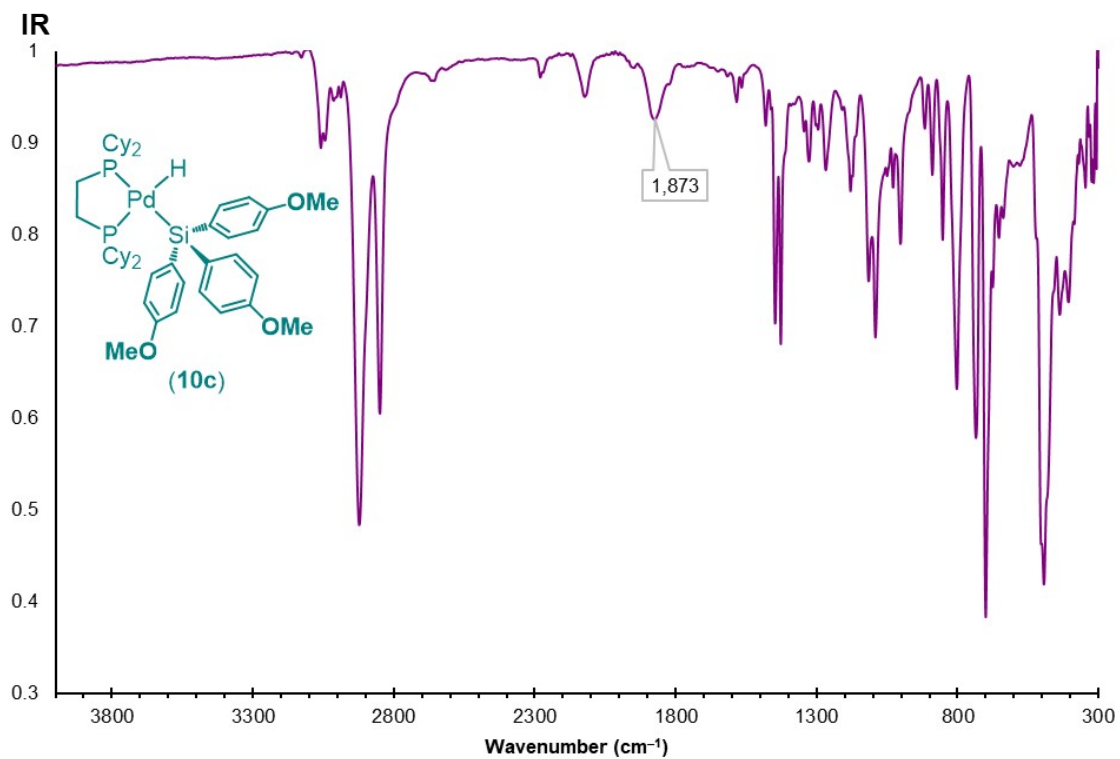


**Figure S141.** IR spectrum of **10c** recorded neat at room temperature.

(dcpe)Pd(H)[Si(4-Me-Ph)<sub>3</sub>] (**10d**)

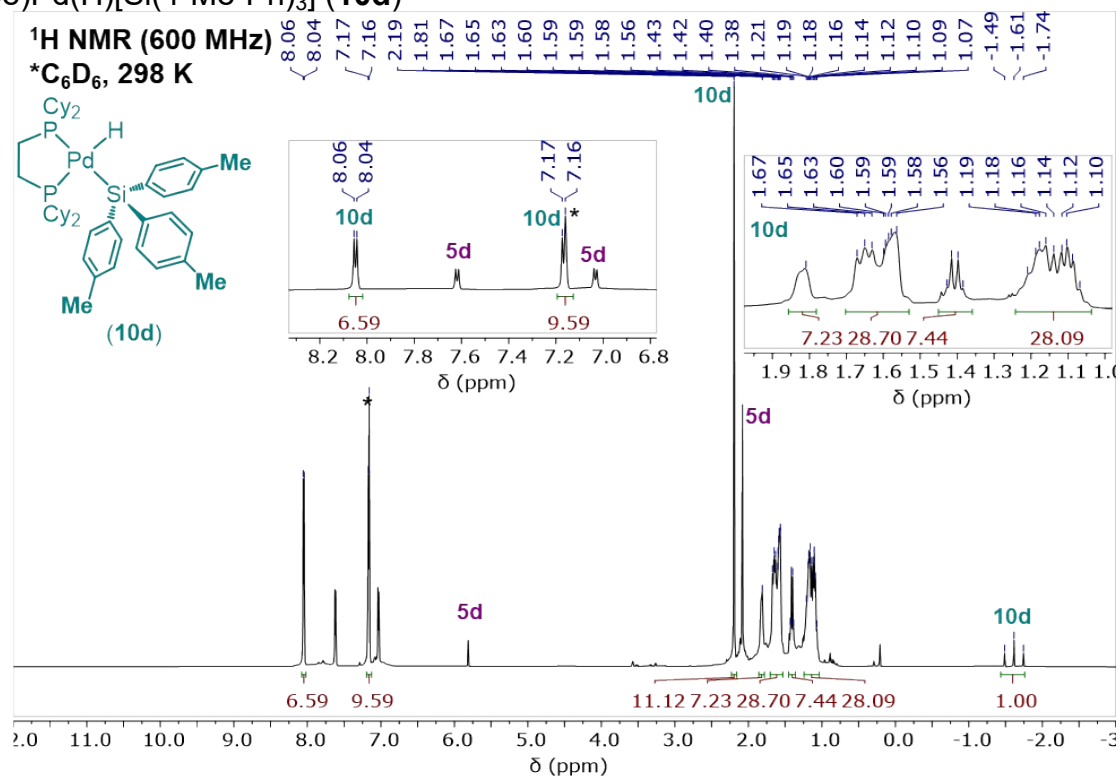


Figure S142. <sup>1</sup>H NMR spectrum of **10d** recorded in C<sub>6</sub>D<sub>6</sub> at 298 K.

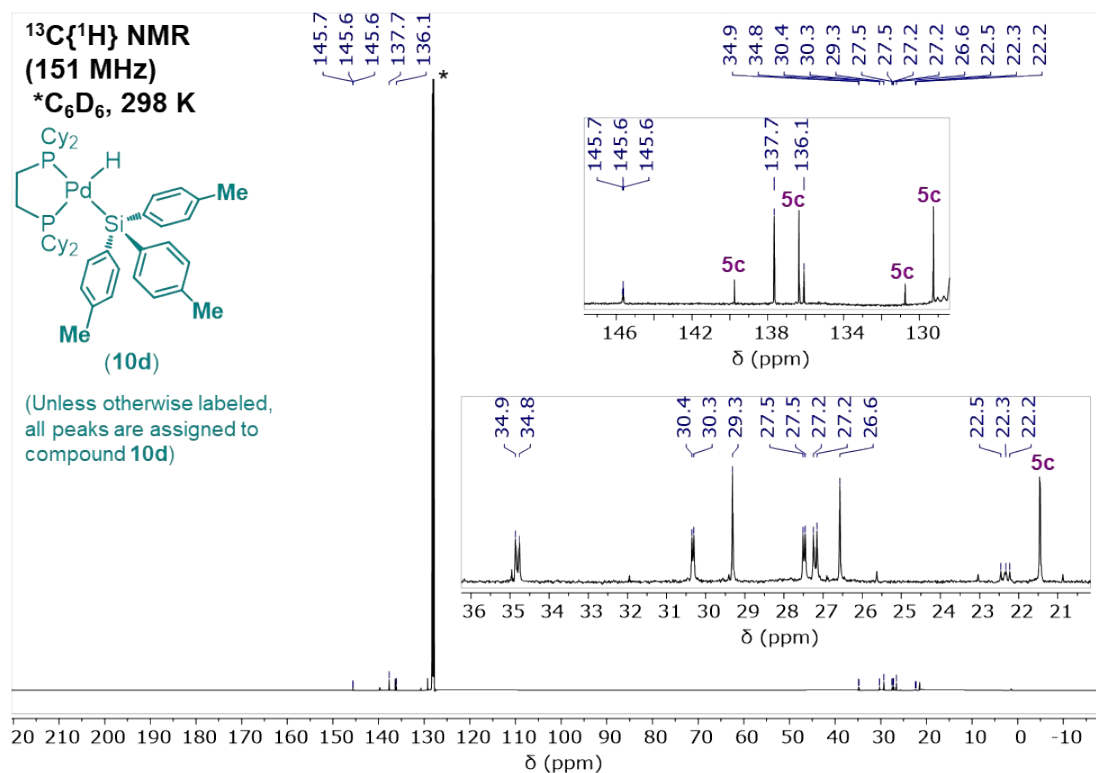
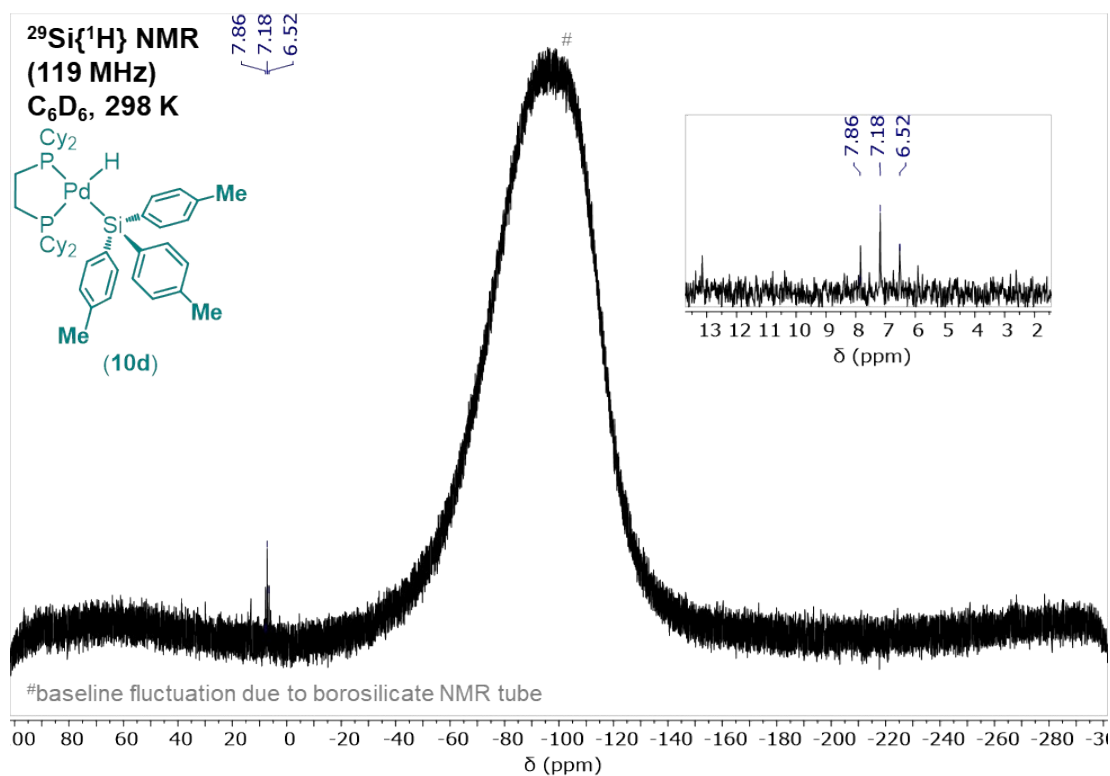
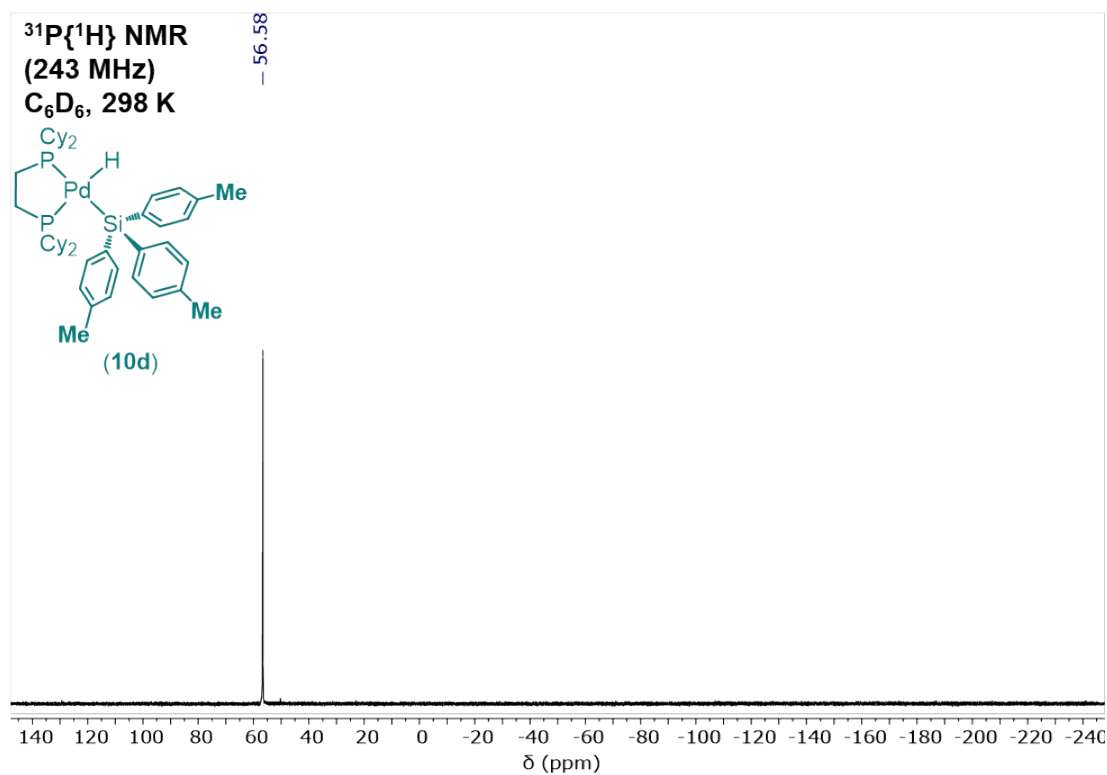


Figure S143. <sup>13</sup>C{<sup>1</sup>H} NMR spectrum of **10d** recorded in C<sub>6</sub>D<sub>6</sub> at 298 K.



**Figure S144.**  $^{29}\text{Si}\{^1\text{H}\}$  NMR spectrum of **10d** recorded in  $\text{C}_6\text{D}_6$  at 298 K.



**Figure S145.**  $^{31}\text{P}\{^1\text{H}\}$  NMR spectrum of **10d** recorded in  $\text{C}_6\text{D}_6$  at 298 K.

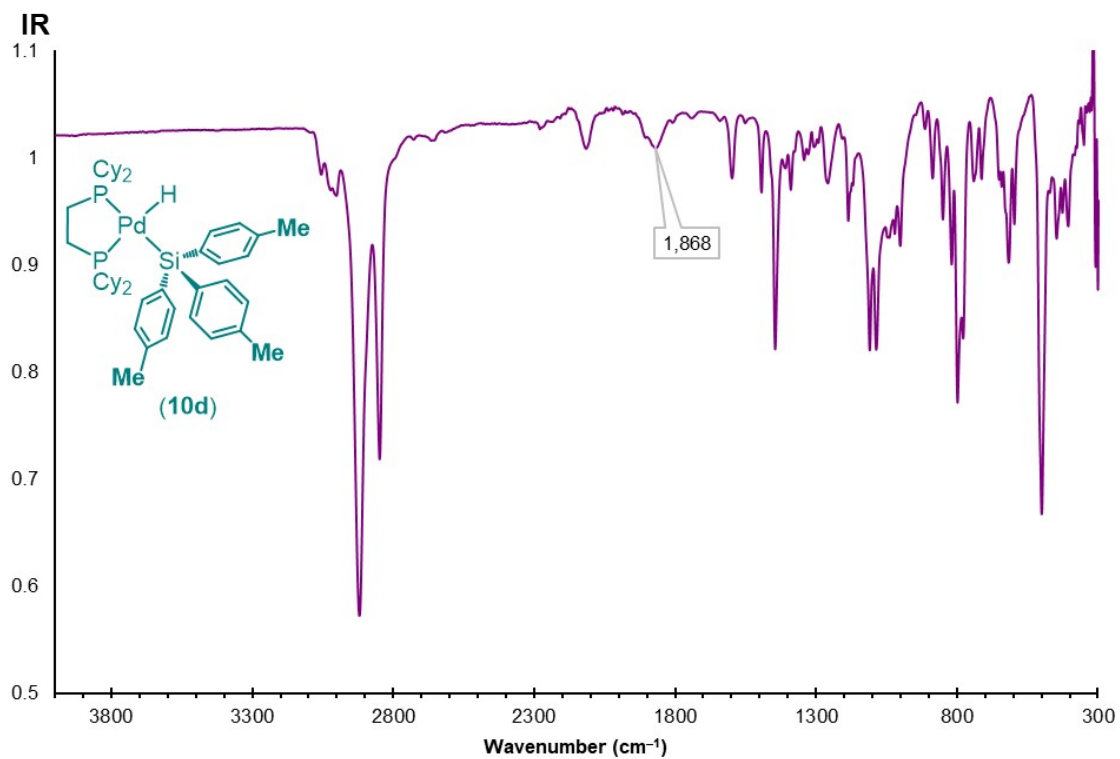


**Figure S146.** IR spectrum of **10d** recorded neat at room temperature.

(dcpe)Pd(H)(SiPh<sub>3</sub>) (**10a**)

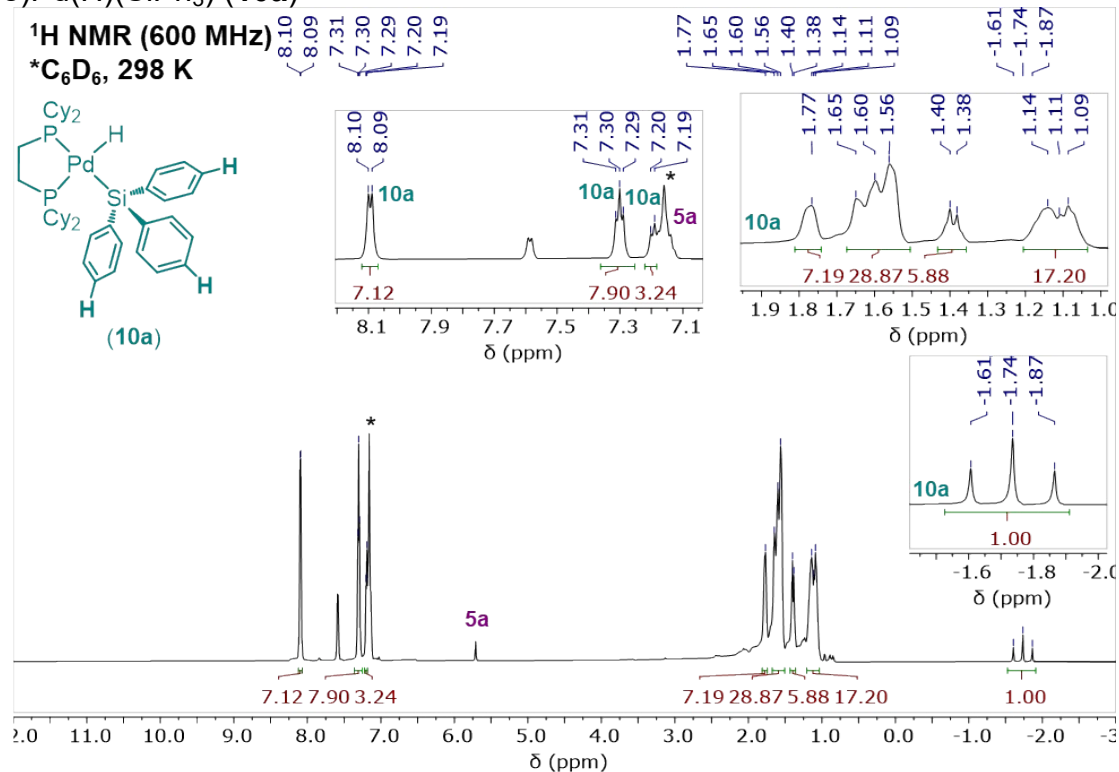


Figure S147. <sup>1</sup>H NMR spectrum of **10a** recorded in C<sub>6</sub>D<sub>6</sub> at 298 K.

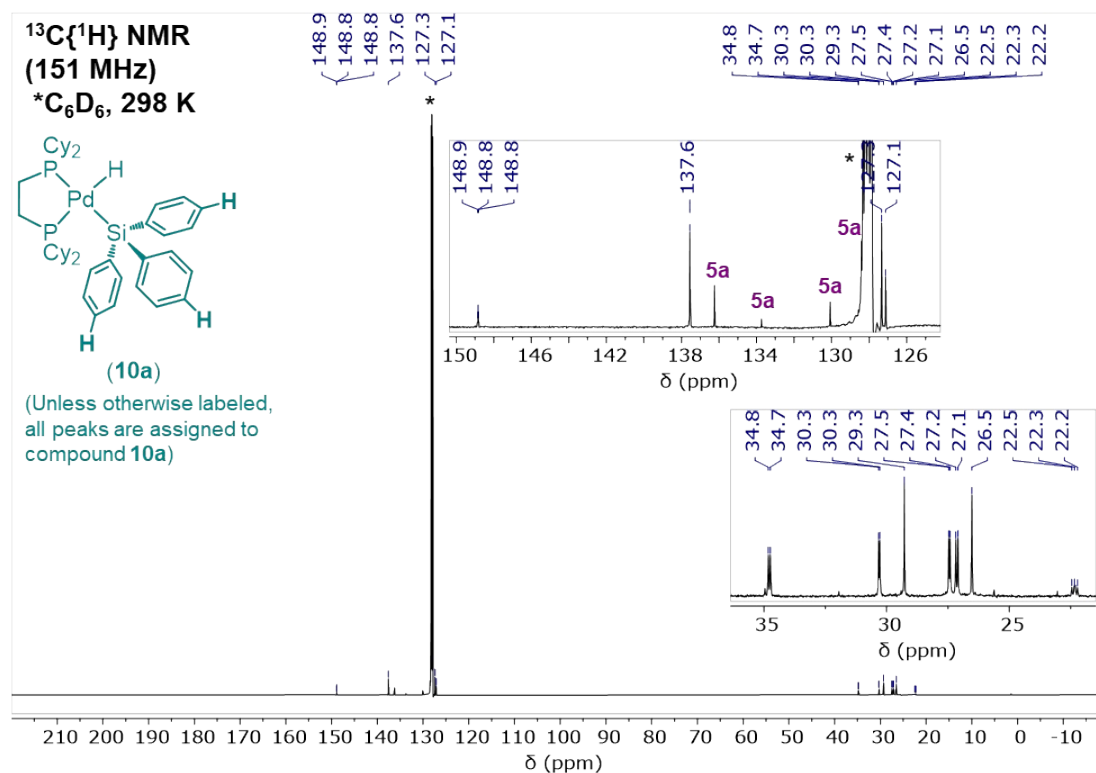
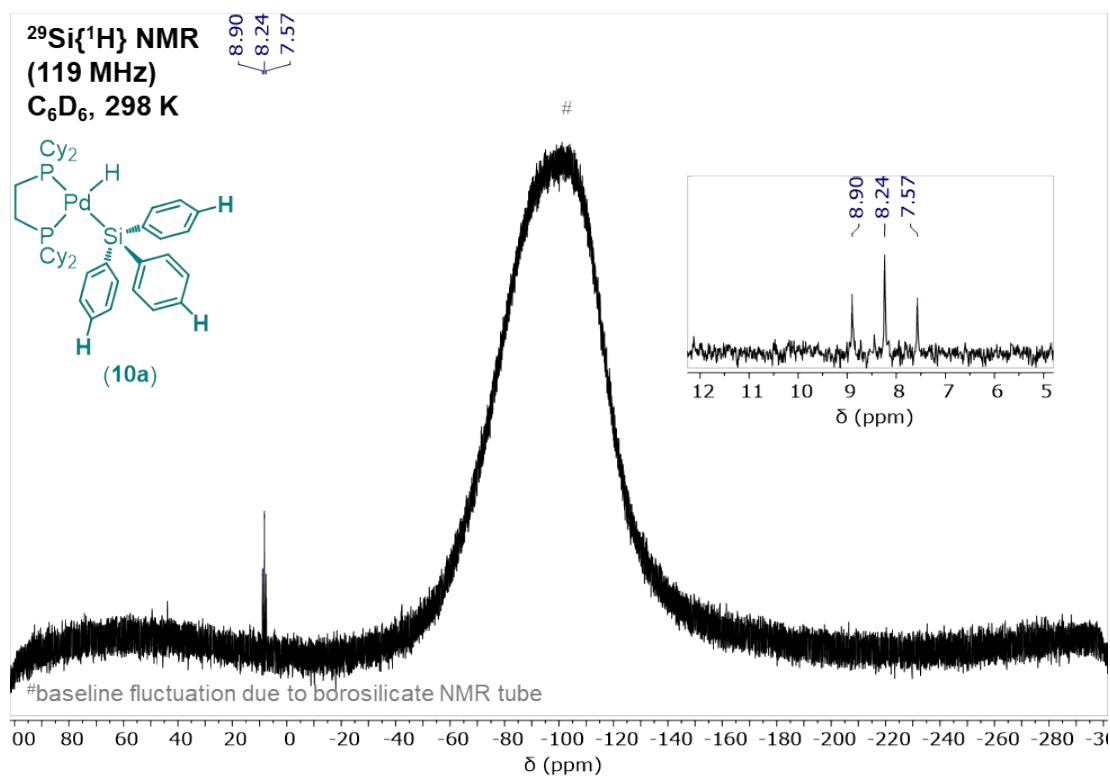
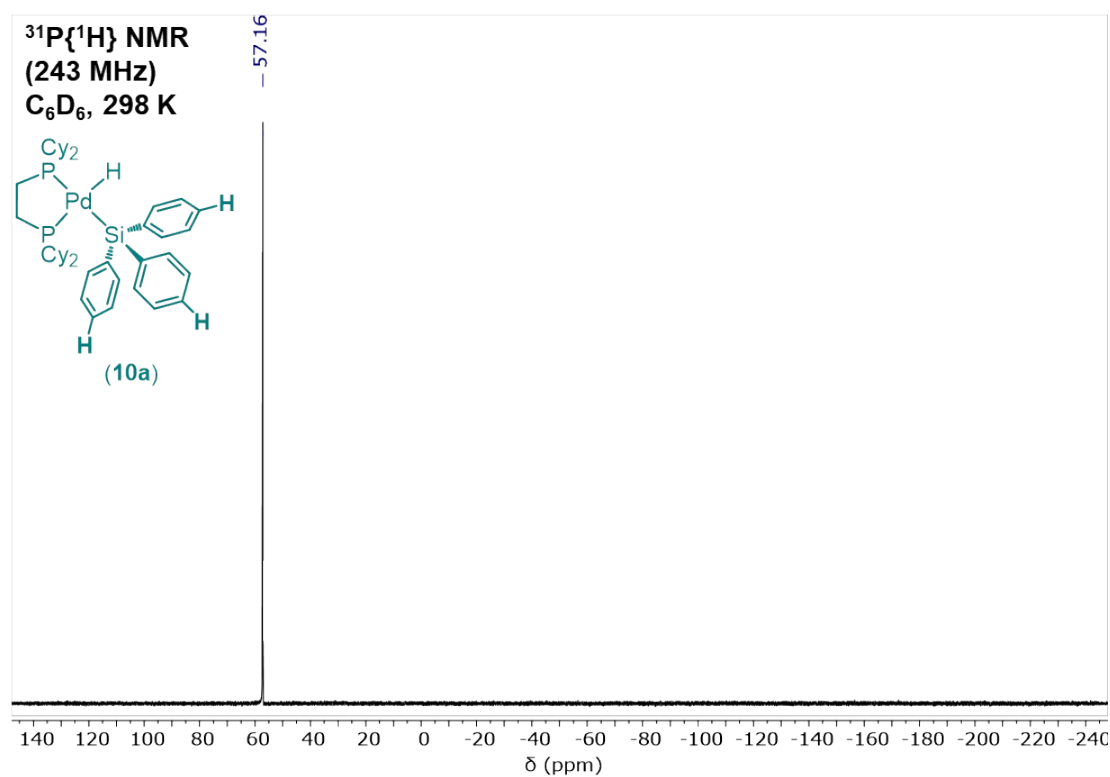


Figure S148. <sup>13</sup>C{<sup>1</sup>H} NMR spectrum of **10a** recorded in C<sub>6</sub>D<sub>6</sub> at 298 K.



**Figure S149.**  $^{29}\text{Si}\{^1\text{H}\}$  NMR spectrum of **10a** recorded in  $\text{C}_6\text{D}_6$  at 298 K.



**Figure S150.**  $^{31}\text{P}\{^1\text{H}\}$  NMR spectrum of **10a** recorded in  $\text{C}_6\text{D}_6$  at 298 K.

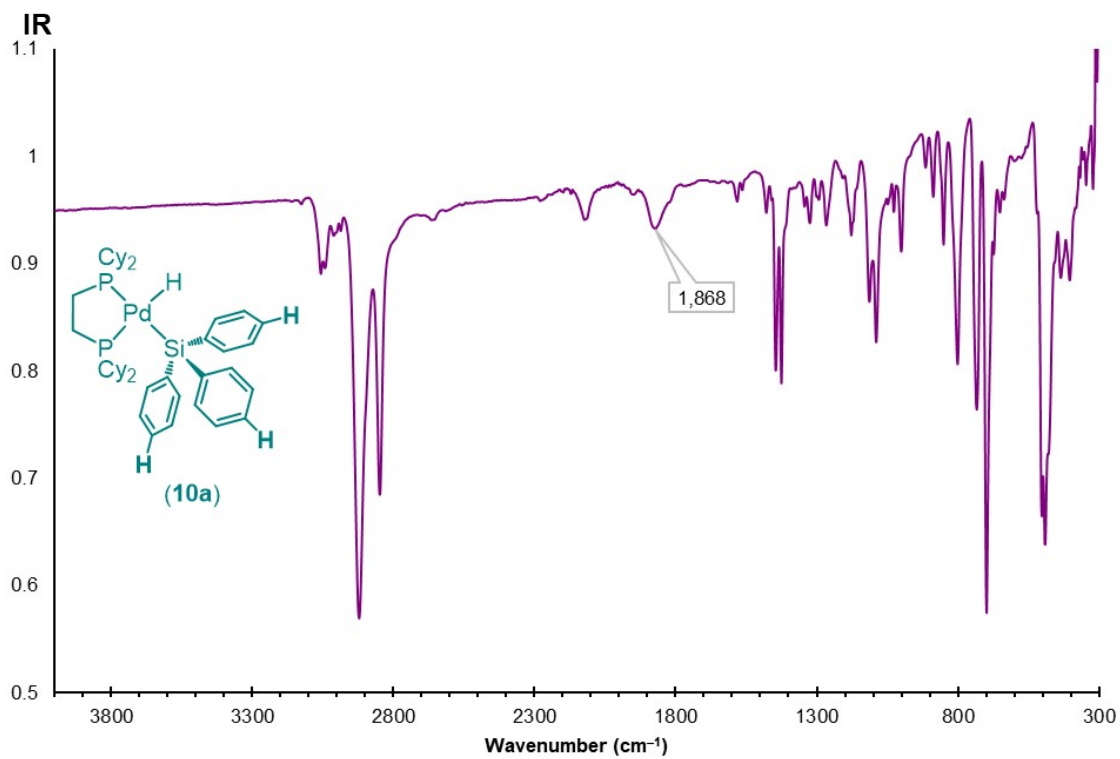


**Figure S151.** IR spectrum of **10a** recorded neat at room temperature.

(dcpe)Pd(D)(SiPh<sub>3</sub>) (**10a-d<sub>1</sub>**)

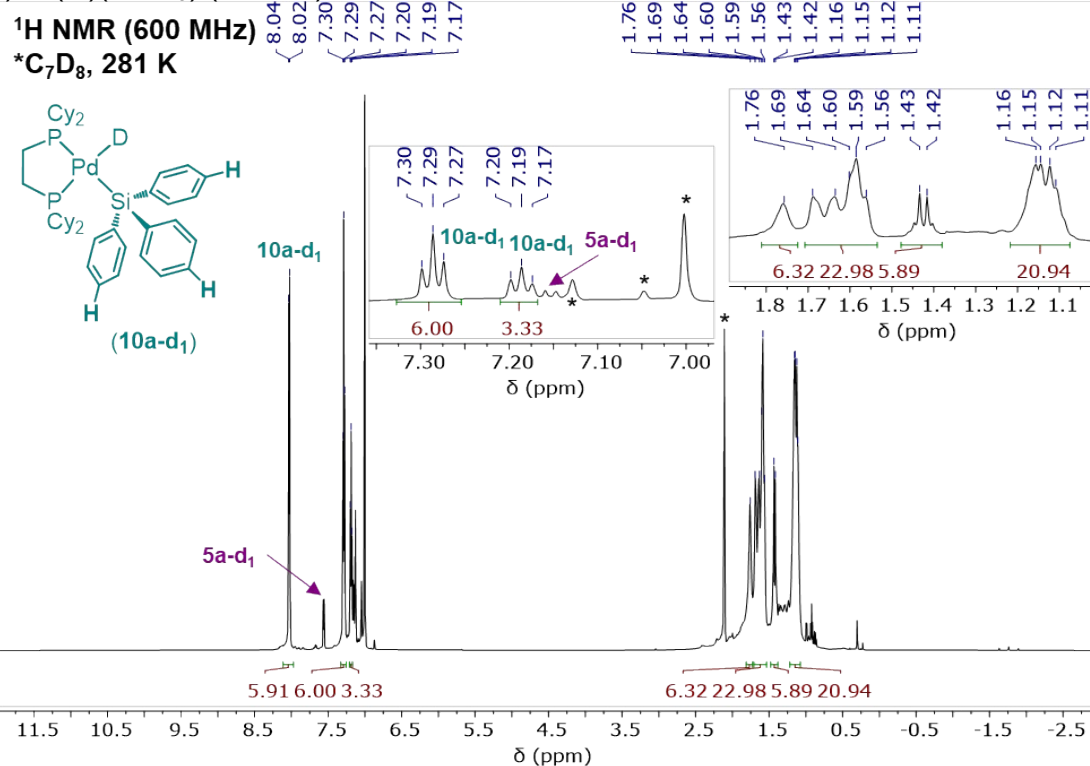


**Figure S152.** <sup>1</sup>H NMR spectrum of **10a-d<sub>1</sub>** recorded in C<sub>7</sub>D<sub>8</sub> at 281 K.

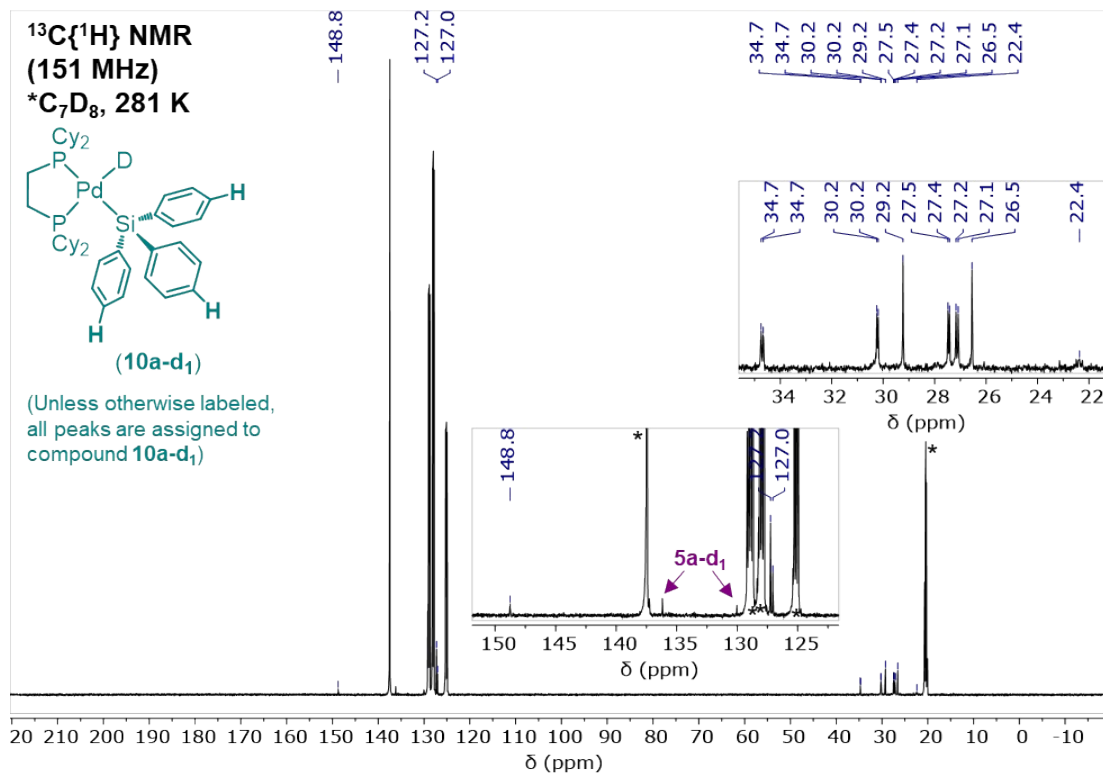


**Figure S153.** <sup>13</sup>C{<sup>1</sup>H} NMR spectrum of **10a-d<sub>1</sub>** recorded in C<sub>7</sub>D<sub>8</sub> at 281 K.

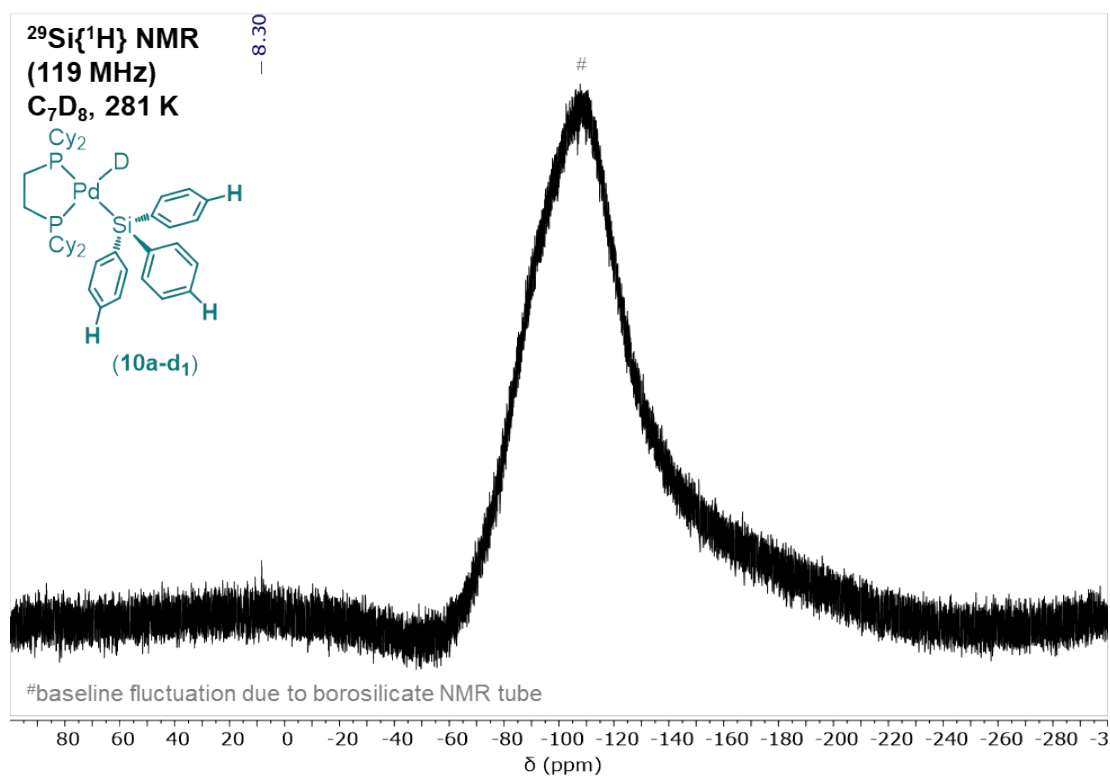


**Figure S154.**  $^{29}\text{Si}\{^1\text{H}\}$  NMR spectrum of **10a-d<sub>1</sub>** recorded in  $\text{C}_6\text{D}_6$  at 281 K.

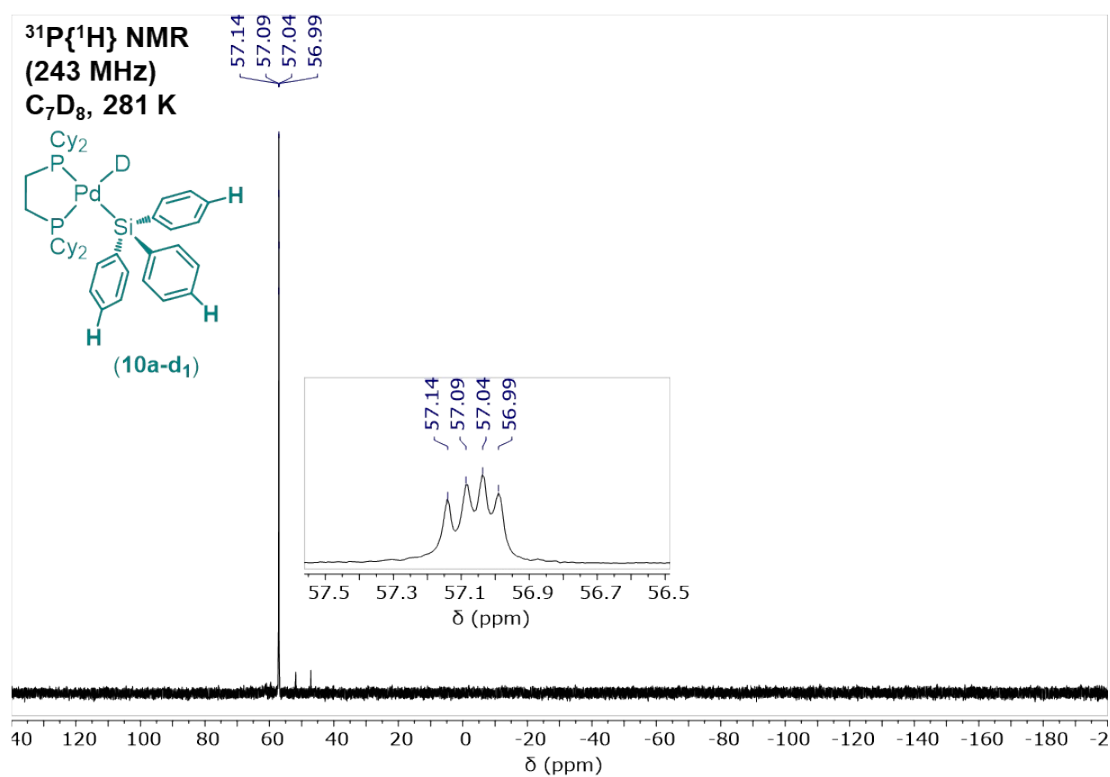


**Figure S155.**  $^{31}\text{P}\{^1\text{H}\}$  NMR spectrum of **10a-d<sub>1</sub>** recorded in  $\text{C}_7\text{D}_8$  at 281 K.

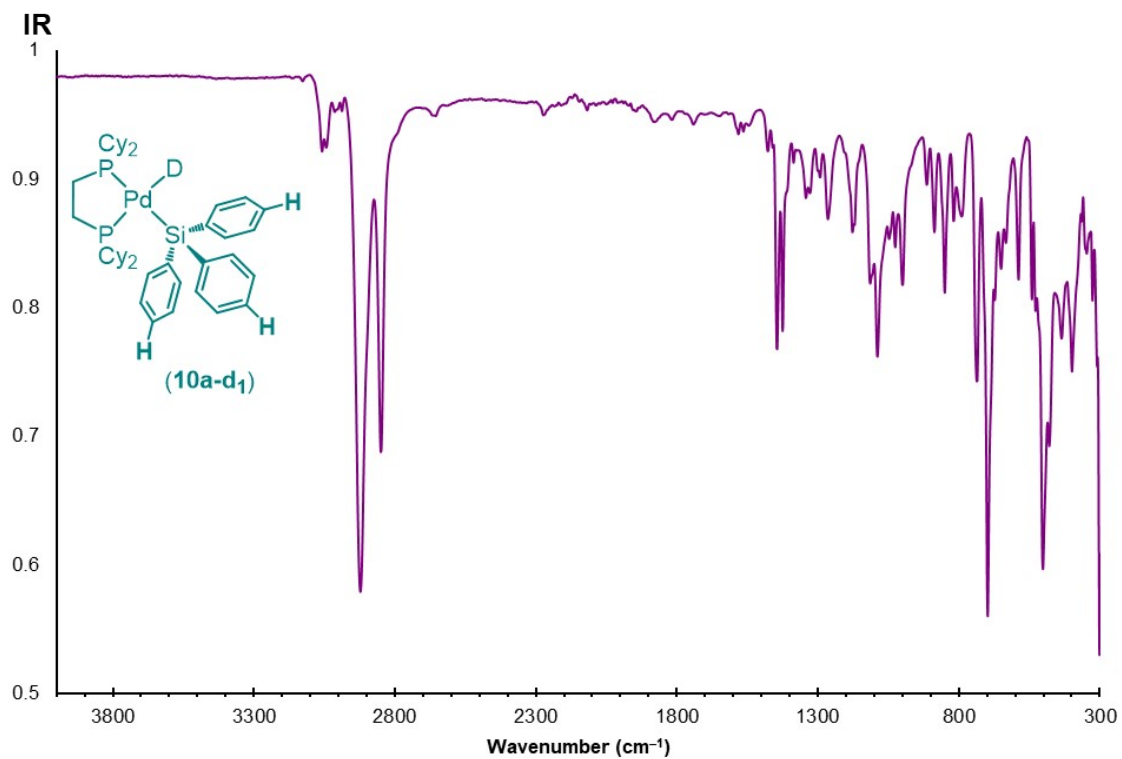


**Figure S156.** IR spectrum of **10a-d<sub>1</sub>** recorded neat at room temperature.

(dcpe)Pd(H)[Si(4-F-Ph)<sub>3</sub>] (**10e**)

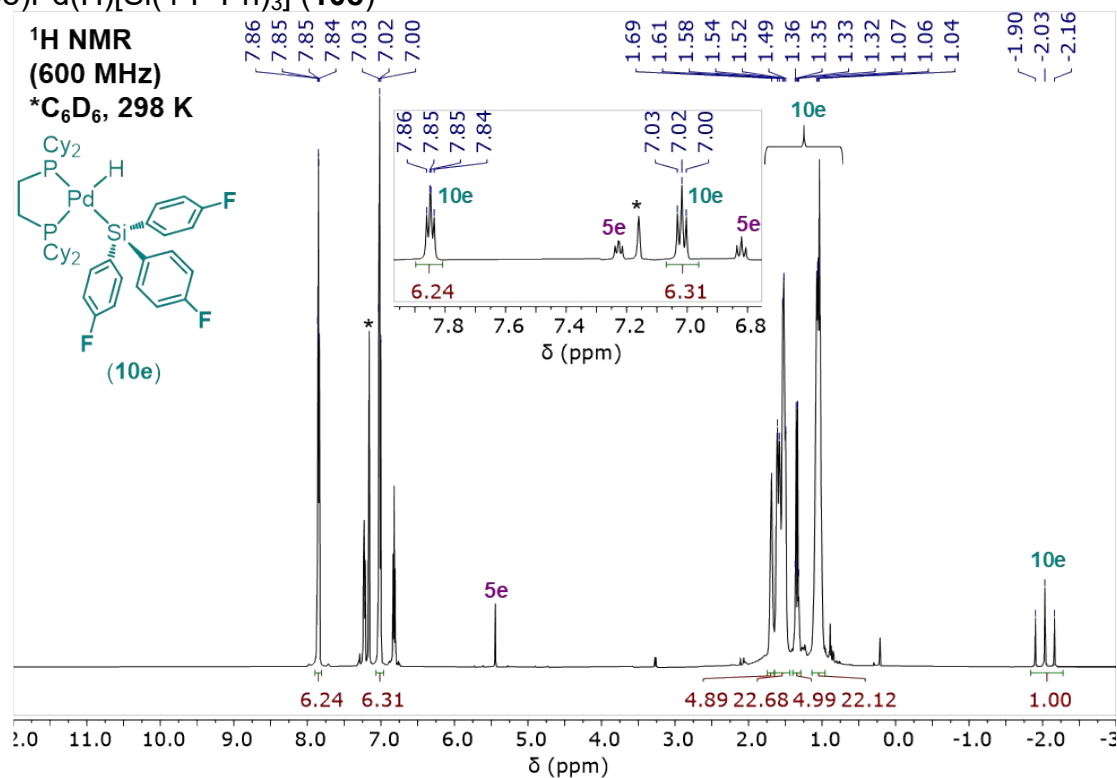


**Figure S157.** <sup>1</sup>H NMR spectrum of **10e** recorded in C<sub>6</sub>D<sub>6</sub> at 298 K.

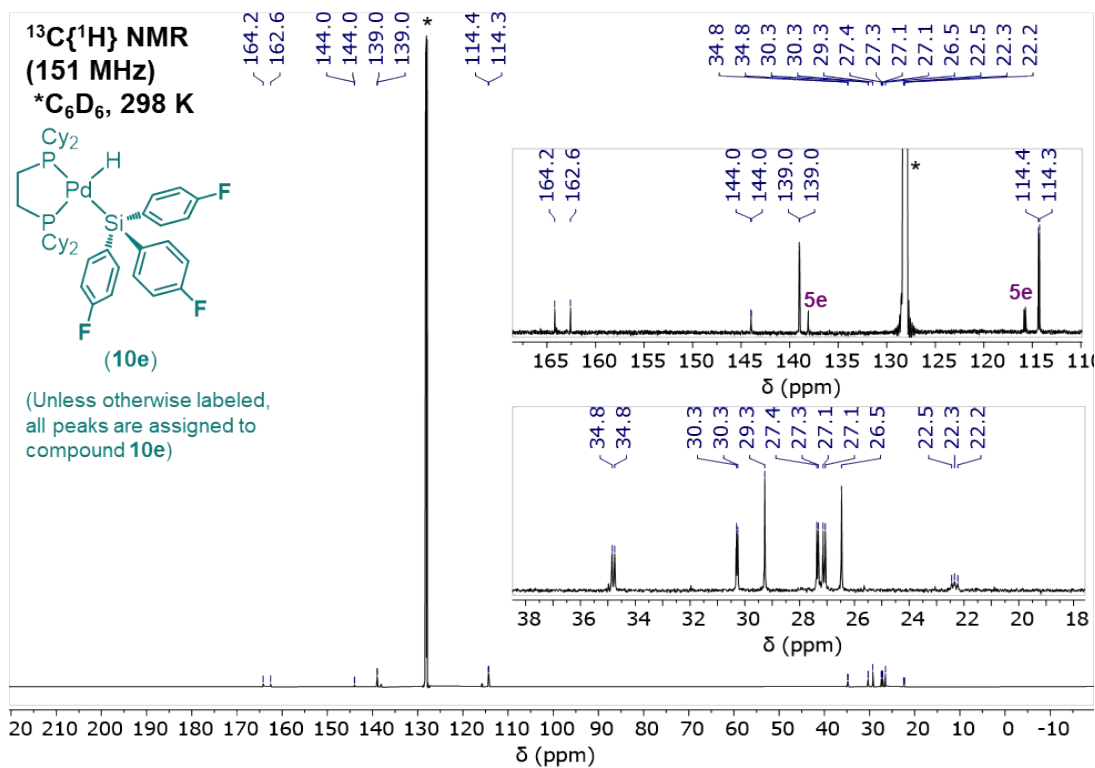


**Figure S158.** <sup>13</sup>C{<sup>1</sup>H} NMR spectrum of **10e** recorded in C<sub>6</sub>D<sub>6</sub> at 298 K.

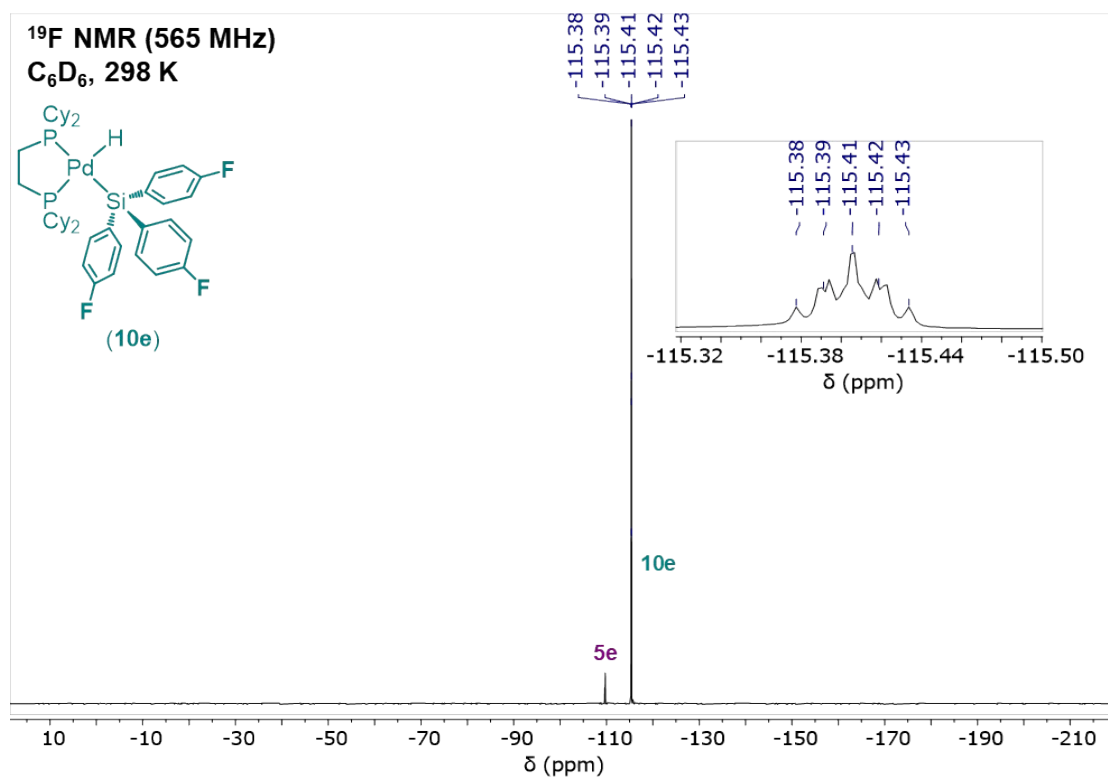


**Figure S159.**  $^{19}\text{F}$  NMR spectrum of **10e** recorded in  $\text{C}_6\text{D}_6$  at 298 K.

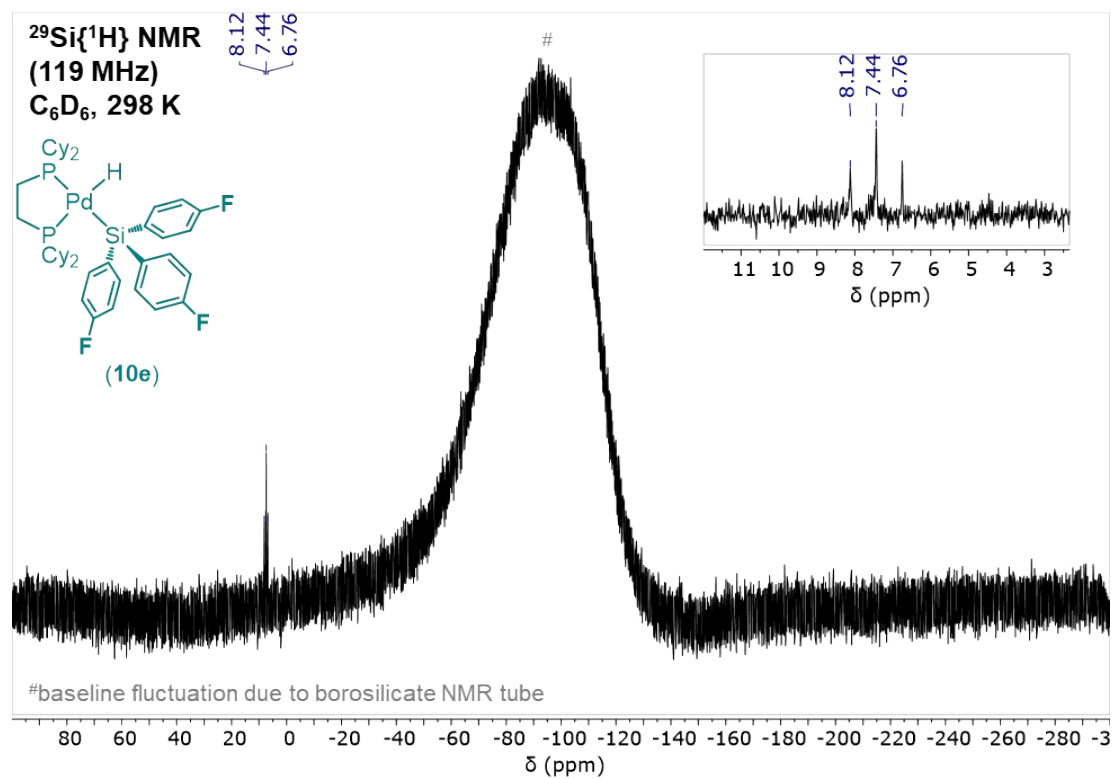


**Figure S160.**  $^{29}\text{Si}\{^1\text{H}\}$  NMR spectrum of **10e** recorded in  $\text{C}_6\text{D}_6$  at 298 K.

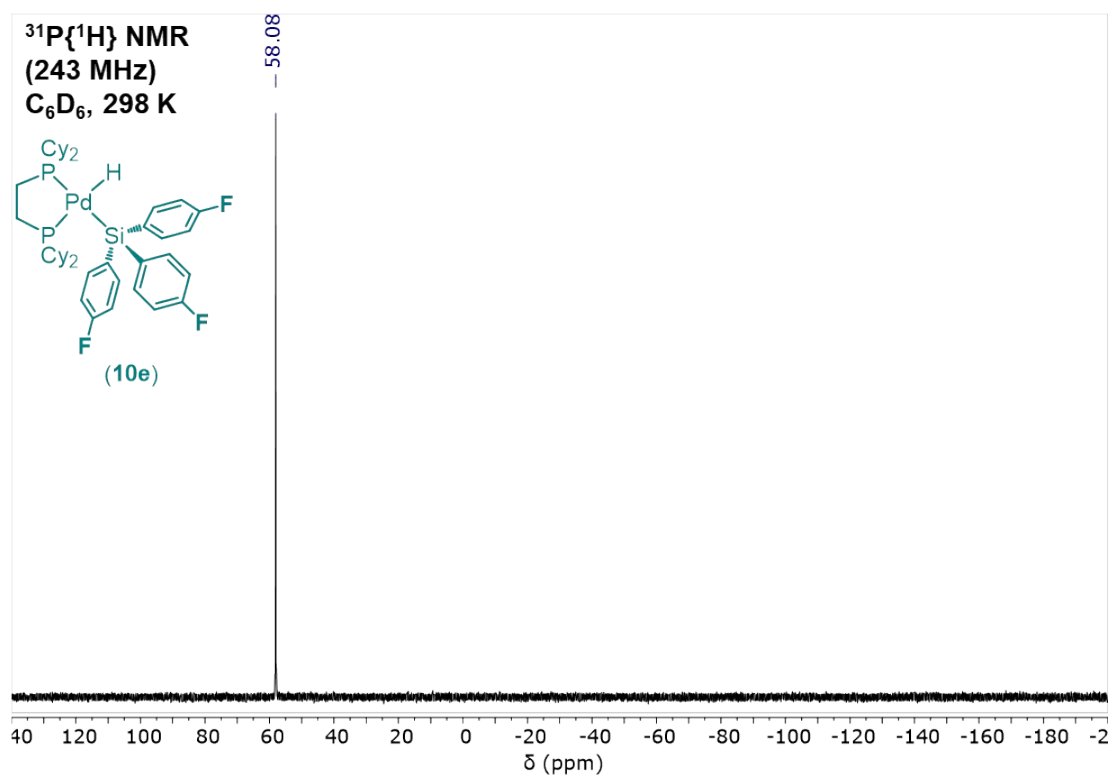


**Figure S161.**  $^{31}\text{P}\{^1\text{H}\}$  NMR spectrum of **10e** recorded in  $\text{C}_6\text{D}_6$  at 298 K.

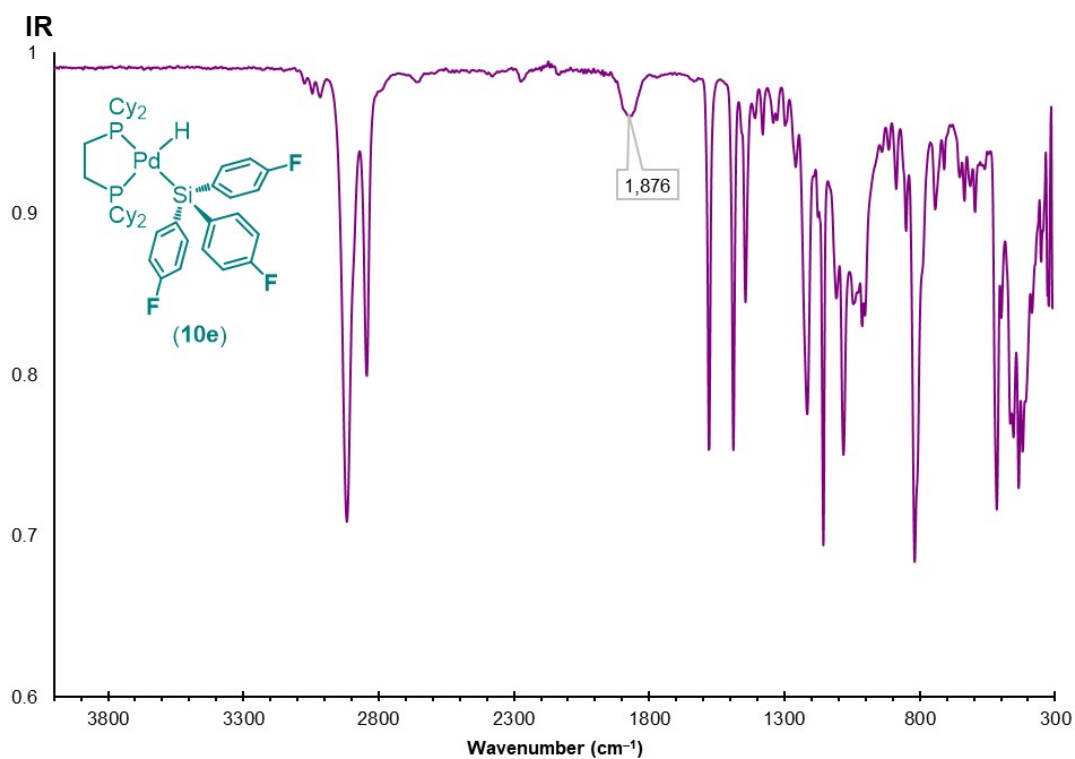


**Figure S162.** IR spectrum of **10e** recorded neat at room temperature.

(dcpe)Pd(H)[Si(4-CF<sub>3</sub>-Ph)<sub>3</sub>] (**10f**)

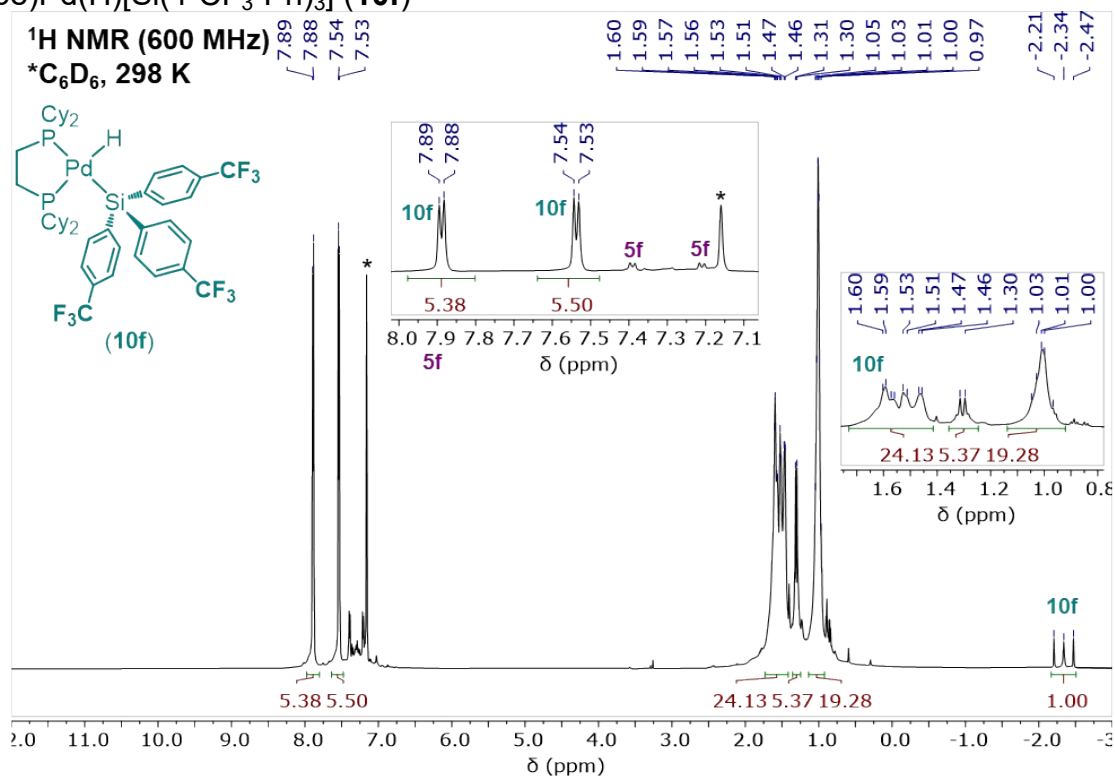


Figure S163. <sup>1</sup>H NMR spectrum of **10f** recorded in C<sub>6</sub>D<sub>6</sub> at 298 K.

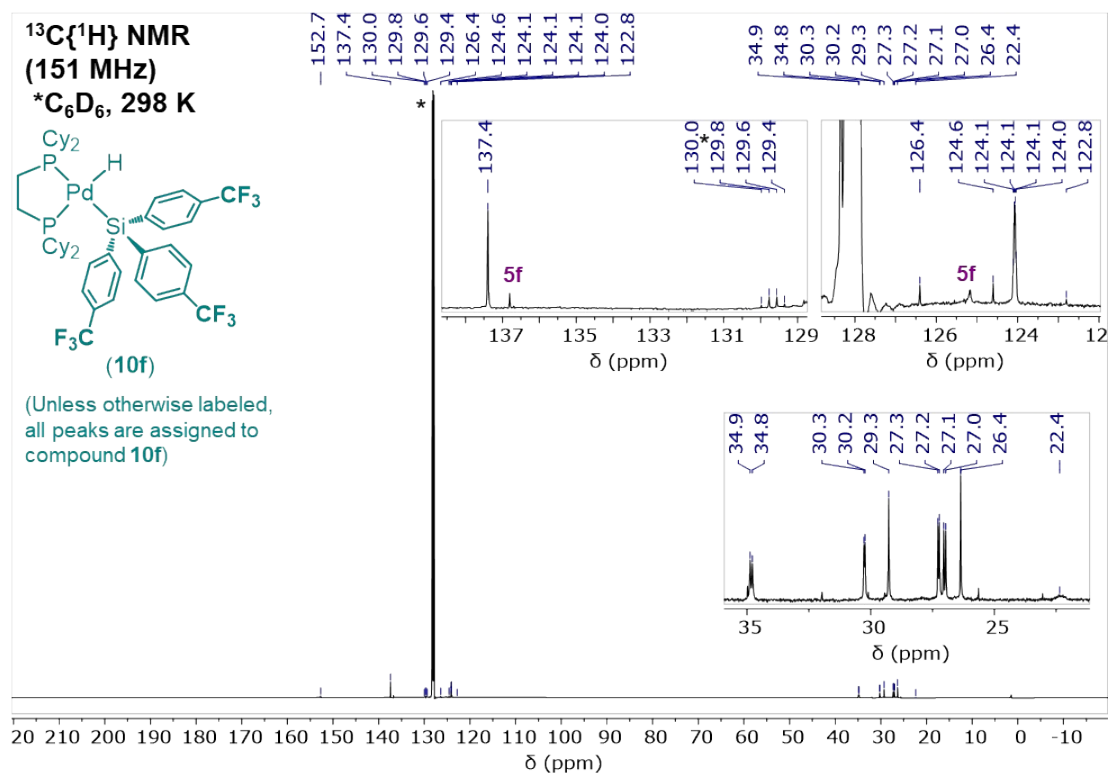
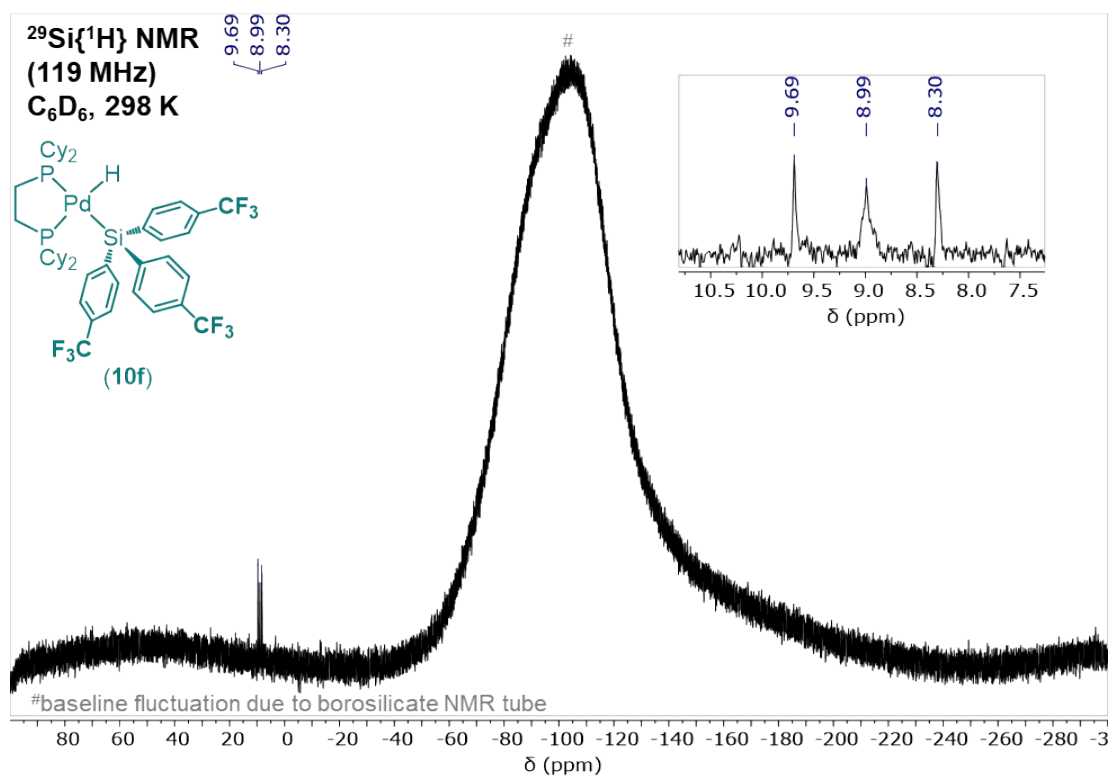
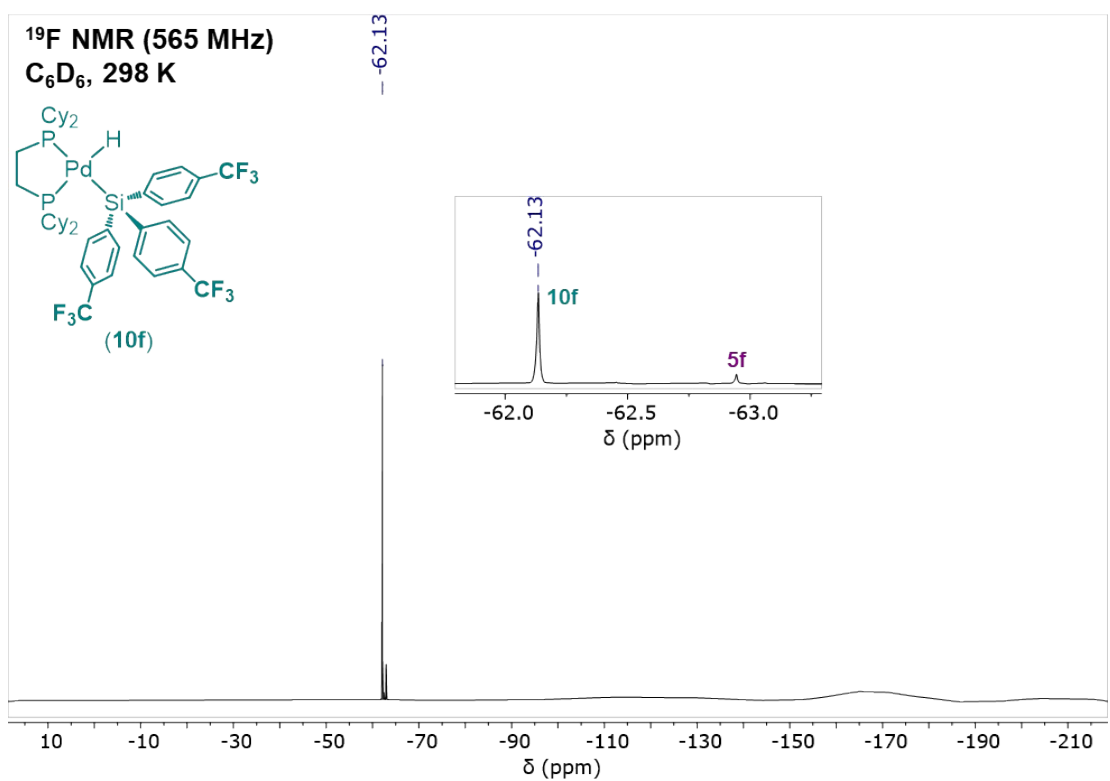


Figure S164. <sup>13</sup>C{<sup>1</sup>H} NMR spectrum of **10f** recorded in C<sub>6</sub>D<sub>6</sub> at 298 K.



**Figure S165.**  $^{29}\text{Si}\{^1\text{H}\}$  NMR spectrum of **10f** recorded in  $\text{C}_6\text{D}_6$  at 298 K.



**Figure S166.**  $^{19}\text{F}$  NMR spectrum of **10f** recorded in  $\text{C}_6\text{D}_6$  at 298 K.

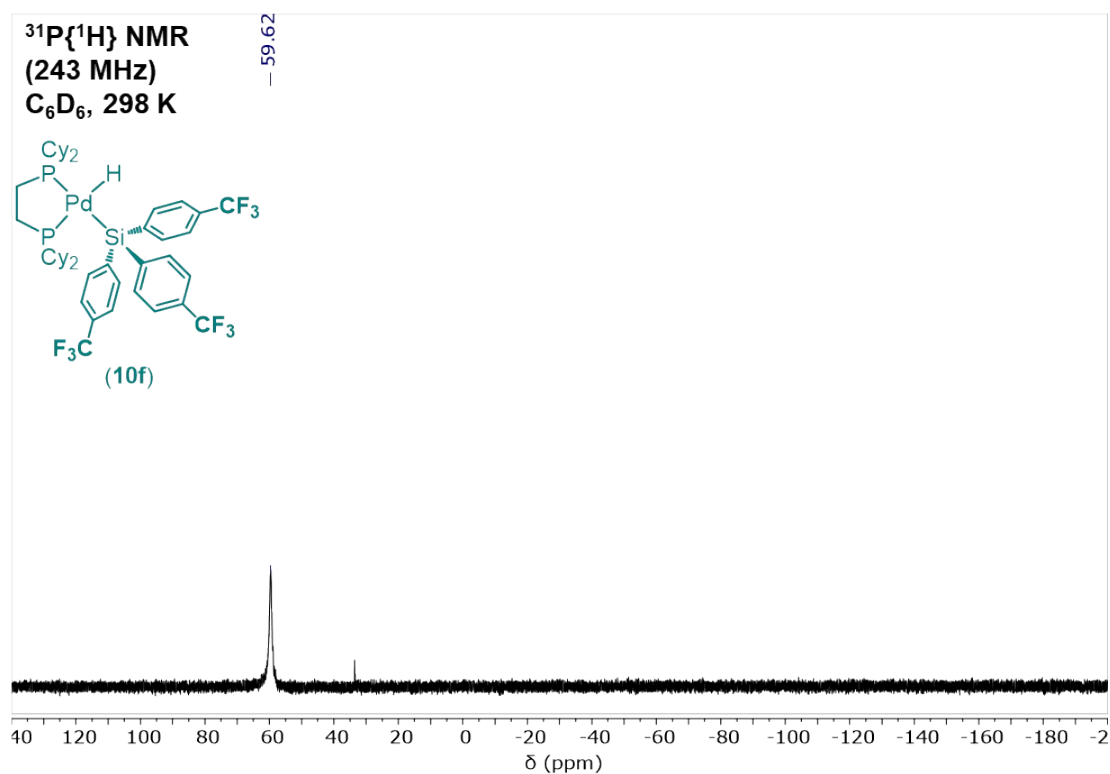


**Figure S167.**  $^{31}\text{P}\{^1\text{H}\}$  NMR spectrum of **10f** recorded in  $\text{C}_6\text{D}_6$  at 298 K.

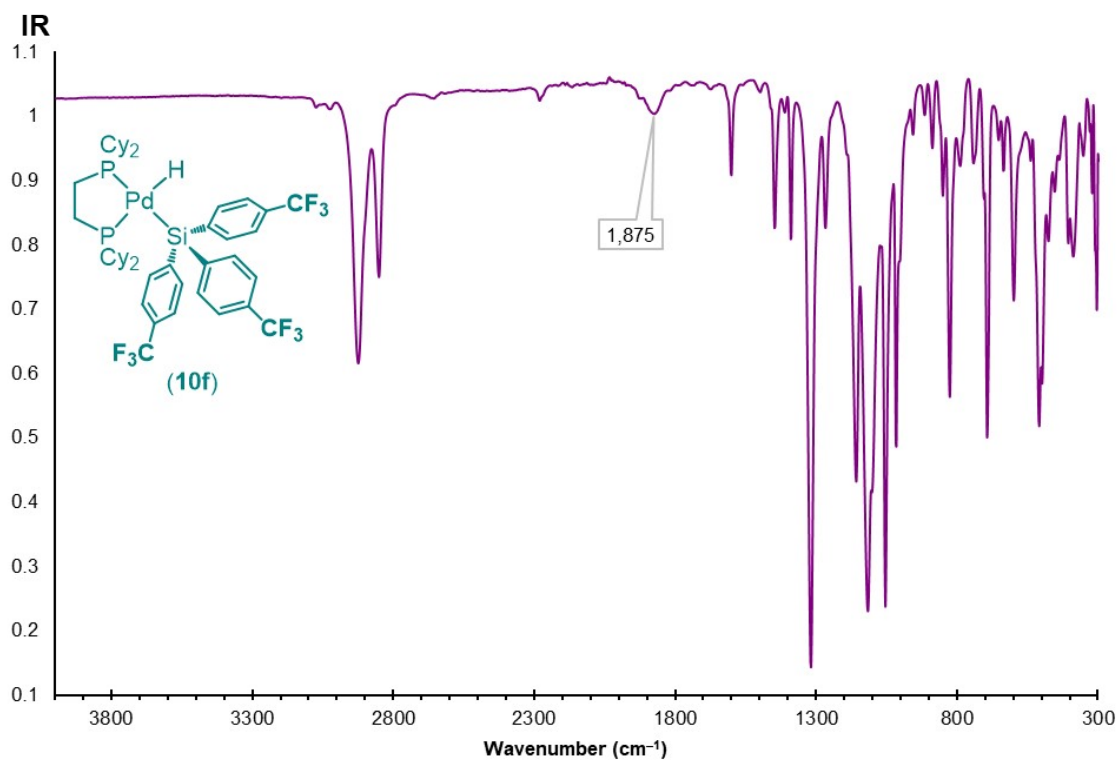


**Figure S168.** IR spectrum of **10f** recorded neat at room temperature.

(dcpe)Pd(H)[Si(4-NMe<sub>2</sub>-Ph)Me<sub>2</sub>] (**8b**)

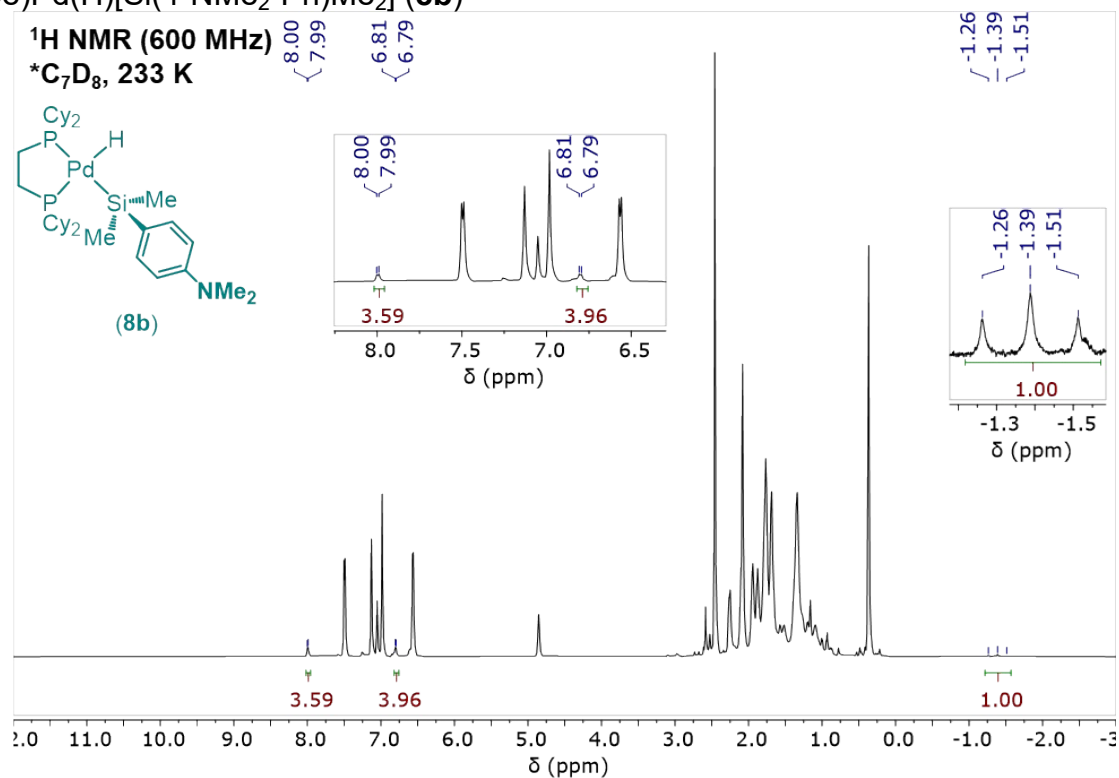


**Figure S169.** <sup>1</sup>H NMR spectrum of **8b** recorded in C<sub>7</sub>D<sub>8</sub> at 233 K.

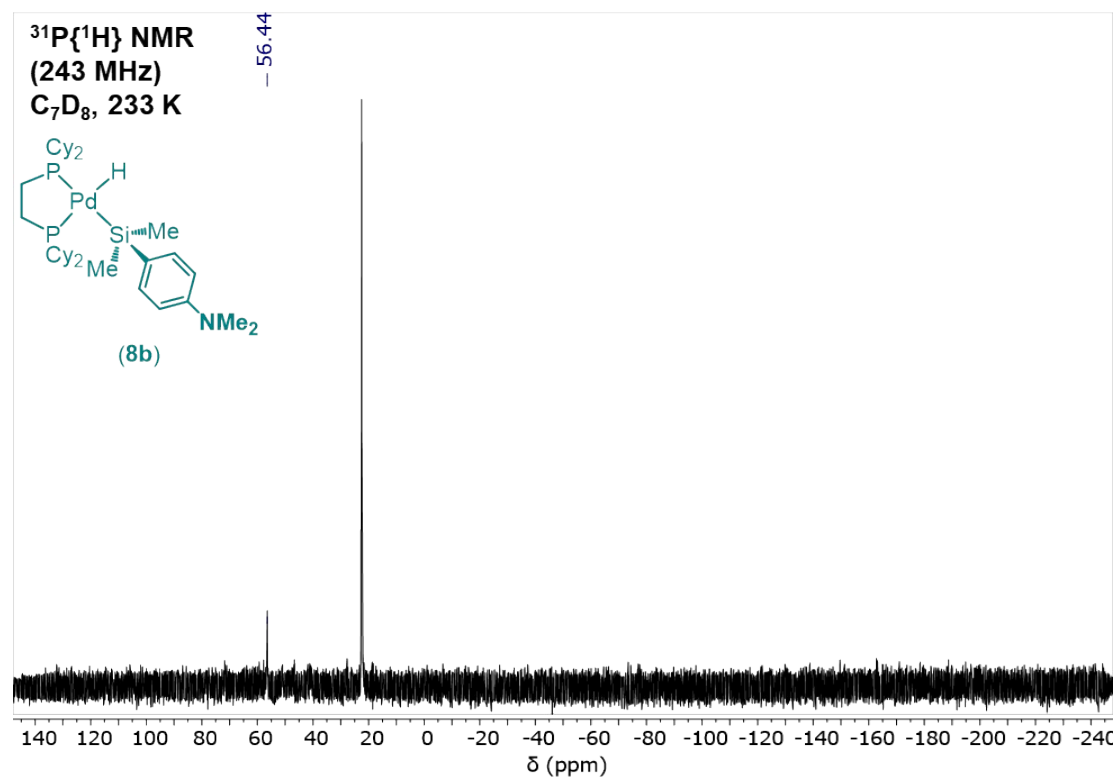


**Figure S170.** <sup>31</sup>P{<sup>1</sup>H} NMR spectrum of **8b** recorded in C<sub>7</sub>D<sub>8</sub> at 233 K.

(dcpe)Pd(H)[Si(4-OMe-Ph)Me<sub>2</sub>] (**8c**)

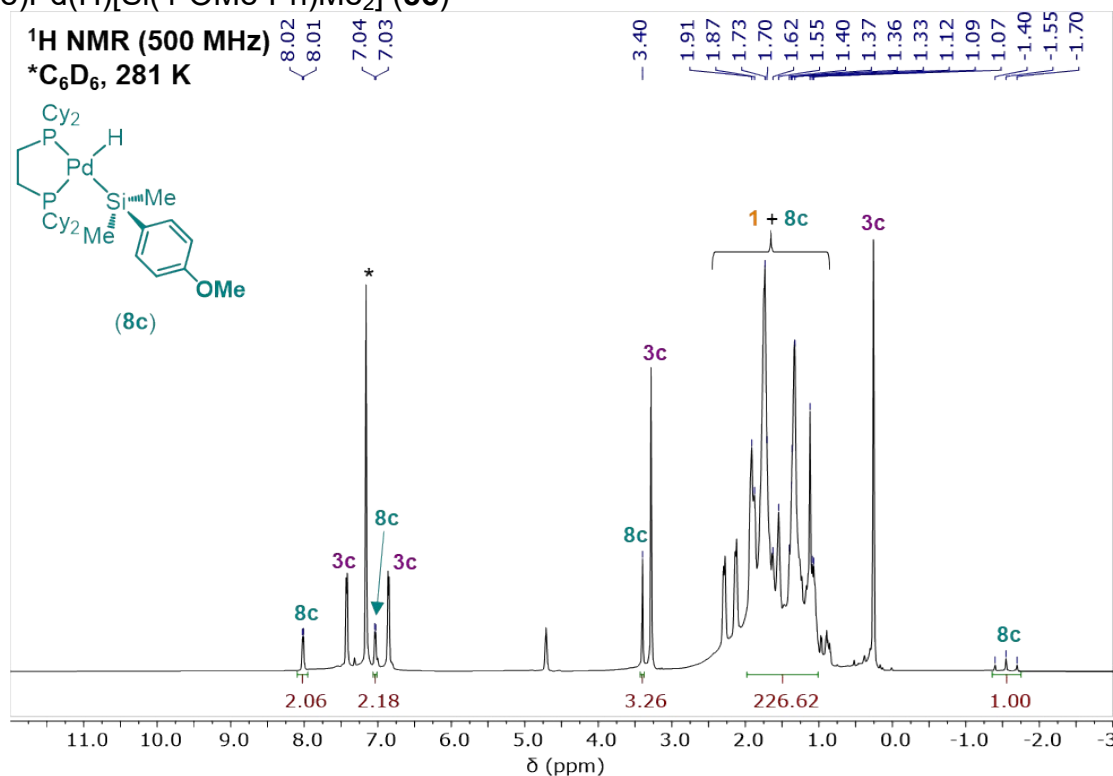


Figure S171. <sup>1</sup>H NMR spectrum of **8c** recorded in C<sub>6</sub>D<sub>6</sub> at 281 K.

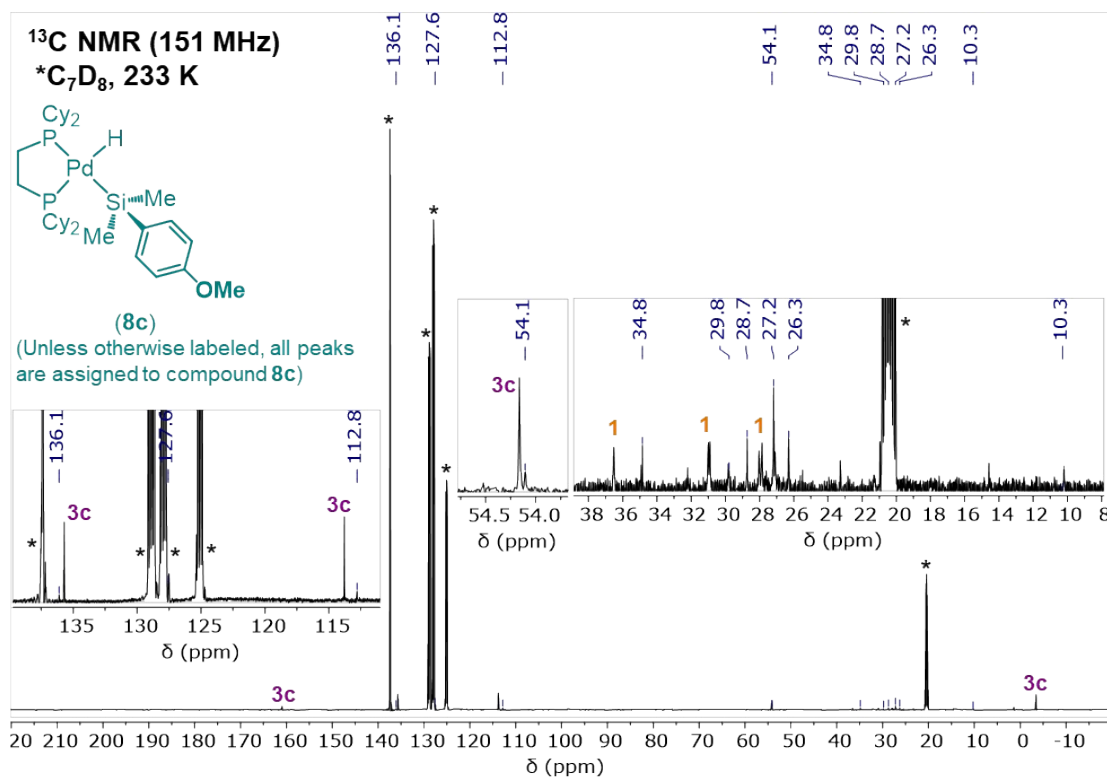
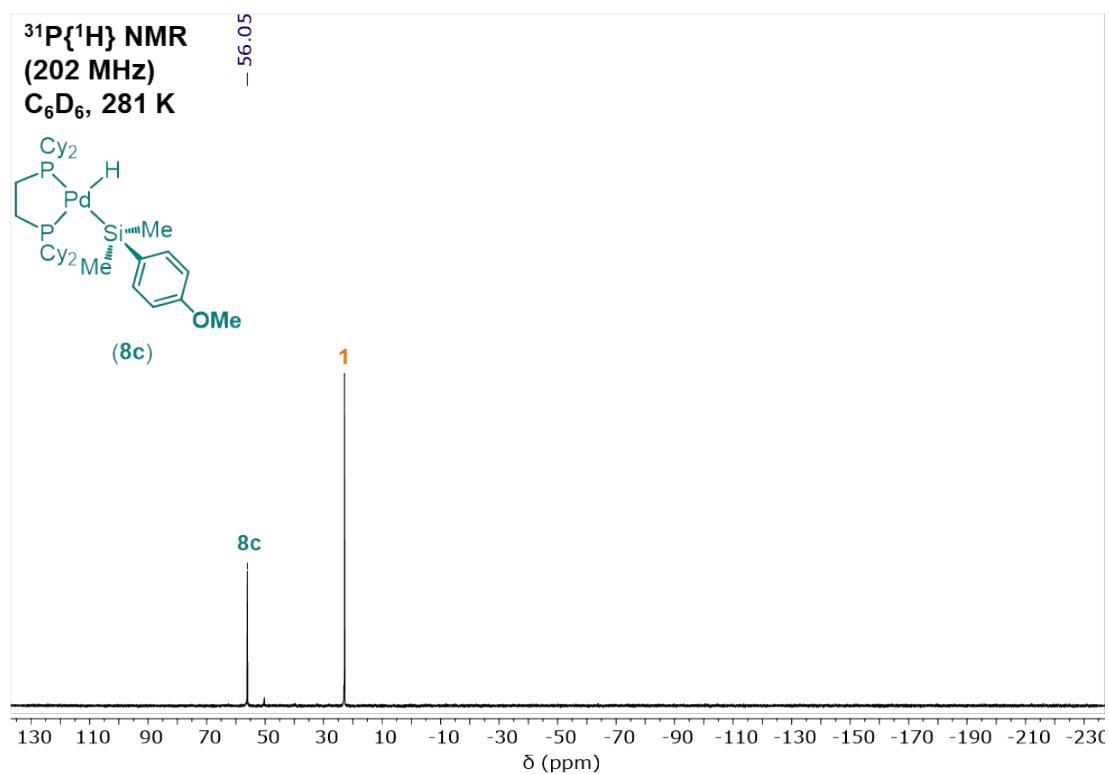
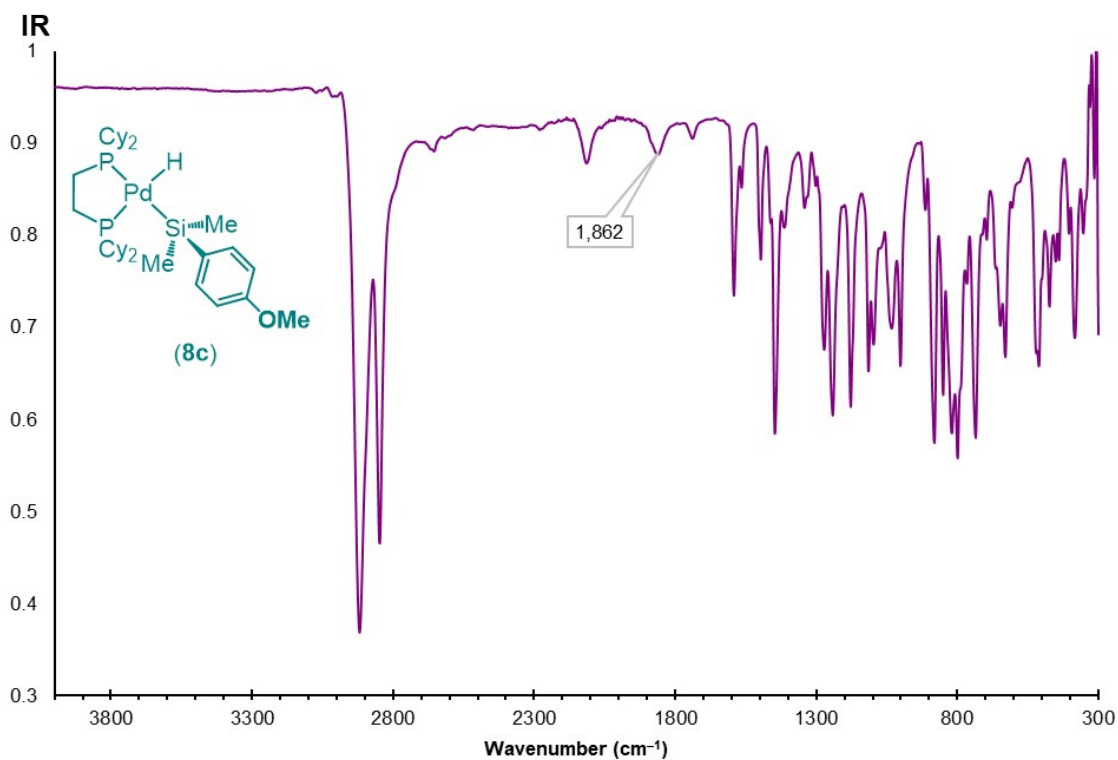


Figure S172. <sup>13</sup>C{<sup>1</sup>H} NMR spectrum of **8c** recorded in C<sub>7</sub>D<sub>8</sub> at 233 K.



**Figure S173.** <sup>31</sup>P{<sup>1</sup>H} NMR spectrum of **8c** recorded in C<sub>6</sub>D<sub>6</sub> at 281 K.



**Figure S174.** IR spectrum of **8c** recorded neat at room temperature.

(dcpe)Pd(H)[Si(4-Me-Ph)Me<sub>2</sub>] (**8d**)

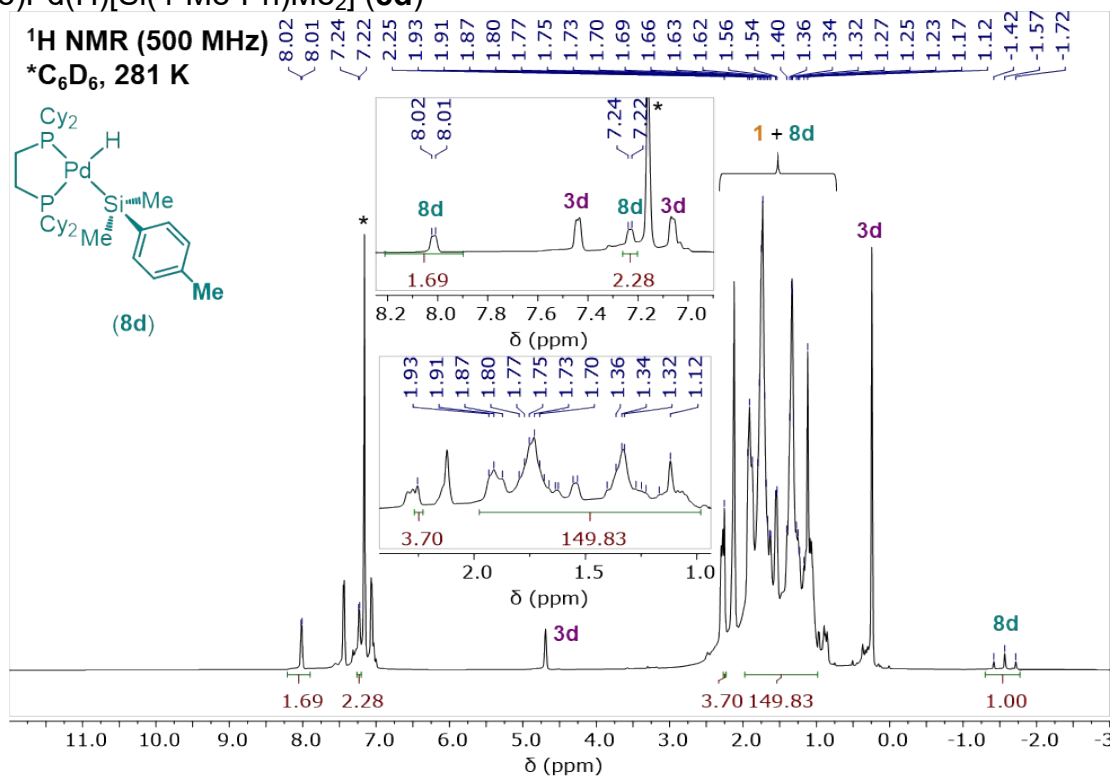


Figure S175. <sup>1</sup>H NMR spectrum of **8d** recorded in C<sub>6</sub>D<sub>6</sub> at 281 K.

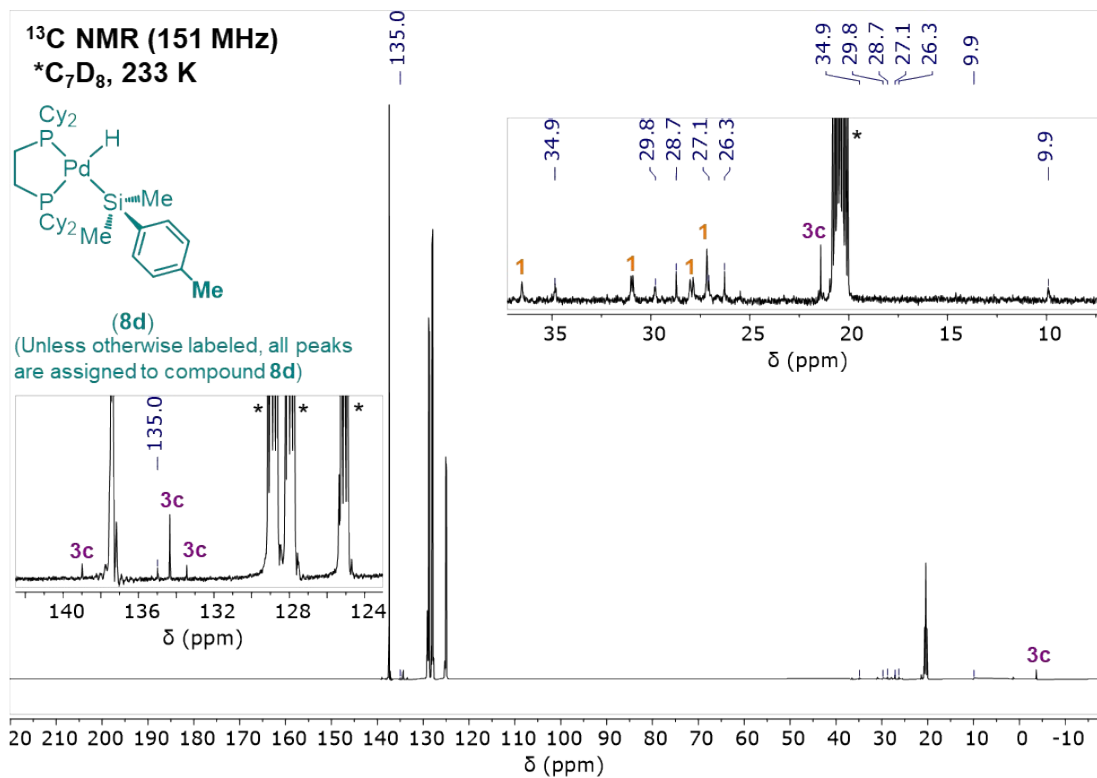
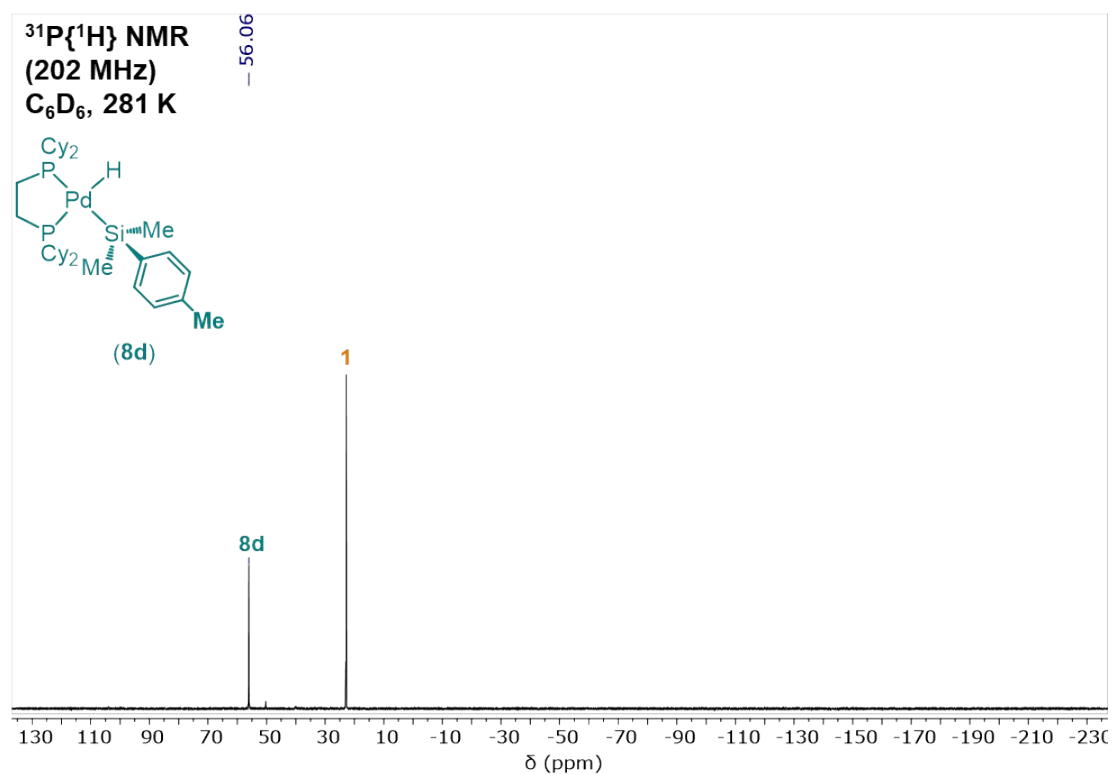
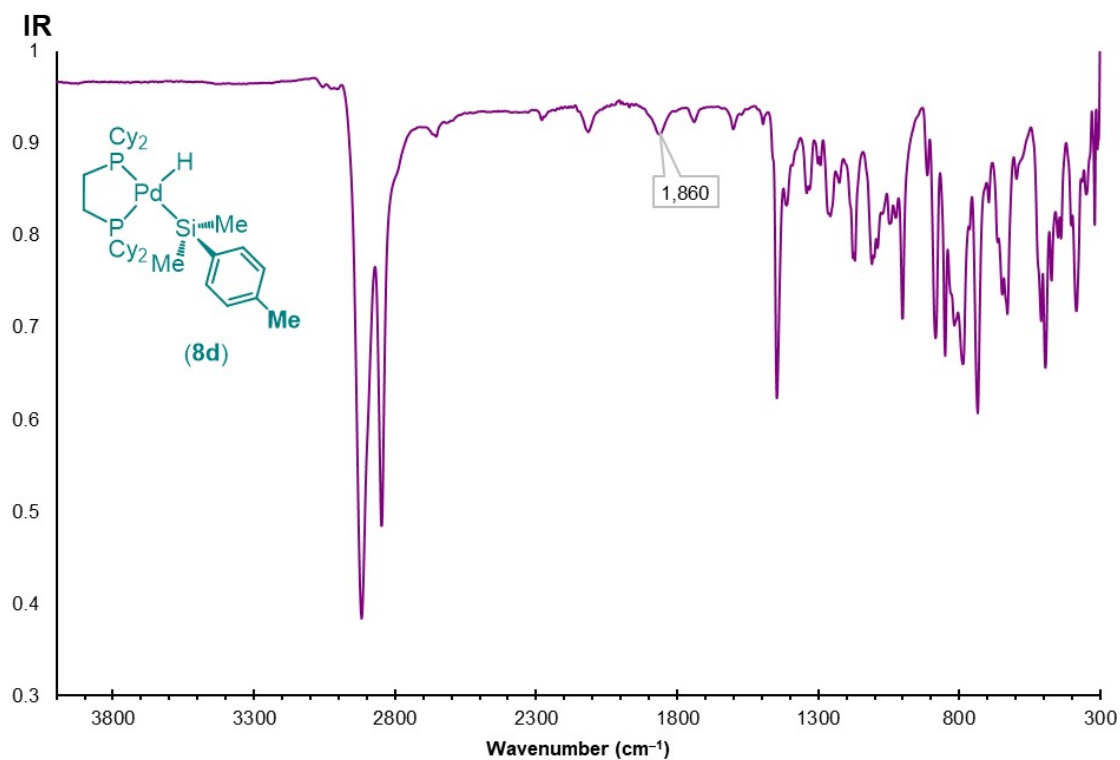


Figure S176. <sup>13</sup>C{<sup>1</sup>H} NMR spectrum of **8d** recorded in C<sub>7</sub>D<sub>8</sub> at 233 K.



**Figure S177.**  $^{31}\text{P}\{^1\text{H}\}$  NMR spectrum of **8d** recorded in  $\text{C}_6\text{D}_6$  at 281 K.



**Figure S178.** IR spectrum of **8d** recorded neat at room temperature.

(dcpe)Pd(H)(SiPhMe<sub>2</sub>) (**8a**)

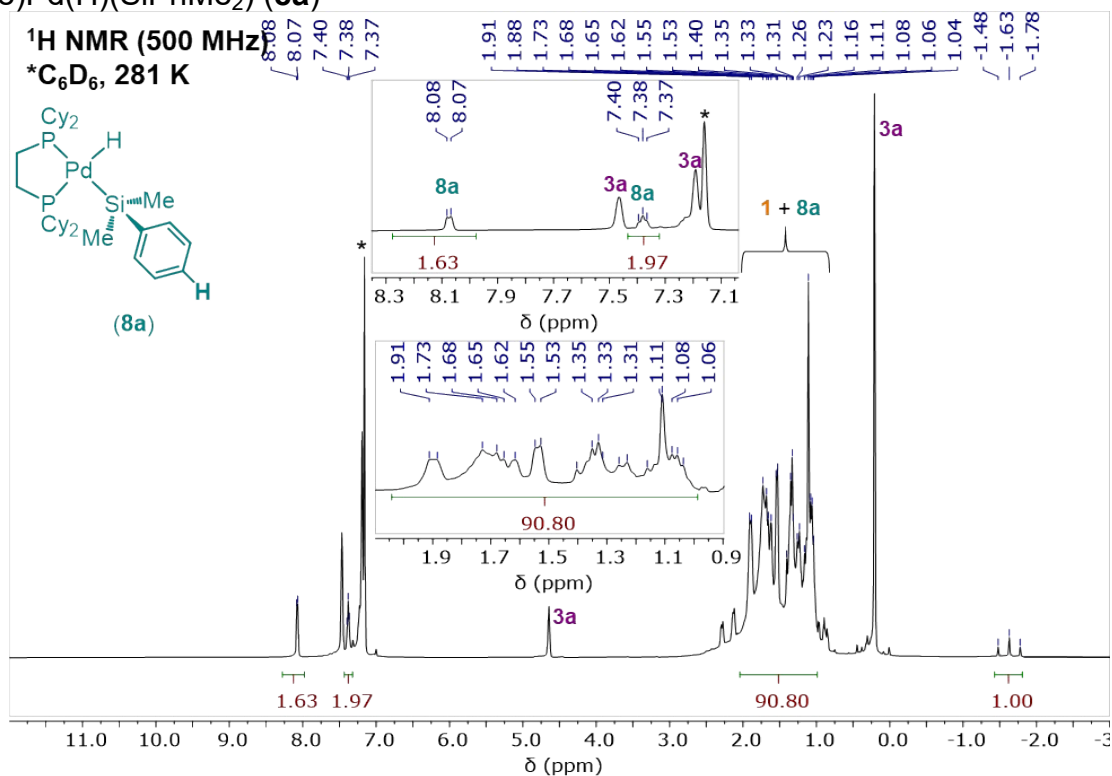


**Figure S179.** <sup>1</sup>H NMR spectrum of **8a** recorded in C<sub>6</sub>D<sub>6</sub> at 281 K.

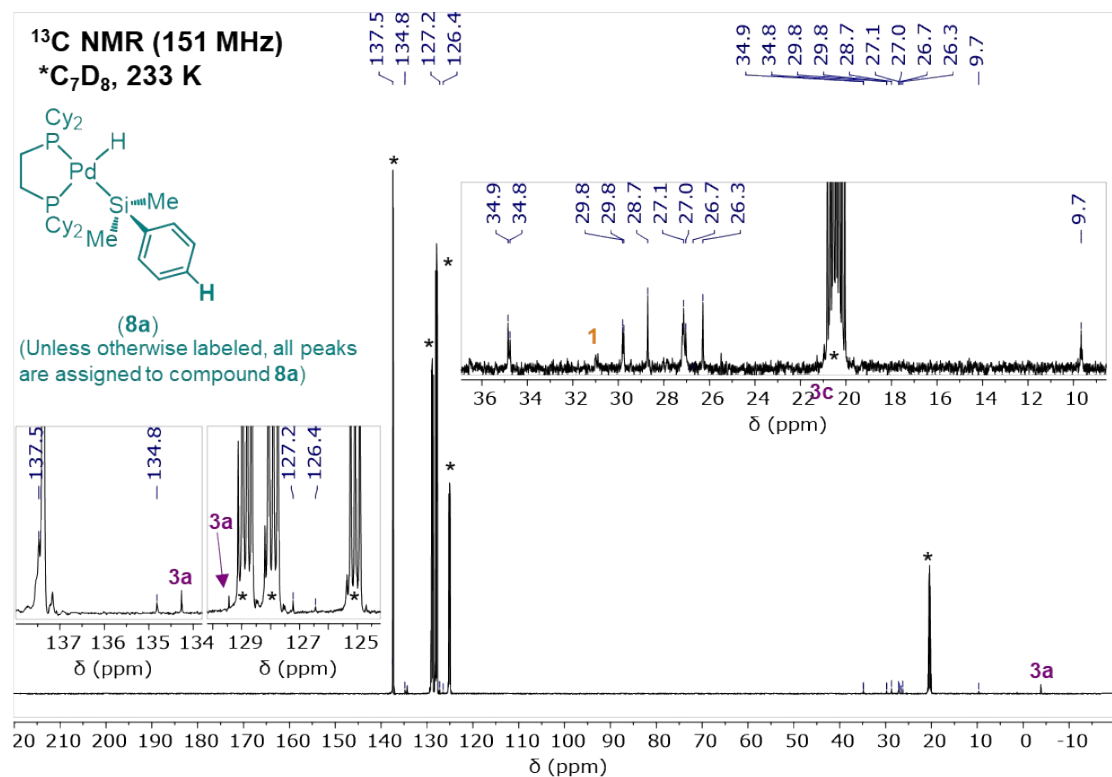


**Figure S180.** <sup>13</sup>C{<sup>1</sup>H} NMR spectrum of **8a** recorded in C<sub>7</sub>D<sub>8</sub> at 233 K.

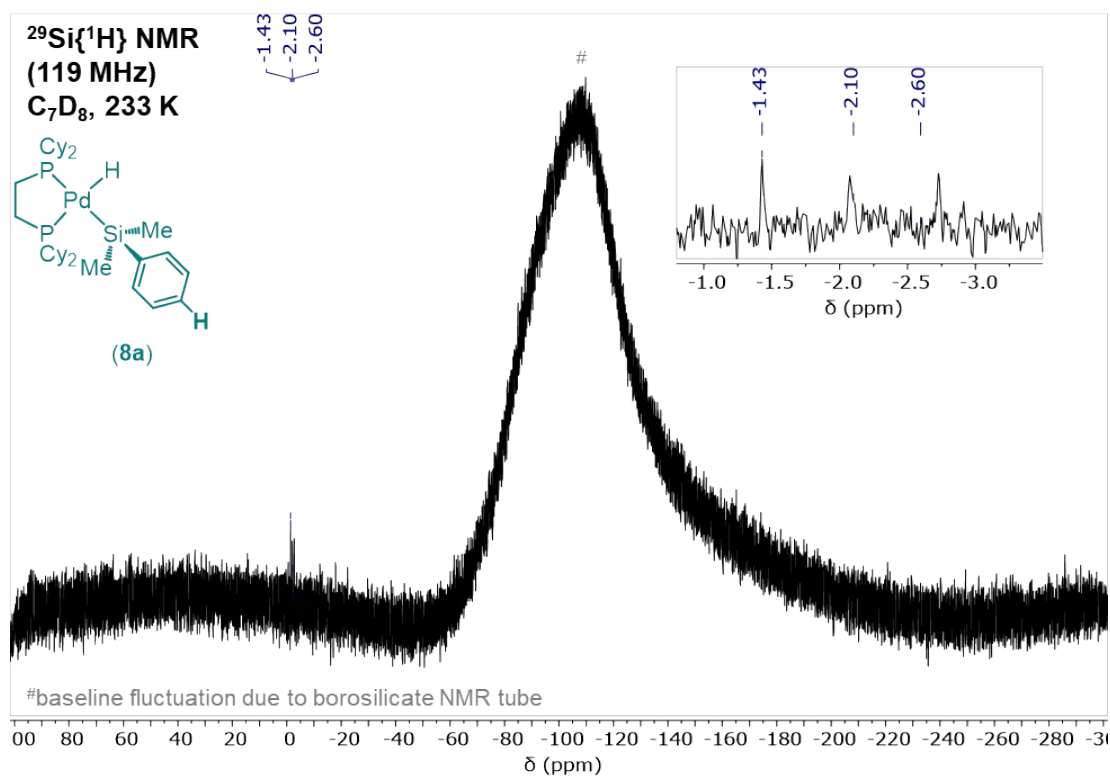


**Figure S181.**  $^{29}\text{Si}\{^1\text{H}\}$  NMR spectrum of **8a** recorded in  $\text{C}_7\text{D}_8$  at 233 K.

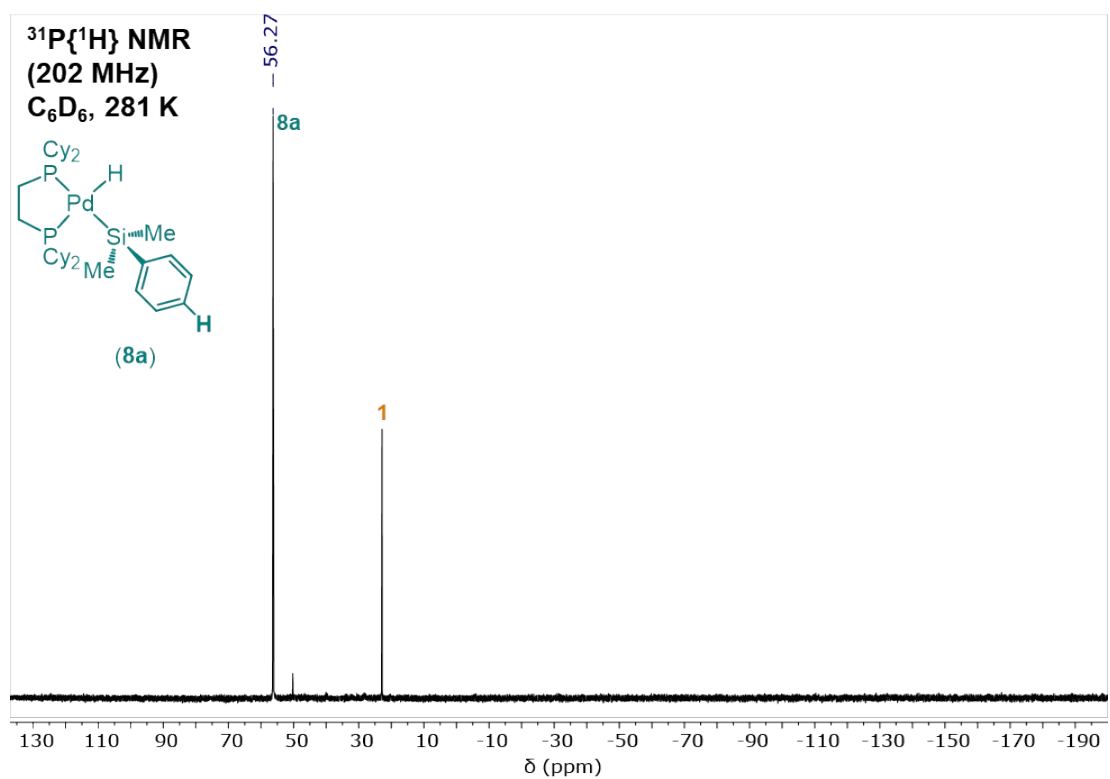


**Figure S182.**  $^{31}\text{P}\{^1\text{H}\}$  NMR spectrum of **8a** recorded in  $\text{C}_6\text{D}_6$  at 281 K.

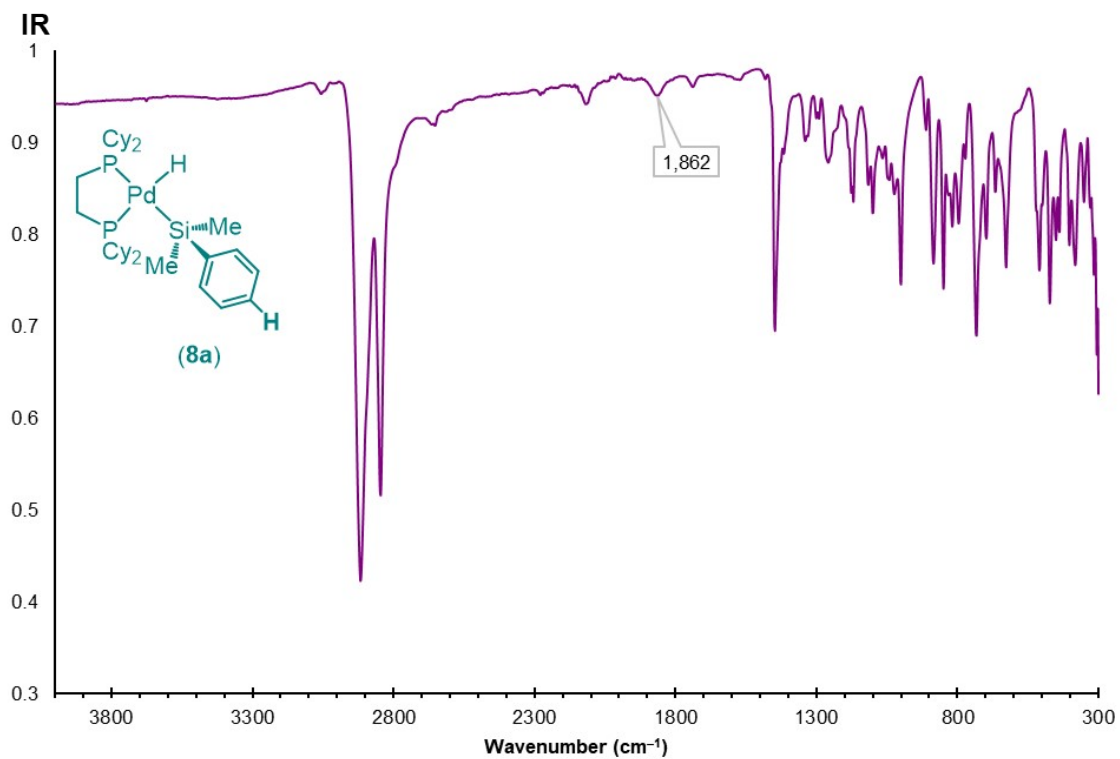


**Figure S183.** IR spectrum of **8a** recorded neat at room temperature.

(dcpe)Pd(D)(SiPhMe<sub>2</sub>) (**8a-d<sub>1</sub>**)

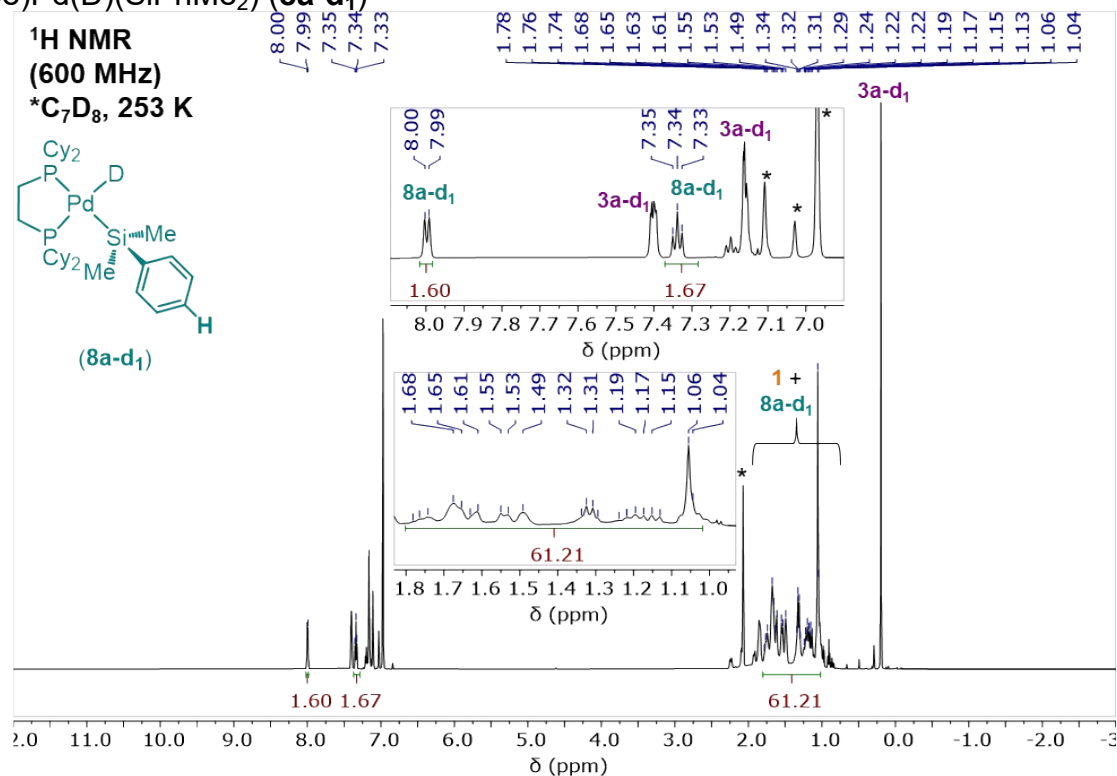


**Figure S184.** <sup>1</sup>H NMR spectrum of **8a-d<sub>1</sub>** recorded in C<sub>7</sub>D<sub>8</sub> at 253 K.

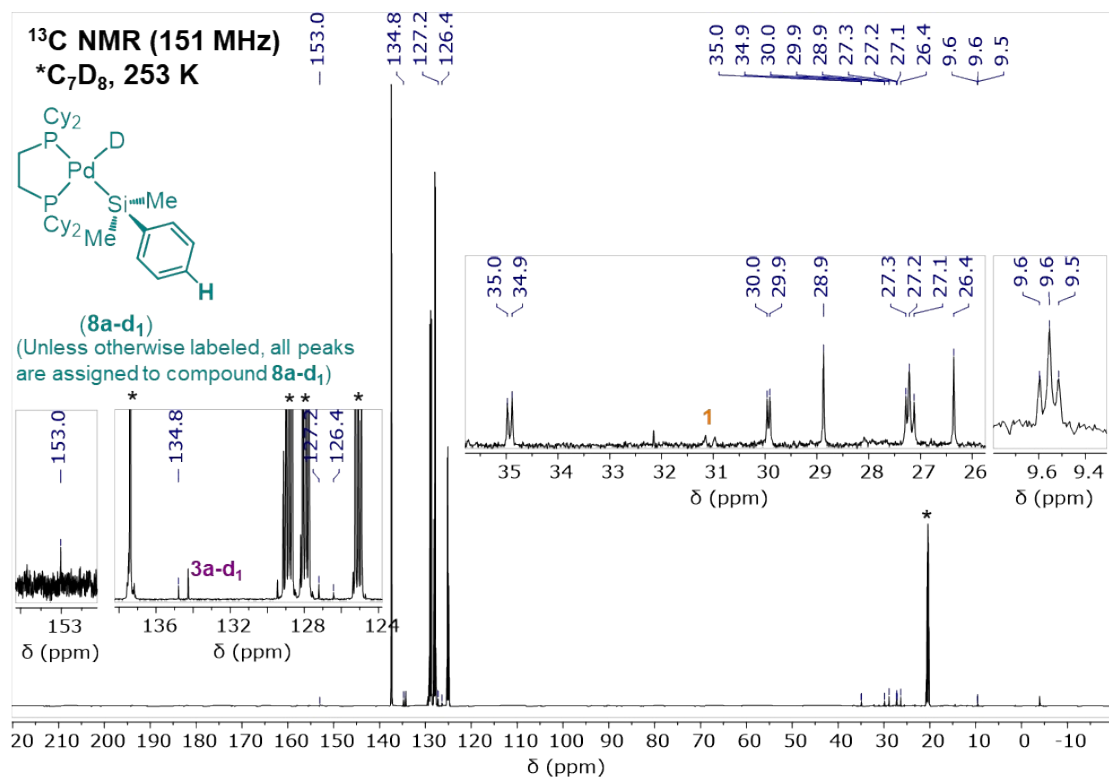


**Figure S185.** <sup>13</sup>C{<sup>1</sup>H} NMR spectrum of **8a-d<sub>1</sub>** recorded in C<sub>7</sub>D<sub>8</sub> at 253 K.

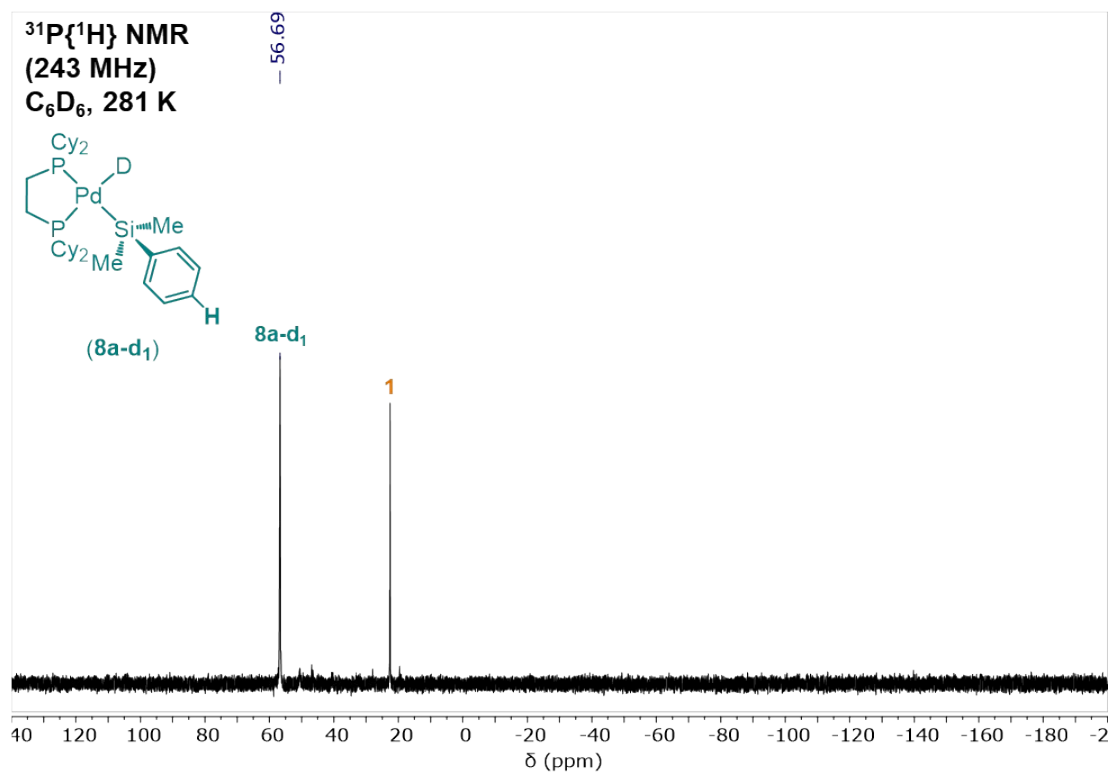


**Figure S186.**  $^{31}\text{P}\{^1\text{H}\}$  NMR spectrum of **8a-d<sub>1</sub>** recorded in  $\text{C}_6\text{D}_6$  at 281 K.

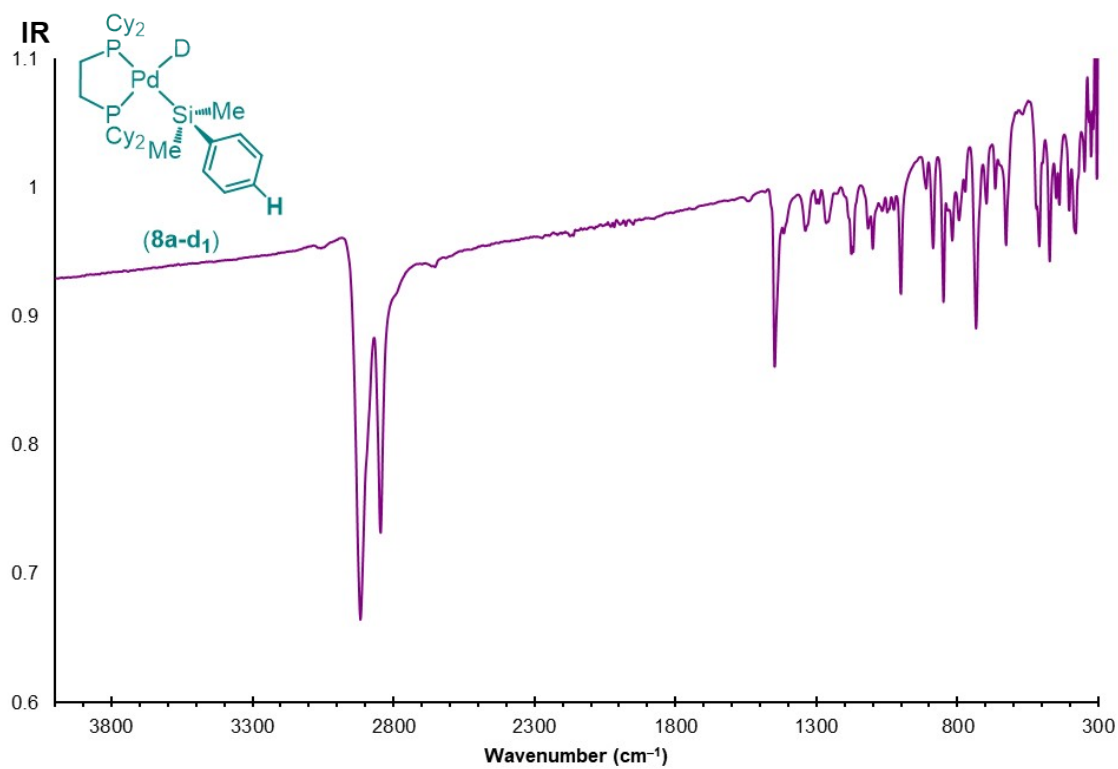


**Figure S187.** IR spectrum of **8a-d<sub>1</sub>** recorded neat at room temperature.

(dcpe)Pd(H)[Si(4-F-Ph)Me<sub>2</sub>] (**8e**)

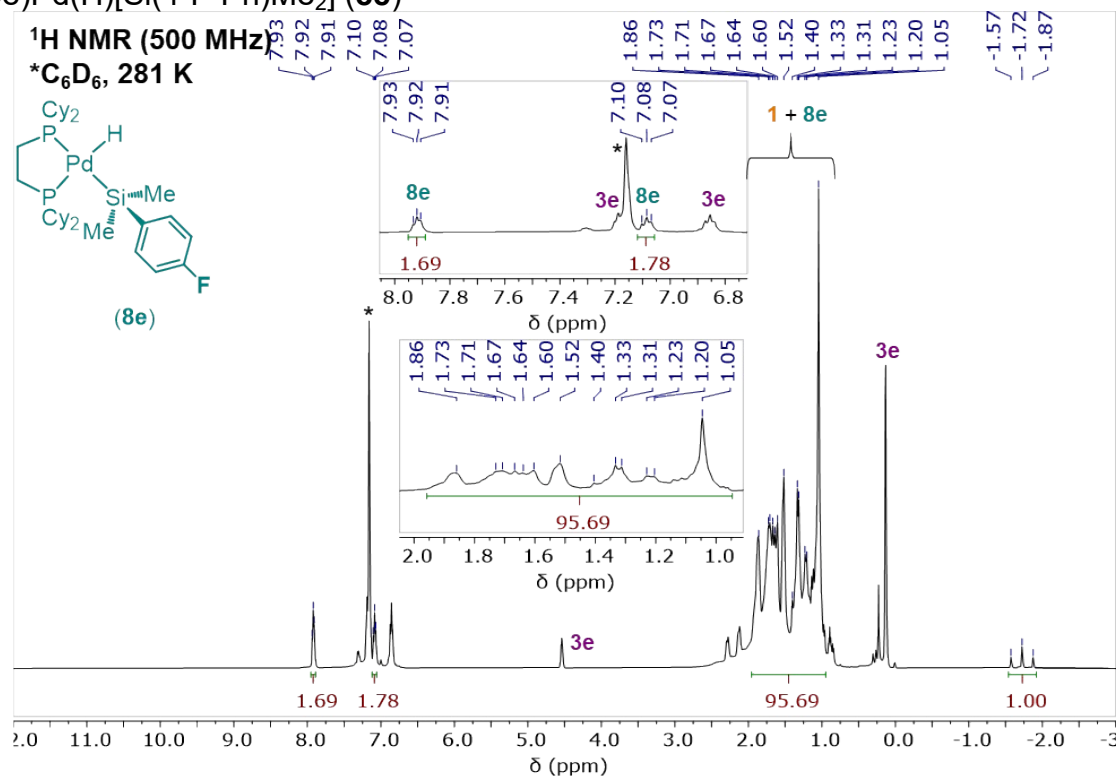


**Figure S188.**  $^1\text{H}$  NMR spectrum of **8e** recorded in  $\text{C}_6\text{D}_6$  at 281 K.

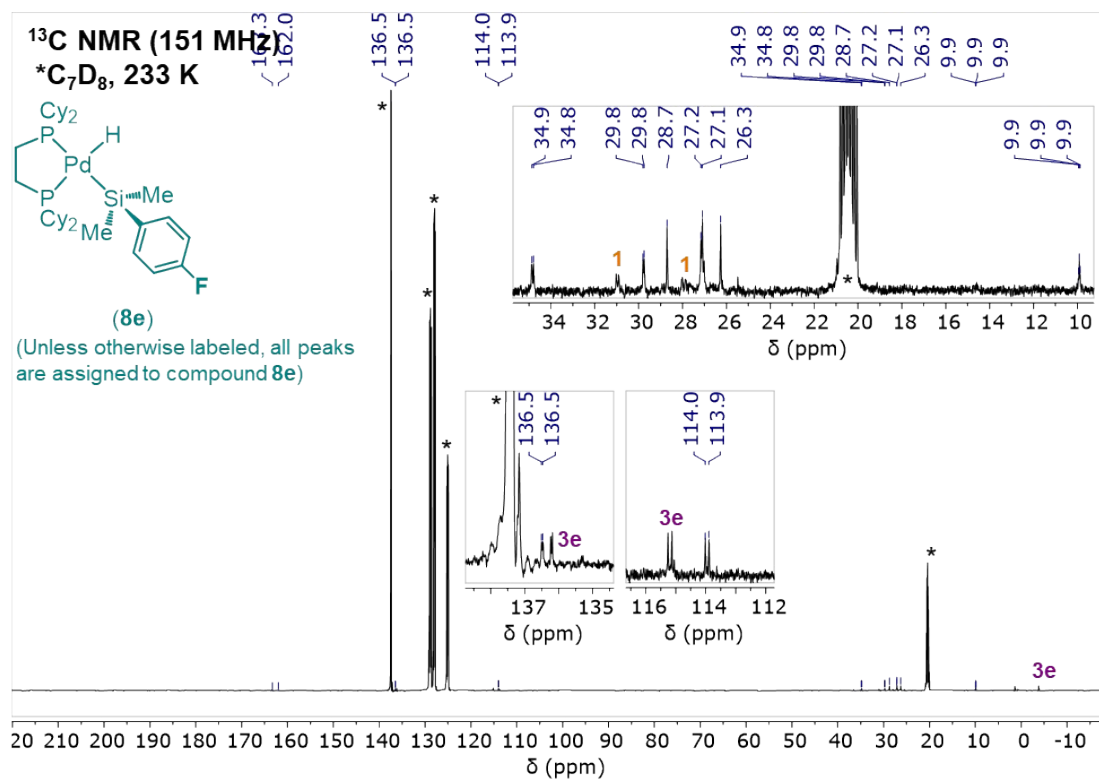


**Figure S189.**  $^{13}\text{C}\{^1\text{H}\}$  NMR spectrum of **8e** recorded in  $\text{C}_7\text{D}_8$  at 233 K.

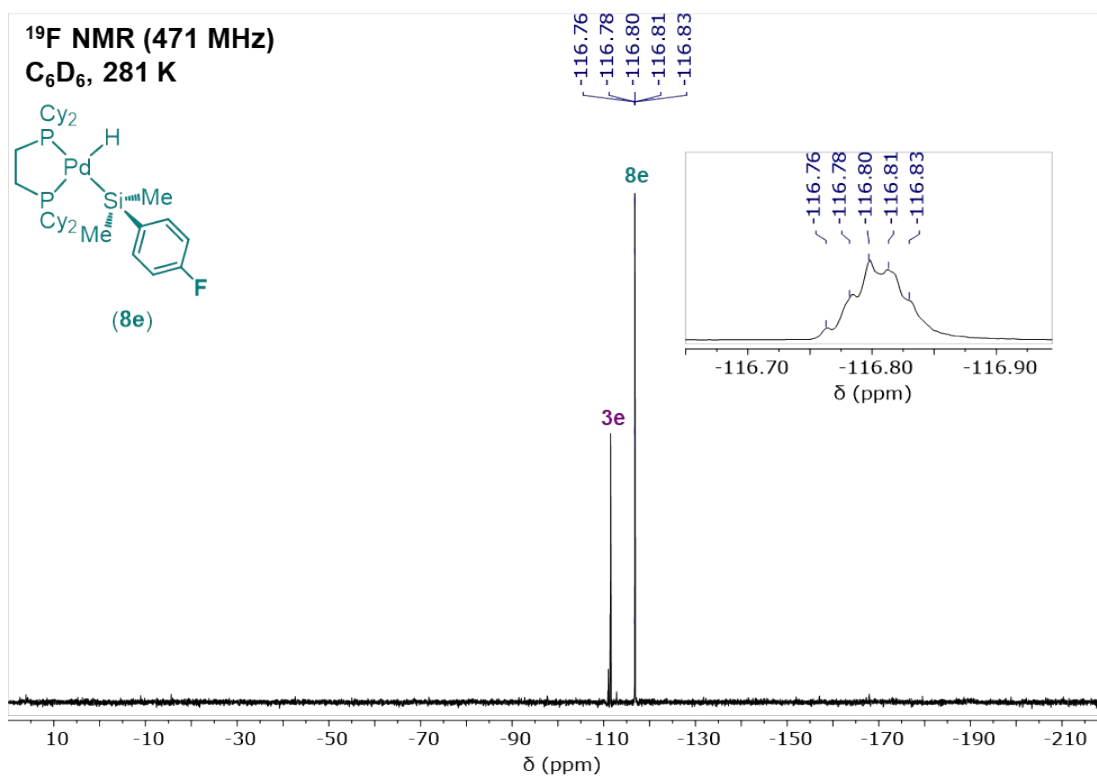


**Figure S190.**  $^{19}\text{F}$  NMR spectrum of **8e** recorded in  $\text{C}_6\text{D}_6$  at 281 K.

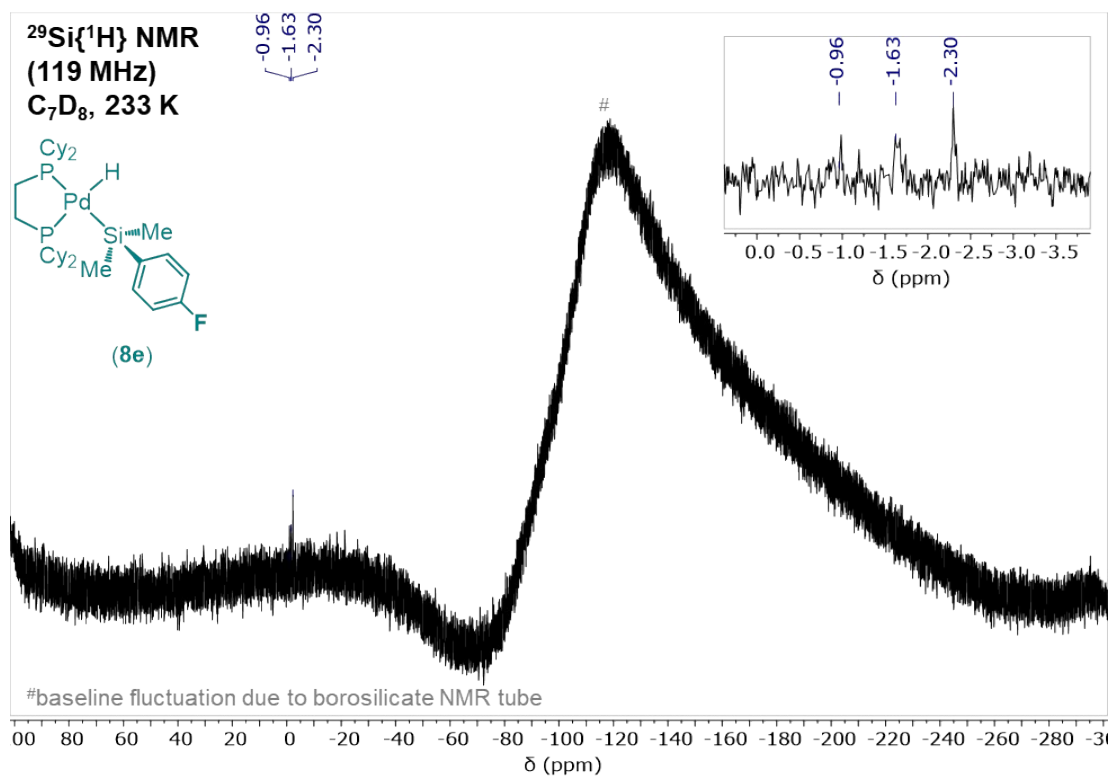


**Figure S191.**  $^{29}\text{Si}\{^1\text{H}\}$  NMR spectrum of **8e** recorded in  $\text{C}_7\text{D}_8$  at 233 K.

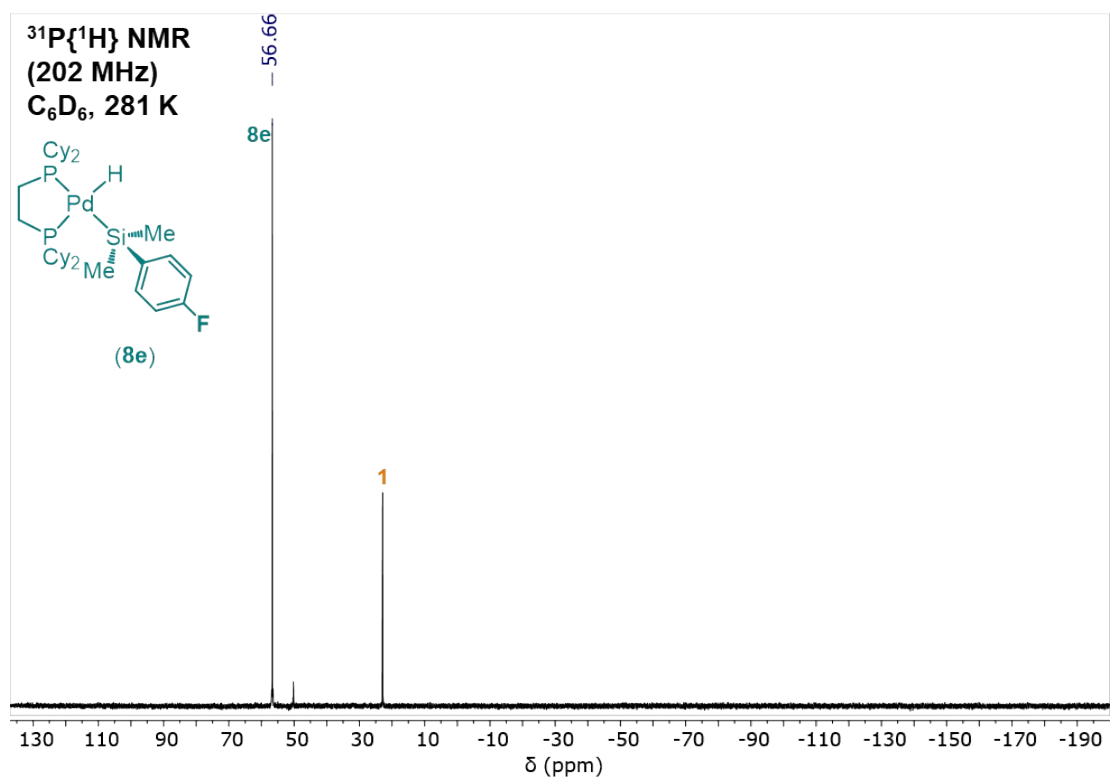


**Figure S192.**  $^{31}\text{P}\{^1\text{H}\}$  NMR spectrum of **8e** recorded in  $\text{C}_6\text{D}_6$  at 281 K.

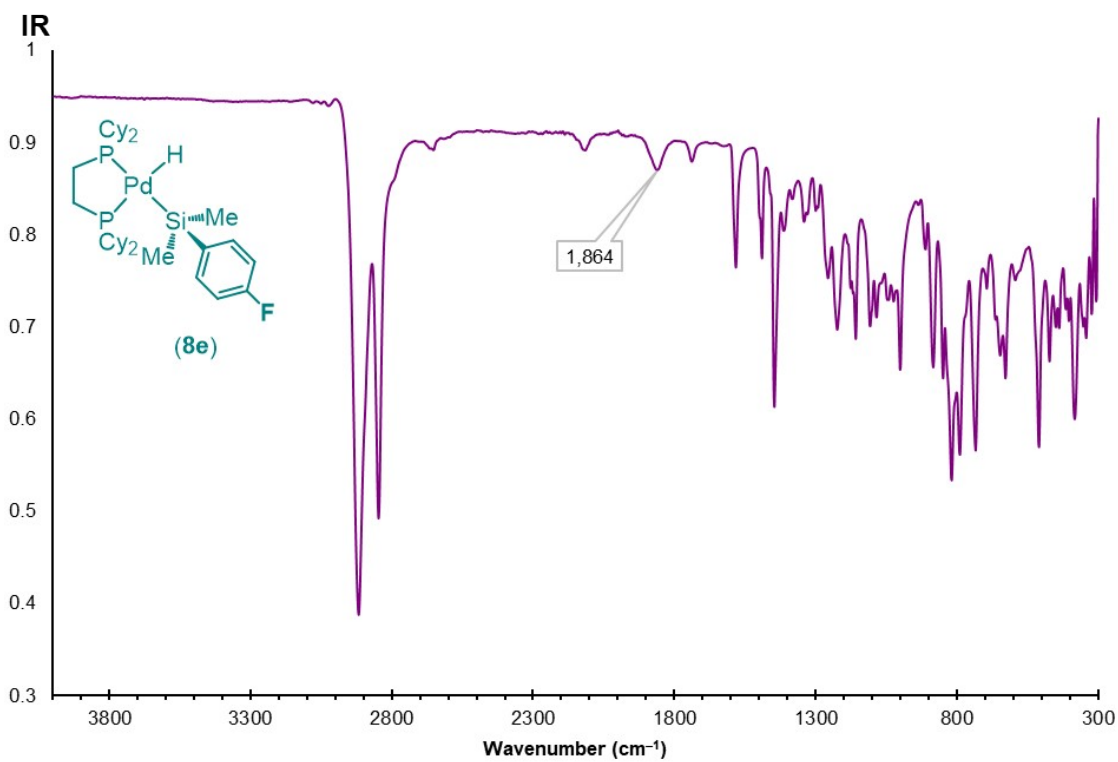


**Figure S193.** IR spectrum of **8e** recorded neat at room temperature.

(dcpe)Pd(H)[Si(4-CF<sub>3</sub>-Ph)Me<sub>2</sub>] (**8f**)

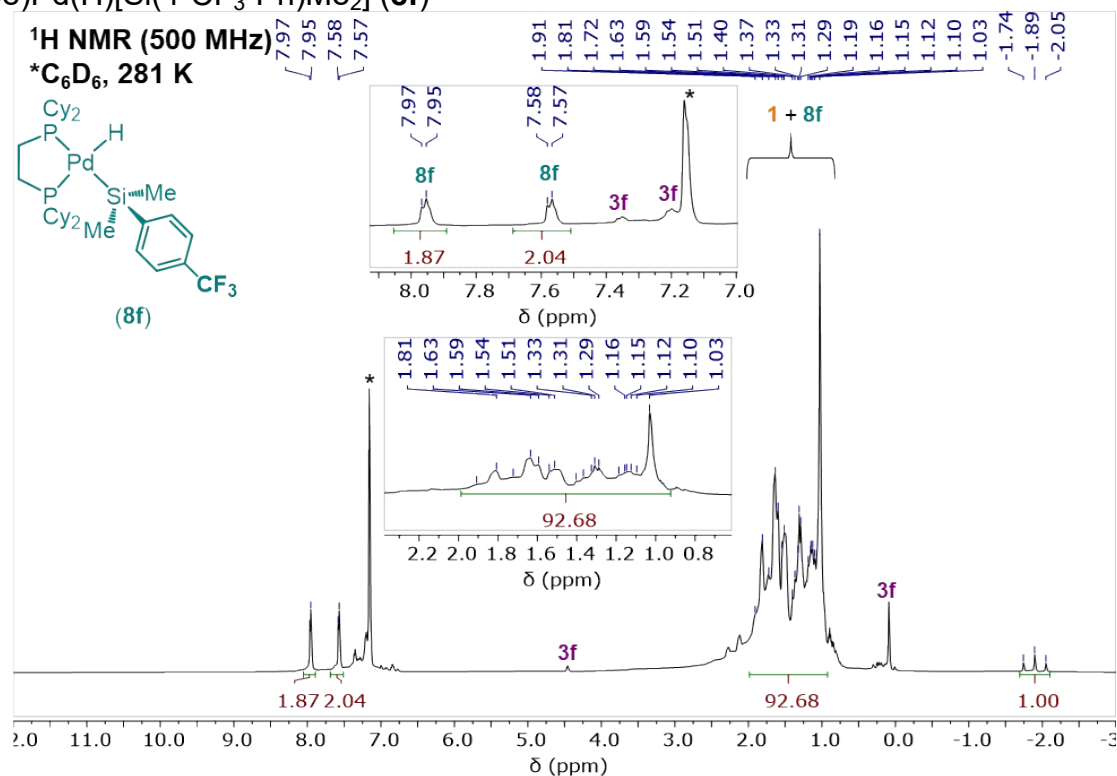


Figure S194. <sup>1</sup>H NMR spectrum of **8f** recorded in C<sub>6</sub>D<sub>6</sub> at 281 K.

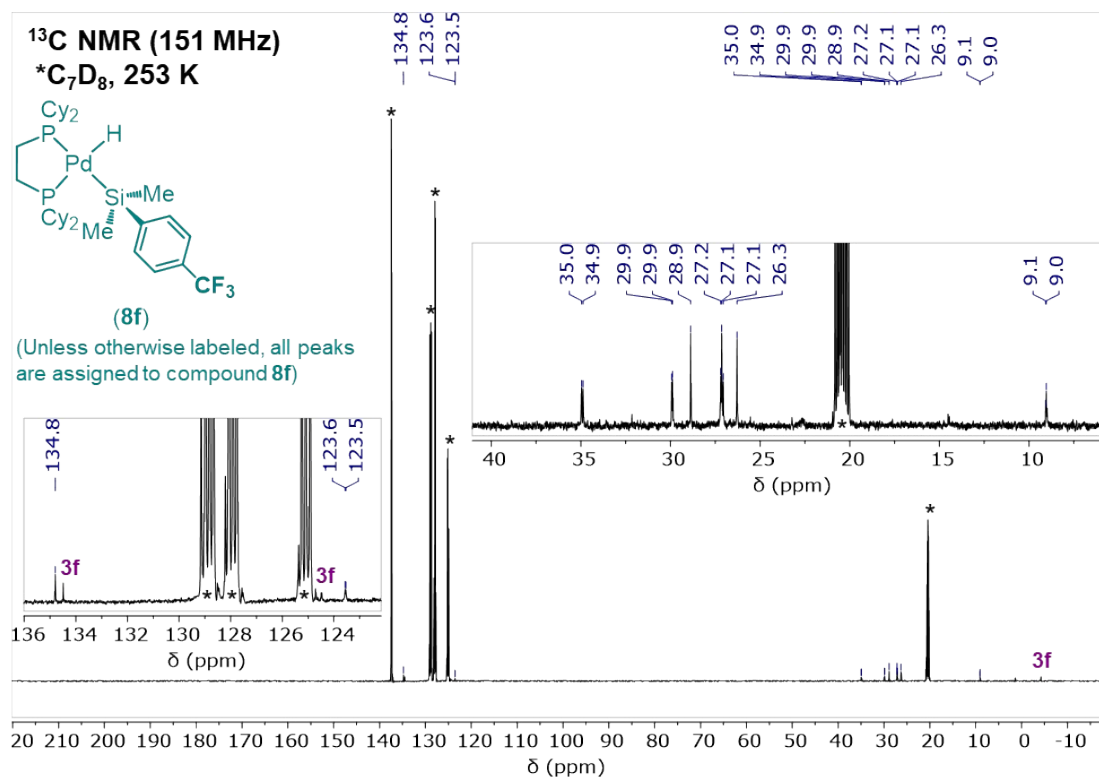
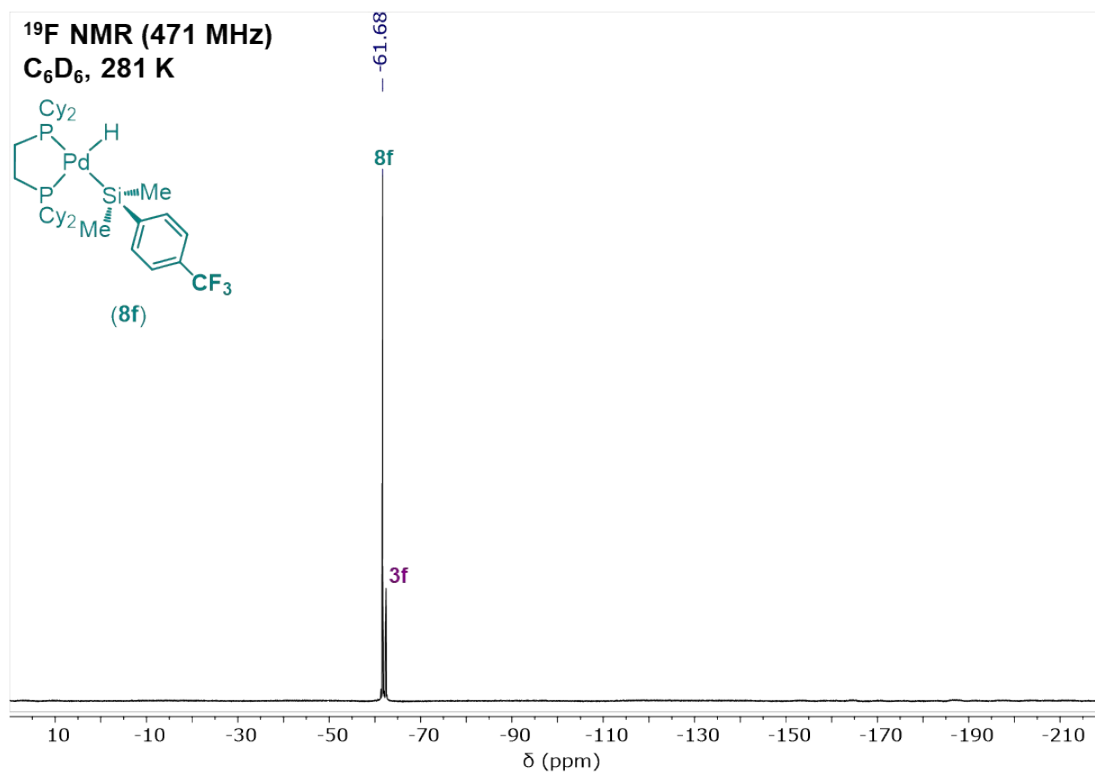
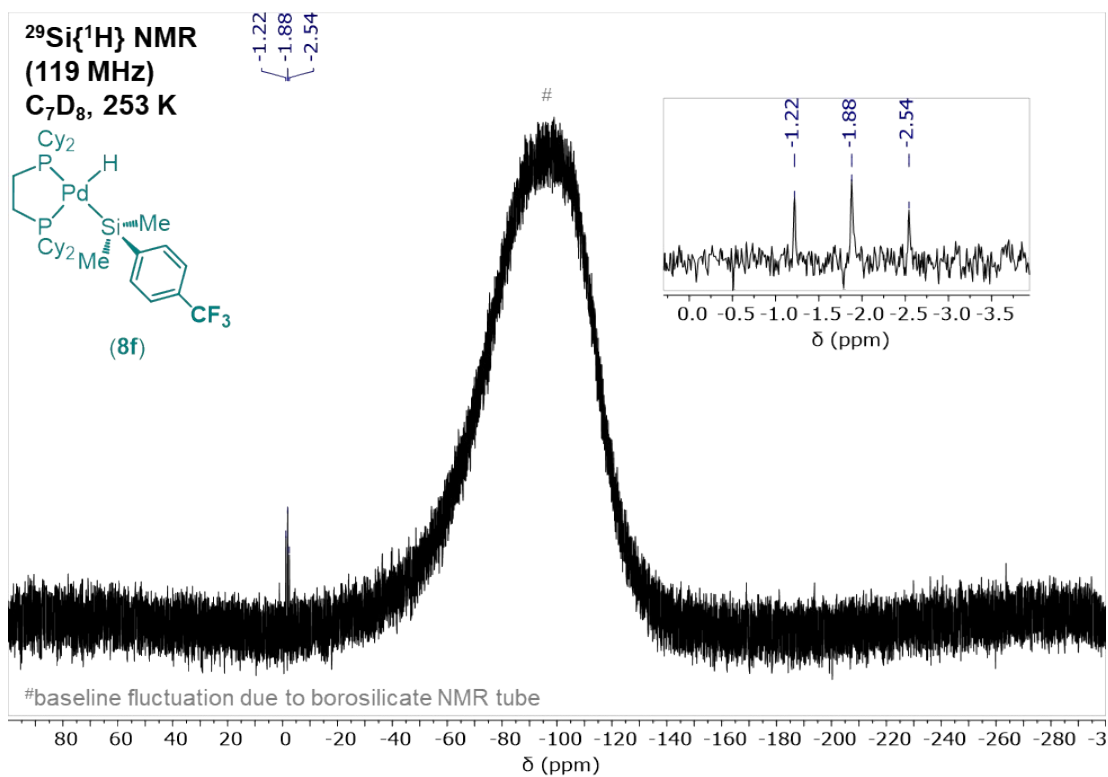


Figure S195. <sup>13</sup>C{<sup>1</sup>H} NMR spectrum of **8f** recorded in C<sub>7</sub>D<sub>8</sub> at 253 K.



**Figure S196.**  $^{19}\text{F}$  NMR spectrum of **8f** recorded in  $\text{C}_6\text{D}_6$  at 281 K.



**Figure S197.**  $^{29}\text{Si}\{^1\text{H}\}$  NMR spectrum of **8f** recorded in  $\text{C}_7\text{D}_8$  at 253 K.

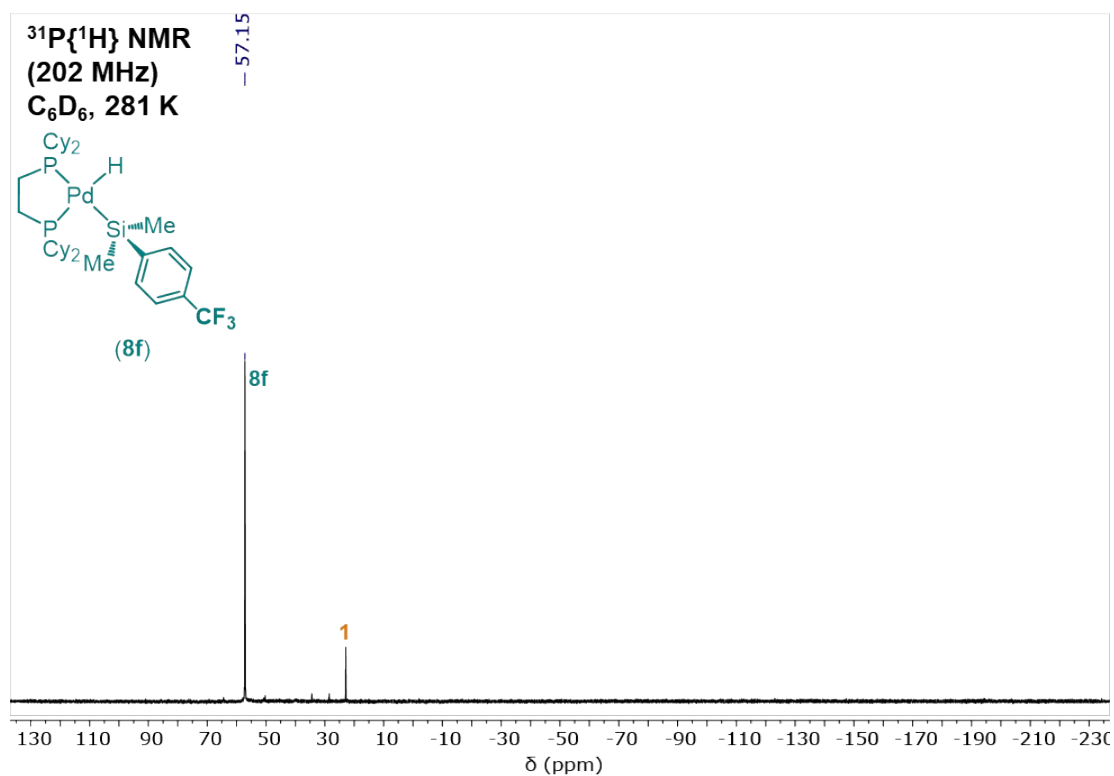


**Figure S198.**  $^{31}\text{P}\{^1\text{H}\}$  NMR spectrum of **8f** recorded in  $\text{C}_6\text{D}_6$  at 281 K.

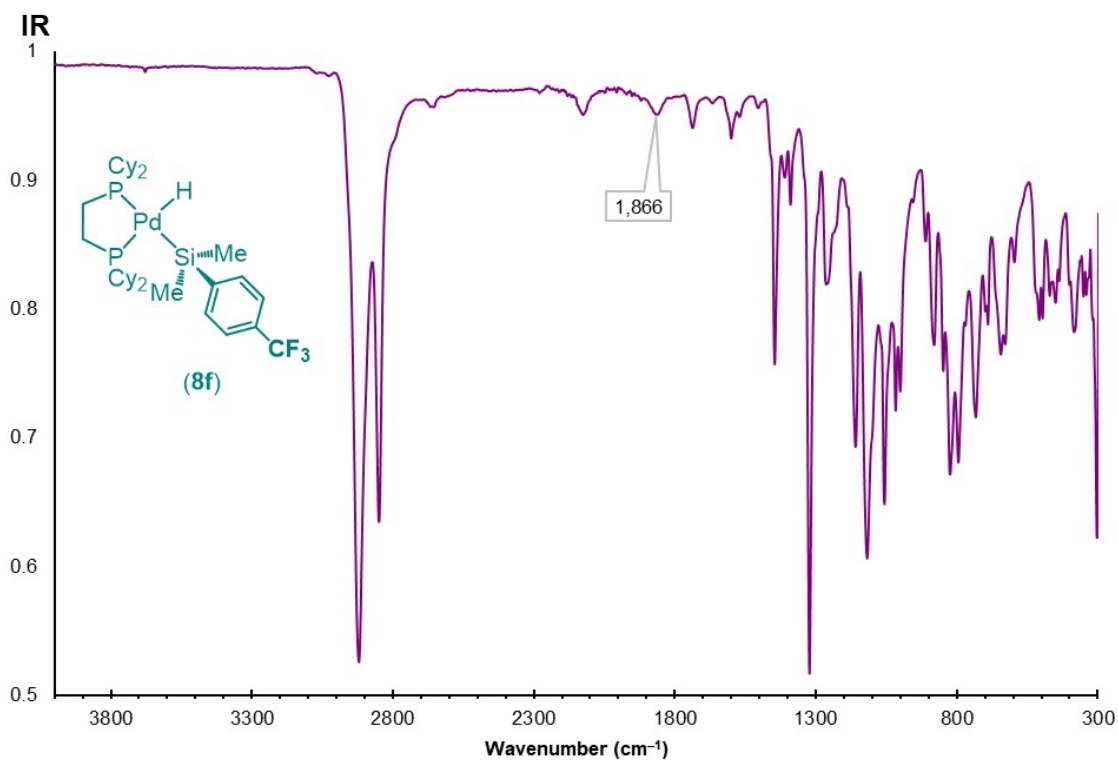


**Figure S199.** IR spectrum of **8f** recorded neat at room temperature.

(dcpe)Pd(H)(SiPh<sub>2</sub>Me) (**9**)

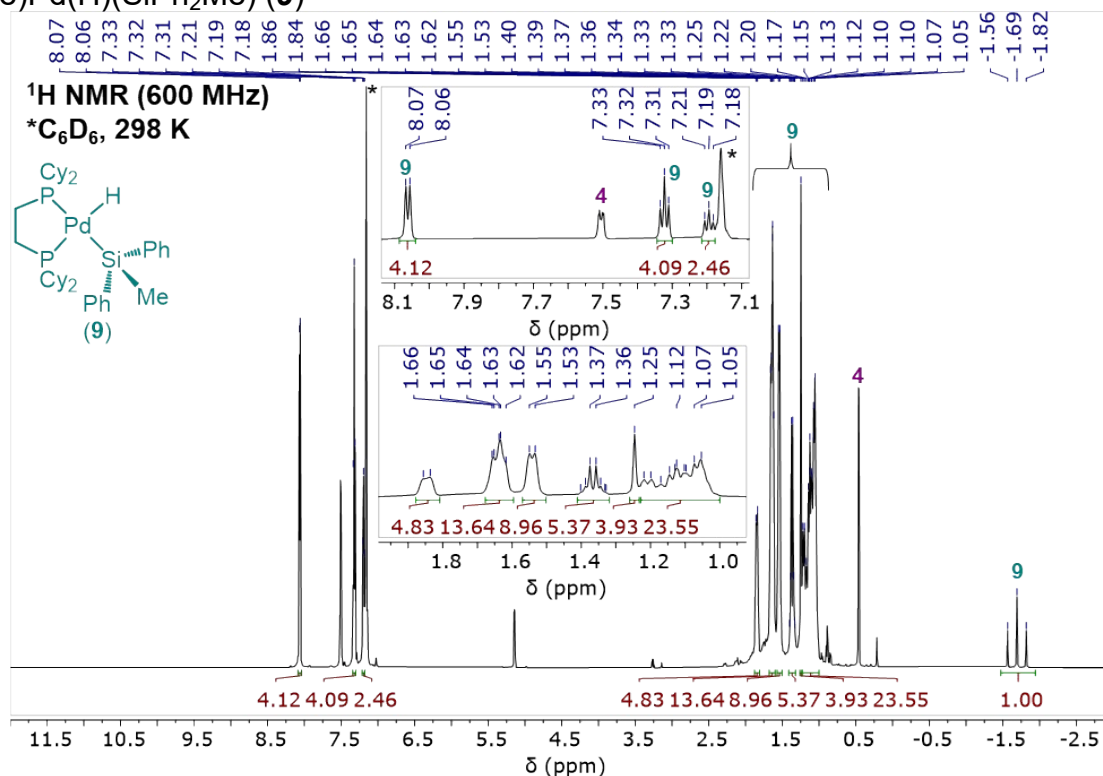


Figure S200. <sup>1</sup>H NMR spectrum of **9** recorded in C<sub>6</sub>D<sub>6</sub> at 298 K.

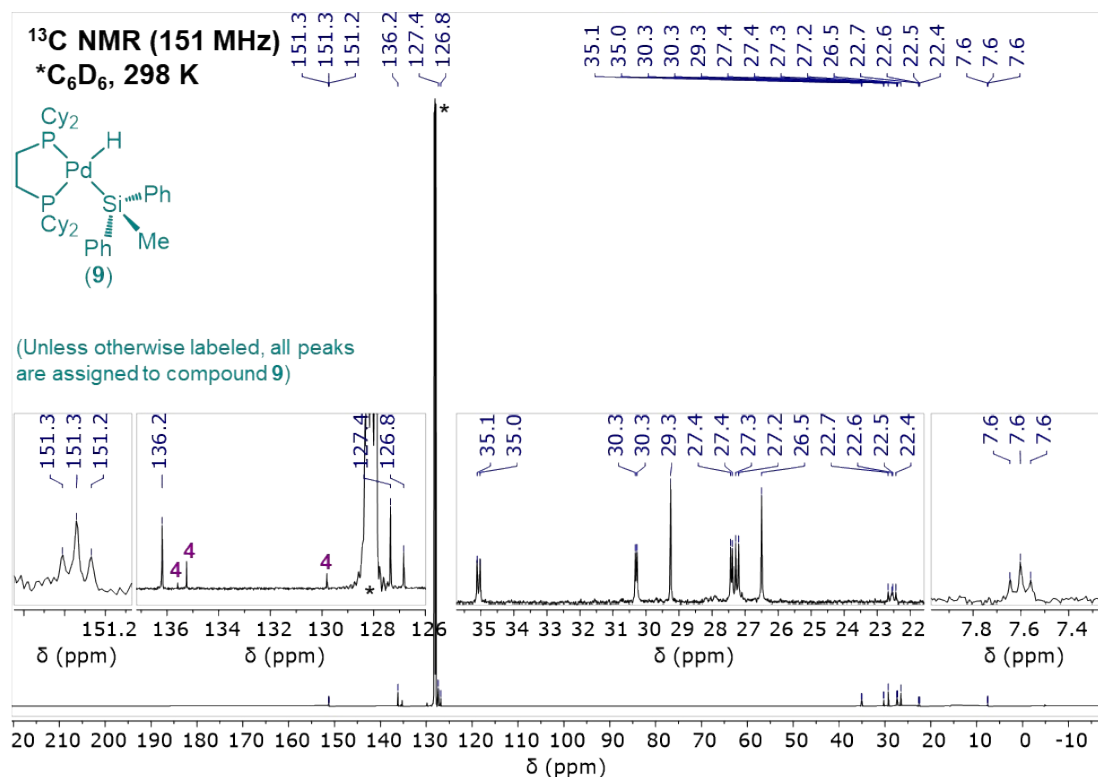
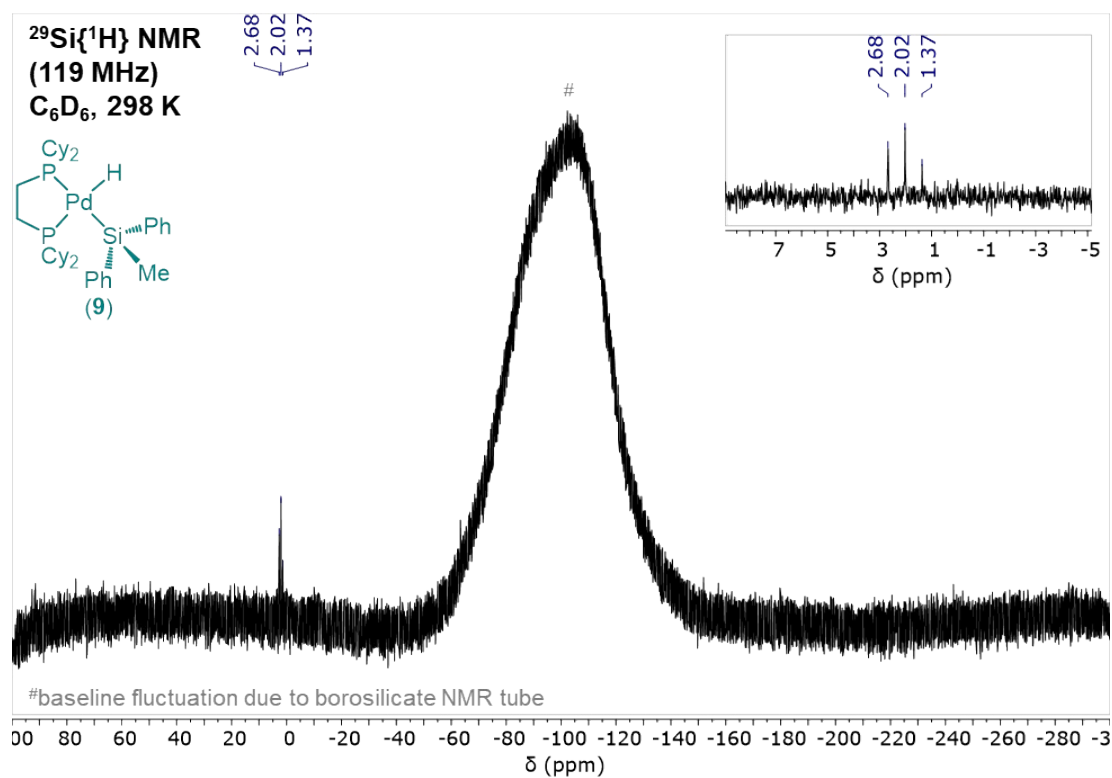
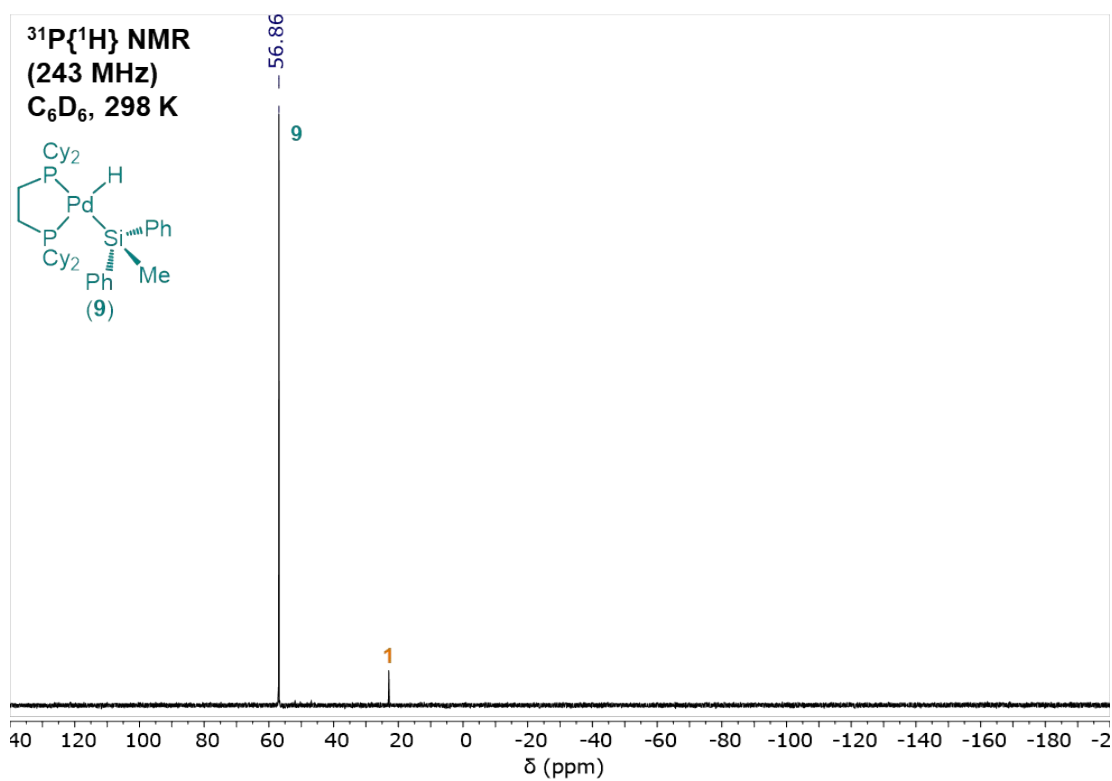


Figure S201. <sup>13</sup>C{<sup>1</sup>H} NMR spectrum of **9** recorded in C<sub>6</sub>D<sub>6</sub> at 298 K.



**Figure S202.**  $^{29}\text{Si}\{^1\text{H}\}$  NMR spectrum of **9** recorded in  $\text{C}_6\text{D}_6$  at 298 K.



**Figure S203.**  $^{31}\text{P}\{^1\text{H}\}$  NMR spectrum of **9** recorded in  $\text{C}_6\text{D}_6$  at 298 K.

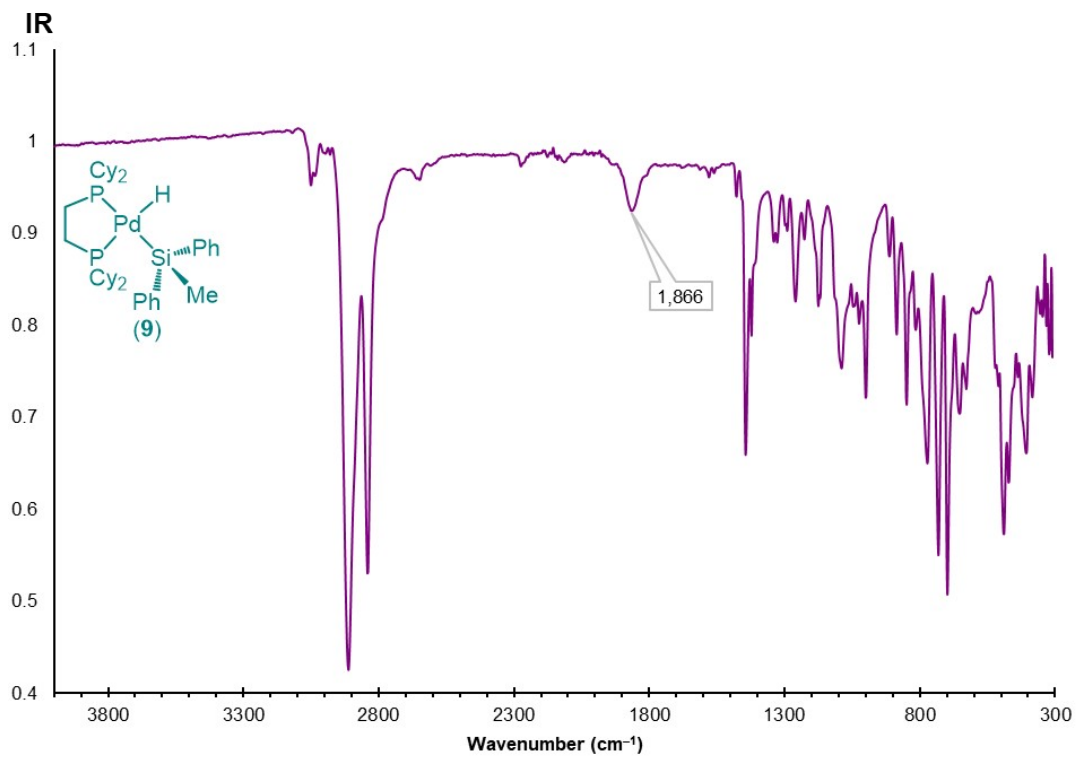


**Figure S204.** IR spectrum of **9** recorded neat at room temperature.

(dcpe)Pd(H)[Si(OEt)<sub>3</sub>] (**11**)

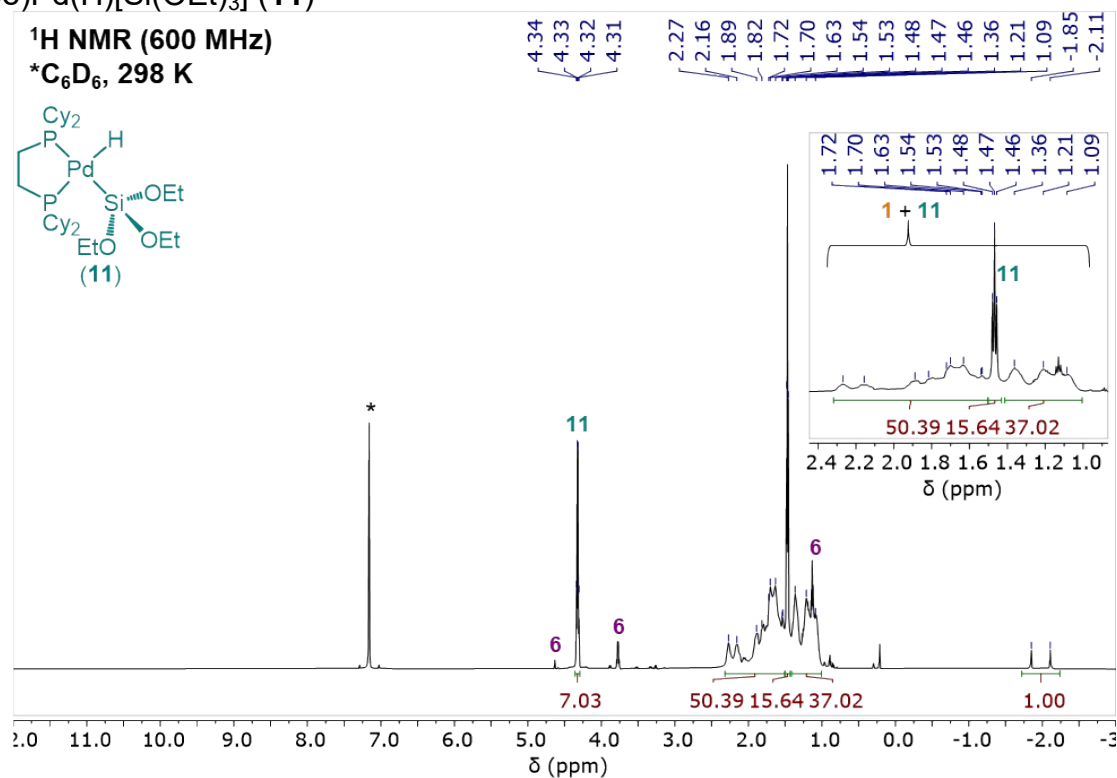


**Figure S205.** <sup>1</sup>H NMR spectrum of **11** recorded in C<sub>6</sub>D<sub>6</sub> at 298 K.

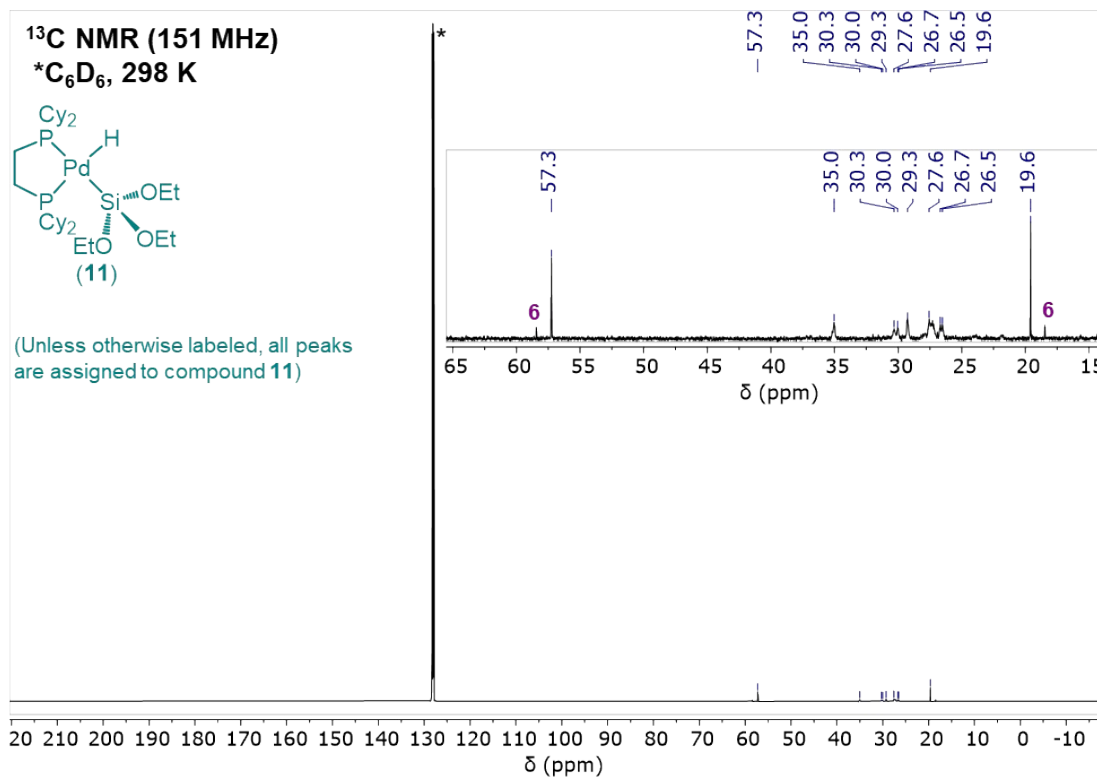


**Figure S206.** <sup>13</sup>C{<sup>1</sup>H} NMR spectrum of **11** recorded in C<sub>6</sub>D<sub>6</sub> at 298 K.

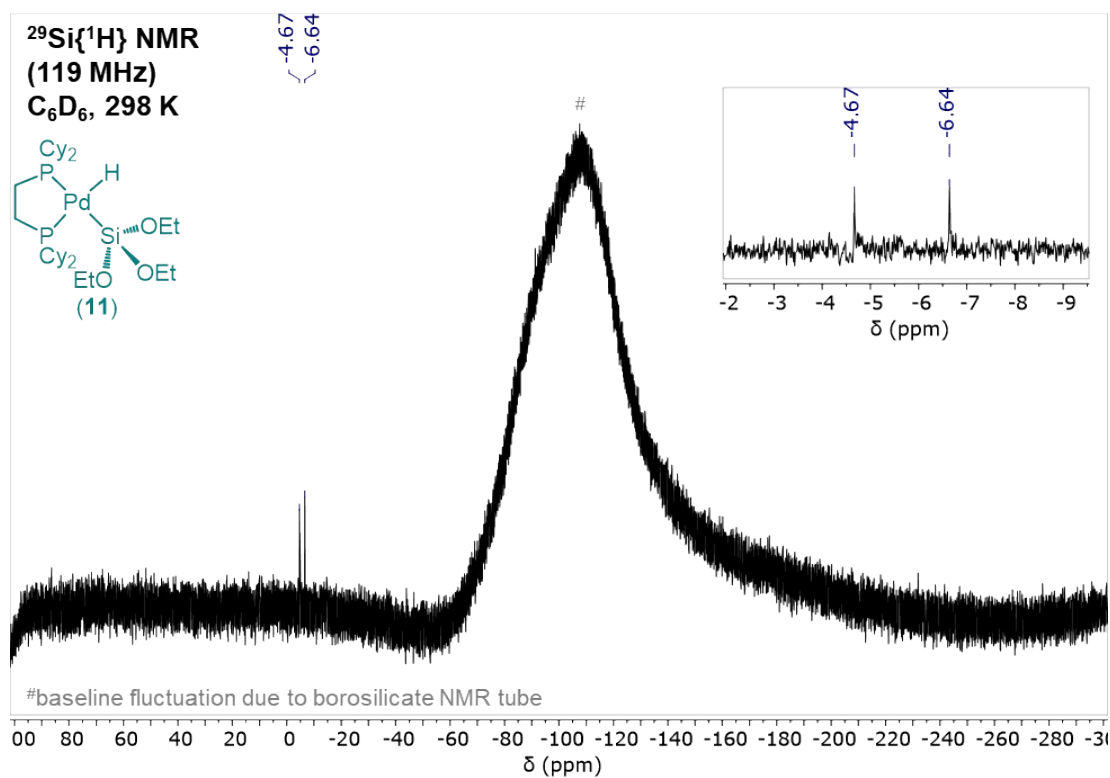


**Figure S207.**  $^{29}\text{Si}\{^1\text{H}\}$  NMR spectrum of **11** recorded in  $\text{C}_6\text{D}_6$  at 298 K.

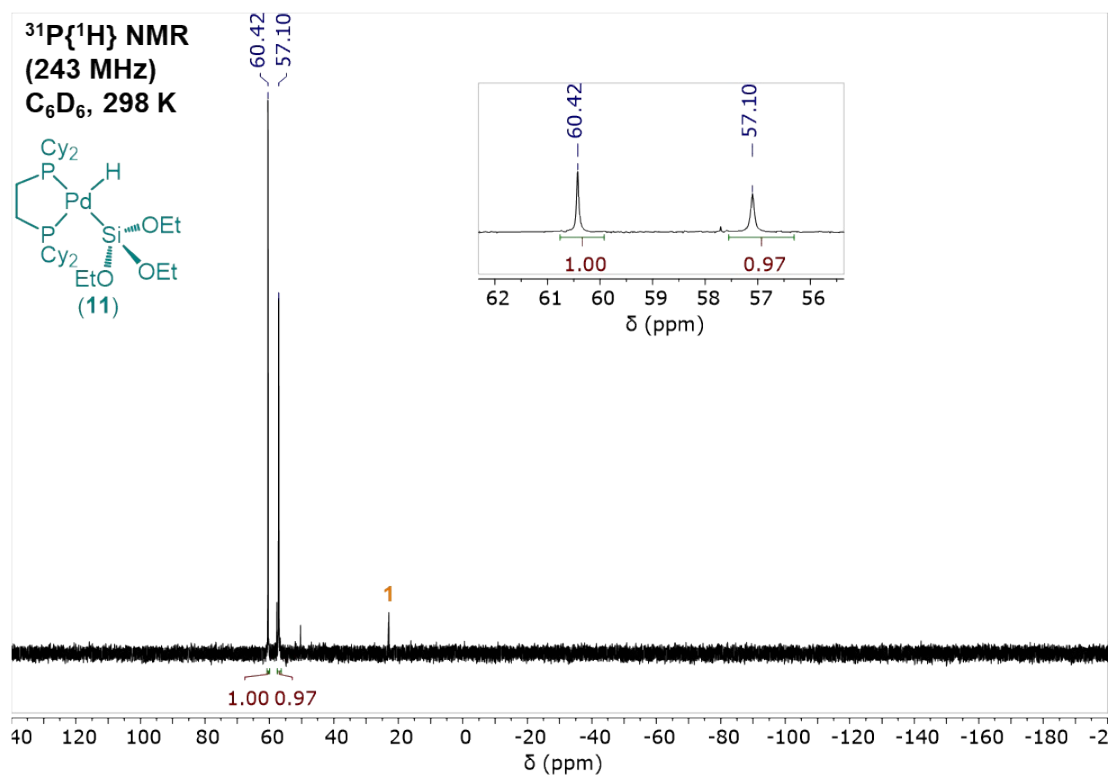


**Figure S208.**  $^{31}\text{P}\{^1\text{H}\}$  NMR spectrum of **11** recorded in  $\text{C}_6\text{D}_6$  at 298 K.

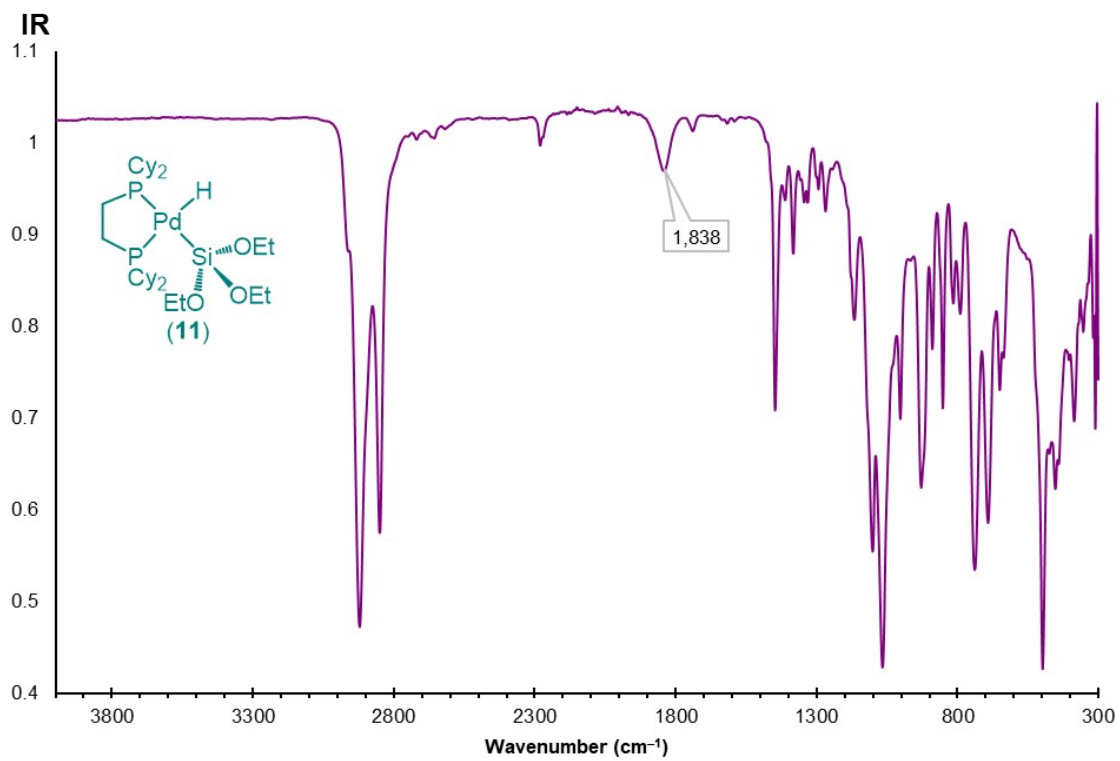


**Figure S209.** IR spectrum of **11** recorded neat at room temperature.

## g. Hydrosilylation Products

(*E*)-1-phenyl-2-[tris(4-methylphenyl)silyl]ethene (**E- $\beta$ -16d**)

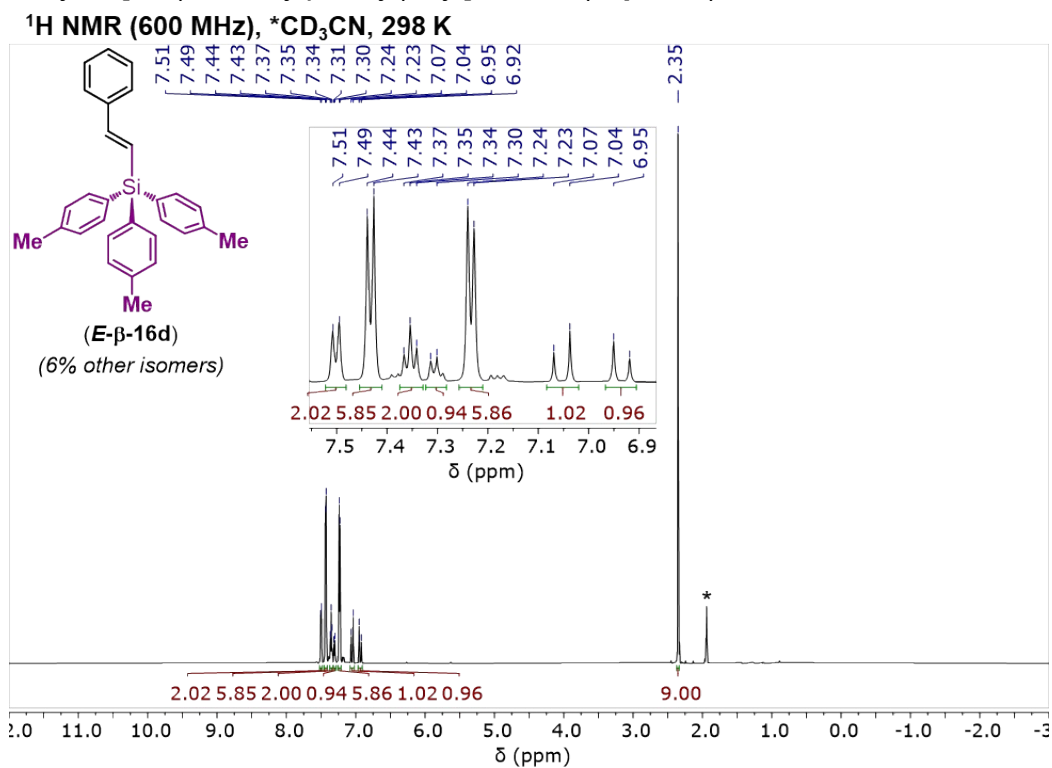


Figure S210. <sup>1</sup>H NMR spectrum of **E- $\beta$ -16d** recorded in CD<sub>3</sub>CN at 298 K.

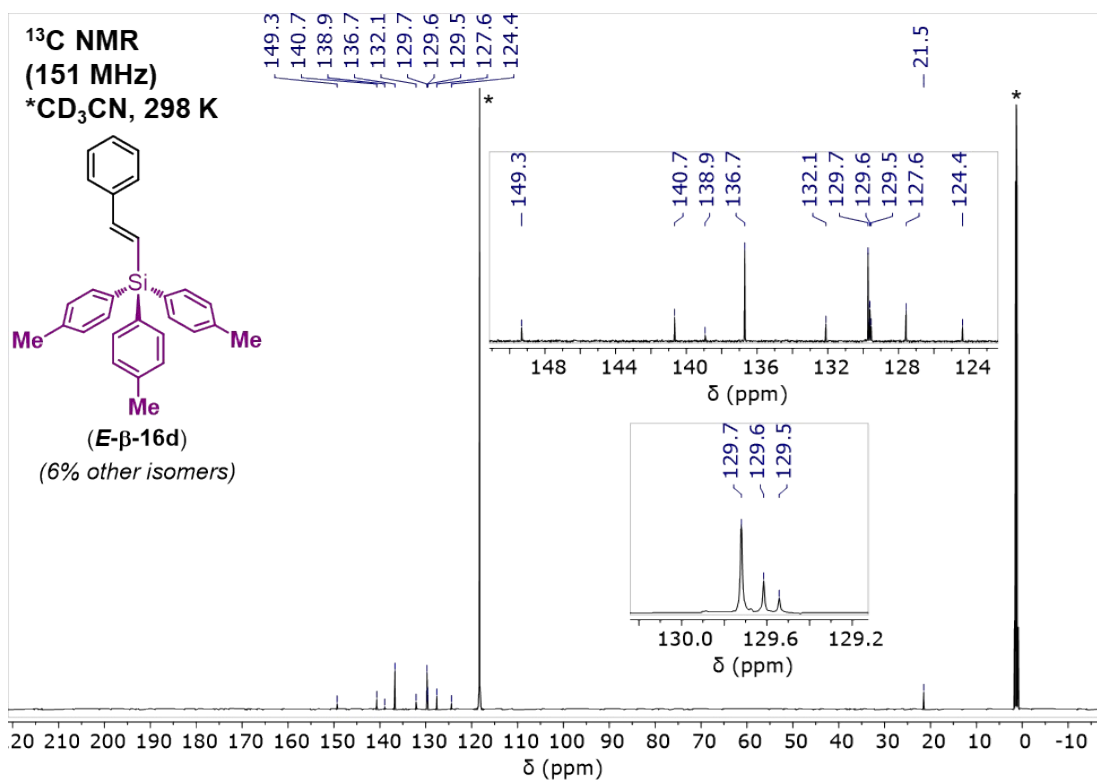
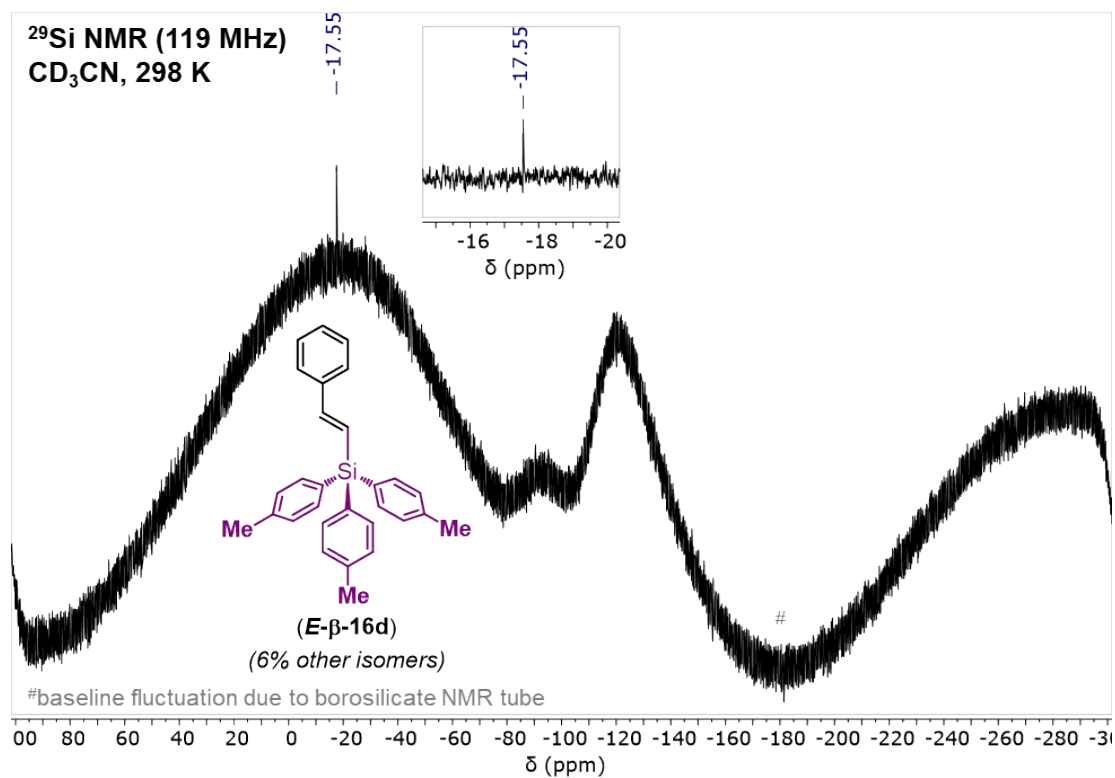
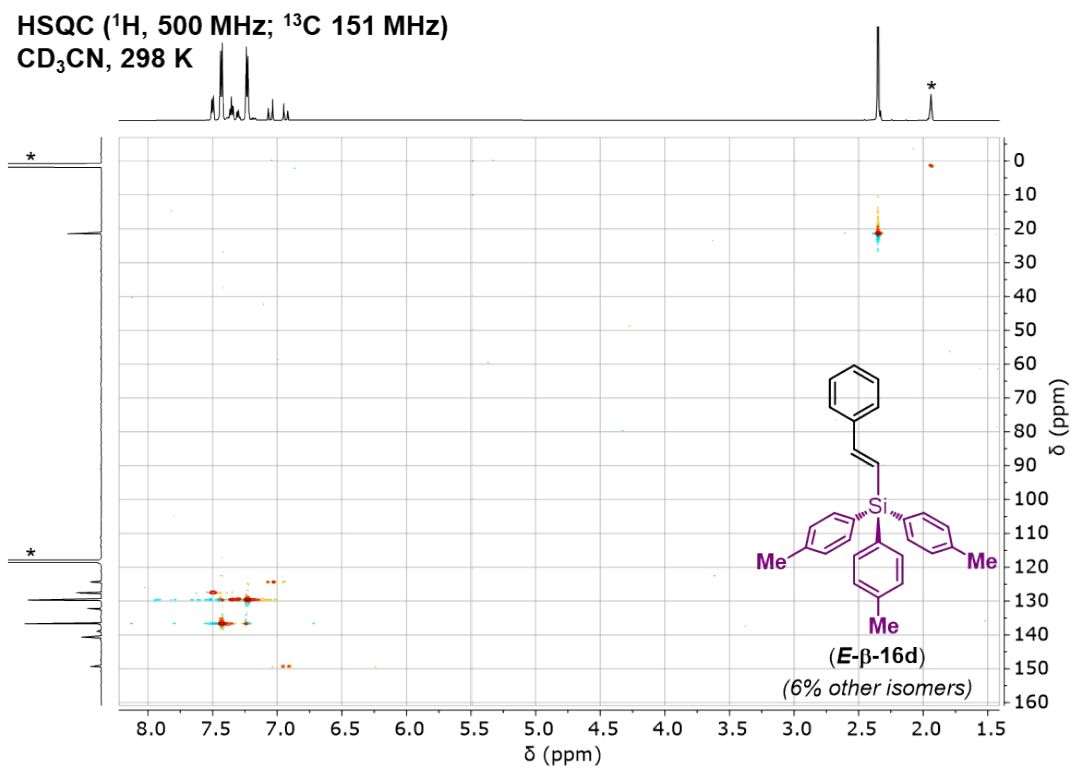


Figure S211. <sup>13</sup>C{<sup>1</sup>H} NMR spectrum of **E- $\beta$ -16d** recorded in CD<sub>3</sub>CN at 298 K.



**Figure S212.** <sup>29</sup>Si{<sup>1</sup>H} NMR spectrum of **E-β-16d** recorded in CD<sub>3</sub>CN at 298 K.



**Figure S213.** HSQC NMR spectrum of **E-β-16d** recorded in CD<sub>3</sub>CN at 298 K.

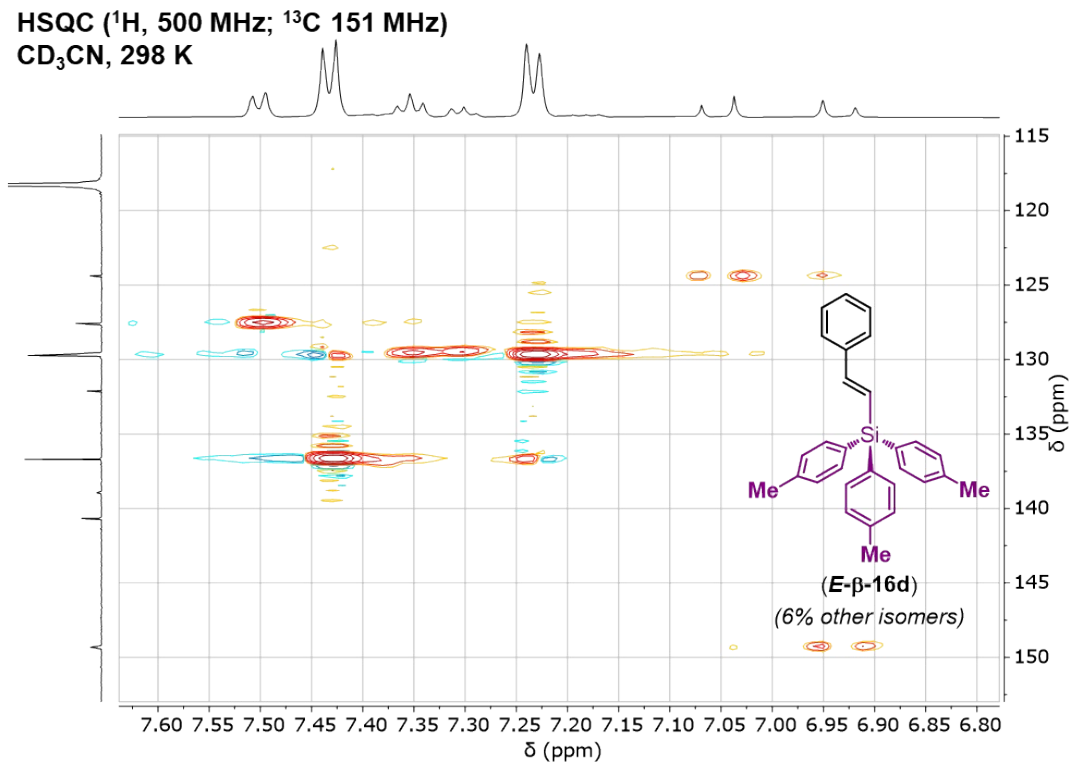


**Figure S214.** Zoom in of aryl region of the HSQC NMR spectrum of **E-β-16d** recorded in  $\text{CD}_3\text{CN}$  at 298 K.

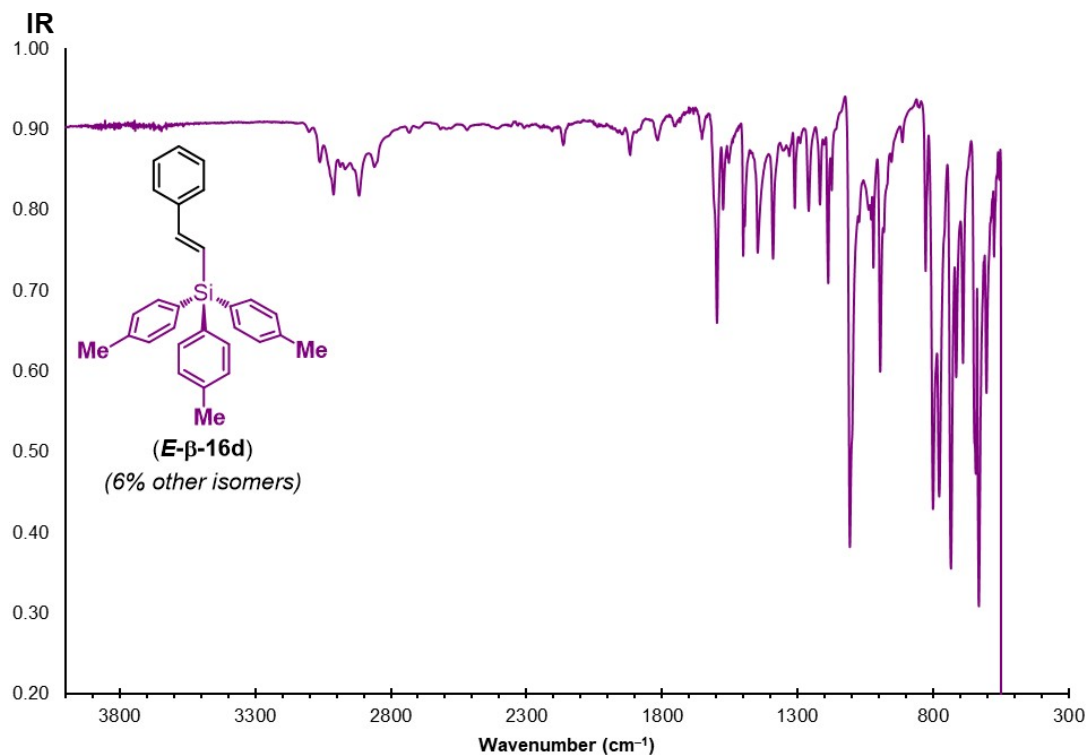


**Figure S215.** IR spectrum of **E-β-16d** recorded neat at room temperature.

(*E*)-1-phenyl-2-(triphenylsilyl)ethene (**E- $\beta$ -16a**)

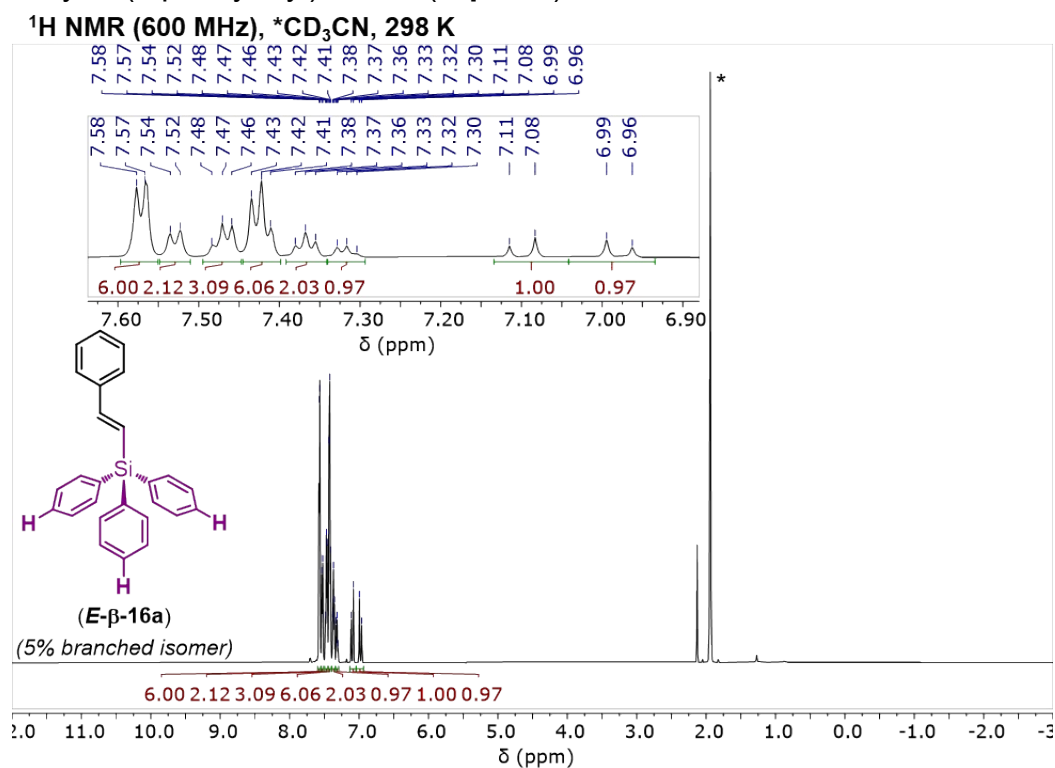


Figure S216. <sup>1</sup>H NMR spectrum of **E- $\beta$ -16a** recorded in CD<sub>3</sub>CN at 298 K.

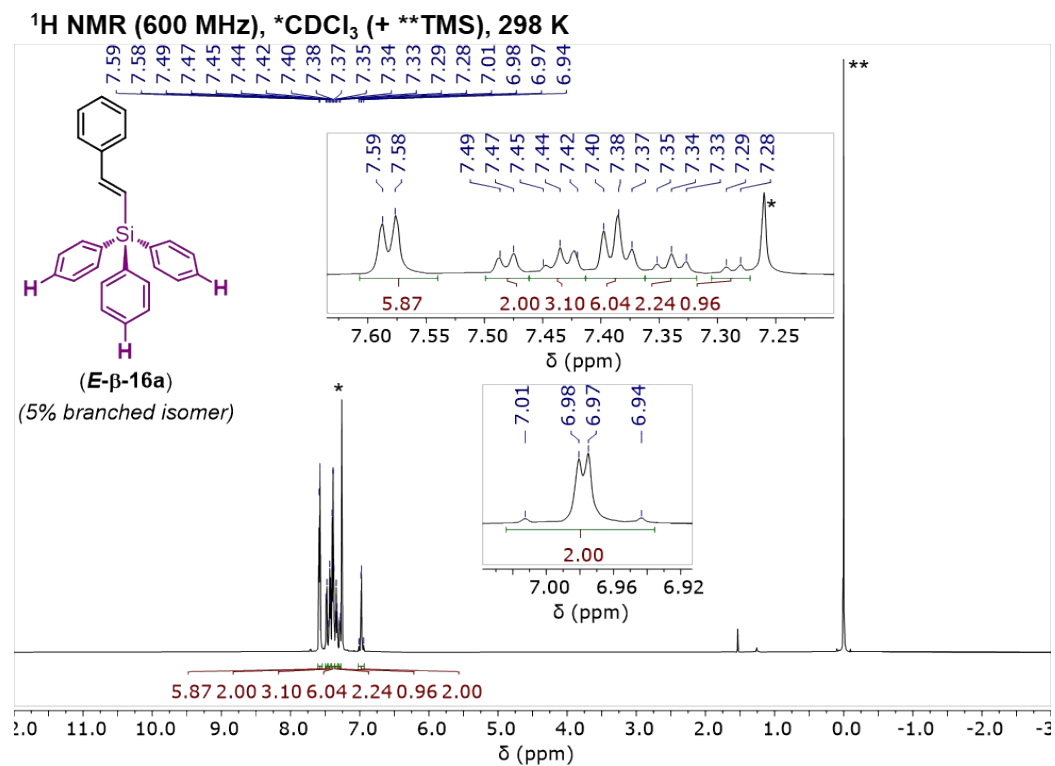
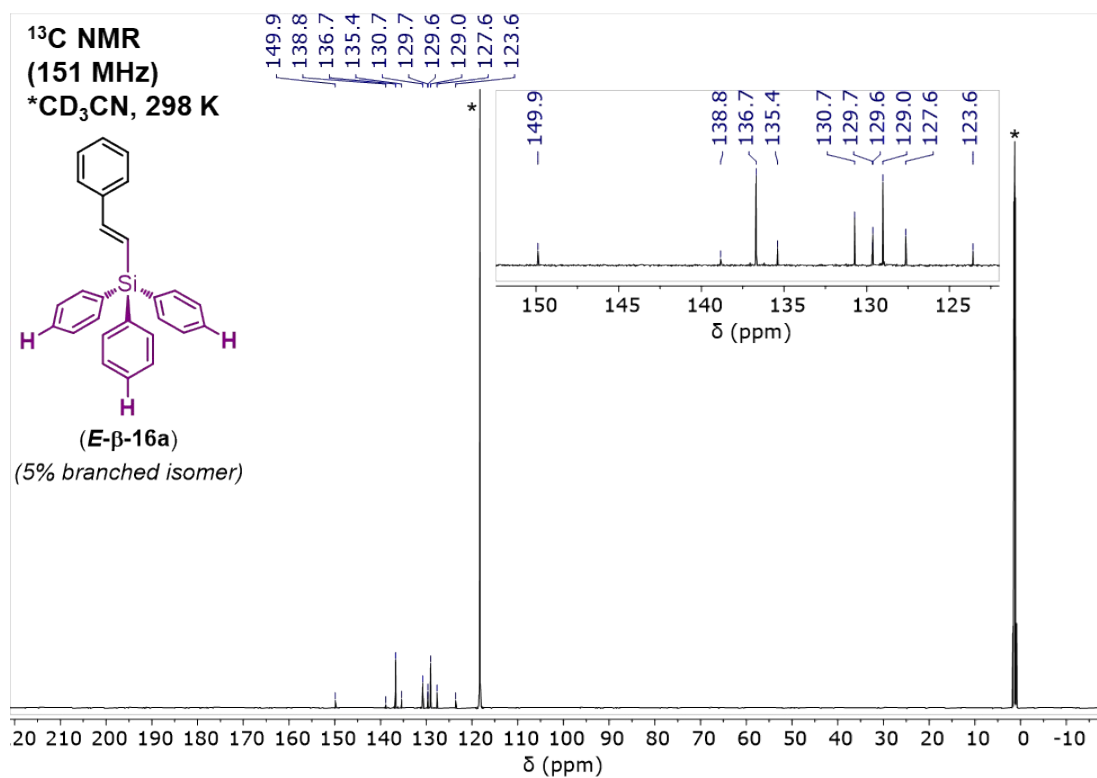
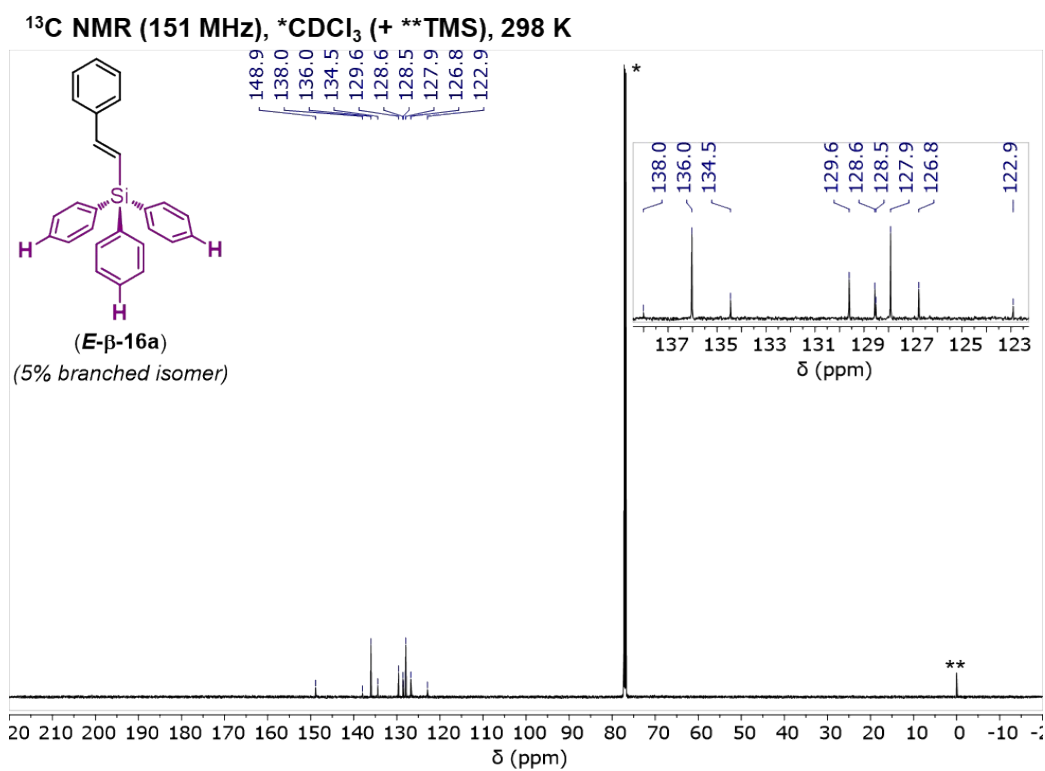


Figure S217. <sup>1</sup>H NMR spectrum of **E- $\beta$ -16d** recorded in CDCl<sub>3</sub> at 298 K.



**Figure S218.**  $^{13}\text{C}\{^1\text{H}\}$  NMR spectrum of **E- $\beta$ -16a** recorded in  $\text{CD}_3\text{CN}$  at 298 K.



**Figure S219.**  $^{13}\text{C}\{^1\text{H}\}$  NMR spectrum of **E- $\beta$ -16a** recorded in  $\text{CDCl}_3$  at 298 K.

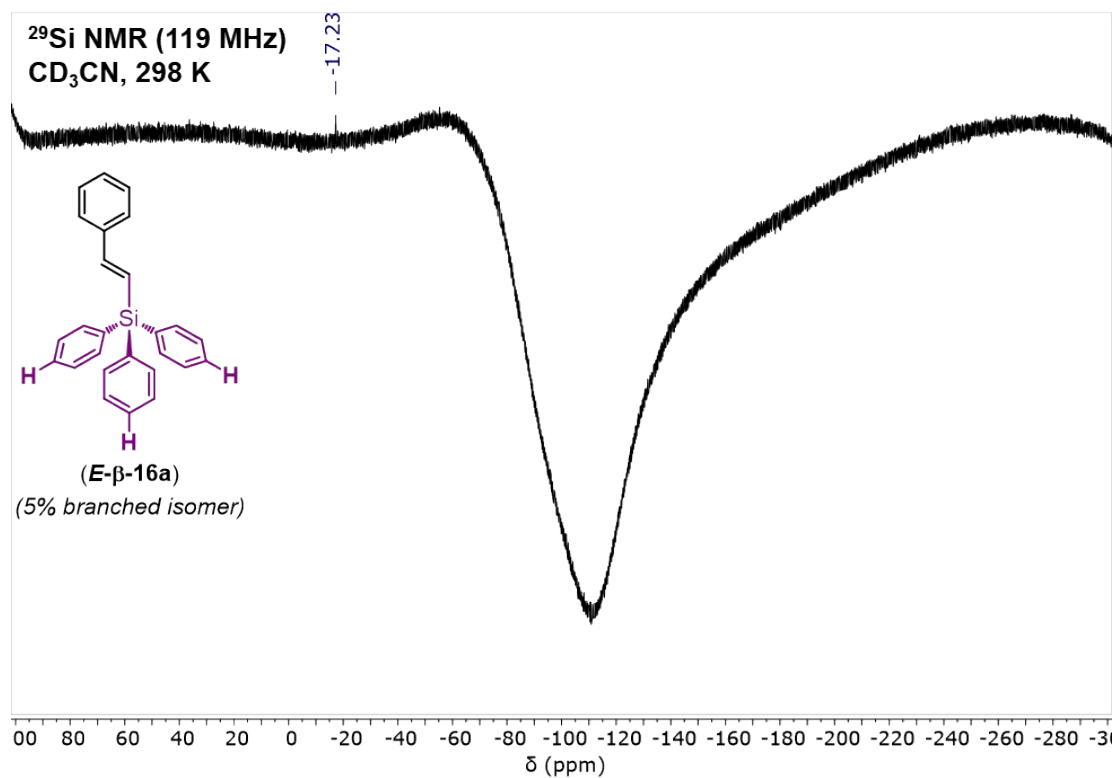


**Figure S220.** <sup>29</sup>Si{<sup>1</sup>H} NMR spectrum of **E-β-16a** recorded in CD<sub>3</sub>CN at 298 K.

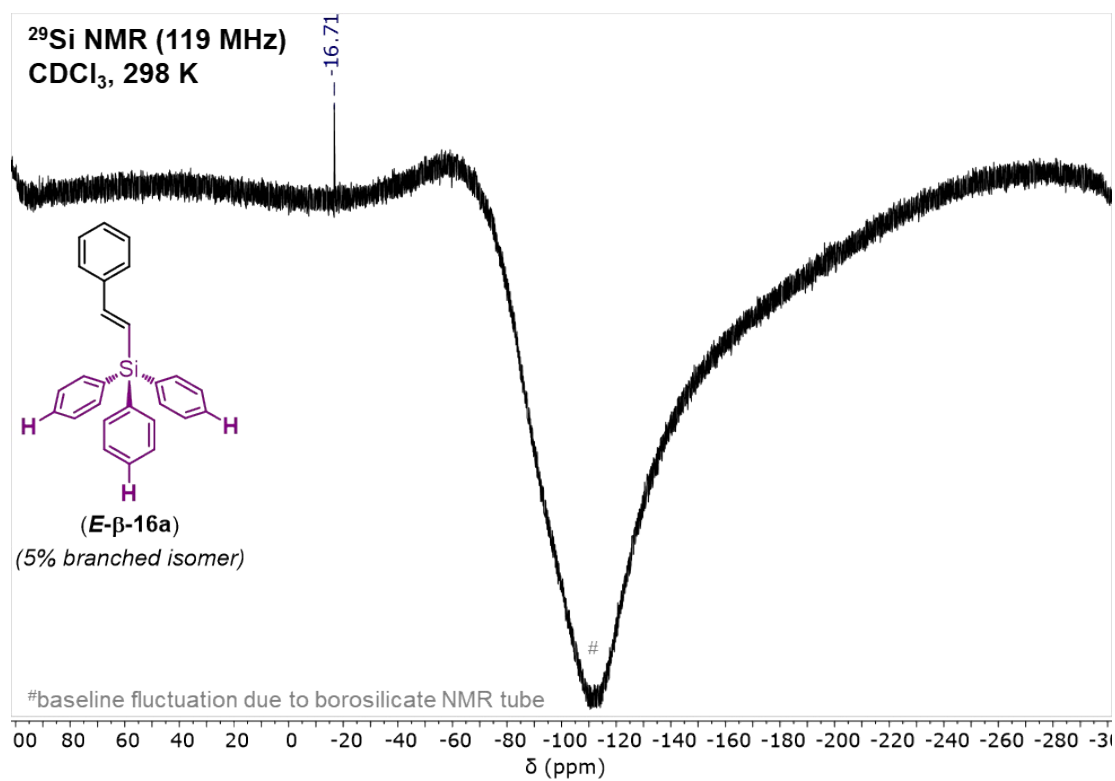


**Figure S221.** <sup>29</sup>Si{<sup>1</sup>H} NMR spectrum of **E-β-16a** recorded in CDCl<sub>3</sub> at 298 K.

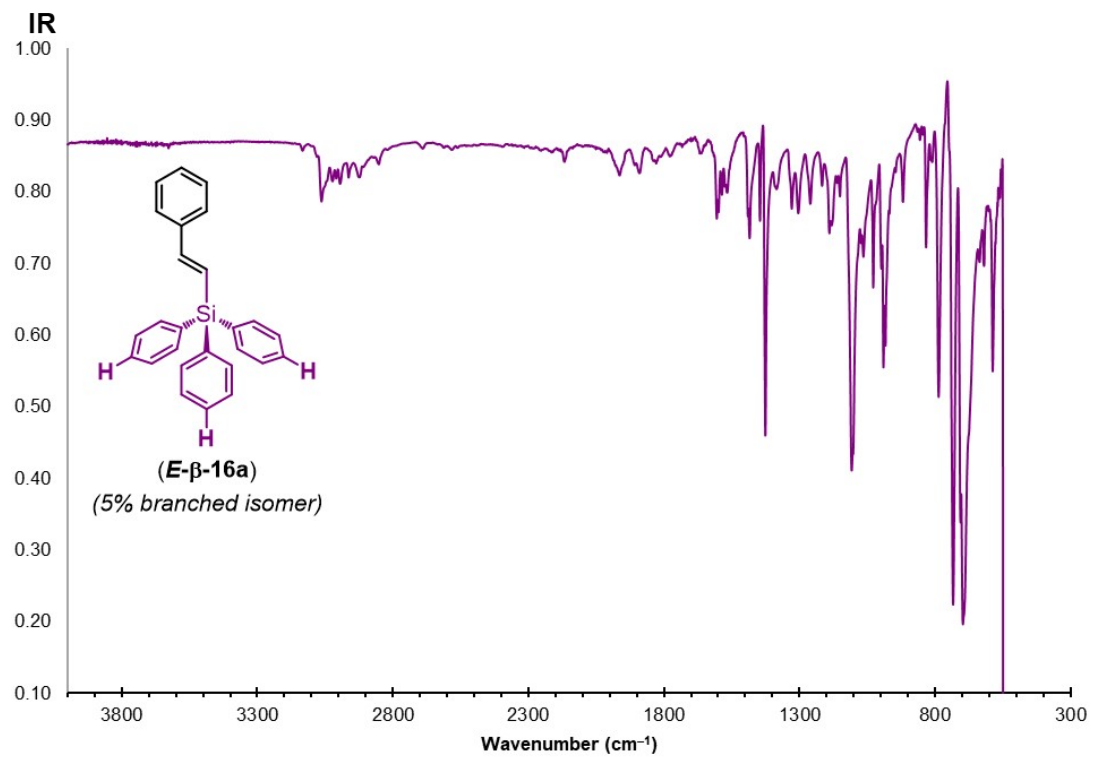


**Figure S222.** IR spectrum of **E-β-16a** recorded neat at room temperature.

(*E*)-1-phenyl-2-[tris(4-trifluoromethylphenyl)silyl]ethene (**E- $\beta$ -16f**)

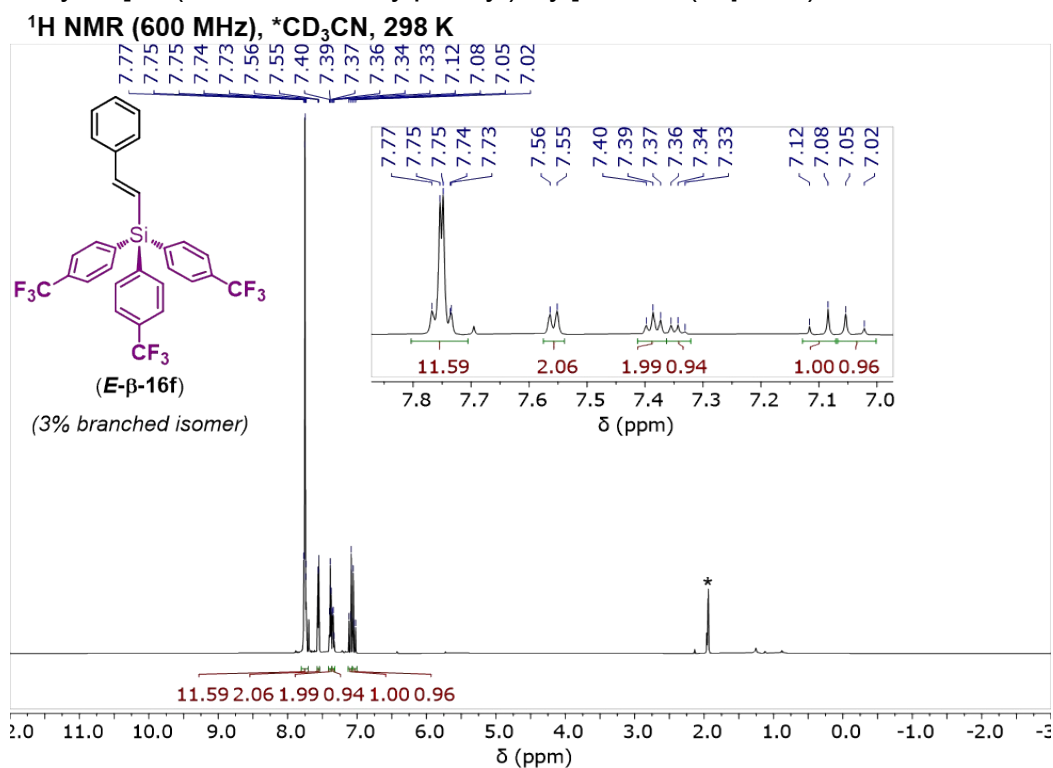


Figure S223. <sup>1</sup>H NMR spectrum of **E- $\beta$ -16f** recorded in CD<sub>3</sub>CN at 298 K.

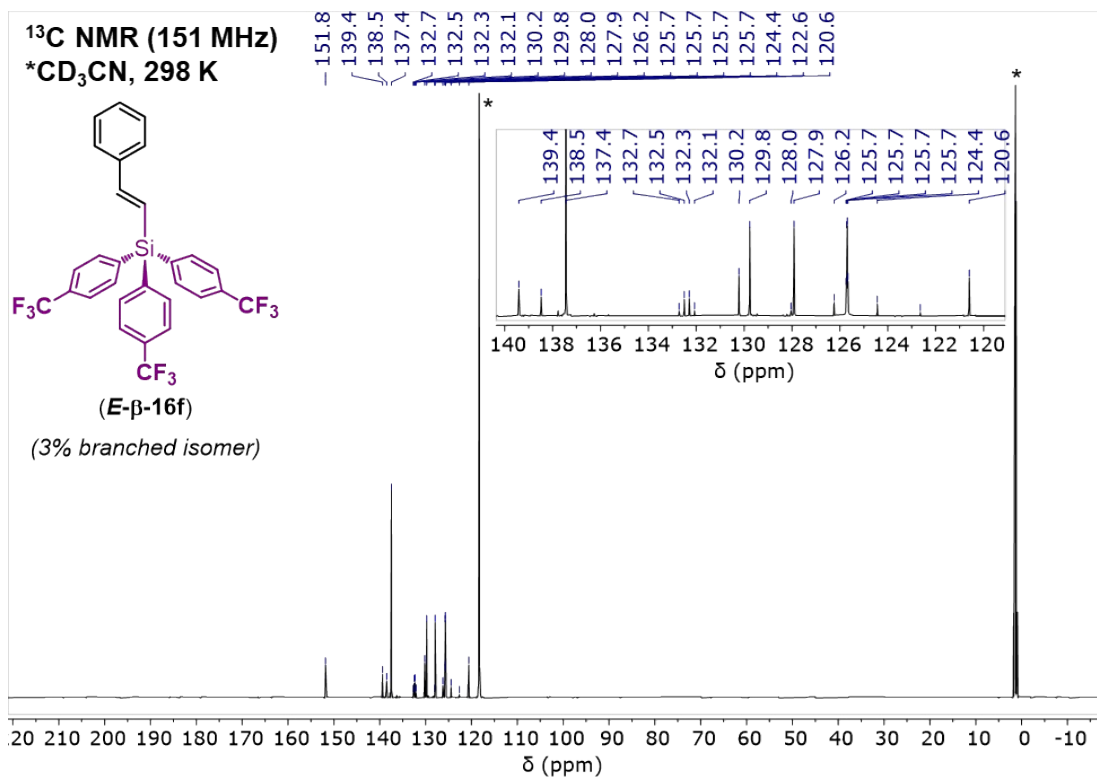
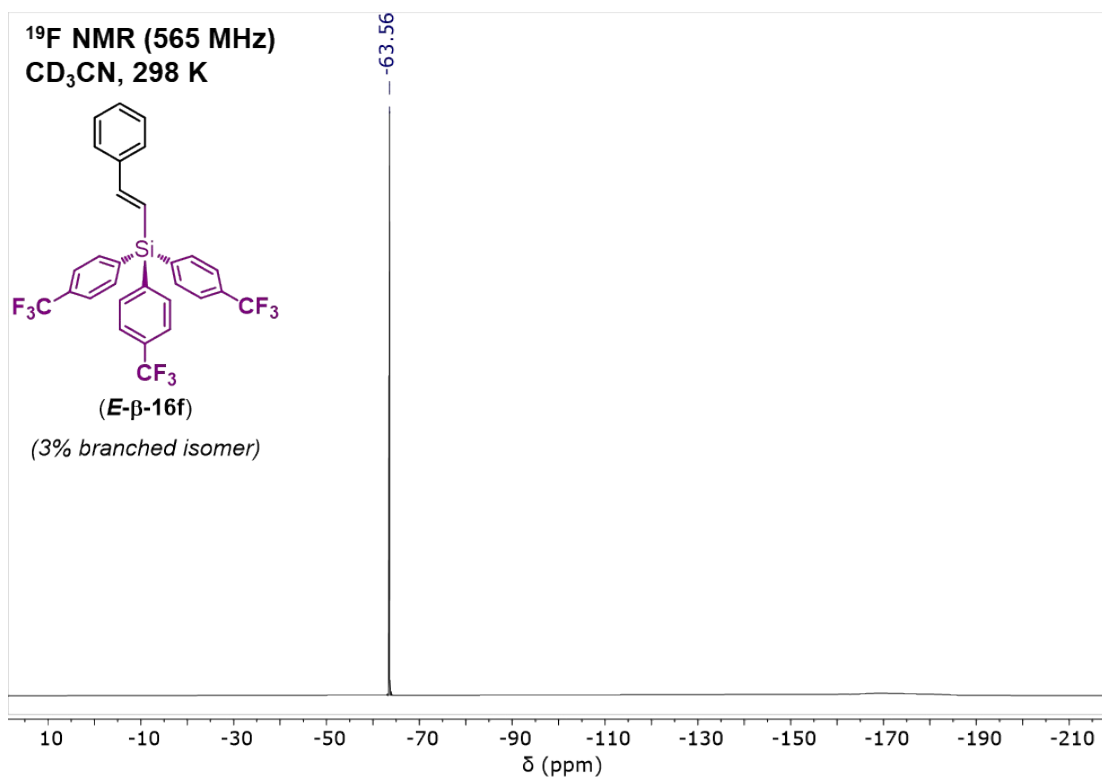
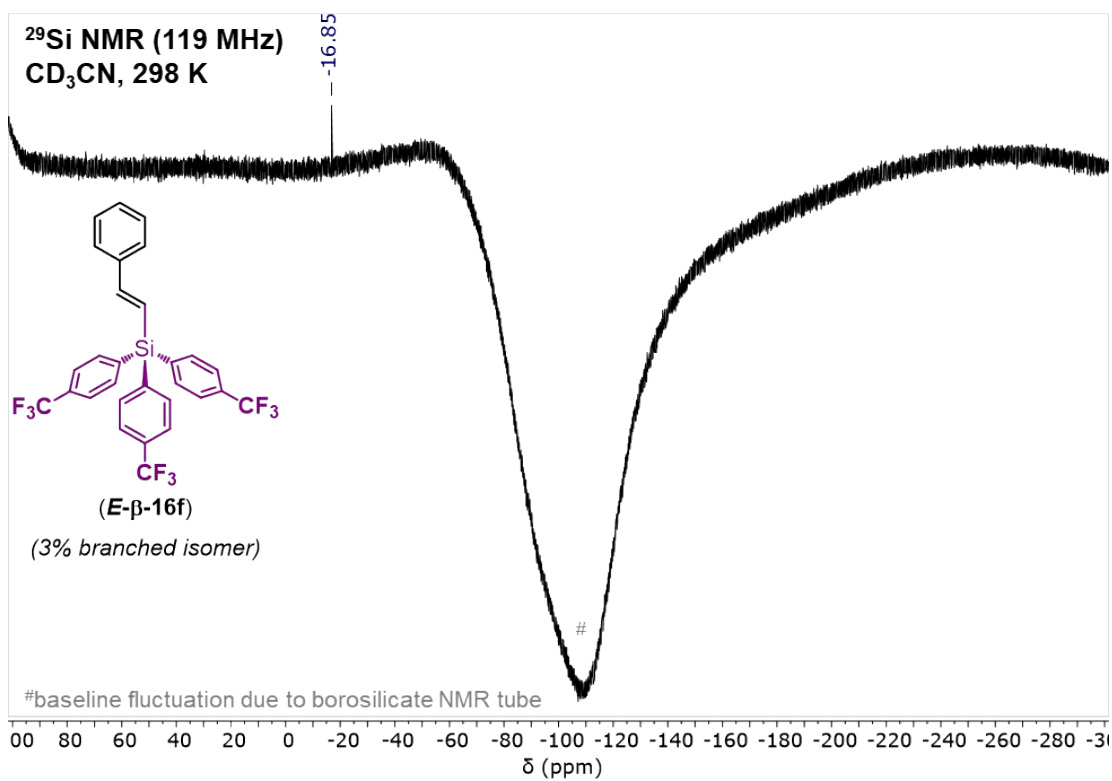


Figure S224. <sup>13</sup>C{<sup>1</sup>H} NMR spectrum of **E- $\beta$ -16f** recorded in CD<sub>3</sub>CN at 298 K.



**Figure S225.** <sup>19</sup>F NMR spectrum of **E-β-16f** recorded in CD<sub>3</sub>CN at 298 K.



**Figure S226.** <sup>29</sup>Si{<sup>1</sup>H} NMR spectrum of **E-β-16f** recorded in CD<sub>3</sub>CN at 298 K.

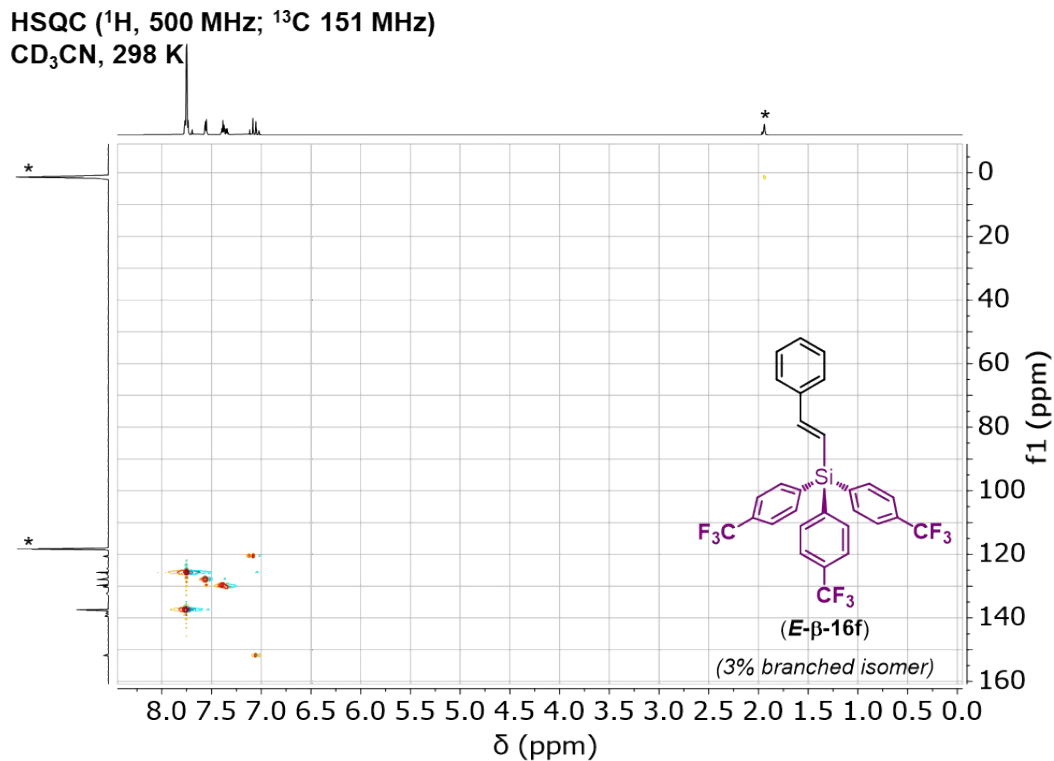


**Figure S227.** HSQC NMR spectrum of **E-β-16f** recorded in  $\text{CD}_3\text{CN}$  at 298 K.

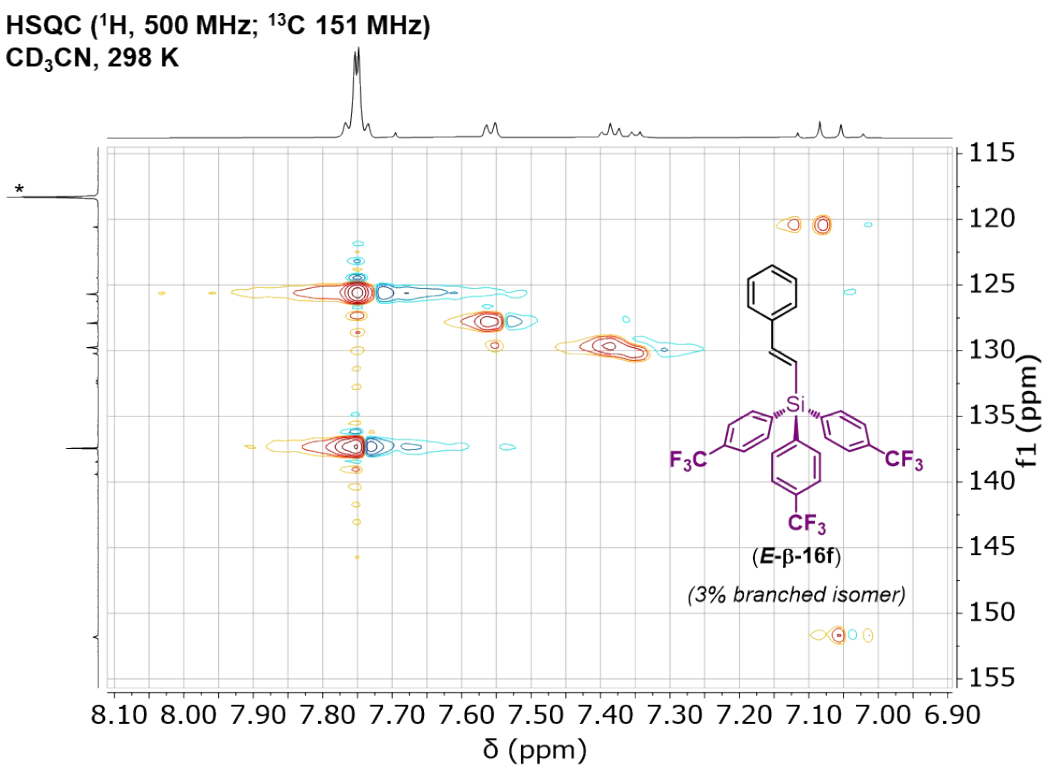


**Figure S228.** Zoom in of aryl region of the HSQC NMR spectrum of **E-β-16f** recorded in  $\text{CD}_3\text{CN}$  at 298 K.

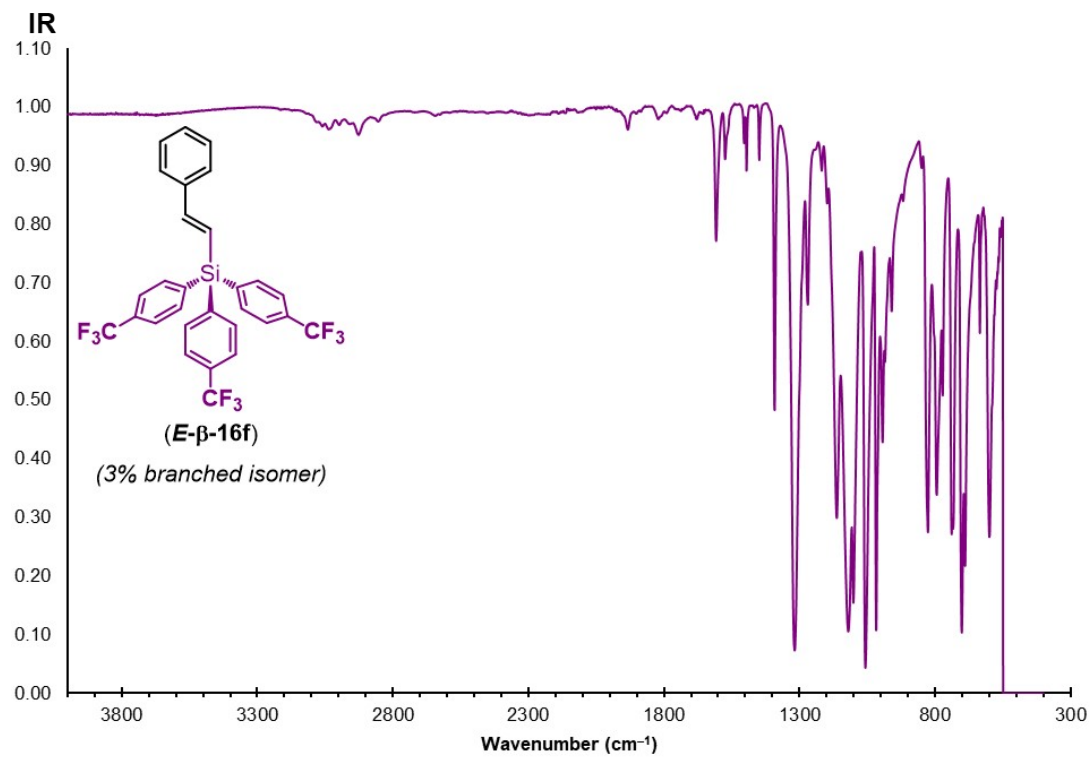


**Figure S229.** IR spectrum of **E-β-16f** recorded neat at room temperature.

## 15. References

1. Diversi, P.; Ingrosso, G.; Lucherini, A.; Lumini, T.; Marchetti, F.; Adovasio, V.; Nardelli, M. Synthesis and thermal decomposition of palladacyclopentane derivatives of the type  $[\text{Pd}(\text{CH}_2\text{CHRCH}_2\text{RCH}_2)\text{L}_2](\text{R} = \text{H} \text{ or } \text{Me})$ . X-Ray crystal structure of  $[\text{Pd}(\text{CH}_2\text{CH}_2\text{CH}_2\text{CH}_2)(\text{bipy})]$ . *J. Chem. Soc., Dalton Trans.* **1988**, 133-140.
2. Reid, S. M.; Fink, M. J. Reductive Routes to Dinuclear d<sup>10</sup>-d<sup>10</sup> Palladium(0) Complexes and Their Redistribution Equilibria in Solution. *Organometallics* **2001**, 20, 2959-2961.
3. Li, H.; Grasa, G. A.; Colacot, T. J. A Highly Efficient, Practical, and General Route for the Synthesis of (R<sub>3</sub>P)<sub>2</sub>Pd(0): Structural Evidence on the Reduction Mechanism of Pd(II) to Pd(0). *Org. Lett.* **2010**, 12, 3332-3335.
4. Akhiani, R. K.; Moore, M. I.; Pribyl, J. G.; Wiskur, S. L. Linear Free-Energy Relationship and Rate Study on a Silylation-Based Kinetic Resolution: Mechanistic Insights. *J. Org. Chem.* **2014**, 79, 2384-2396.
5. Nakagawa, Y.; Chanthamath, S.; Fujisawa, I.; Shibatomi, K.; Iwasa, S. Ru(II)-Pheox-catalyzed Si-H insertion reaction: construction of enantioenriched carbon and silicon centers. *Chem. Commun.* **2017**, 53, 3753-3756.
6. Savella, R.; Zawartka, W.; Leino, R. Iron-Catalyzed Chlorination of Silanes. *Organometallics* **2012**, 31, 3199-3206.
7. Gandhamsetty, N.; Park, S.; Chang, S. Selective Silylative Reduction of Pyridines Leading to Structurally Diverse Azacyclic Compounds with the Formation of sp<sup>3</sup> C-Si Bonds. *J. Am. Chem. Soc.* **2015**, 137, 15176-15184.
8. Hansch, C.; Leo, A.; Taft, R. W. A survey of Hammett substituent constants and resonance and field parameters. *Chem. Rev.* **1991**, 91, 165-195.
9. Anslyn, E. V.; Dougherty, D. A., *Modern Physical Organic Chemistry*. University Science Books: 2006.
10. Ramey, K. C.; Louick, D. J.; Whitehurst, P. W.; Wise, W. B.; Mukherjee, R.; Moriarty, R. M. A line width method for determining chemical exchange rates from NMR spectra. *Org. Magn. Reson.* **1971**, 3, 201-216.
11. Gasparro, F. P.; Kolodny, N. H. NMR determination of the rotational barrier in N,N-dimethylacetamide. A physical chemistry experiment. *J. Chem. Educ.* **1977**, 54, 258.
12. Motoda, D.; Shinokubo, H.; Oshima, K. Efficient Pd(0)-catalyzed hydrosilylation of alkynes with triorganosilanes. *Synlett* **2002**, 1529-1531.
13. Zhang, L.; Oestreich, M. Copper-Catalyzed Cross-Coupling of Vinylodonium Salts and Zinc-Based Silicon Nucleophiles. *Org. Lett.* **2018**, 20, 8061-8063.
14. G. M. Sheldrick, Bruker/Siemens Area Detector Absorption Correction Program, Bruker AXS, Madison, WI, 1998.
15. Sheldrick, G. Crystal structure refinement with SHELXL. *Acta Crystallogr. C* **2015**, 71, 3-8.
16. Yang, L.; Powell, D. R.; Houser, R. P. Structural variation in copper(I) complexes with pyridylmethanamide ligands: structural analysis with a new four-coordinate geometry index,  $\tau_4$ . *Dalton Trans.* **2007**, 955-964.
17. Okuniewski, A.; Rosiak, D.; Chojnacki, J.; Becker, B. Coordination polymers and molecular structures among complexes of mercury(II) halides with selected 1-benzoylthioureas. *Polyhedron* **2015**, 90, 47-57.

18. Nakata, N.; Fukazawa, S.; Kato, N.; Ishii, A. Palladium(II) Hydrido Complexes Having a Primary Silyl or Germyl Ligand: Synthesis, Crystal Structures, and Dynamic Behavior. *Organometallics* **2011**, *30*, 4490-4493.
19. Barrett, B. J.; Iluc, V. M. Metal-ligand cooperation between palladium and a diphosphine ligand with an olefinic backbone. *Inorg. Chim. Acta* **2017**, *460*, 35-42.